Snow Removal and Ice Control Technology

TRANSPORTATION
RESEARCH
BOARD

NATIONAL
RESEARCH
COUNCIL

Snow Removal and Ice Control Technology

Selected Papers Presented at the

Fourth International Symposium
Reno, Nevada
August 11–16, 1996

Sponsored by

Transportation Research Board
Nevada Department of Transportation
American Association of State Highway and Transportation Officials
World Road Association–PIARC
Federal Highway Administration

TRANSPORTATION
RESEARCH
BOARD

NATIONAL
RESEARCH
COUNCIL

Contents

Foreword

The Fourth International Symposium on Snow Removal and Ice Control Technology was held in Reno, Nevada, on August 11–16, 1996. The Symposium was conducted by the Transportation Research Board (TRB) Committee on Winter Maintenance in cooperation with the Nevada Department of Transportation, the American Association of State Highway and Transportation Officials, the World Road Association–PIARC, and the Federal Highway Administration.

The objective of the Symposium was to provide a forum for the exchange of information about state-of-the-art research and technology applications to improve snow removal and ice control operations in transportation systems. Sixty-one papers were presented in the areas of policy and management, infrastructure and snow control, materials and applications, equipment, travel surface, environment and health, road weather information systems and forecasting, and safety and visibility. Papers were authored by maintenance engineers and researchers from Austria, the Czech Republic, Denmark, Finland, Germany, Japan, New Zealand, the Netherlands, Norway, Russia, Sweden, the United Kingdom, and the United States.

All papers in this report were reviewed and accepted for publication through TRB's peer review process established according to procedures approved by the Governing Board of the National Research Council. Papers were refereed by the TRB Committee on Winter Maintenance with committee members and other, outside experts serving as reviewers. The process included a minimum of three reviews and author revisions based on review comments.
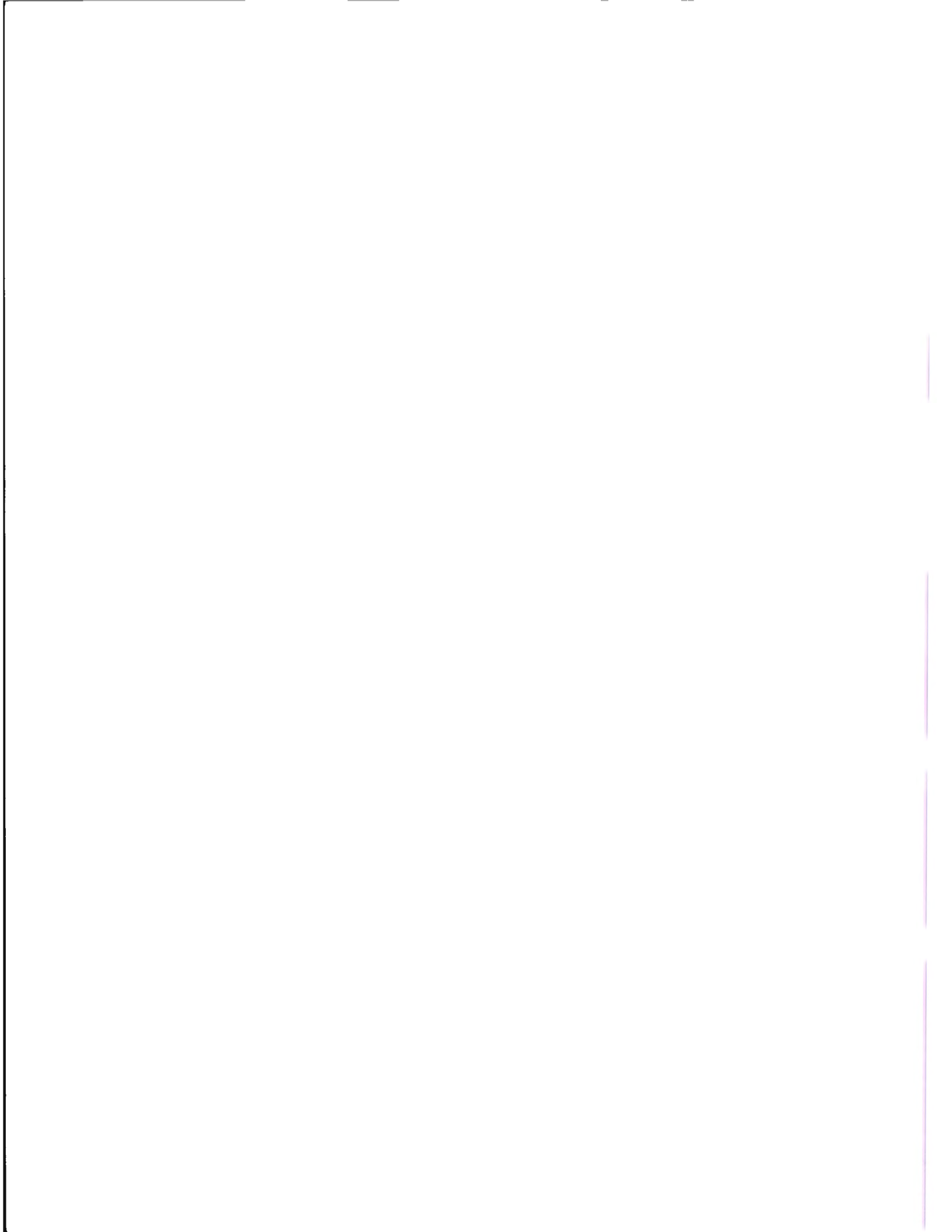
PART 1
POLICY AND MANAGEMENT
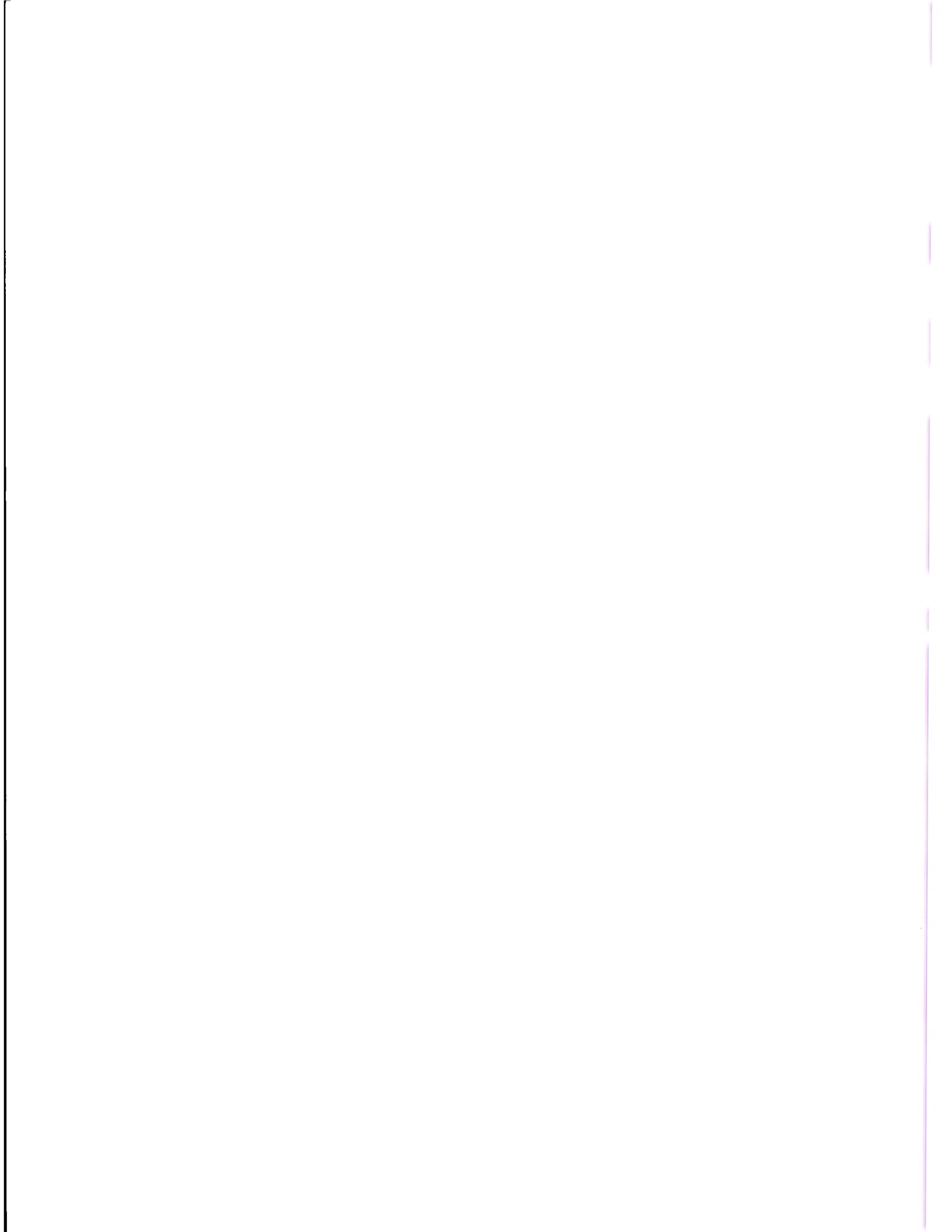
Winter Maintenance in the Netherlands

Maarten Noort, *Meteo Consult, The Netherlands*

Traffic and transport are of vital importance to the Netherlands. The country has an average winter temperature of just above 0°C, and winter maintenance is important to keep roads open and safe. The organization and strategy of winter maintenance are discussed. Special attention is given to the National Ice Warning System, which has been installed on highways and secondary roads in the Netherlands. This system, along with regional weather reports, weather radar, and road-surface forecasts provided by experienced meteorologists, gives authorities up-to-date road and weather conditions. The combination of winter maintenance, knowledge of road management, and meteorology appears to be a success in the Netherlands. In 3 years, Meteo Consult, a private weather service, has significantly enlarged its share in the market. Experience in the Netherlands has shown that free competition in meteorological assistance (which is not common in Europe) can improve quality in road management without reducing traffic safety or increasing cost.

Traffic and transport are of vital importance to the Netherlands. Because of its favorable location, the large ports of Rotterdam and Amsterdam, and Schiphol International Airport, the Netherlands is a main gateway to Europe. Roads and waterways are essential elements of the transport system and account for a significant part of the Netherlands' national income.

For the Netherlands to continue to be Europe's distribution hub, the infrastructure must be efficient to use.

Transport is and will continue to be a growth sector. The continued unification of Europe moves markets. The extension of the European Union and the fading of the borders with Eastern Europe will accelerate this process. Consequently, investment in infrastructure, safety, and environmental protection has become a priority for the present government. A population of 15.5 million in only 41.6 km^2, 6 million cars, 500,000 vans, and 90,000 trucks all seriously test the capacity of the Dutch road system.

The activities necessary to keep roads clear and safe for driving during the winter months are explained, as is the interaction of the government authorities that coordinate winter maintenance in the Netherlands.

CLIMATE

The Netherlands, located in northwestern Europe, has a maritime climate with relatively mild, humid winters. The warming effects of the Gulf Stream generate a predominately westerly wind, which in turn has a marked influence on temperature. Because of the high level of precipitation, which in the winter is mostly rain, road surfaces tend to be wet. Despite the relatively mild winters, the average January air temperature is 1.9°C. The changeable weather leads to hazardous road conditions,

```
126  Air frosts
 44  Ice days
                                    126
                                     44
            91
            40
                                    131
      100      107                   40
       24       26

   63
   11

                             96
 Winter 95/96                20
 © Meteo Consult 1996
```
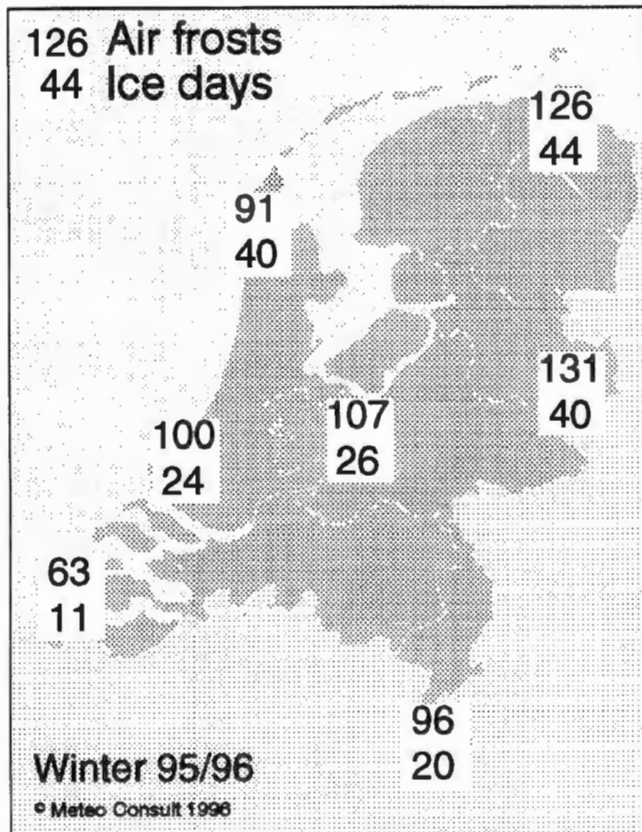
FIGURE 1   The climatological diversity of the Netherlands, winter of 1995–1996.

which mainly are caused by the freezing of wet sections as well as the formation of a layer of ice through condensation or freezing fog. Snow and freezing rain are infrequent. Winter maintenance mainly is based on the preventive treatment of highways and secondary roads by salting. In the colder Northeast, severe weather occurs considerably more often than in the warmer Southwest (Figure 1). High humidity combined with temperatures below freezing results in conditions that require the Dutch government to maintain a well-structured winter maintenance program.

WINTER MAINTENANCE ORGANIZATION

The Netherlands has three government authority levels; each authority maintains its own road system. The public authorities maintain more than 2500 km of main roads, and the county authorities are responsible for about 50 000 km of secondary and tertiary roads. The municipalities maintain about 50 000 km of municipal roads.

The supervision of main roads is the responsibility of about 25 geographically based divisions. County authorities divide the maintenance and control of their roads into several areas. The municipalities are responsible for their own road systems and, together with the counties, also are responsible for bicycle paths (nearly 20 000 km), which are maintained as well.

During winter maintenance, all authorities are autonomous. However, public and county authorities consult each other regularly on an executive level; thus, the two levels of authority have established similar procedures for winter maintenance. The main goal is to prevent hazardous road conditions, and this is done through salt spreading. Both organizations use the prewetted technique for spreading operations. The public and county authorities both purchase or refurbish equipment and material (e.g., spreaders, snowplows, and salt) before the winter season begins and store these items in several locations for easy access during the winter months. The trucks needed for spreading operations (Figure 2) are rented from the transportation industry, and the drivers are hired from the same industry. The costs are based on a standard amount per year plus an amount for every spreading operation. If the spreading operation takes longer than 3 hr the costs relate to the actual hours worked.

Municipalities, on the other hand, use their own trucks. In the municipalities, the changeover from the dry salt technique to the prewetted technique has not been completed. About 70 percent of the larger municipalities use the prewetted technique. In smaller municipalities, the changeover has not made much progress.

Within the public and county authorities are generally three coordinators who take turns being on duty. When hazardous conditions first appear the coordinator informs one of the workers in each area. The truck drivers are contacted and they begin spreading operations. After the spreading operation, the driver returns to the area headquarters, and more spreading operations are ordered, if necessary.

With the help of a computer program, all spreading routes have been optimized during the last few years. The duration of a spreading operation on each route is about 45 min. The time it takes to alert the drivers, put

FIGURE 2   Truck with prewetting solution being loaded with salt in a maintenance yard.

the spreader on the truck, load the salt, and perform the spreading operation is a maximum of 2 hr. A fixed snowplow route takes about 1 hr to complete. Spreading is done mainly in the evening or just before the a.m. peak, to disturb traffic as little as possible.

The county authorities have a similar organization but take longer to spread, typically 1.5 to 2 hr for secondary roads.

In municipalities, where spreading operations are done by the local authorities, a clear difference exists between the time it takes a main road and secondary roads to receive treatment. Integration among routes is limited. In addition, organization of spreading and salt storage management is rarely integrated among authorities.

As mentioned, the prewetted technique is frequently used. In general, calcium chloride ($CaCl_2$) is the wet component used in prewetted spreading operations. Quantities of salt used depend on conditions.

Freezing of wet road sections caused by dropping temperatures is the most common form of road ice in the Netherlands. In general, this can be prevented by application of 5.5 g of sodium chloride (NaCl) per square meter. Porous asphalt (drain asphalt), which is often used for main roads, needs a higher dosage (11 g/m^2).

Road ice caused by condensation also may be prevented by the application of 5.5 g sodium chloride per square meter. The Netherlands road authorities use preventive measures as much as possible, especially for approaching snow or freezing rain. Fifteen g of sodium chloride per square meter prevents the snow from attaching to the asphalt. During snowfall, 15 to 20 g/m^2 sodium chloride is applied to the road surface right after plowing. Normally, a dry salt is used in this case. In the

Netherlands both evaporated (vacuum) salt and rock salt are used. The heavy metals in the salt are limited to 10 ppm. In addition, the division of grains has its limit. The maximum permitted size is 3.15 mm. Larger grains are permitted when a price reduction is stipulated, as are fine materials.

Snow is removed from bicycle paths with a revolving broom instead of a snowplow.

NATIONAL ICE WARNING SYSTEM

Prevention is the best policy for main and secondary roads. Without the required data regarding ice conditions, road authorities may order needless spreading operations, resulting in wasted money and resources. Adequate planning also reduces environmental pollution caused by the thawing agents. Porous asphalt requires special attention. Measuring points installed along sections of porous asphalt have improved the winter maintenance capability of road authorities.

In 1989, the first phase of the National Ice Warning System was installed. The experience gained led to a series of improvements, mainly in the reliability of the system. By the end of 1994 the ice warning system had been installed on all highways and on most of the county roads. The measuring points on the county roads often run in conjunction with the highway system. In addition, measuring stations have been installed on the municipal roads. The procedures and communication of the National Ice Warning System were fixed in functional specifications so that several contractors could participate in the project.

The ice warning system consists of several elements (Figure 3). First, the measuring stations along the road
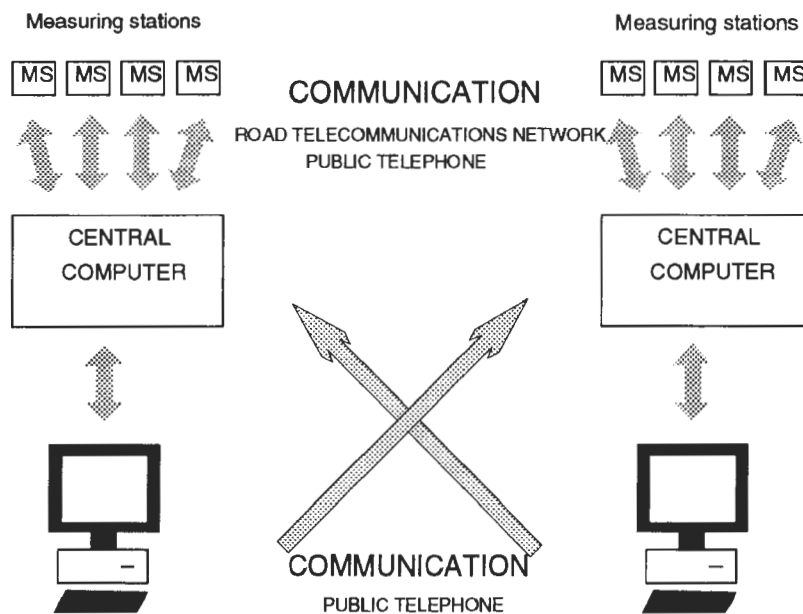
FIGURE 3 National Ice Warning System communication system.

collect relevant data measured on or near the road. The collected data are then retrieved by a central computer, either through the emergency telephone network or, if such a system is not available, through the public telephone network. The computer collects the data from measuring stations in its district every 5 min. If the data are transmitted through the public telephone network, they are collected once or twice every 24 hr. However, in situations in which road ice is likely to occur, the data are collected on a much more frequent basis. Of course, current data from measuring stations can be retrieved whenever the road authority in charge considers the data to be essential.

By using the public telephone network, all road authorities can establish a connection with the central computer with a modem-equipped personal computer. Through the telephone network, a connection to the central computer system can be obtained from anywhere. If hazardous conditions are expected in one or more places, the central computer, on the basis of programmed parameters, sends a semaphone or telephone alarm signal to the road authority in charge of the road sections involved. Because the parameters of the ice warning system produce alarm signals before the road actually becomes icy, authorities can carry out preventive spreading actions.

Communication between the personal computer and the central computer is standardized, which means that all the ice detection systems in the Netherlands use the same communication algorithms. As a result, road authorities can collect data for areas outside their own districts and use the data as a solid basis for their spreading decisions (Figure 4).

Measuring Station

The roadside measuring station is one of the most important elements of the National Ice Warning System. To determine the position of a measuring station, thermal mapping is carried out under prescribed conditions. These conditions include light winds, cloudless skies, and temperatures around freezing. Thermal mapping indicates the coldest spots of a specific section of the road system. The pertinent road authorities apply these data to their experience to establish the first areas of road ice formation.

The Netherlands' infrastructure contains many bridges and flyovers. Since bridges and flyovers receive no heat from the subsoil, they often are the first places to become icy. Yet, under certain circumstances, road ice easily develops in many other places, including elevated roads and roads near forests and large water surfaces. In addition, the low position of the sun in winter allows entrances and exits to highways, especially those on the north side, to become hazardous. Through review of these critical
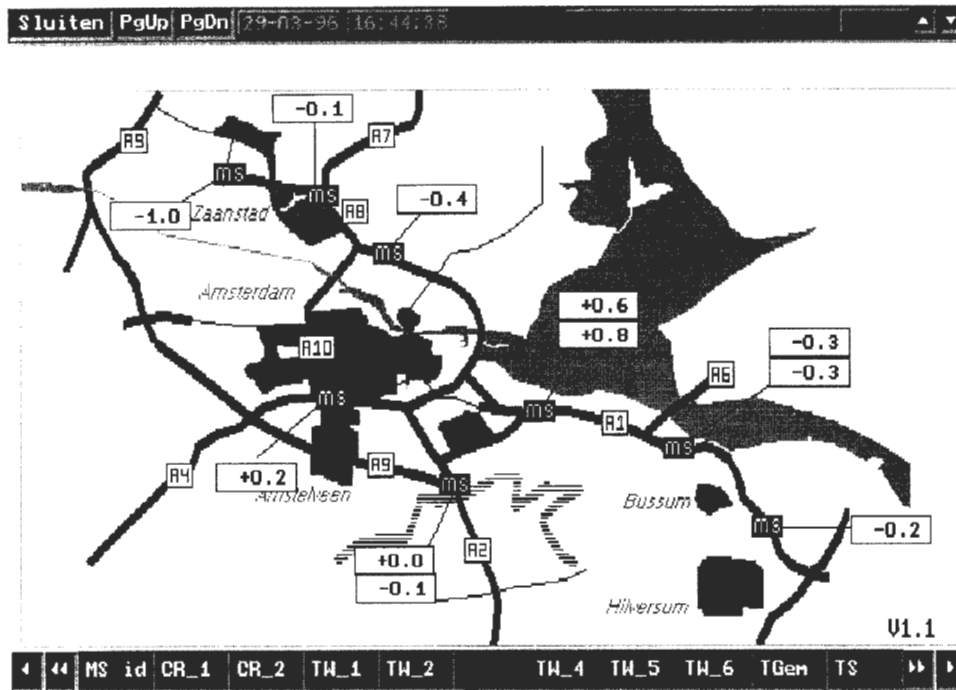
FIGURE 4   Road temperatures around Amsterdam, January 7, 1996, 8:30 a.m. Highest temperature is for a steel bridge. Measuring stations around the country provide such relevant data to road managers.

spots, a safe distribution of the measuring stations can be established within each district.

Currently, 300 measuring stations are situated on primary and secondary roads throughout the Netherlands. These computers are linked to 20 central computers, and the last central computer was installed in December 1994. Near the measuring stations, several temperature sensors are installed a little below the road surface. In the case of multilane superhighways, the temperature sensors are installed in the wheel track of the left lane; because of lower traffic intensity, this lane is colder than the more-traveled right lane. Moreover, the road is equipped with sensors that apply the principle of conductance to their measurements to provide information on the general condition of the road surface. These conditions may include a dry, wet, or salt-covered roadway. The temperature under the road bed is measured in several places. These values provide the road authority with information on possible warm or cold reservoirs in the subsoil. A maximum of 12 temperature sensors and condition sensors can be connected with a measuring station.

In addition to road surface data the measuring stations also record air temperature and humidity, as well as precipitation and, in some places, the speed and the direction of the wind (Figure 5). On the basis of air temperature and humidity values, the dew point is calculated. A comparison of the road surface temperature and the dew point indicates if humidity will settle on the road surface, which can cause road ice through condensation (Figure 6).

Decisions about spreading operations are made not by the ice warning system but by the road authority in charge. Because of the present parameters the road authority is warned more than 2 hr before hazardous conditions occur. On the basis of an evaluation made from the data provided by its own system and, if necessary, by adjacent ice warning systems, the road authority then makes a decision. In addition, meteorological forecasts play an essential part in the decision.

Sprinkler Equipment

The Netherlands abounds in waterways. Many bridges cross the country's rivers and canals, and a number of these bridges have steel frames. Especially during clear

FIGURE 5 Illustration of measuring station, January 7, 1996, 8:30 a.m. Air temperature, humidity, dew point, and precipitation are shown in upper left box. Road temperature and conditions are shown at sensor locations in roadway. Note that road temperature is below freezing and air temperature is above freezing.
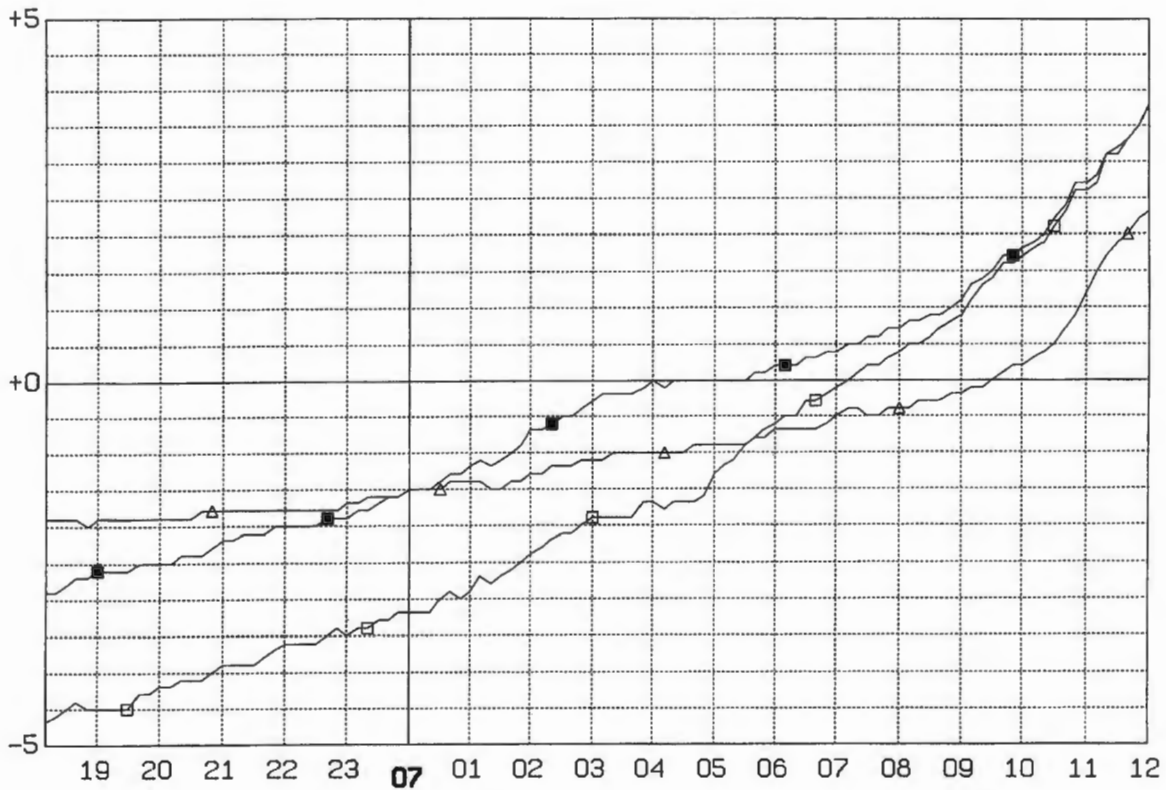
FIGURE 6   Road temperature (△), air temperature (■), and dew point (□) presented in graph form. Note that road temperature rises more slowly than air temperature. Road temperature passes freezing point 5 hr after air temperature.

and windless nights the temperature of the road surface of these steel bridges often drops below freezing, whereas the temperature of adjacent road sections may stay well above freezing. The humid maritime climate often causes condensation on these bridges. To the surprise of drivers, steel bridges often become slippery during spring and autumn. To prevent this, many steel bridges have been equipped with an ice warning system, which alerts the road authority to potential hazardous road conditions. Instead of sending a warning signal to a road authority, however, some ice warning systems independently activate a sprinkler system permanently located on the bridge (Figure 7). The sprinkler system sprays a 20 percent sodium chloride solution on the road surface. Five bridges have been equipped with the automatic sprinkler system, which has produced satisfactory results.

METEOROLOGICAL SERVICES

Several years ago there was little cooperation between road authorities and meteorologists. The most important source of information was weather reports broad-

cast on the news. Since then cooperation has accelerated and enormous progress has been made by combining the knowledge of road authorities with the knowledge of meteorologists.

All road authorities autonomously decide which meteorological products they need and who will supply

FIGURE 7   Sprinkler head spraying NaCl over bridge road surface.

these products. Road authorities often use several meteorological products provided by their meteorology firm to obtain information about conditions that may favor dangerous winter road conditions.

Regional Weather Reporting

One product developed by meteorologists for road authorities is a regional weather report. This report, which details the possibility of road ice, was developed by meteorologists by using knowledge of the types of hazardous roads in coordination with their experiences with weather conditions. The authorities receive a detailed report for the first 24 hr and a 5-day forecast detailing the possibility of winter conditions.

In addition to providing regional weather reports, meteorologists also warn road authorities of snow or freezing rain several hours before it reaches their areas. From that moment the road authority watches the situation with the help of weather radar.

Weather Radar

Radar pictures are available to all road authorities in the Netherlands (Figures 8 and 9). Through contact with the host computer, an updated picture is available every quarter of an hour. Detailed information about a specific area can be obtained by using the magnifying feature included in the program's package. By using the network of main roads, the road authority can relatively easily see the velocity and the direction of the precipitation. European countries do not exchange weather radar yet, so symbols are used outside the Dutch border. This system does, however, allow road authorities to increase their knowledge of current environmental conditions. During the 1996–1997 winter, road authorities used the German weather radar. Especially during an easterly circulation, these data considerably improve road-condition forecasts. The weather radar of Great Britain is not available to the Dutch market because it is too expensive.

Road Surface Forecasts

Many models for road surface forecasts have been developed. These models, which are based mainly on physical processes (e.g., balance of heat), considerably improved the "nowcast" (short-term forecast) conditions for the road authorities. In these models, data from the ice warning system are incorporated into the meteorological formula. From these models, nowcast
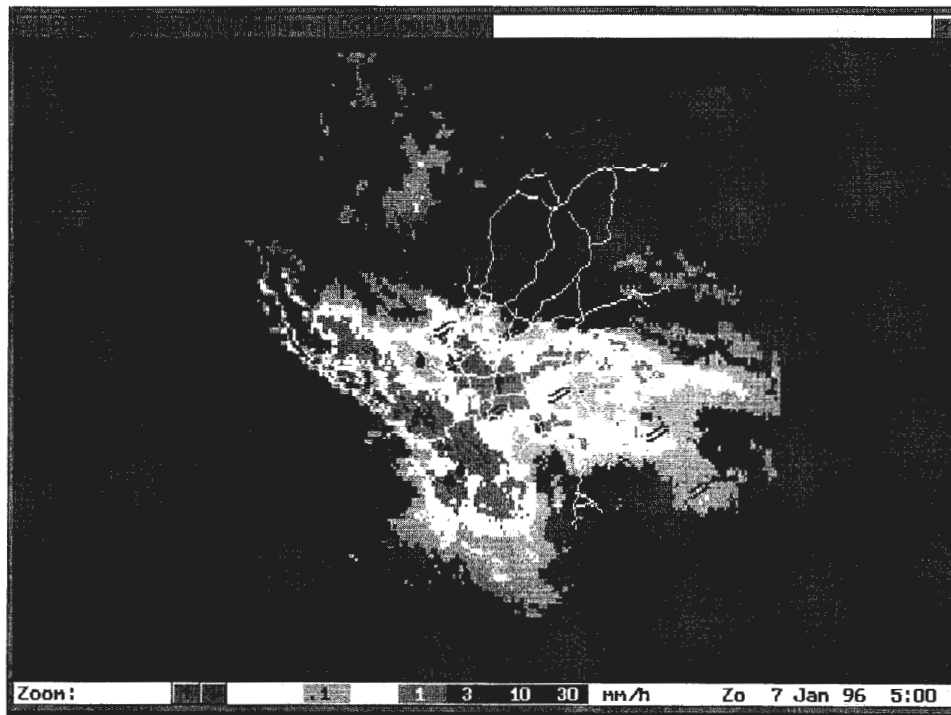
FIGURE 8   Weather radar indicating freezing rain over southern Netherlands and rain over northern Belgium.
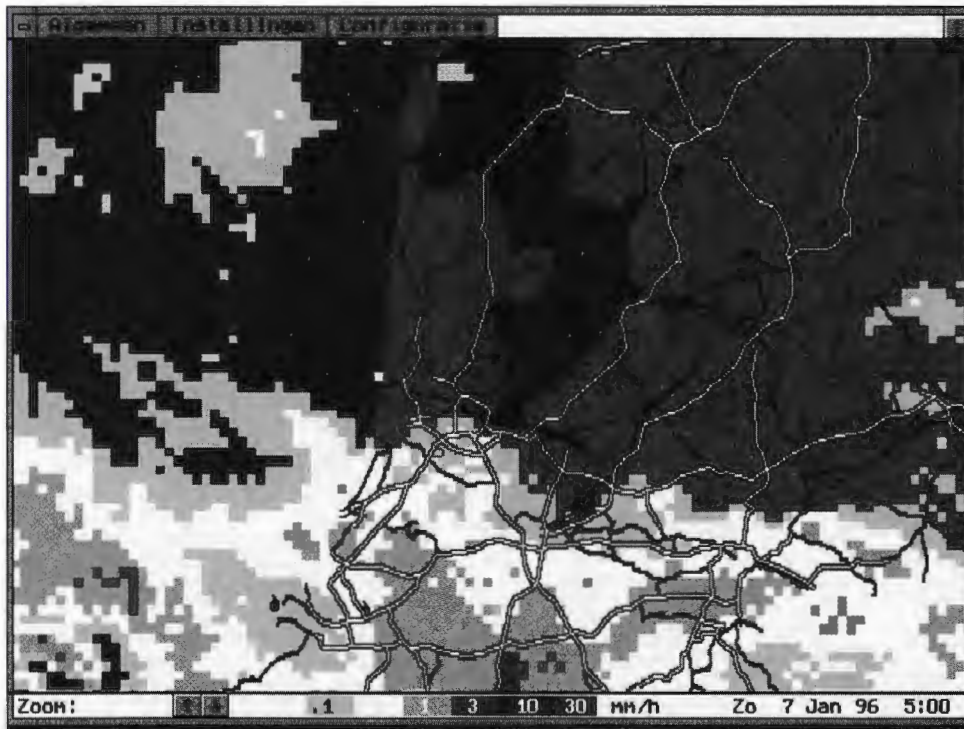
FIGURE 9   Use of road overlay to determine position of precipitation.

and long-term forecasts are generated for the road authority. To keep the information as accurate as possible, special measures have been taken. First, a meteorological database at Meteo Consult, a private weather service, is kept up to date with the most recent data 24 hr a day. In addition, the central computer of the ice warning system also gathers the data of the measuring stations.

When the road authority contacts the central computer, which is protected by a password security system, to get information from the ice warning system, the central computer immediately contacts the meteorological computer. Via a modern connection the actual data of the ice warning system can be passed on. The most up-to-date meteorological data can be connected to the ice warning system data and the model of road surface forecasts can present, in 1 min, the most up-to-date road surface forecast. Spreading decisions are based on this forecast (Figure 10). By using data from the winter of 1994, two road-surface forecast models used in the Netherlands were compared. The first, the icebreak model, was developed by Vaisal/TMI and is used by the National Weather Service. This model, based on physical processes, was compared to a statistical model, which was developed by Meteo Consult. It was clear that the statistical model is responsible for a more exact road surface forecast than is the

physical model. It was further concluded from this comparison that a temperature sensor under the road surface construction is necessary to make correct road surface forecasts.

Designated Meteorologists

Increased knowledge of ice warning systems and meteorology encouraged a few divisions of the main road network to ask Meteo Consult for assistance in winter maintenance. Subsequently, seven meteorologists broadened their knowledge of winter maintenance and ice warning systems. During the winter, the meteorologists work 24 hr a day to ensure optimal operation of the ice warning system. The road authorities receive the collected data from the meteorologists. Decisions for spreading operations can be based on the data. During unclear situations, an inspection of the roadway is carried out following close consultation between the meteorologist and the road manager. Cooperation between road authorities and meteorologists has improved through this type of regular contact. The same seven meteorologists also are responsible for other meteorological services, such as regional weather reports.
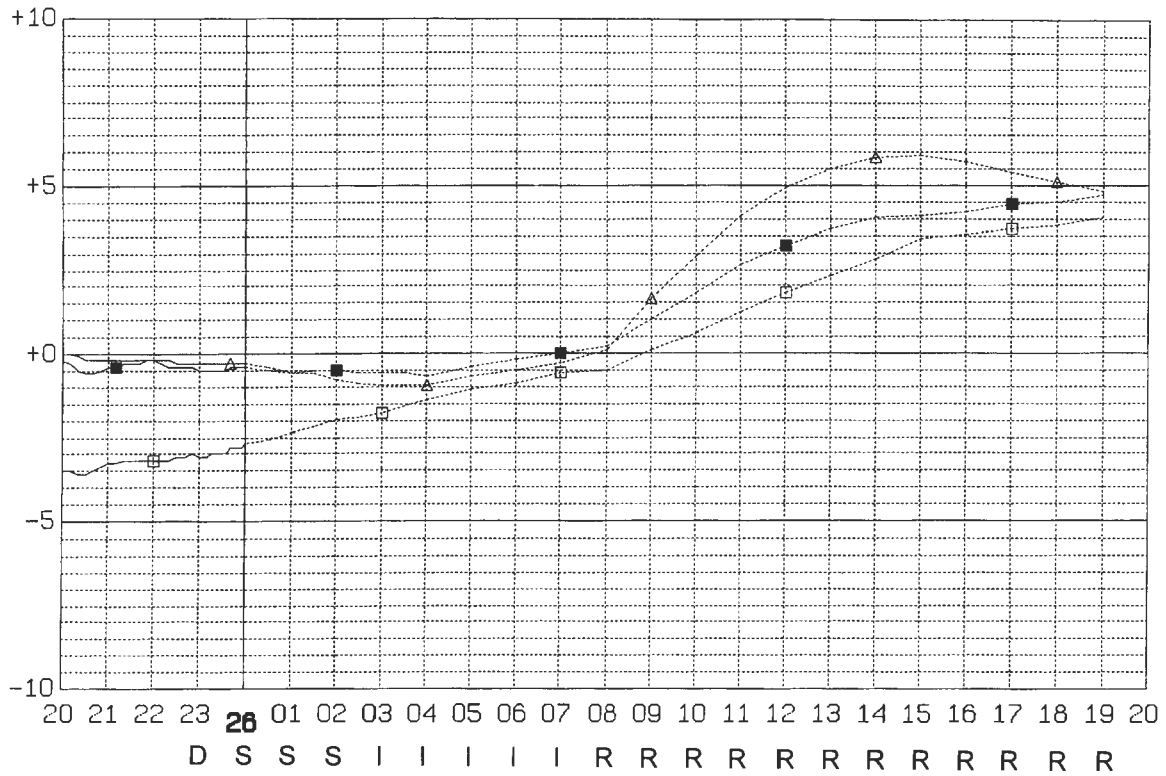
FIGURE 10   Four hours of measured data at the left (solid lines). Forecast from midnight on right (dotted lines). Road surface temperature (△), air temperature (■), and dew point (□) are shown. Forecast indicates snow (S) and freezing rain (I), followed by rain (R).

CONCLUSION

The combination of winter maintenance, knowledge of road management, and meteorology appears to be a success in the Netherlands. In 3 years, Meteo Consult, as a private weather service, has been able to enlarge its share in the market from 0 to 80 percent.

However, in most European countries only one provider (the national weather service) is available to supply road authorities with meteorological services. Experience in the Netherlands has proven that free competition can improve quality in this part of road management, without reducing traffic safety or increasing cost.

Weather-Related Traffic Management in the E18 Finnish Test Area

Yrjö Pilli-Sihvola, *Finnish National Road Administration*

The test area prepared for the demonstration of weather-related traffic management telematics solutions is the E18 corridor running from Turku along the southern coast regions of Finland via Helsinki and Kotka to Vaalimaa on the Russian border. The corridor also includes maritime links from Turku to Stockholm, Sweden; from Helsinki to Stockholm, Travemunde (Germany), and Tallinn (Estonia); and from Kotka to various ports in Germany, as well as road and rail links from Vaalimaa to St. Petersburg, Russia. An overview reflecting the initial phase of the test project is presented.

The total length of the Finnish part of the E18 roadway is about 350 km. The average daily traffic on E18 varies from 2,500 vehicles near the Russian border to 35,000 vehicles near Helsinki. The average daily traffic at the border station in Vaalimaa is about 1,000 vehicles. In Turku the traffic crossing the border is about 1,300 vehicles per day and in Helsinki about 1,400 vehicles per day. The corridor runs through three Finnish National Road Administration (Finnra) districts, each of which has its own weather and road surface condition monitoring center (RWMC), which in turn exchange information among themselves and with the national traffic information center in Helsinki. The regional RWMCs in Turku, Helsinki, and Kouvola serve the entire corridor. There are nine RWMCs in Finland in all. Several variable message signs warn of the slippery road conditions along the corridor. A 14-km motorway section on the eastern part of the corridor near Kotka has 36 automatic speed-limit signs, controlled by weather and road surface conditions, and 5 automatic information signs. Road weather stations and traffic monitoring stations are placed at 3- to 30-km intervals along the corridor, and weather monitoring centers have immediate access to these stations.

BACKGROUND

Finnra seeks to improve traffic flow and safety and increase driving comfort as much as possible. Environmental considerations are taken into account. Transport telematics is intended to increase the effectiveness of traffic control, traffic information, and winter maintenance.

Adverse weather conditions are a significant traffic safety problem in Finland. Almost half of winter accidents occur during bad weather or road conditions. Road users are not always aware of the road conditions and the risk of driving during wintertime. Road conditions quite often are estimated to be better than they really are. An increase in international traffic in Finland may increase the risk of accidents because foreign drivers may not be accustomed to the winter conditions on Finnish roads. Weather-related traffic management is one way to handle traffic safety problems and to improve traffic flow during adverse weather conditions.

Road transport telematic systems are becoming more common around the world and especially in Europe. In

Finland telematic solutions are used, for example, to decrease the negative effects of unexpected poor road conditions on traffic safety. The existing telematic infrastructure in Finland and especially on the E18 test area creates a firm base for new transport telematic applications. The data transmission networks are highly developed and reliable. The network of the global system for mobile communications (GSM) covers the entire 350-km-long road section. Finnish citizens are accustomed to using different types of modern telematic equipment to receive information.

The level of winter road maintenance will be improved in the Trans-European Road Network in Finland. One way to improve maintenance is preventive salting, which requires exact and real-time information on road surface conditions as well as good weather forecasts.

The need for several types of information for safe driving is increasing as is development of information processing systems. Automatic data collection and information processing will lead to automatic distribution of information to drivers. The road authorities must be ready for this development.

VISION FOR WEATHER-RELATED TRAFFIC MANAGEMENT

The E18 test area from Turku via Helsinki to Vaalimaa will provide the following features:

- Weather and road surface conditions, road surface friction, status of maintenance activities, and traffic information will be available continuously for the entire corridor.
- Forecasts of road conditions and traffic a few hours ahead will be possible.
- All information systems concerning the E18 road section will be compatible.
- Information from Sweden, Estonia, and Russia may be received before a driver crosses the border.
- Information about unexpected traffic situations will be available to road users via information systems.
- Speed limits will be controlled according to the road surface conditions and traffic.
- Locally situated variable information signs will be used whenever needed.
- Prevailing information media will be used effectively both before and during the trip.
- Elderly drivers will be considered in the planning of telematic applications.
- Some of the information may have a direct effect on vehicles.

In the future a uniform information service will be available in understandable form to drivers of any nationality in the E18 test area.

OBJECTIVES OF E18 TEST AREA

Telematic solutions are being tested and evaluated in the E18 test area. The goal is to improve traffic safety and flow, to improve driving comfort by means of traffic management, to supply information, and to provide more effective winter road maintenance. The project is running from 1995 to 1999. The E18 test area from Turku to Vaalimaa will be one part of the transport telematic corridor from Sweden via Finland to Russia. The main parts of the study being carried out on the E18 test area are as follows:

- Development of data collecting methods to a new level.
- Development of data handling that corresponds to the new data collecting methods.
- Development of information analysis and road-condition forecasting.
- Development of information distribution and automation of message generation to the road users' information systems.
- Evaluation of the system as a technical system and evaluation of the effects of the system on traffic.

DEVELOPMENT OF INFORMATION SYSTEMS

Current Systems

Finland has more than 200 road weather stations and about 200 traffic monitoring stations. Road weather monitoring video cameras complement the information received from road weather monitoring stations. Three weather radar serving the southern part of Finland are located in Turku and Helsinki and near Kouvola. The basic information of the road surface conditions and weather comes from the observation systems shown in Figure 1. The data are collected with the road weather information system. On the test area there are already 14 road weather and traffic monitoring stations and five video cameras.

Thermal mapping of the entire test road section was done during autumn 1995. Thermal mapping helps to situate the new monitoring stations at the right spots. Thermal mapping information also helps to widen the information of the local road weather monitoring stations to include the other sections of the road.

Planned Systems

Monitoring of weather and road conditions will be improved on the 60-km-long road section in the western part of the test area. Fifty to 60 new road surface condition
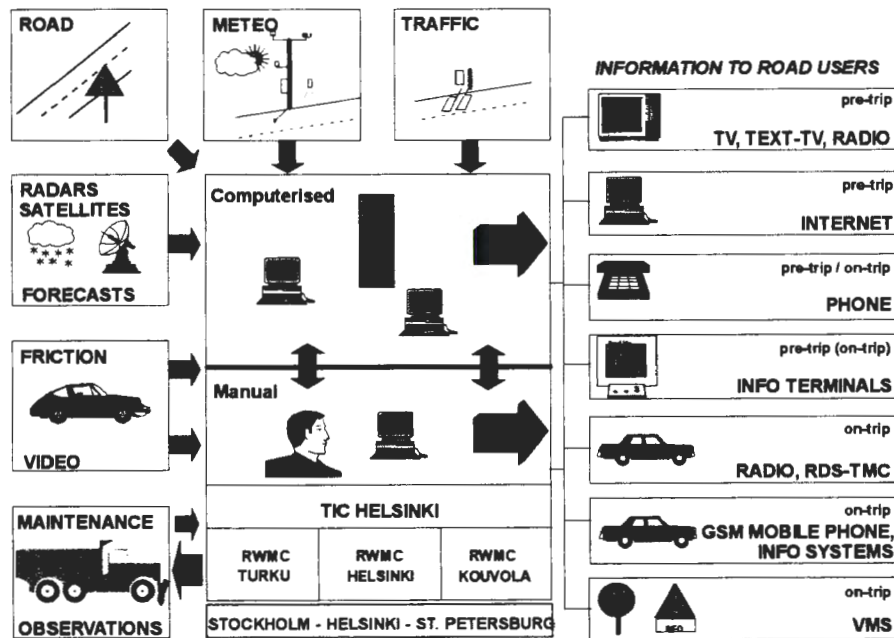
FIGURE 1   Schematic of information system.

measuring stations will be installed. Observations will be made at every kilometer on that road section. There will also be additional but fewer monitoring stations in the eastern part of the test section. The information gathered will be added to the road weather information system.

Still video pictures are transmitted from moving vehicles to the information system by the GSM-based transmitting methods. During the test, the cameras may be installed on buses driving along the test road section.

Road surface temperature and friction data will be collected by floating car sensors. The equipment that measures the friction will be installed at first on a test vehicle, but it is planned that the equipment also can be fitted to maintenance trucks and buses. Preventive salting will be made more effective with the longitudinal measurements of the road surface temperature and friction.

The maintenance activities will be stored in the new road condition information database. Every RWMC will keep the information in real time in the database so that the information may be used in all information centers whenever needed.

Data Handling Systems

Software applications of the information system will be made according to the European technical standards for telematic architecture. The information is bound to the place and to the coordinates. Data exchange among neighboring countries will be automated in part. A great deal of the information is stationary so that it may be updated by manual data transfer.

All the information (road surface condition, weather, traffic, maintenance, incidents, and so on) is recorded in the databases. The databases of each data collection system form a family of databases, and the user interface program collects all needed information from each database through the data management application. The user interface is based on the map interface called arcview. The information can be shown on the map base or in time series. Message management is used when the information must be sent quickly and directly to the road user, for example, slipperiness warnings via the radio data system–traffic message channel (RDS-TMC).

In the development of the forecasting model for road surface conditions, the prevailing methods are used in combination with new weather forecasting methods. It is important to define the responsibilities of the different road weather monitoring centers for feeding data to the systems. Within the test area are four information centers: Helsinki traffic information center, Turku RWMC, Uusimaa RWMC, and Kouvola RWMC.

Use of the Information

Road users can obtain information about prevailing road conditions, traffic, and so forth before and during their trips. Information is available via television, radio, Internet, RDS-TMC, in-vehicle information systems, telephone service, variable message signs, and infoterminals (at service stations and border stations). National

information networks like TELMO or Teletext provide access via television or modem to real-time weather data and forecasts.

The new data transfer techniques are being tested in the E18 telematics project. Data transfer from the floating cars to the road-user terminals via GSM techniques is a new way to transfer data. GSM is already a European standard and offers many possibilities for the development of different kinds of message exchange, such as short messages and cellular broadcasting.

Variable message signs are used to warn drivers about slippery road conditions, traffic congestion, incidents, maintenance activities, animals on the road, and other hazards. The automatic weather-related speed limit signs and information boards are being tested on the eastern test road section near Kotka. The posted speed limit varies automatically according to the road conditions and weather. During adverse weather conditions the speed limit is 80 km/h, and in good conditions it is 100 km/h during midwinter and 120 km/h in other seasons.

More accurate information about the road conditions is also transmitted to the road maintenance personnel to improve the maintenance work.

Conclusions

Greatly increased information on the E18 test area will be available to road maintenance personnel and road users within the next 2 years. Careful evaluations of the effects of the information will be done during the third year of the project. The main areas of the evaluation will be

- System functionality,
- Comparison of measurements from the local monitoring stations and floating cars,
- Road condition forecasting,
- Pre-trip and on-trip information to the road user,
- Effects on winter maintenance,
- Effects on traffic safety and fluency,
- Information or ergonomical aspects, and
- Economic aspects (cost-benefit analysis).

Although various road surface monitoring stations and sensors already exist, the reliability of the information must be examined and estimated. The need for more reliable information increases when the information is used to control the traffic signs, information boards, and various information delivery media.
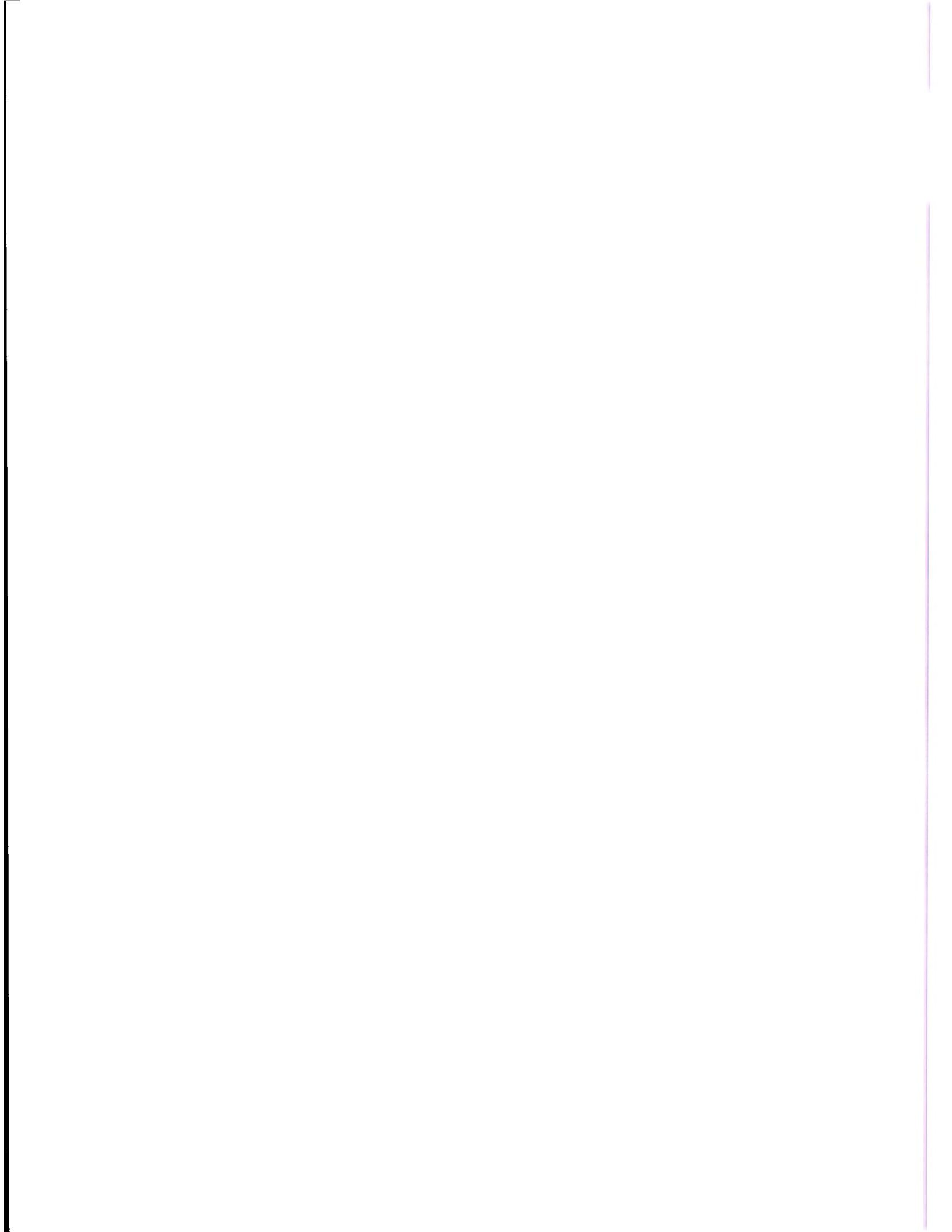
PART 2
INFRASTRUCTURE AND
SNOW CONTROL
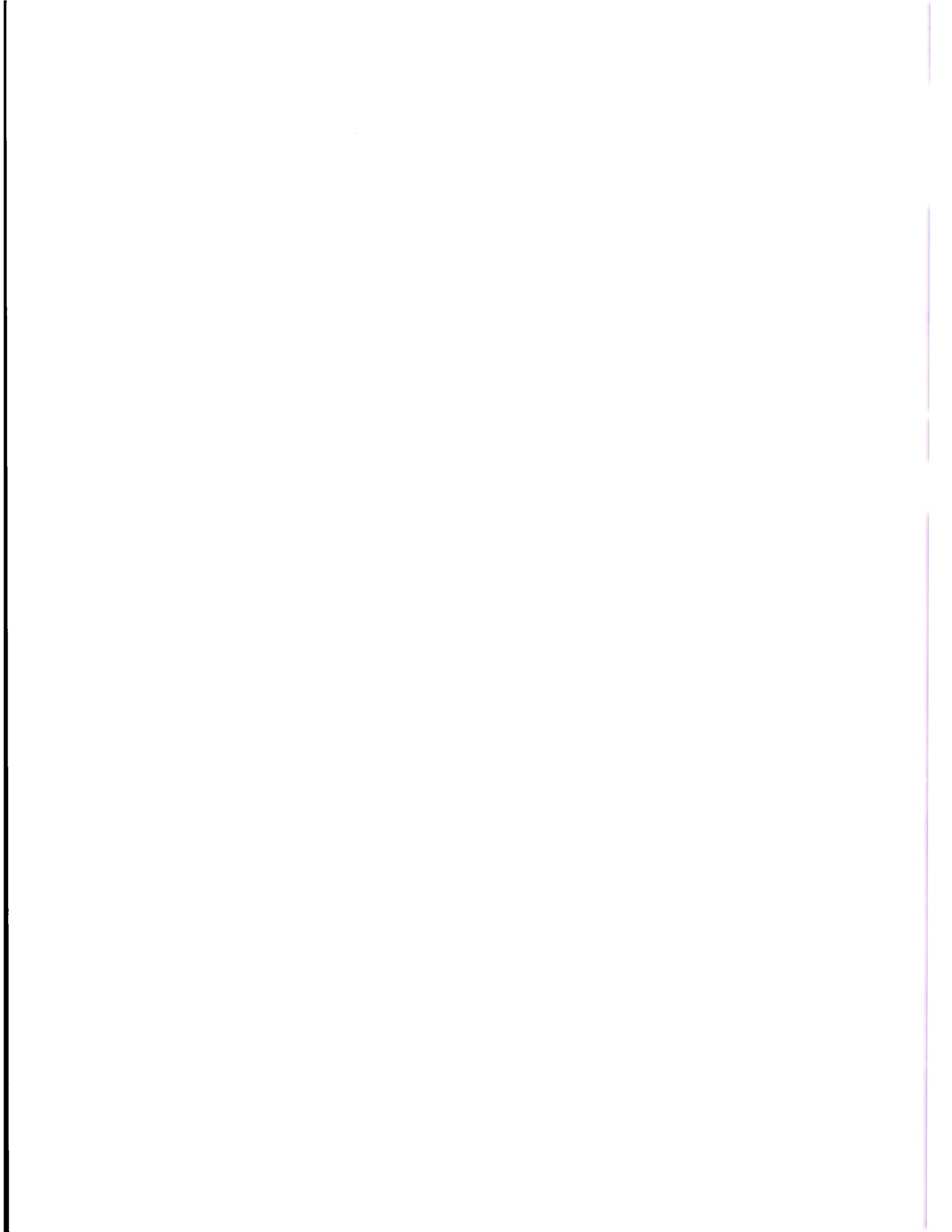
Model Experiment and Field Observation of a Snow Avalanche Deflector

Kazunori Fujisawa, *Public Works Research Institute,*
Ministry of Construction, Japan

A study of the jumping-up phenomenon that occurs when a snow avalanche strikes an inclined plane was carried out. The study is important to the design of avalanche deflectors and arrestors. The behavior of an avalanche colliding with a deflector was recorded at 4-sec intervals in the field, and jumping height and length were analyzed. The results of the analysis suggest that jumping-up velocity (V_a) is less than striking velocity (V_b) against a deflector. The velocity reduction coefficient (k) is defined as V_a/V_b, and physical significance is also considered. A model experiment, in which a snow avalanche struck an inclined plane, was examined to clarify the relationship between the velocity reduction coefficient (k) and the angle of incidence (ϕ). Jumping-up height and length of the full-scale avalanche that struck the deflector were explained by using the velocity reduction coefficient (k).

A deflector is a snow avalanche protection measure constructed to control moving avalanches to protect roads and the like from damage. It is assumed that snow avalanches jump upward when they strike deflectors, so it is possible to deflect an avalanche with a structure that is taller than the jumping height. For this reason, research to clarify the behavior of a snow avalanche striking a deflector will provide information of great value in the planning and design of deflectors.

CASE STUDY

A hamlet stands in the foothills of Mt. Gongendake in Maseguchi in the community of Nou in Niigata Prefec-

ture, Japan. On January 26, 1986, the hamlet was devastated by a surface-layer avalanche descending from the slope of Mt. Gongendake. Disaster protection facilities constructed to protect the village from future snow avalanches include deflectors at three sites located short distances from the slope. The Niigata Prefecture Erosion Control Section used a videotape system to observe snow avalanches occurring on the slope of Mt. Gongendake, and on February 26, 1992, it obtained a video record of a snow avalanche striking Deflector 1, the deflector installed closest to the slope.

The snow avalanche is clearly observed from 15:28:56, but it is impossible to clearly observe the jumping of the avalanche after 15:30:04. Because the video images were taken at 4-sec intervals, this period was covered by 18 frames. This snow avalanche is assumed to have been a surface-layer avalanche because the pictures obtained during and immediately before the avalanche do not show any accumulated snow sliding down the slope of Mt. Gongendake. It was a relatively large-scale and flowing avalanche, and weather information from a nearby meteorological observation station indicated that the temperature on the slope where the avalanche occurred was low up to that day.

Figure 1 is a time series display made by copying the boundary conditions of the avalanche from the video images. Because the avalanche furrow topography and the steep cliffs can be confirmed (in black, Figure 1) with reference to their locations, a time series display on a plane diagram of the location of the tip of the avalanche until it struck the deflector and of the boundary shape of the avalanche afterwards can be created (Figure 2). Because
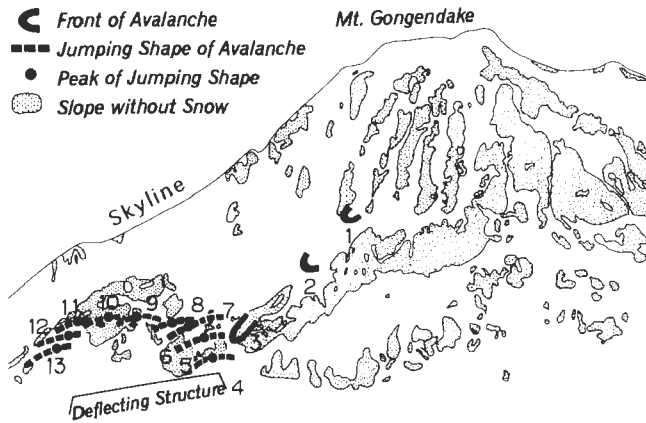
FIGURE 1 Time series diagram of snow avalanche behavior. Numbers indicate location of avalanche at 4-sec intervals.

the snow avalanche striking the deflector probably jumped in the length direction of the deflector along the deflector surface, the apparent jumping height of the avalanche can, with reference to the value of G in Figure 3, be found geometrically assuming that $H' = G + [C - (*)]$. (*) is the altitude at the location of $\bigcirc 4$, which is shown in Figure 2 and Table 1. To obtain the actual avalanche jumping height, it is necessary to deduct the snow depth from the apparent values obtained. The maximum apparent values from each frame were organized as H' in Table 1, and the locations
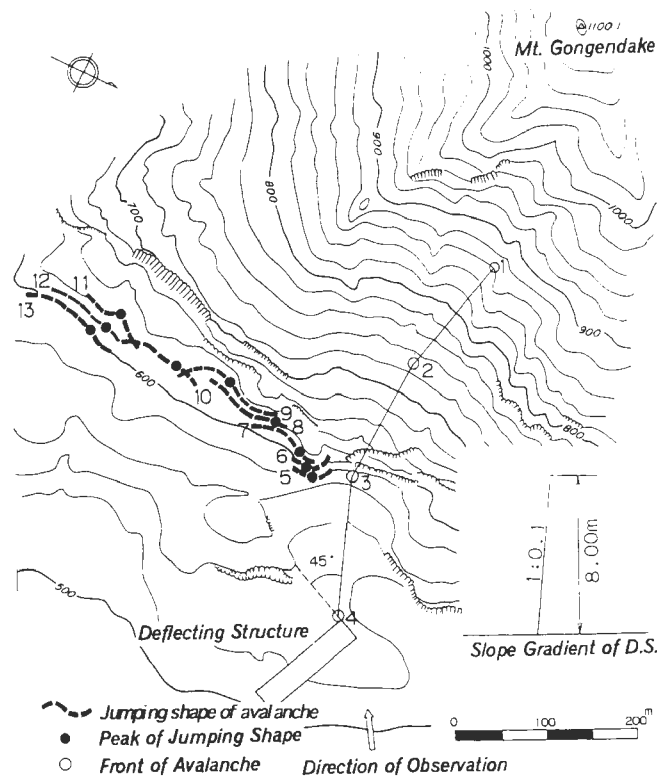
FIGURE 2 Plane diagram based on Figure 1.

at which they occurred are marked in Figure 1 and Figure 2 with black circles.

The maximum value of the apparent snow avalanche jumping height H' shown in Table 1 is 34 m, but because the interval between the images was 4 sec, it is assumed that the maximum value of H' is a little higher than 34 m. Although the accumulated snow depth around the deflector was not measured, the depth of the snow was probably very deep—probably greater than 2 m—because the depth of the snow around the spot where the video camera was installed was 2 m, and debris produced by snow avalanches descending from the slope of Mt. Gongendake was observed to pile up in front of the deflector, as it did every year. For these reasons, an estimate of the jumping height of an actual snow avalanche of about 30 m probably is close to the truth.

STUDY OF ENERGY DISSIPATION MECHANISM

The resistance to a snow avalanche is assumed to be the resistance generated by boundary friction and the resistance generated by internal friction. The resistance caused by the internal friction is assumed to consist of the resistance caused by contact between snow ice particles, the resistance produced by the turbulence of the air between the snow ice particles, and the resistance generated by the nonelastic collisions of snow ice particles. According to the particle flow resistance model (1), it is possible to represent the resistance stress caused by the internal friction (τ) as follows by using the contact resistance stress of the particles (τ_y), the turbulence resistance stress of the air (τ_f), and the impact resistance stress between the particles (τ_g).

$$\tau = \tau_y + \tau_f + \tau_g$$
$$\tau_y = \sigma_m \times \mu_k$$
$$\tau_f = \eta\left(\frac{du}{dy}\right) + \rho\ell^2 \left|\frac{du}{dy}\right|\left(\frac{du}{dy}\right)$$
$$\tau_g = \left(\frac{\pi}{12}\right)\sin^2 \alpha \left(1 - e^2\right)\sigma\left(\frac{1}{b}\right) D^2 \left(\frac{du}{dy}\right)^2$$

where

σ_m = vertical effective stress,
μ_k = kinematics friction coefficient,
η = coefficient of viscosity of the air,
ρ = density of the air,
ℓ = mixture length of the air based on the Prandtl,
du/dy = velocity gradient between particle rows,
α = striking angle of the particles,
e = reaction coefficient of the particles,
σ = concentration of the particles,
b = coefficient stipulating the particle interval, and
D = diameter of the particles.

$$F = (A-E) * D/B + E$$
$$G = F - C$$
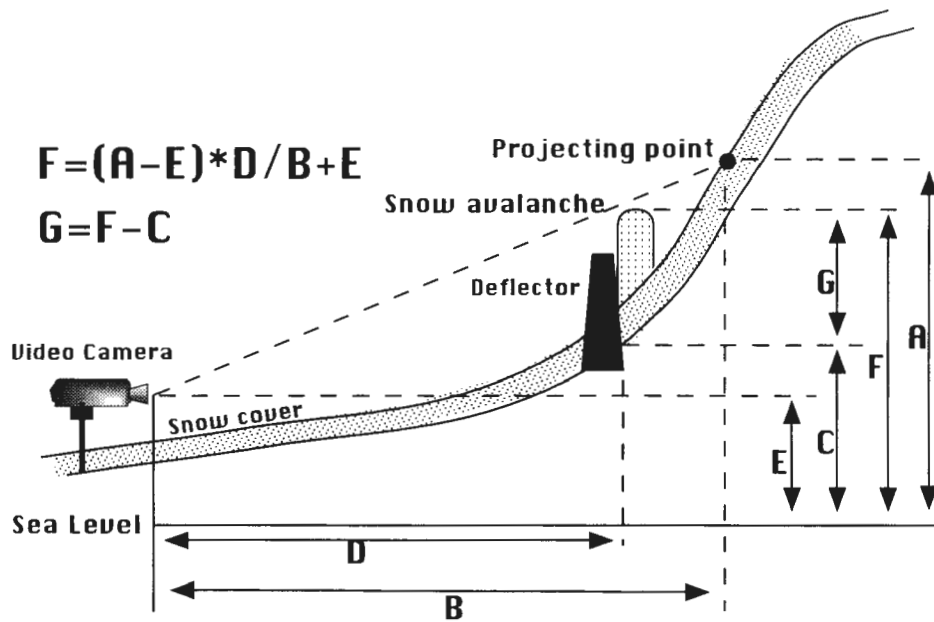
FIGURE 3   Geometric calculation for avalanche jumping height.

TABLE 1   Geometric Analysis of Avalanche Jumping Phenomenon in Collision with Deflector 1

No.	Time	A(m)	B(m)	C(m)	D(m)	E(m)	F(m)	G(m)	A.J.H. H'(m)	H.D. (m)	J.L. L(m)
1	15:28:56					281					
2	15:29:00	B.C.	B.C.	B.C.	B.C.	281	B.C.	B.C.	B.C.	138(35)	B.C.
3	15:29:04					281				134(34)	
4	15:29:08	U.K.	U.K.	530(*)	1238	281	U.K.	U.K.	U.K.	166(42)	U.K.
5	15:29:12	580	1396	530	1236	281	546	16	16	7	7
6	15:29:16	590	1406	530	1234	281	552	22	22	5	12
7	15:29:20	600	1426	530	1232	281	557	27	27	5	17
8	15:29:24	620	1460	530	1220	281	564	34	34	21	38
9	15:29:28	630	1510	518	1202	281	559	41	29	39	77
10	15:29:32	630	1540	507	1180	281	548	41	18	46	123
11	15:29:36	620	1610	494	1160	281	525	31	- 5	37	160
12	15:29:40	610	1600	480	1156	281	519	39	- 11	16	176
13	15:29:44	610	1600	474	1152	281	518	44	- 12	14	190

A.J.H.; Appeared Jumping Heights   B.C. ;   Before Collision
H.D. ;   Horizontal Distances   U.K. ;   Unknown
J.L. ;   Jumping Lengths

In the case of a snow avalanche that strikes a snow avalanche deflector, when the direction of the motion of a snow avalanche changes, the effect of inertial force is added to τ_y. It is forecast that at the same time as the turbulence of the flow increases and the mixture distance of the air increases, both the striking velocity between the particles, which governs τ_g, and the striking frequency rise. Because this means that the resistance of τ_y, τ_f, and τ_g increases, the velocity of the avalanche after it strikes the deflector is less than its striking velocity. If the striking velocity is V_b and the velocity after striking is V_a, then $V_a/V_b = k$ is defined as the velocity reduction coefficient. The value of k plays an important role in governing the jumping of an avalanche. But as this study has revealed, because the velocity reduction caused by the striking occurs during a period from the beginning of the impact at the particle level to the point where the direction of the motion has completely changed, the values of V_a and k are not defined at the striking point. Finding this value of k analytically is difficult, so it is estimated from snow ice particle striking experiments.

Study of Motion of Mass Points Striking a Plane

As shown in Figure 4, four angles based on the collision of mass points with a plane are defined. Considering the motion of an avalanche striking the deflector surface (Surface B) in the direction from I to O along the plane of incidence of the snow avalanche (Surface A), the angle of incidence of the snow avalanche that strikes Surface B (ϕ) and the run-up angle to Surface B (ψ) can be represented by using θ and β.

$$\phi = \sin^{-1}(\sin\theta \cdot \sin\beta) \tag{1}$$

$$\psi = \cos^{-1}\frac{\cos\theta}{\cos[\sin^{-1}(\sin\theta \cdot \sin\beta)]} \tag{2}$$

If the vertical Surface C is introduced to Surface B, which includes the incidence line, and the position of IV is set such that $\angle$ I,IV,O = 90°, the straight line I,IV is the normal line of Surface B and $\angle$ I,IV,III = 90° is established at the same time. And if the position of III is set such that $\angle$ O,III,IV = 90°, the straight line O,III is the normal line of the plane I,III,IV, and $\angle$ O,III,I = 90° is established at the same time. It is possible for this formula to be derived from the relationship of the edge and the angle of the tetrahedron O,I,III,IV. However, if $\theta = \beta = 90°$, ψ cannot be assessed.
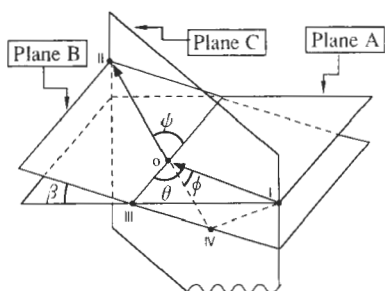
Because the angle of incidence (ϕ) is a key factor governing the velocity reduction coefficient, it can now be understood that to estimate the value of k, it is necessary to perform an experiment in which the angle of incidence is varied. The simplest method for performing a striking experiment in which the angle of incidence is varied is shown in Figure 4: $\theta = \beta = 90°$, and Surface A is horizontal, where $\beta = \phi$ is established simultaneously. This permits the jumping height of an avalanche to be represented as follows from a model of a body that moves on a plane under the effects of bottom surface friction and the resistance of gravity. However, μ is the kinematics friction coefficient of the deflector surface and the snow avalanche.

$$H = \frac{(kV_b)^2 \sin\phi}{2g(\sin\phi + \mu\cos\phi)} \tag{3}$$

Experimental Assessment of Velocity Reduction Coefficient

A horizontal flow of a collection of small snow ice particles was caused to strike a plane, $\theta = 90°$, at varying angles of incidence (ϕ) to measure the striking velocity (V_b) and the run-up height on the plane. The model avalanches flowed down a chute with a length of 3 m and a width of 40 cm. A horizontal table surface was connected to the chute at its bottom end and the model was installed on a table (Figure 5). The velocity of the avalanche when it collided with the model could be varied from 3 to 6 m/sec by varying the gradient of the chute. The model was made of FRP resin panels with a length of 1 m and a width of 2 m. The collision angle θ of the avalanche and the slope gradient β of the collision surface were varied by changing the incline and direction of the panels of the model. A mesh with sides 5×5 cm was drawn on the resin panels to measure the behavior of the avalanche. The samples used for the experiment were ice particles with a central grain size of about 1 mm and accumulation density between 0.4 and 0.5 (g/cm^3) prepared by pulverizing ice in a laboratory at a temperature of −10°C. The avalanche collision velocity was found by installing two beam sensors near the bottom of the chute and calculating the velocity from the time gap between two measured points and the distance between the two points.

FIGURE 4 Illustration accounting for angle of incidence ϕ, jumping angle ψ, deflecting angle θ, and slope gradient β.
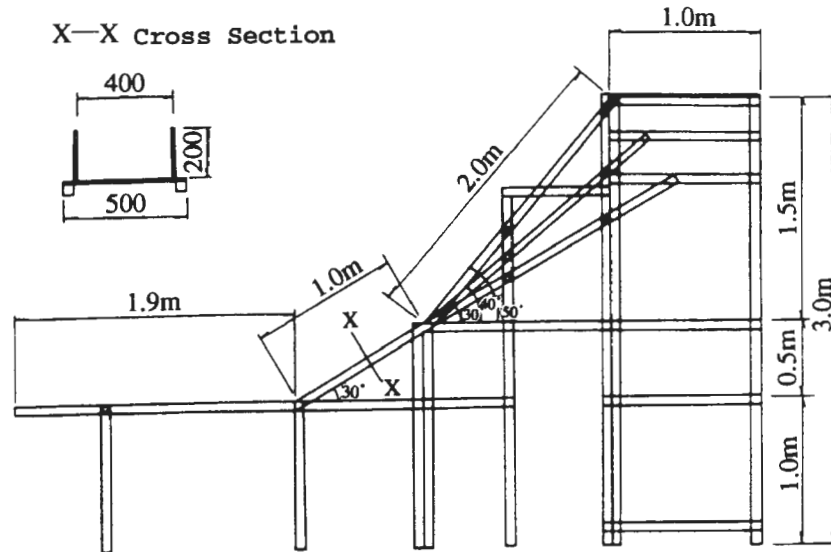
FIGURE 5   Model avalanche chute.

The behavior of a snow avalanche striking a plane varies according to the angle of incidence (φ). When φ is 45° or 60°, the snow avalanche moves in such a way that it runs up the deflector plane; then, as time passes, the width of the snow avalanche gradually increases. When the angle of incidence is 90°, the snow avalanche not only jumps up along the surface of the deflector when it strikes the surface, but it also sprays to the left and right, forming an expanding semicircle. Part of the tip of the snow avalanche consists of particles that collide with the deflector surface and then bounce back, but this is a temporary condition not repeated by the following snow, and the height at which the snow jumps backward is lower than the height it jumps up. To use Equation 3 to estimate k, it is necessary to set the value of k. Figure 6 is a schematic diagram of the test apparatus used to find the kinematics friction coefficient of the plane and the snow ice particles. As the cart was pulled at a fixed velocity by a motor, the tension of the rope connecting a sampler filled with snow ice particles mounted on top of the cart to the wall was recorded. The recorded data indicate that when the cart was pulled by the motor, breaking the adhesion of the snow ice particles to the deflector surface required large initial force, but that after that stage the force remained

almost constant. The experiment was conducted with the sampler filled with snow ice particles and with an empty sampler. When the results for the snow ice particles and for the sampler are represented by the subscripts $_0$ and $_1$ respectively, the results are as follows: from $F_0 = \mu_0 N_0$, $F_1 = \mu_1 N_1$, $F_{0+1} = F_0 + F_1$ to $\mu_0 = (F_{0+1} - F_1)/N_0 = 0.23$. ($F$, μ, and N represent the friction force, kinematics friction coefficient, and vertical effectiveness, respectively.)

Figure 7 shows the relationship of the calculated values obtained by using Equation 3, ignoring k, with the measured snow avalanche jumping height values, revealing that the value of k is found from the inclination of the regression straight line. Figure 8 shows the results of an organization of the relations of the angles of incidence (φ) with the estimated velocity reduction coefficient (k). But φ is represented as degree.

FIGURE 6   Schematic illustration of kinematic friction test.
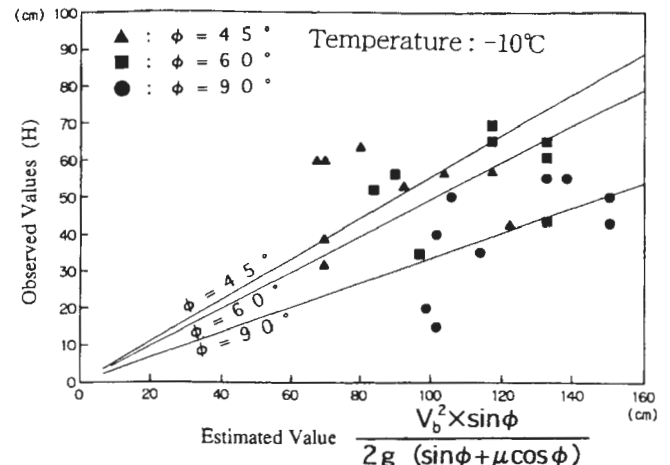
FIGURE 7   Comparison of measured jumping height values and calculated jumping height values.
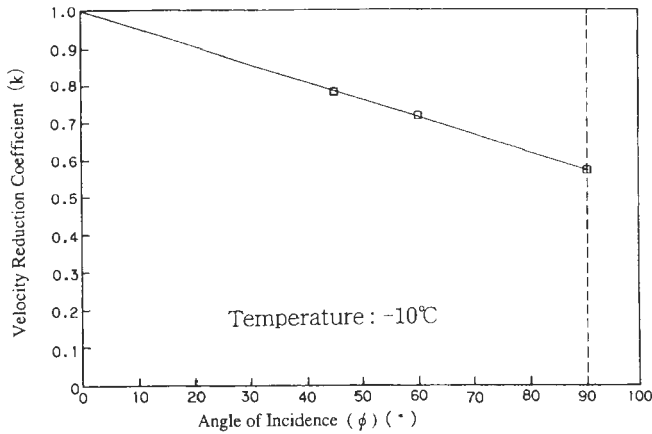
FIGURE 8 Relationship between velocity reduction coefficient and angle of incidence.

$$k = 1 - 4.7 \times 10^{-3} \cdot \phi \tag{4}$$

STUDY OF RUN-UP ANGLE OF AN AVALANCHE STRIKING A PLANE

The organization of all the preceding results should permit a description of the avalanche after striking as the motion of an object with the initial conditions run-up velocity kV_b and run-up angle ψ. But in a case in which $\theta = \beta = 90°$, although it was impossible to assess the run-up angle (ψ) by using a motion model of mass points as explained previously, during the experiment the run-up of the snow avalanche could be observed. This suggests differences between the striking phenomenon of mass points on a plane and a flow of concentrated snow ice particles. It can be assumed that the flow of concentrated snow ice particles not only strikes the plane but also influences the run-up angle of the snow avalanche through the collisions between the particles.

When the experiment was performed with the inclination of the deflector surface (β) held constant at 90° and the deflector angle (θ) varied, as shown in Figure 9, several lines were formed on the surface of the snow ice particles that ran up the deflector surface, indicating the course of the motion. Observation of the run-up angle to the surface of the deflector from the course of the motion of the group of particles with the maximum run-up height revealed that this value is the deflector angle (θ). Figure 9 is a schematic diagram of the behavior of an avalanche striking a deflector in a case in which $\beta = 90°$ and $\theta = 60°$. The avalanche that struck the deflector ran up along the surface of the deflector at various run-up angles and formed a fan-shaped front pointed in the deflector direction. As the top of this front flowed in the deflector direction, it separated from the surface of the deflector and fell to rest in front of the deflector. This behavior was observed not only at the front; it continued throughout the entire flow. This reveals that it is not possible to represent the run-up angle when a flow of concentrated particles strikes a plane as a constant value.

When a flow of concentrated particles such as a snow avalanche strikes a plane, the form of motion usually observed after the impact is the particles spreading in the lateral direction. The lateral expansion of the particles is caused by collisions between the particles, and this influences the run-up velocity and run-up angle of the particles. In the case of particles moving from A toward and striking Plane B at angle of incidence ϕ, as shown in Figure 10, flow direction OB after the impact changes only γ degrees to become motion from O toward C. In Plane ABOD, if ψ is defined as the angle of incidence of Plane AOC at right angles to Plane B, ψ can be written as follows:

$$\Phi = \cos^{-1}(\cos\gamma \cdot \cos\phi) \tag{5}$$

If the angle γ is defined in the counterclockwise direction, the run-up angle and the velocity reduction coefficient are corrected as shown, with reference to Equations 2 and 4:

$$\Psi = \psi + \gamma \tag{6}$$

$$K = 1 - 4.7 \times 10^{-3}\Phi \tag{7}$$
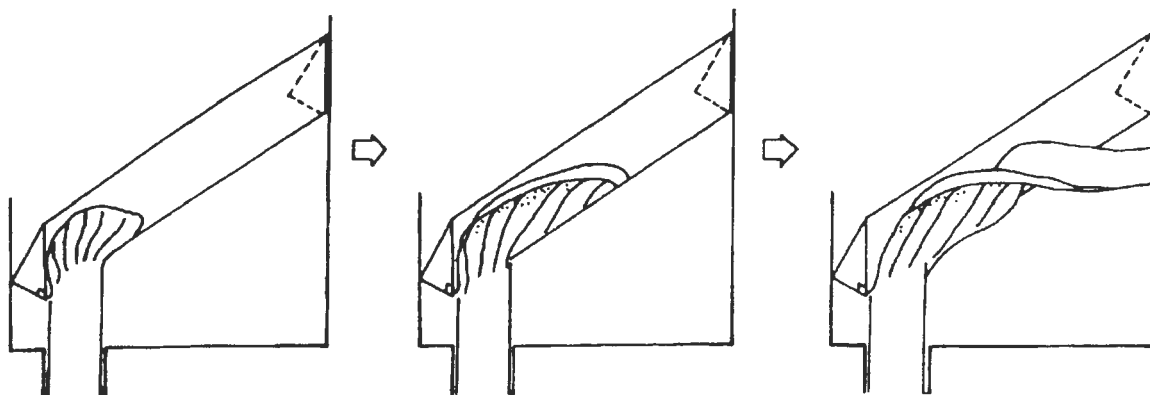
FIGURE 9 Schematic diagram of behavior of snow avalanche striking deflector.
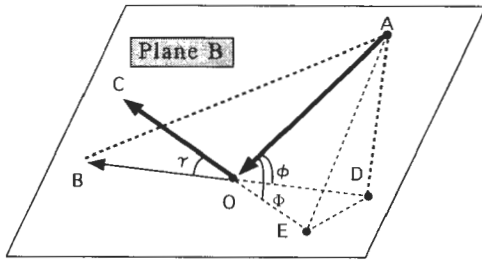
FIGURE 10   Illustration accounting for lateral spread and angles ϕ, Φ, and γ.

FIGURE 11   Definition of symbols used in analysis.

Representing the run-up angle and the run-up velocity as the function of the angle γ provides the grounds for the explanation of the behavior (the formation of a fan-shaped front with a tip in the downstream direction as shown in Figure 1 and Figure 9) of a snow avalanche striking a deflector.

The jumping height of the snow avalanche striking Deflector 1 is about 30 m. The height of the action of the friction on the deflector surface is equal to the height of the deflector above the snow, and on the basis of the snow accumulation environment around the deflector as described earlier, the snow depth is estimated to be about 4 m. For these reasons, it is assumed that the jumping height would differ little even if the resistance caused by the friction were ignored. The free motion of an object thrown into the air can be represented as shown in the following and in the coordinate system shown in Figure 11.

$$\frac{dy}{dt} = KV_b \sin \Psi - g \sin \beta \cdot t \tag{8}$$

$$\frac{dx}{dt} = KV_b \cos \Psi \tag{9}$$

Accordingly, H_1 and L_1 are as follows.

$$H_1 = \left(KV_b \sin \Psi\right)^2 / 2g \sin \beta \tag{10}$$

$$L_1 = \left(KV_b\right)^2 \sin \Psi \cos \Psi / g \sin \beta \tag{11}$$

Conditions when the snow avalanche struck Deflector 1 were the following: V_b was 42 m/sec, θ was 45°, β was 84.3°, and the $H_1 - \gamma$ relationship was as shown in Figure 12. The calculated value of γ, which provides the highest value of H_1, is 68°, and $H = H_1 \sin \beta = 35$ m. This result is a little larger than the observed jumping
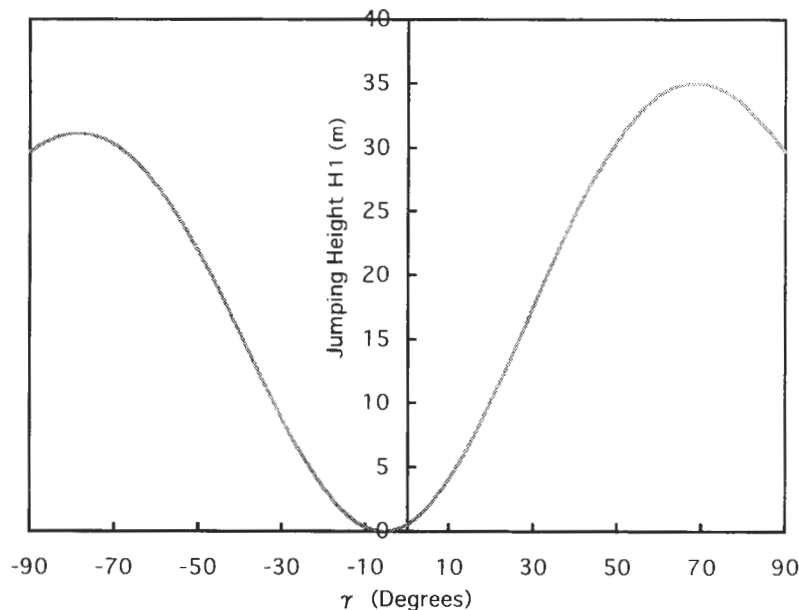
FIGURE 12   Jumping height variations with angle γ.

height of 30 m. The angle at which this avalanche actually ran up the deflector cannot be confirmed because the deflector itself hid the motion, and because only one videotape frame was obtained every 4 sec. Also, the value of L_1 was calculated as 21 m, which is smaller than the jumping length shown in Table 1 (L is 38 m to 77 m). Because the interval between video images was 4 sec, it was impossible to specify the location indicating the maximum jumping height, and because the width of the snow avalanche that jumped was 10 or greater when it struck Deflector 1, it is impossible to conclude that the calculated jumping length was short. At this stage, it would be difficult to verify any more than this; new data are needed.

SUMMARY AND FUTURE CHALLENGES

This paper describes the jumping of snow avalanches incorporating the velocity reduction coefficient based on the velocity reduction mechanism and run-up angle of an avalanche striking a plane. An attempt was made to use a single case study to confirm the height and length of the jumping of an avalanche, but because the results were incomplete, more research is necessary.

When a design intended to deal with a high-speed avalanche is planned, it will be difficult to consider realistically a deflector that can handle the jumping height of the avalanche, and the height of the deflector designed will be too small. Accordingly, the shape and height of the deflector surface and its deflector effects must be confirmed. Because it is impossible to ignore the effects of the deposited snow, such as snow blown against the deflector on the effective height of the deflector surface (height above the snow), research on a transparent deflector surface should be performed.

REFERENCE

1. Kitahara, I., H. Yoshimatsu, and K. Fujisawa. Study of the Mechanics of Debris Flow and Its Simulation Model. *Landslide—Journal of Japan Landslide Society*, Vol. 28, No. 2, Sept. 1991, pp. 9–19.

Cost-Benefit Analysis of Snow-Removing Channels in an Urban Area with Heavy Snowfall

Kazuyuki Morohashi, *Foundation System Research and Development Institute of Japan*
Teruyoshi Umemura, *Department of Mechanical Engineering, Nagaoka University of Technology, Japan*

In an urban area with heavy snowfall, such as the northwest coast of Japan bordering the Japan Sea, snow often becomes a serious obstacle. Therefore, advanced means of snow removal, such as a snow-removing channel, are required. The snow-removing channel, an open channel constructed on the shoulder of a road to provide water flow, can remove a large amount of snow quickly. However, because of the high construction costs, a benefit-cost analysis of the snow-removing channel is conducted to help determine whether a channel should be constructed. A method for estimating benefits of the snow-removing channel is proposed. The benefits are considered to consist of reduction of snow damage and snow removal costs. The reduction of snow damage costs is calculated from land value of and expenses incurred for the closed area that would be opened through the introduction of the channel. The reduction of snow removal costs is calculated from the costs of snow removal equipment. The present method is applied to the snow-removing channel system in the central area of Tokamachi City, Japan, which is about 1.9 km² and has a population of 15,000. The average annual maximum snow depth is 2.5 m. The total length of the channel is 43.2 km and water at the rate of 2.1 m³/sec is pumped up from rivers to remove snow. The calculated benefits of the snow-removing channel system vary, equaling 84, 294, 394, and 516 million yen a year according to the annual maximum snow depth of 1.45 m (1991), 2.26 m (1994), 3.28 m (1985), and 3.67 m (1983), respectively. In addition, the benefit-cost ratios are given as 0.31, 1.10, 1.46, and 1.89, respectively. It is concluded that this system is economically effective when the annual amount of snowfall is more than the average.

In an urban area with heavy snowfall, the development of modern automotive society and the resulting change in lifestyle have caused residents serious snow problems. Residents cannot maintain their urban life without snow removal, and advanced means of snow removal are required.

A snow-removing channel, an open channel with water flow that is usually constructed on the shoulder of a road, is one method of effective snow removal. Residents throw the snow that has fallen on roofs, in yards, and on roads into the channel to create more open space and to keep roads clear for transportation. However, the construction costs for the snow-removing channel are fairly high, making the decision to build difficult for the local government. The decision to construct could be made effectively if the economic benefits of the channel were known. As yet such an evaluation has not been conducted.

The amount of snow damage in an urban area with heavy snowfall was defined and calculated (1), which makes possible the evaluation of the benefits of a snow-removing channel. The present study applies the evaluation method to the urban area of Tokamachi City, Japan, where a system of snow-removing channels is being constructed. The annual benefits and costs of the system are calculated and the system's economic effectiveness is evaluated from benefit-cost ratios.

METHOD OF BENEFIT-COST ANALYSIS

To evaluate economic effectiveness of a snow-removing channel in a given place, snow damage and snow removal costs before and after the introduction of the channel are compared. Assume that the snow removal cost is C_1 and the amount of snow damage is D_1 before the introduction of a snow-removing channel and C_2 and D_2 after the introduction, as shown in Figure 1. C_2 includes the cost of the snow-removing channel, C, and ΔC_1 in Figure 1 indicates the reduction of C_1 by introducing the snow-removing channel.

The economic effectiveness of the channel can be judged by comparing $C_1 + D_1$ and $C_2 + D_2$. Specifically, the snow-removing channel is considered to be economically effective if

$$C_1 + D_1 > C_2 + D_2 \tag{1}$$

Because C_2 equals $C_1 - \Delta C_1 + C$, as shown in Figure 1, Equation 1 is written as

$$\left(D_1 - D_2\right) + \Delta C_1 > C \tag{2}$$

Let the left side of Equation 2 be defined as the benefit of the snow-removing channel, B, which consists of the benefit $B_1 = D_1 - D_2$ and benefit $B_2 = \Delta C_1$. Both B and C are evaluated in annual amounts and the degree of economic effectiveness is expressed by benefit-cost ratio B/C.

Benefit B_1

By means of the method proposed by Umemura et al. (1), the annual amount of snow damage, D, in a given place is expressed as

$$D = \bar{k}(rL + F)A \tag{3}$$

Before Introduction   After Introduction

SNOW DAMAGE D_1 D_2

SNOW REMOVAL COSTS C_1 ΔC_1 C C_2

Cost of Snow Removing Channel
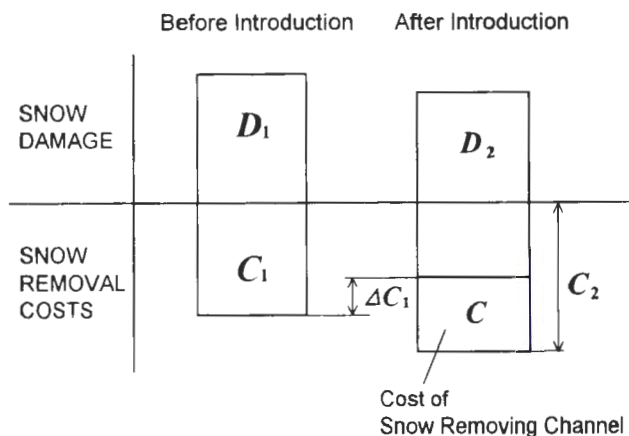
FIGURE 1   Economic effects of snow-removing channel.

where

    $\bar{k}$ = annual mean seasonal drop factor in utilization,
    r = annual rate of interest,
    L = land value of a unit area,
    F = annual expense of a unit area for facilities at the location, and
    A = area of the location (m^2).

$\bar{k}$ means $\Sigma\, k/365$ where k is the daily seasonal drop factor in utilization and $\Sigma\, k$ is the annual sum of k. Here k is 0 if the location can be used completely in a snowy season as well as a nonsnowy season and k is 1 if the location cannot be used at all in a snowy season because of snow cover. k has a value between 0 and 1 if the place is partly used in a snowy season. Thus $\bar{k}$ is given as

$$\bar{k} = \frac{R \cdot N}{365} \tag{4}$$

where R is the average value of snow-covered area/given place area for N days, and N is the number of snow cover days given by the local meteorological observatory. Because the snow damage D_1 and D_2 in Figure 1 are expressed as $\bar{k}_1(rL + F)A$ and $\bar{k}_2(rL + F)A$ from Equation 3, the benefit B_1 can be expressed as

$$\begin{aligned} B_1 = D_1 - D_2 &= \left(\bar{k}_1 - \bar{k}_2\right)\left(rL + F\right)A \\ &= \frac{\left(R_1 - R_2\right)N}{365}\left(rL + F\right)A \end{aligned} \tag{5}$$

Benefit B_2

Benefit B_2, the reduction of C_1 through introduction of the snow-removing channel, is mainly brought about by the decreased need for trucks for snow disposal. Thus let B_2 be evaluated as

$$B_2 = C_T \cdot W \cdot A \tag{6}$$

where

    C_T = cost of transportation work by trucks for 1 ton of transported snow,
    W = annual amount of transported snow in a unit area of A', and
    A' = snow-covered area where snow removal by trucks is to be replaced by the snow-removing channel.

SNOW-REMOVING CHANNEL SYSTEM IN TOKAMACHI CITY

This method is applied to the snow-removing channel system in Tokamachi City, which is being constructed in

TABLE 1 Specifications for Snow-Removing Channel System

Total channel length	43.2	km
Pipeline length	6.76	km
Channel width	0.5	m
Channel depth	over 0.5	m
Water flow depth	0.2	m
Water resource from rivers	2.1	m³/sec

the urban area of 1.9 km² where 15,000 residents live. This city has a heavy amount of snowfall; the average annual maximum snow depth is 2.5 m and the greatest depth on record is 4.25 m.

Table 1 shows the specifications for the snow-removing channel system. The system consists of open channels, pipelines, and pumps for water supply. Water at the rate of 2.1 m³/sec is pumped up from two rivers for 11 hr/day and distributed to each channel route according to the timetable.

Snow Removal Area

Only residents of houses near snow-removing channels, in general, use the channels to remove the snow from the roads, sidewalks, and housing sites around them. Therefore, the snow removal area that benefits from the snow-removing channel system can be divided into three parts: roads, sidewalks, and housing sites. In cases in which channels are constructed on both sides of the road, the area from the center of the road to the back of the housing site, which has a depth of 20 m, is the snow removal area, as shown at A in Figure 2. In cases in which channels are constructed on one side of the road, the area between the back lines of housing sites on either side of the channel, each with a depth of 20 m, is the snow removal area, as shown at B in Figure 2.

The benefits of the system depend on the snow removal area and its means of snow removal. Therefore, in the snow removal area, the benefits are evaluated on six items: (a) roads cleared by snow removal machines, (b) roads with snow-melting pipes, (c) sidewalks cleared by snow removal machines, (d) sidewalks with arcades, (e) housing sites with snow transportation demand (e.g., where houses require roof snow removal and the spaces around the houses are not large enough), and (f) housing sites without snow transportation demand (e.g., hous-
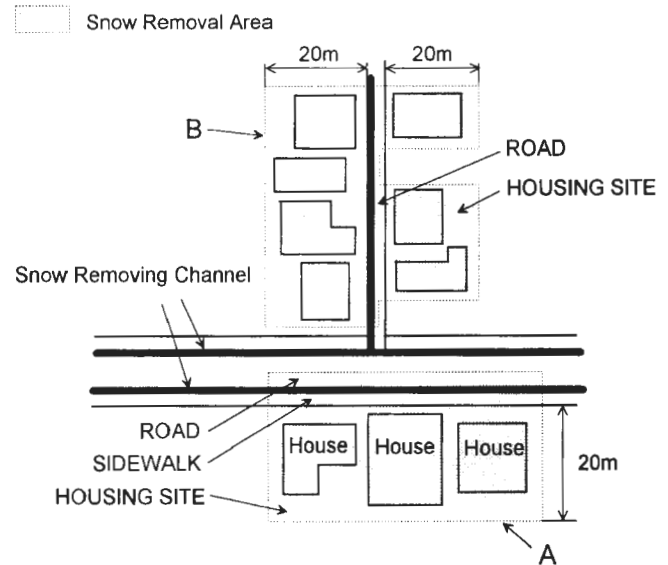
FIGURE 2 Snow removal area of channel system.

where houses have the equipment for melting the roof snow). Equations 5 and 6 are applied to each item to evaluate the benefits of B_1 and B_2, respectively.

Evaluation of Benefit B_1

Table 2 shows the values of R_1, R_2, and A in Equation 5 for each item. In roads cleared by snow removal machines, R_1 is estimated to be 0.16, taking into consideration that the road shoulder, about 16 percent of the road area, is partly covered with snow. R_2 is 0 on the assumption that all the snow on the shoulder is thrown into the channels after the introduction of the system. In roads with snow-melting pipes and sidewalks with arcades, both R_1 and R_2 are 0 because there is almost no snow cover. In sidewalks cleared by snow removal machines, R_1 is estimated to be 0.39, taking into consideration that about 39 percent of the sidewalk area is covered with snow, and R_2 is 0 on the assumption that all the remaining snow on the sidewalk is thrown into the channels after their introduction. In housing sites, R_1 is 0.34 and R_2 is 0.28, reflecting the results of a questionnaire administered to the residents of Tokamachi City.

TABLE 2 Values for Benefits Evaluation

Item in Snow Removal Area	R_1	R_2	A (m²)	A' (m²)
Roads by snow removal machines	0.16	0	72,980	21,890
Roads with snow melting pipes	0	0	25,930	0
Sidewalks by snow removal machines	0.39	0	6,700	3,590
Sidewalks with arcades	0	0	6,580	6,580
Housing Sites with snow transportation demand	0.34	0.28	400,990	400,990
Housing Sites without snow transportation demand	0.34	0.28	139,360	0

Moreover, r of 0.06 in Equation 5 is given as the typical rate of interest used in the previous study (1), and L for each item is taken from the street values in the snow removal area. F in Equation 5 is 2,460 yen/m^2 on roads and sidewalks, calculated from the recent records of the costs for road construction and maintenance in Tokamachi City. On the other hand, F on housing sites is negligible.

Evaluation of Benefit B_2

C_T in Equation 6 is 1,063 yen/ton, which is calculated from the snow removal records in Tokamachi City, where snow rotary plows and dump trucks (11-ton capacity) have been utilized for snow transportation.

A' for each item is shown in Table 2. On roads cleared by snow removal machines, A' is the area of the shoulder, which is 30 percent of A. On roads with snow-melting pipes, A' is 0 because the snow transportation works are not needed. In sidewalks cleared by snow removal machines, A' is the area 1.2 m wide and 2992 m long where snow is removed by small rotary plows. In sidewalks with arcades, A' is the roof area of arcades, which is equal to A. In housing sites with snow transportation demand, A' equals A, and in housing sites without snow transportation demand, A' equals 0.

W in Equation 6 on each item is calculated through computer simulation by using the models shown in Figures 3 through 6. These models simulate the distribution of removed snow by using the daily observed snow cover data in Tokamachi City. In these models, W is calculated as the sum of the daily amount of transported snow that cannot be displaced and then transported.

Figure 3 is the model of roads cleared by snow removal machines. When the depth of snow on the roadway reaches 10 cm (density of 100 kg/m^3), it is moved to the shoulder by a tractor with a blade plow. When the snow depth reaches 1.1 m (density of 300 kg/m^3), the limit to displace snow by the tractor with a blade plow, the snow on the shoulder is loaded by a snow rotary plow onto a dump truck and transported. The shoulder width is 30 percent of the road width.

FIGURE 4   Model of sidewalks cleared by snow removal machines.

Figure 4 is the model of sidewalks cleared by snow removal machines. When the depth of snow cover on the sidewalk reaches 15 cm (density of 100 kg/m^3), the snow on the 1.2 m width in the sidewalk is moved to the shoulder by a small rotary plow. When the depth of snow on the shoulder reaches 1.1 m, it is transported in the same manner as in the model of roads cleared by snow removal machines.

Figure 5 is the model of sidewalks with arcades. When the roof snow depth on the arcade reaches 1 m (density of 200 kg/m^3), it is manually thrown down to the shoulder and transported immediately by a rotary plow and dump truck.

Figure 6 is the model of housing sites with snow transportation demand. When the roof snow depth on the house reaches 1 m (density of 200 kg/m^3), it is manually thrown down to the ground around the house. When this snow depth exceeds 2.5 m (density of 350 kg/m^3), the excess is transported so that it does not touch the eaves of the house.

COSTS AND ANALYSIS

The annual cost of the system, C, consists of construction costs, maintenance costs, and running costs. The construction cost is 243 million yen a year, which is determined by the evaluated cost of the total construction, 4,860 million yen, divided by an assumed life span of 20 years. The maintenance cost is 5 million yen a year, obtained from the recent records in Tokamachi City. The running cost, annual electricity charges for the pumps, is

FIGURE 3   Model of roads cleared by snow removal machines.
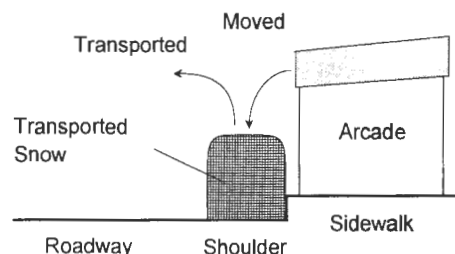
FIGURE 5   Model of sidewalks with arcades.
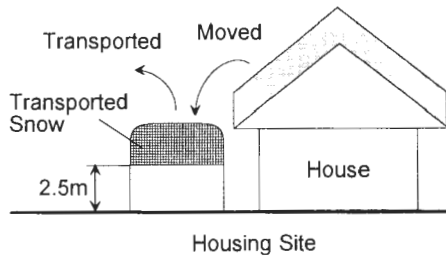
FIGURE 6 Model of housing sites with snow transportation demand.

FIGURE 7 Benefit and cost of system versus annual maximum snow depth.

evaluated at $5 + 0.12N$ million yen a year, assuming that the pumps are operated 11 hr/day for snow cover days N. The sum of those costs, C, is calculated as

$$C = 253 + 0.12N \quad (\text{million yen}) \tag{7}$$

By using the snowfall and snow depth data for 20 years, from 1975 through 1994, the benefits, costs, and benefit-cost ratios of the snow-removing channel system in Tokamachi City are calculated as shown in Table 3. The total benefit divided by the total cost for the 20 years is 0.85, proving that this system is not economically effective. However, the economic effectiveness depends on the amount of snowfall. For example, the benefit-cost ratios for the first decade (1975–1984, average annual maximum snow depth of 2.77 m) and the second decade (1985–1994, 1.94 m) are 1.08 and 0.62, respectively.

Figure 7 shows the relationship between the annual benefits and costs and the annual maximum snow

depths for the 20 years. The benefits increase in an accelerated manner as the maximum snow depths increase, but the costs are almost constant. Consequently, the benefit-cost ratios are expressed by the same plot as the benefits according to the scale of the right vertical axis. From this result, it follows that when the annual maximum snow depth is greater than about 3 m, the system has an annual benefit-cost ratio of more than 1, making the system economically effective.

Figure 8 shows the benefit B_1 and B_2 on roads, sidewalks, and housing sites in representative years of light (1991), average (1994), and heavy (1983) snowfall. Figure 8 indicates that B_2 is more than B_1, and the major factor in the benefits is housing sites. B_2 for housing sites

TABLE 3   Results of Benefit-Cost Analysis

	Snow Data		Results of Calculation			
	Maximum Snow Depth	Snow Cover Days	Benefit $B1$	Benefit $B2$	Cost C	B/C
Year	(m)	(days)	(million yen)	(million yen)	(million yen)	
1975	2.82	126	44	149	268	0.72
1976	3.15	142	50	247	270	1.10
1977	3.09	131	46	345	269	1.45
1978	1.14	95	33	16	264	0.19
1979	3.05	104	37	235	266	1.02
1980	3.77	141	50	555	270	2.24
1981	1.79	129	45	53	269	0.36
1982	2.29	105	37	154	266	0.72
1983	3.67	166	58	458	273	1.89
1984	2.97	126	44	247	268	1.09
1985	3.28	140	49	345	270	1.46
1986	1.89	111	39	66	266	0.39
1987	2.15	102	36	153	265	0.71
1988	0.81	76	27	10	262	0.14
1989	1.91	87	31	49	263	0.30
1990	2.30	109	38	233	266	1.02
1991	1.45	113	40	44	267	0.31
1992	1.72	123	43	46	269	0.33
1993	1.63	119	42	62	267	0.39
1994	2.26	123	43	251	268	1.10
Total			832	3,718	5,346	0.85
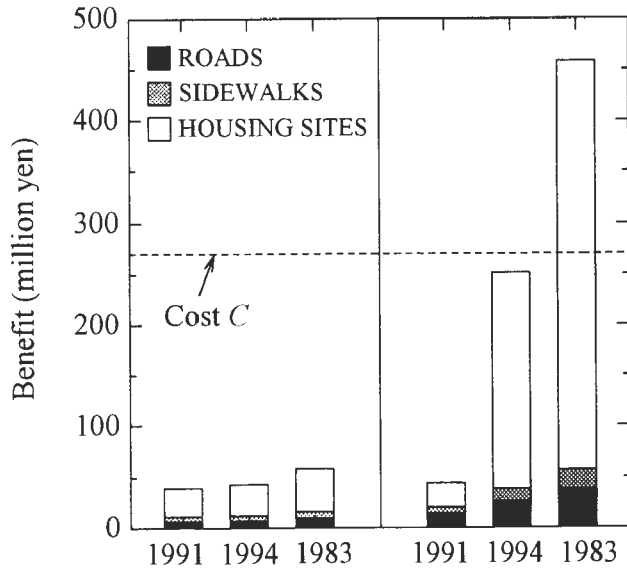
FIGURE 8   Benefit B_1 and B_2 on roads, sidewalks, and housing sites in representative years.

increases considerably with an increasing amount of snowfall. This is because the amount of snow transported by trucks increases dramatically as the frequency of roof snow removal increases. This characteristic of B_2 appears to determine the economic effectiveness of the system.

CONCLUSIONS

A method for evaluating the economic effectiveness of a snow-removing channel has been proposed and applied to the snow-removing channel system in Tokamachi

City. The annual benefits, costs, and benefit-cost ratios have been calculated for 20 years, from 1975 through 1994, and conclusions were made.

First, the economic effectiveness of the system is dependent on the amount of snowfall. For example, the system is effective for the first decade (average B/C = 1.08) but not effective for the second decade (average B/C = 0.62). Second, the annual benefits B increase with the annual amount of snowfall, but the annual costs C are almost constant. The critical value for economic effectiveness (B/C = 1) is attained at an annual maximum snow depth of about 3 m. Third, the benefit B_2 is more than B_1. The major factor for B_2 is housing sites, and B_2 increases considerably as the amount of snowfall rises.

This method is applicable to other places for which a snow-removing channel is planned. It can contribute to the selection of the measures against snow damage.

ACKNOWLEDGMENT

REFERENCE

1. Umemura, T., S. Kamimura, and H. Otaki. Snow Damage in an Urban Area with Heavy Snow Fall. *Journal of Natural Disaster Science*, Vol. 13, No. 1, 1991, pp. 1–11.

Winter Maintenance on Porous Asphalt

Maarten Noort, *Meteo Consult, The Netherlands*

In 1986, porous asphalt (drain asphalt or open-graded asphalt) was introduced in the Netherlands. By 1997, approximately 40 percent of all highways in the Netherlands had been paved with this open asphalt. The main reason for the use of porous asphalt is its ability to reduce traffic noise and improve traffic safety. The increase in the use of open porous asphalt in the last couple of years has shown that its winter behavior deviates from that of normal dense asphalt. The main causes of the different behavior of porous asphalt, compared with dense asphalt, are its responses to temperature, humidity, and salt on the road surface. Discussed here is the maintenance required by the three principal forms of slipperiness: that caused by freezing of wet road sections, that caused by a small amount of moisture (condensation, sublimation, and freezing fog), and that caused by precipitation such as snow and freezing rain. Under "normal" Dutch winter conditions (in which slipperiness is caused mainly by the freezing of the wet road surface), winter maintenance of porous asphalt roads will not cause significant problems for the highway authority, requiring only a high consumption of salt to keep the road safe. However, in the case of freezing rain, the difference in friction between porous asphalt and dense asphalt is considerable. In highly intense freezing rain, a layer of ice will swiftly form on porous asphalt and cause a subsequent loss of friction.

In 1986, porous asphalt (drain asphalt or open-graded asphalt) was introduced in the Netherlands on a large scale because of its ability to reduce traffic noise and improve traffic safety. Porous asphalt is believed to increase traffic safety because it can minimize splash and spray and hydroplaning. An inquiry also made it clear that drivers appreciated the comfort of porous asphalt roads. By 1997 about 40 percent of the Dutch main road network had been improved with porous asphalt. Aside from the positive qualities, porous asphalt roads have some disadvantages, including high construction costs and a reduction in friction preceding construction. Recently it became clear that, immediately after construction, the friction of porous asphalt roads is insufficient.

Since the introduction of porous asphalt in the 1970s, highway departments have had to combat adverse conditions associated with the asphalt and wintry conditions. During the winter of 1978–1979, it became clear that winter behavior of the open porous asphalt strongly differs from that of a normal dense upper layer. Because of the relatively short sections of porous asphalt on the road and lack of experience, road authorities were not aware of the different treatment needed for this new layer. It was thought that more experience with open asphalt would help to solve the problems.

The first winters following large-scale construction gave no reasons to change this conclusion. An adaptive treatment for different types of slipperiness gave good results. Insight into the mechanism of slipperiness on porous asphalt made it clear that freezing rain on a road surface that was below the freezing point could cause a large reduction in friction. Because of a lack of freezing rain through the early 1990s, different views could not be examined. Laboratory tests, carried out by the Onderzoek Centrum voor de Wegenbouw (1), indicated the opposite of the theory that porous asphalt reduced friction. During these laboratory tests with simulated freezing rain, it was shown that porous asphalt, without any gritted salt, provided better friction than an upper layer of dense road surface. This may have been caused by breakage of the ice on porous asphalt.

This study deals with the properties of porous asphalt and the mechanisms that change them. By finding these

mechanisms, which are caused mainly by different types of precipitation, slipperiness of porous asphalt upper layers can be combated.

BEHAVIOR OF POROUS ASPHALT

The main advantages of porous asphalt are thought to be the following:

- Traffic noise reduction,
- Traffic safety,
- Road capacity,
- Absence of splash and spray,
- Absence of hydroplaning,
- Absence of reflection from the road surface,
- Visible road marks, and
- Lack of ruts in the road surface.

A recent study completed by the Netherlands Ministry of Transport shows that there is no difference in traffic safety between road surfaces of dense and porous asphalt. Driver comfort is the main advantage of porous asphalt.

The main disadvantages of porous asphalt are

- Lifetime cost,
- Dirt build-up,
- Recycling,
- Mechanical damage, and
- Winter maintenance.

Maintenance of porous asphalt is the main problem for the road authority.

A ministry of transport survey shows that in the following situations porous asphalt requires close monitoring in winter conditions:

- Roads with low traffic volume,
- Roads on an incline,
- Roads with a limited superelevation,
- Hard shoulders,
- Changes from cold to warm temperatures,
- Snow remaining on the road surface,
- Slipperiness caused by condensation,
- Slipperiness caused by freezing rain, and
- Changeovers from porous asphalt to dense asphalt concrete.

As noted in a report on winter maintenance of porous asphalt (2), the main causes of the different behavior of porous asphalt relative to that of dense asphalt concrete are temperature, humidity, and salt on the road surface.

Temperature Behavior

Since the construction of the National Ice Warning System in the Netherlands, the temperature behavior of porous asphalt has become clear. Many useful measurements were obtained by using this system, especially from roads with one lane of porous asphalt and the other lane of dense asphalt concrete. The road temperature data (winter of 1986–1987) from the ice warning system confirmed that, on average, the porous asphalt drops below freezing sooner, and as the air temperature rises, the temperature of the porous asphalt stays below freezing longer than that of a comparable road section of dense asphalt (Figure 1). The data also show that the maximum temperatures of porous asphalt are often lower than the maximum temperatures of dense asphalt. The measurements also indicate that the minimum temperatures of porous asphalt are often a little higher than those of dense asphalt.

In addition, when the air temperature rises after a cold period, the temperature behavior of porous asphalt causes a colder road surface than that of a comparative road section of dense asphalt. When the air temperature remains at or a little above freezing, and cold weather has been prolonged, porous asphalt sections remain below freezing considerably longer than do comparable dense asphalt road sections (Figure 2).

Humidity Behavior

Voids in porous asphalt ensure that precipitation is slowly drained to the shoulder as a result of the super-elevation of the road. Some of the precipitation remains behind in the pores (Figure 3). In the winter roads dry slowly because traffic brings moisture back to the surface of the road. The transport of moisture is caused by the air pumping effect of vehicle tires.

Remaining moisture combined with the average lower temperature of a porous asphalt section suggests that this open asphalt is more sensitive to freezing on wet road sections. If an ice warning system is present, this slipperiness will be indicated by a warning to the road authority. The sensors of the ice warning system signal slipperiness in time to prevent dangerous situations.

Behavior with Regard to Salt on Road Surface

When a frozen wet road section is forecast (because of falling temperatures), preventive spreading operations should take place before a layer of ice adheres to the road. In these conditions the prewetted salt technique is used to spread the salt onto the road. The mixture used consists of dry sodium chloride (NaCl) grains and a sodium chloride or calcium chloride ($CaCl_2$) solution
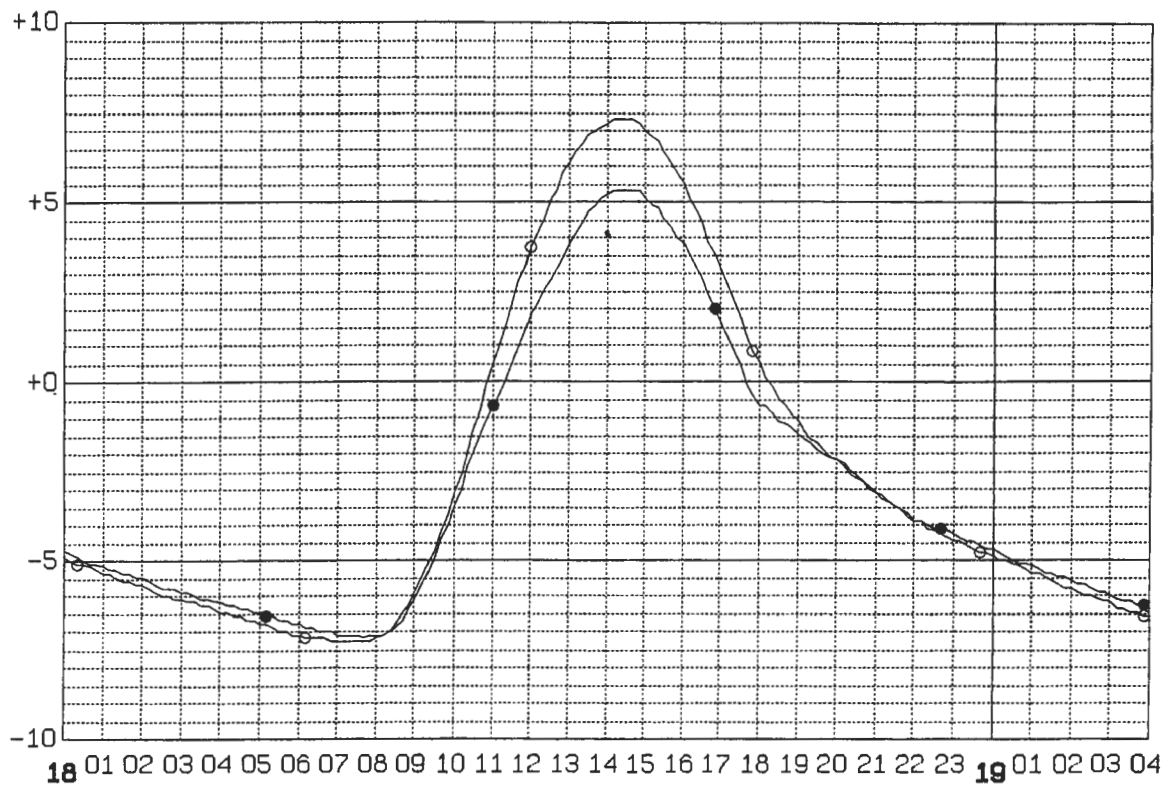
FIGURE 1   Characteristic path of porous asphalt temperature (●) compared with dense asphalt (○) concrete. Porous asphalt remains below freezing longer.
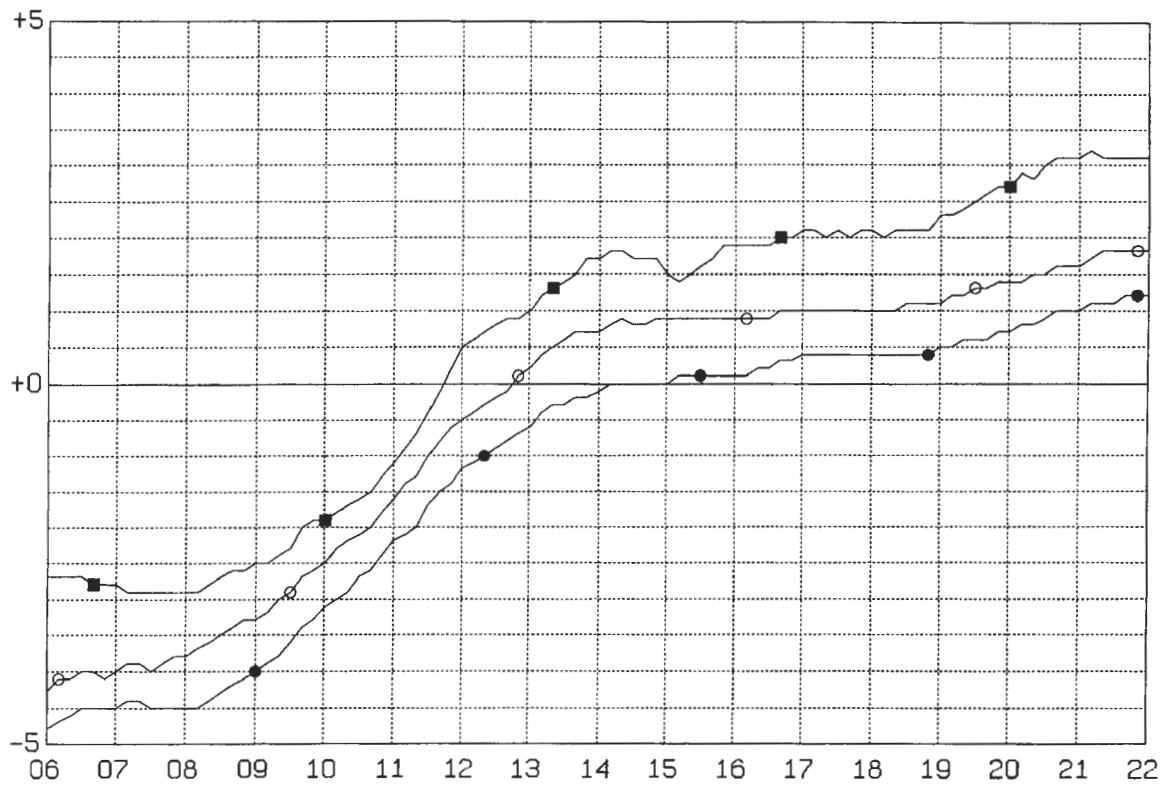
FIGURE 2   Temperature path of porous asphalt road section (●) versus temperature path of dense asphalt road section (○), and air temperature (■), following cold period.
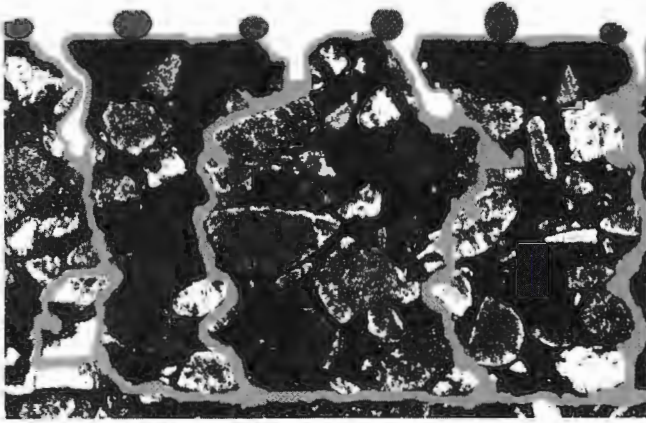
FIGURE 3 Distribution of water in voids of porous asphalt. Only a thin layer of water and salt grains is present on surface.

(16 percent). The mixture is made on a spreading sheet and is immediately on the road (Figure 4).

On road sections of dense asphalt this salt mixes with the moisture on the surface. The resulting salt solution freezes only when the temperature falls below the freezing point of the mixture, which is substantially lower than the freezing point of water. Small amounts of falling precipitation are neutralized, and the wet road section is not slippery. In addition, traffic considerably accelerates the mixing process and distributes the salt on the road.

The amount of salt for spreading operations is doubled (11 g/m^2) on porous asphalt because it contains more moisture. On porous asphalt, the salt is distributed evenly on the road, and only a small amount of the salt disappears into the voids. As on dense asphalt, the air pumping effect of tires accelerates the mixing process, even within voids of the porous asphalt. Conversely, nearly all the salt applied to dense asphalt remains on the road surface. The amount of the salt solution slowly decreases, because the crown of the road causes mois-

ture to flow away from the road. The salt solution can also be blown away or transported by traffic.

Although more spreading operations are needed on porous asphalt, the amount of salt solution on the surface of the porous road is less than that on dense asphalt concrete. The distributed salt mixes with the moisture inside the voids of porous asphalt (because of the air pumping effect), the salt dissolves, and the resulting salt solution prevents moisture from freezing. Also, little salt solution remains on the surface of porous asphalt because of the material's draining properties. The largest amount of salt solution is in the voids (Figure 5). Through the air pumping effect of tires, fresh salt solution is transported continuously to the road surface (Figure 6). The salt solution stored in the voids is available for thawing the road surface. In general, a driver does not notice any difference between porous asphalt and dense asphalt concrete as long as sufficient traffic is on the road.

If moisture (precipitation, condensation, or fog) is not added to the road surface, the salt solution becomes concentrated through evaporation. Ultimately, small salt crystals surface, which on dense asphalt concrete are evident in a whitening of the road surfaces as the salt dries. On dense asphalt concrete, the small white salt crystals slowly disappear over time. This disappearance is influenced by traffic. On porous asphalt the salt remains for a considerably longer period, mainly in the voids of the asphalt. A survey of different types of slipperiness may show the properties of porous asphalt during other, more critical circumstances.

SLIPPERINESS

Slipperiness may be divided into three principal forms:

• Slipperiness caused by freezing of wet road sections; the available moisture on the road surface causes slipperiness as temperatures fall.

FIGURE 4 Prewetted salt is spread on surface before ice layer forms.
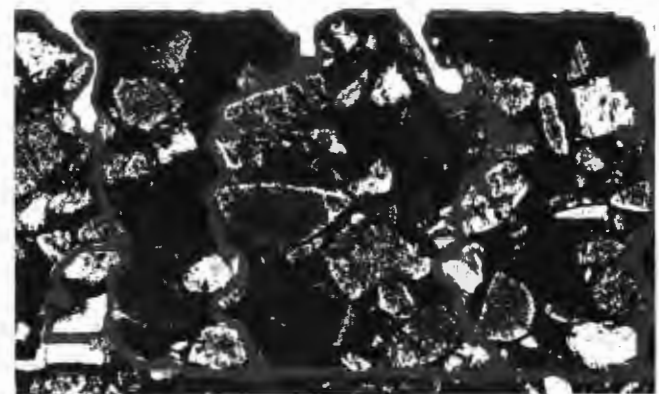
FIGURE 5 Distribution of salt on road surface and in voids of porous asphalt. Only a small amount of salt remains on surface.

FIGURE 6 Air pumping effect of tires. Moisture visible behind tire has been sucked out of voids of porous asphalt. This effect transports thawing agent to surface and allows surface to remain wet.

FIGURE 7 If balance between salt solution in voids and on road surface is disturbed, a small amount of precipitation may be sufficient to reduce surface friction.

- Slipperiness caused by a small amount of moisture (condensation, sublimation, and freezing fog).
- Slipperiness caused by precipitation. All types of precipitation, including hail, snow, ice rain, and freezing rain, can cause slipperiness.

Freezing of Wet Sections

When wet road sections freeze, no differences distinguish porous asphalt from dense asphalt concrete after preventive spreading operations. In these cases, the amount of moisture on the road surface must be monitored. If a large amount of moisture is present, more salt must be distributed to reach the intended lower freezing point. In comparison with dense asphalt concrete, a double quantity of salt is needed to neutralize the moisture in the voids of porous asphalt.

Small Amount of Moisture

A difference between porous asphalt and dense asphalt concrete is evident when the road surface temperature is below freezing and a small amount of moisture falls on the road. A considerable difference in friction can arise on road surfaces if they are below freezing and spreading operations already have been carried out. This situation can occur if the balance of the salt solution in the voids is disturbed because of diminishing traffic intensity (Figure 7). A small amount of new moisture on the road surface of porous asphalt then reduces the friction of the road surface. On dense asphalt concrete this reduction of friction does not occur because the amount of salt on the surface is sufficient to prevent reduction.

Experience has shown that condensation or freezing fog on well-gritted porous asphalt, in combination with normal (or nightly) traffic intensity, does not cause a reduction in friction. In contrast, the less-traveled hard shoulder turns white, and friction may be reduced. Even so, during periods of fog and road surface temperatures below freezing, slipperiness must be monitored. Fog that changes into drizzling rain can greatly reduce friction.

At night porous asphalt is more sensitive to the lowering of friction because of the disturbed balance between the voids and the surface. A suitably instrumented ice warning system can warn road authorities of drizzling rain so that extra spreading operations may be implemented.

In the Netherlands, air temperatures at or just below freezing often occur and are likely to cause complications. Under these circumstances temperatures of the road surfaces of bridges (porous and dense) and viaducts often drop below freezing. Frozen bridges and viaducts are caused by a lack of warmth in their foundations. The adjacent road sections, which can consist of either porous asphalt or dense asphalt concrete, remain at or rise above freezing at the same time. In this case a large difference in friction can occur.

If spreading operations are followed by a dry period, the salt distributed on dense asphalt concrete slowly disappears from the effects of traffic. A porous asphalt road section also dries out under these circumstances. The salt, however, does not disappear—small crystals remain in the voids of porous asphalt. These salt crystals dissolve again if new precipitation occurs, even as road surface temperatures drop below freezing. Traffic transports this solution to the surface of the road, and the salt buffer helps to make the porous asphalt passable. As the action of traffic transports this solution to the surface of the road, the salt barrier allows the porous asphalt to remain passable and unfrozen.

Precipitation

Different types of precipitation can cause slippery roads. The following comments on different types of precipitation apply to both porous asphalt and dense asphalt concrete.

Snow

In the Netherlands, snow may occur when road surface temperatures are above or below freezing. When road surface temperatures are above freezing, a slippery road surface may occur briefly on both porous asphalt and dense asphalt concrete. Afterward, the heat in the road surface melts the snow, which results in normal friction along the road surface. In general, porous asphalt is colder, so snowfall on this asphalt can cover the road surface earlier than on dense asphalt surface (Figure 8).

When snow falls during a period of below-freezing surface temperatures, all types of asphalt need preventive spreading treatment. Spreading before initial snowfall is the only way to prevent icing of the road. If roads are left untreated, snow crushed by traffic becomes ice. During snowfall, the behavior of porous asphalt differs from that of dense asphalt concrete. The performance of the porous asphalt road varies and is dependent on traffic intensity and the salt buffer present in the voids of the asphalt. If spreading operations are not carried out before initial snowfall, a porous asphalt road is more passable than a dense asphalt concrete road because of the salt buffer. During periods of high traffic intensity and snowfall, the performance of a porous asphalt road section, in general, does not differ from that of dense asphalt concrete. During periods of low traffic intensity, it becomes more difficult to maintain the quality of the road. For example, less-traveled porous asphalt exit

FIGURE 8 Hard shoulder of porous asphalt next to dense asphalt concrete road surface. Shoulder is fully covered with snow because without traffic action, salt remains in voids rather than transferring to surface.

ramps become slippery faster than do exit ramps of dense asphalt concrete (Figure 9).

Hail

When precipitation is hail, the temperature of the road is nearly always above freezing. Both dense asphalt concrete and porous asphalt are affected, although the slipperiness is temporary because the heat of the road quickly melts the hail.

Freezing Rain

In freezing rain, the friction levels of the two road surfaces differ considerably. In addition to friction, recognition of black ice by road users is important in freezing-rain circumstances. During periods of snowfall, road users can easily detect visually differences in friction between porous asphalt and dense asphalt concrete. During freezing rain, road users cannot usually perceive the difference.

Whether precipitation reaches the ground in the form of snow or freezing rain depends on the temperature of the upper layers of air. The colder upper layer of air is responsible for the condensation of water to ice crystals (snow). If snow falls through layers of below-freezing air temperatures, the snow keeps its original form. If the snow passes through layers with air temperatures above freezing, the snow crystals melt. When this occurs, the precipitation can remain in liquid form or freeze, depending on atmospheric conditions of the lowest layers. If the ground or the air right above the surface is below freezing, the rain freezes on contact; otherwise it falls as unfrozen rain (Figure 10). Almost immediately after the supercooled drop reaches the road surface, it congeals. Salt melts the first freezing rain, as is the case with snow. After this solution is transported to the voids (as a result of gravity), the amount of salt on

FIGURE 9 Evident difference in behavior of main road and shoulder (porous asphalt) and exit ramp (dense asphalt).
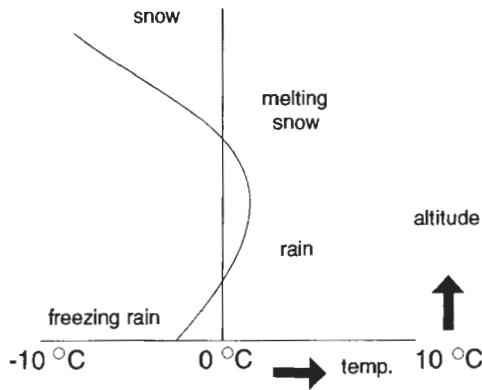
FIGURE 10 Form of precipitation at ground level depends on temperature of upper layers of air.

the surface of porous asphalt has decreased considerably. The continuing freezing rain quickly forms a layer of ice, which is caused by a lack of salt. Average higher intensity of precipitation on the road surface and higher density of freezing rain (1 cm snow equals 0.1 cm water) influence the balance between the thawing agent in the voids and the thawing agent on the road surface.

During periods of snow, the action of traffic maintains a good balance between the salt in the voids and the salt on the road surface. The melting process of snow (as a result of the weight of the vehicles and the balance in transport of salt to the road surface by the air pumping effect) prevents a strong reduction in friction.

During periods of steady freezing rain, the balance between the salt solution in the voids and the salt solution on the road surface of porous asphalt is disturbed. This disturbed balance is caused by quicker succession of freezing raindrops, higher density, quicker transport of the thawing agent, and a layer of ice, which forms immediately. In the case of high intensity of freezing rain, the layer of ice forms swiftly and causes a subsequent loss of friction.

Solutions for Slipperiness Caused by Freezing Rain

With sufficient traffic intensity, porous asphalt and dense asphalt behave more or less the same. However, freezing rain negatively influences the performance of porous asphalt. Especially at changeovers between porous asphalt and dense asphalt, the road user becomes aware of the difference in slipperiness. At these changeovers, the friction of dense asphalt concrete is often sufficient, whereas the friction of porous asphalt is often greatly reduced.

A variety of techniques can be used to reduce slipperiness caused by freezing rain. Often a combination of these techniques is used. On many main roads in the

Netherlands, displays have been installed that indicate reduced speed limits because of road conditions. In addition, these displays force traffic to use one lane, which optimizes the air pumping effect of tires. At some locations without displays, traffic is forced to proceed in a column. Positive results have been obtained by this method. Portable signal boards located at changeovers between dense and porous asphalt are also used to warn road users. During periods of freezing rain, the media also frequently warn road users of the dangers associated with porous asphalt. Since the 1996–1997 winter, the Dutch government has distributed information about the properties of porous asphalt at border crossings.

If the road surface is covered with a layer of ice during periods of freezing rain, sodium chloride is spread to remove this layer. If the layer of ice is thin, the operation often succeeds, and the road surface is temporarily ice free. With continuous freezing rain, a new layer of ice forms. Although spreading operations temporarily improve the friction of the road surface considerably, they also have negative effects. When salt melts the layer of ice, an endothermic reaction (heat depletion) takes place. During this reaction heat is drawn from the environment. Since the air contains little heat, the reaction takes heat from the road surface. Thus, as a result of the spreading (melting) operation, the road surface temperature can fall between 1 and 2°C.

In the case of slowly rising temperatures, the porous asphalt remains critical for a longer period than does dense asphalt (Figure 11). Slipperiness occurs for a considerably longer period on porous asphalt. An improvement can be obtained by adding solid $CaCl_2$ to sodium chloride. The hygroscopic character of $CaCl_2$ brings about an exothermic (heat-producing) reaction when the solution is mixed with water or ice. This hastens the thawing process. A mixture of $CaCl_2$ with sodium chloride (40/60) is expected to give the best result. The first tests with this mixture were carried out during the 1996–1997 winter. During this test, the layer of ice melted quickly. However, it could not be concluded that the heat from the $CaCl_2$ reaction abolished the cooling effect caused by the endothermic reaction of sodium chloride. Moreover, during periods with steady freezing rain, this thawing agent is transported into the voids, and the road surface becomes slippery again. More tests are needed because the mixture of $CaCl_2$ and NaCl also has practical disadvantages associated, for example, with storage and handling.

Distributing sand to reduce the slipperiness caused by freezing rain is not advisable. Sand is covered by new freezing rain, or it is transported into the voids, if enough moisture is available on the road. Only when freezing rain stops does sand improve the friction of the road. Meanwhile, the sand changes the structure of the
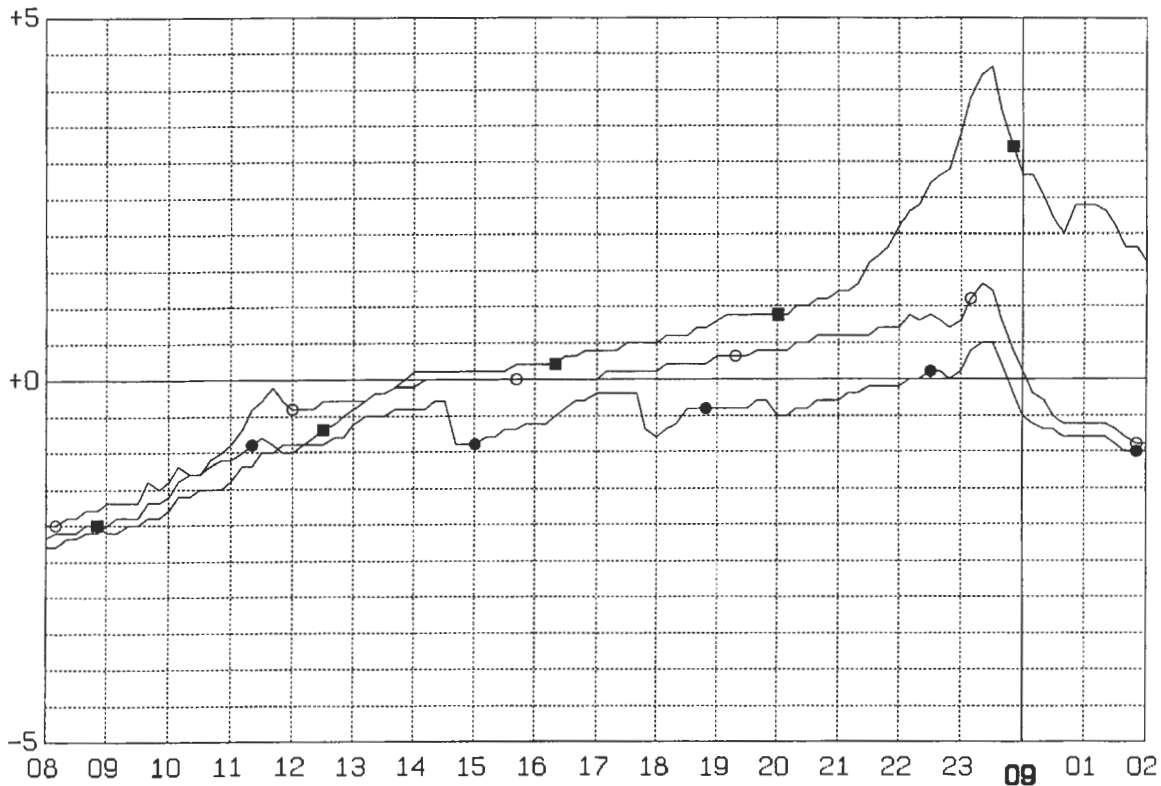
FIGURE 11   Road surface temperature of porous asphalt (●) and dense asphalt (○), January 8, 1996. Fall in temperature of porous asphalt at 14:30, 17:40, and 20:00 is caused by gritting operations. Also shown is air temperature (■).

porous asphalt. The voids are filled with sand, and the desirable transport of water is disturbed after a period of freezing rain. It is doubtful whether it is possible to remove the sand by using cleaning techniques.

Perhaps temporary elimination of the porous asphalt structure is a solution. Some material that is poorly soluble in water can be used to close the voids of porous asphalt temporarily. After a while rain should open the voids again. As such an option, calcium sulfate ($CaSO_4$) must be explored as the spreading agent. $CaSO_4$ is easily obtained and relatively inexpensive. The material is poorly soluble in water (0.2 wt%) and would not cause many problems for the environment or for road authorities.

CONCLUSION

Dutch winters are characterized by unsettled weather. Temperatures can pass the freezing point several times, often in one day. Long cold periods with a great deal of pre-

cipitation are rare. Because of their nondense structure and their temperature and humidity behaviors, roads made of porous asphalt require greater attention from the highway authority than do comparable roads made of dense asphalt concrete. Winter maintenance of porous asphalt roads does not cause the highway authority many worries under normal Dutch winter conditions, in which slipperiness is caused mainly by the freezing of wet road surfaces. Only in the case of freezing rain does the driving quality of porous asphalt become considerably less than that of comparable dense asphalt concrete.

REFERENCES

1. Coene, Y. Winter Behavior of Porous Asphalt (in Dutch). Laboratory freezing rain tests. RV 29/87, Onderzoek Centrum voor de Wegenbouw, Brussels, Belgium, 1987.
2. Noort, M. *Winter Maintenance on Porous Asphalt.* Ministry of Transport, Delft, The Netherlands, 1991.

PART 3
MATERIALS AND APPLICATION
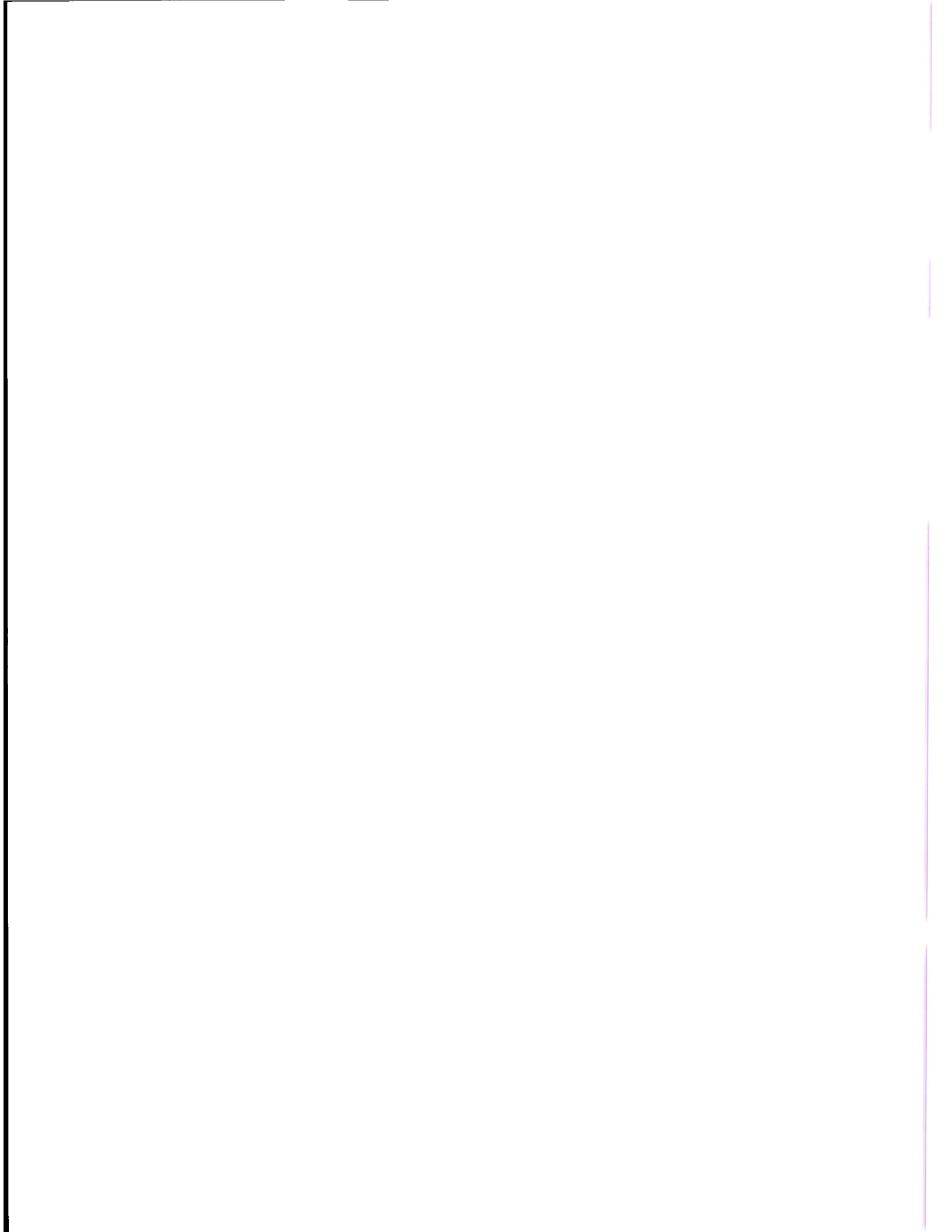
Guidance for Successful Anti-Icing Operations Based on U.S. Experience

Robert R. Blackburn, *Blackburn and Associates*
Stephen A. Ketcham, *U.S. Army Corps of Engineers*
  Cold Regions Research and Engineering Laboratory
L. David Minsk, *Hanover, New Hampshire*

Highway anti-icing is the snow and ice control practice of preventing the formation or development of bonded snow and ice by timely applications of a chemical freezing-point depressant. The application of a chemical freezing-point depressant onto a highway pavement when a winter storm starts or before precipitation begins inhibits the development of a bond between snow and ice and the pavement surface. Moderate, periodic reapplication of the chemical during the storm can continue this effect. Such preventative operations are the core of an anti-icing program. A successful anti-icing program provides the maintenance manager with two major capabilities: the capability of maintaining roads in the best conditions possible during a winter storm and the capability of doing so efficiently. As a consequence, anti-icing has the potential to provide the benefit of increased traffic safety at the lowest cost. However, to achieve this benefit the maintenance manager must adopt a systematic approach to snow and ice control and must ensure that the performance of the operations is consistent with the objective of preventing the formation or development of bonded snow and ice. Such an approach requires considerable judgment, methodical use of available information sources, and timely operations that anticipate or respond promptly to icy conditions.

Guidance for successful anti-icing operations has been developed. This guidance is based on an analysis of data obtained during the winters of 1993–1994 and 1994–1995 in the 15 states participating in FHWA Test and Evaluation Project 28 and also on relevant experiences and the review of anti-icing practices in Strategic Highway Research Project H-208. Specific and concise guidance for anti-icing operations for six winter weather events has been formulated. The weather events are light snow storms, light snow storms with periods of moderate or heavy snow, moderate or heavy snow storms, frost or black ice, freezing rain storms, and sleet storms. The maintenance action for each event is defined for several pavement temperature ranges and associated temperature trends, and for initial and follow-up operations. The actions considered depend on the pavement temperature and other conditions and include application of chemicals, either alone or in combination with plowing, application of abrasives, plowing only, or doing nothing. Solid, liquid, and prewetted solid chemical application rates are suggested as appropriate. These rates are not to be considered fixed values but rather the middle of a range to be selected by an agency according to local conditions and experiences.

Detailed guidance for successful anti-icing operations is contained in the 1986 FHWA publication, *Manual of Practice for an Effective Anti-Icing Program: A Guide for Highway Winter Maintenance Personnel*, Report FHWA-RD-95-202.

Anti-Icing Field Evaluation

Stephen A. Ketcham, *U.S. Army Corps of Engineers*
Cold Regions Research and Engineering Laboratory
L. David Minsk, *Hanover, New Hampshire*

Anti-icing is the snow and ice control practice of preventing the formation or development of bonded snow and ice by timely applications of a chemical freezing-point depressant. This definition derives from U.S. snow and ice control practice observed in anti-icing field evaluations for the Strategic Highway Research Program and FHWA. The FHWA project and the implications of its results for implementation of an anti-icing program are described. This definition and the diversity of operations that can lead to anti-icing success are the focus of this paper. A framework for communication and technology transfer among practitioners is provided to complement guidance contained in the project's manual of practice.

"**A**nti-icing is the snow and ice control practice of preventing the formation or development of bonded snow and ice by timely applications of a chemical freezing-point depressant." This definition of highway anti-icing comes from *Manual of Practice for an Effective Anti-Icing Program: A Guide for Highway Winter Maintenance Personnel (1)*. It derives from U.S. snow and ice control practice observed during the Strategic Highway Research Program (SHRP) project H-208, Development of Anti-Icing Technology (2), and the Federal Highway Administration (FHWA) Test and Evaluation Project 28 (T&E 28), Anti-Icing Technology, which was managed by the Cold

Regions Research and Engineering Laboratory (CRREL) under contract to FHWA (3). The definition is notable because it implies both specific and nonspecific actions for implementation. In particular, although it specifies anti-icing as a practice based on chemical application for preventing the formation or development of a bond between pavement and snow or ice, it does not suggest the type of chemical operations to perform or how operational decisions should be made. This generality is intentional, because the maintenance operations of T&E 28 clearly showed that the desired anti-icing result can be achieved by using a variety of operational methods and decision-making tools. For example, one group may be successful using rock salt or prewetted rock salt as the applied chemical freezing-point depressant, but another group operating under similar conditions may be successful with a different chemical in liquid form. The stated intention, to prevent the formation or development of bonded snow or ice, must be clarified. Preventing the *formation* of bonded snow or ice means that the bond simply does not form. Preventing the *development* of bonded snow or ice means that, while snow or ice is bonded to the road during some period of the storm, the strength of the bond is mitigated. In the case of formation, although bare pavement conditions are often achieved, slush, loose snow, and nonbonded packed snow are also commonly observed. In the case of development success can be achieved even with sustained periods of weakly or mod-

erately bonded snowpack or ice. Thus, although a "successful" anti-icing operation can result in a variety of conditions that are slippery, these conditions are always more desirable than is strongly bonded snow or ice, which is difficult to remove and thereby provides low traction for extended periods. It may be surprising that anti-icing success can mean conditions ranging from slush to loose snow to packed snow. Yet this was observed during T&E 28. The positive implication is that anti-icing practices, although diverse, can be further engineered to achieve a desired target level of effectiveness. For example, with adequate resources, operations on one highway might be designed to prevent bonded snow or ice at all times, whereas operations on another highway might be designed to prevent development of a strong bond so that all snow or ice can be readily removed within a certain time, perhaps, after the end of a storm or before a heavy traffic period.

By focusing on the formation and development of the bond, the definition centers on the effectiveness of anti-icing practices rather than on reduced costs or any other secondary objective or benefit. This focus is consistent with the observed practices of T&E 28 participating agencies, which, because of the demanding effectiveness requirements of high service levels, have been instinctively implementing elements of anti-icing practices for years. Anti-icing above all should be seen as a practice that, because of its preventive nature, provides a high level of maintenance effectiveness, and not as a practice that automatically results in lower cost. The secondary issue of savings depends on current practice—for example, what level of service current practice supports, what materials it uses, whether it provides more deicing than anti-icing, and what information sources it uses. Nonetheless, because anti-icing has evolved within U.S. practice to mean a modern snow and ice control strategy that makes systematic use of new technologies including road weather information systems (RWISs), site-specific weather and pavement temperature forecasts, and sophisticated spreader and plowing equipment, it has become synonymous with efficiency. Indeed, the modern practice of anti-icing provides a maintenance manager with two major capabilities: the capability to maintain roads in the best condition possible during a winter storm and the capability to do so efficiently. As a consequence, anti-icing has the potential to provide the benefit of increased traffic safety at the lowest attainable cost. However, to achieve this benefit the maintenance manager must follow a systematic approach to snow and ice control and must ensure that the performance of the operations is consistent with the objective of preventing the formation or development of bonded snow and ice—generally throughout the entire storm. Such an approach requires considerable judgment, methodical use of available information sources, and operations that anticipate or respond promptly to icing conditions. The initial definition reflects this approach in its reference to *timely* applications of chemicals.

An anti-icing field evaluation program was designed by CRREL and conducted under T&E 28. This paper briefly describes the field evaluation and implications of the results for implementation of an anti-icing program. By focusing on the definition of anti-icing and the diversity of operations that can lead to anti-icing success, the paper offers practitioners a broad framework for communication and technology transfer. Additional descriptions of the field evaluation and its results are contained in reports of the project (1,3).

EXPERIMENTAL AND DATA ANALYSIS TECHNIQUE

The field evaluation of T&E 28 included a two-winter, experimental anti-icing study at 16 sites in 15 states—California, Colorado, Iowa, Kansas, Maryland, Massachusetts, Minnesota, Missouri, Nevada, New Hampshire, New York, Ohio, Oregon, Washington, and Wisconsin—and an analysis of the experimental data. The evaluation comprised field operations and experiments conducted by state highway agency personnel, and the data analysis consisted of graphical and statistical analysis conducted by CRREL.

The general approach of the anti-icing experiments, and many of the specific techniques of the experiments, followed the experimental concept and techniques of the preceding SHRP project H-208 (2). As they were in SHRP H-208, the experiments were conducted at the sites by using different anti-icing and conventional treatments. They were conducted during a variety of storm events that reflected the nature of storms at each site and at the various geographical locations over the two-winter period of the study. An experiment consisted of anti-icing operations on a test section, conventional operations on a control section, documentation of the operations, and data collection during a single storm. The anti-icing operations of T&E 28 were conducted according to treatment strategies that were developed by personnel at each site so that the results would provide knowledge of locally designed anti-icing programs. This approach also furthered the implementation objectives of the project. The conventional operations were intended to reflect the standard practice at the site, with no influence from the anti-icing operations.

More than 200 storm data packages were submitted by the states for the 2 years of the study, and considerable documentation was provided in each storm package. Documents included weather and pavement temperature

forecasts; RWIS and other weather data; logs of the operations and data collection; traffic data; and, for selected sites and storms, cost data. Operation logs included the type, proportions or concentration, and application rate of each major chemical component of all chemical treatments, the snow plowing operations, the type and application rate of any abrasives that were placed, and any other operations.

The on-road data collection consisted primarily of precipitation observations, friction measurements, and pavement condition observations. The friction measurements at all sites were made with a commercially available deceleration-type friction meter that was installed in an agency sedan or pickup truck used as the measurement vehicle. The friction measurements and pavement condition observations were focused on the wheel paths of the driving lanes, and several measurements and observations were made during each pass of the measurement vehicle. An additional observation was made to judge whether the driving lane of the test section or the driving lane of the control section provided the better traction, or whether there was no perceivable difference.

The data analysis examined and interpreted the operations and their results, established significant differences between the effectiveness of test and control operations, established conditions under which anti-icing is effective, and developed statistically based conclusions and recommendations for practice. Storm data sets were analyzed individually and in blocks of a given season and site. Results from a single storm provided a "close-up" of the operations and their effectiveness, and results from several storms at a site allowed the "big picture" to appear.

The fundamental results from a single storm were the graphical data histories and the operations summaries. Data histories of two storms and two sites are given as examples in Figures 1 and 2. Figure 1 displays data from the January 23–25, 1995, storm at the New York site, located in the Rochester metropolitan area a few miles south of
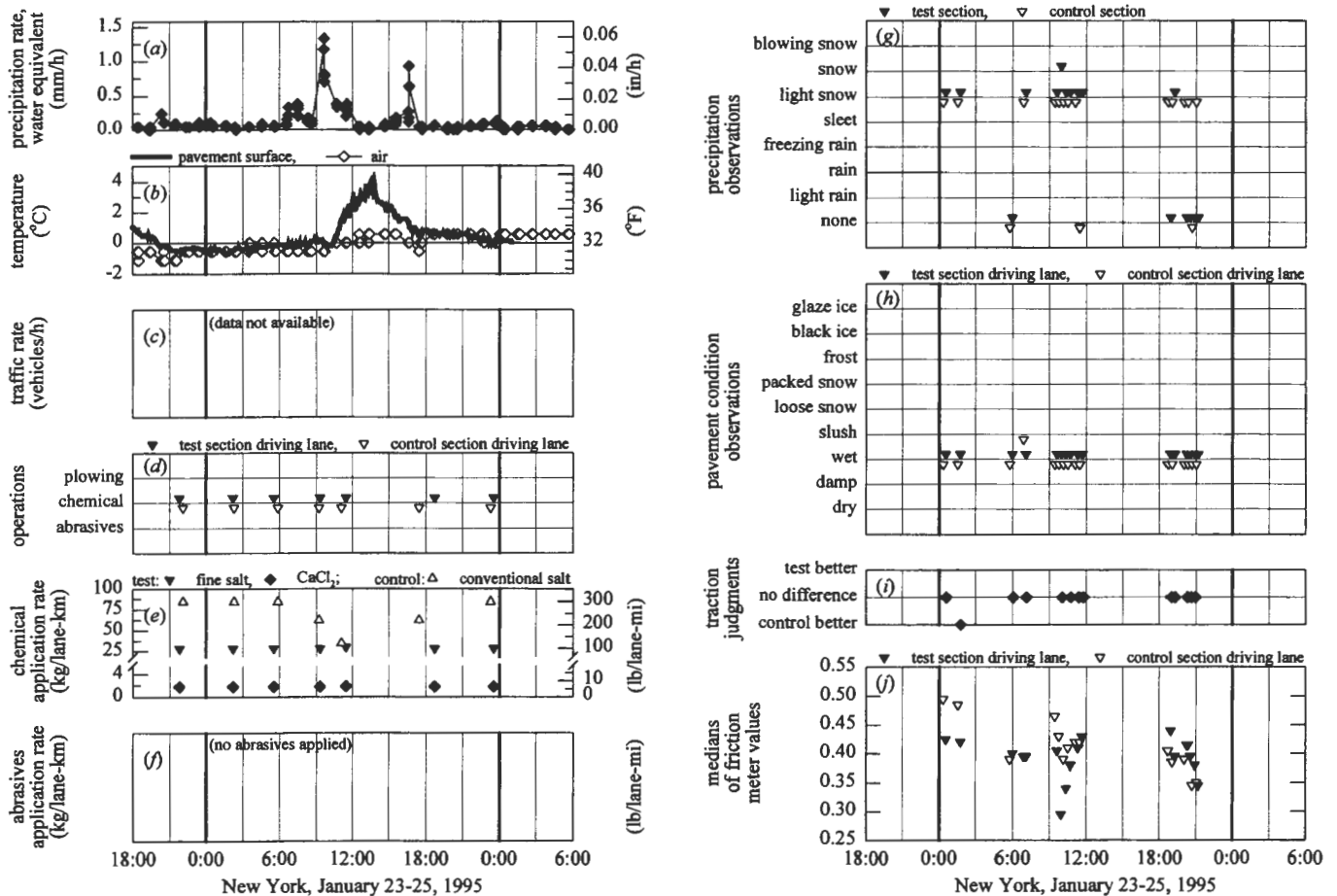
FIGURE 1   Data histories of storm of January 23–25, 1995, New York site, asphalt pavement section: (a) water equivalent precipitation rate, (b) temperature, (c) traffic rate, (d) operations, (e) chemical application rate, (f) abrasives application rate, (g) precipitation observations, (h) pavement condition observations, (i) traction judgments, (j) medians of friction meter values.
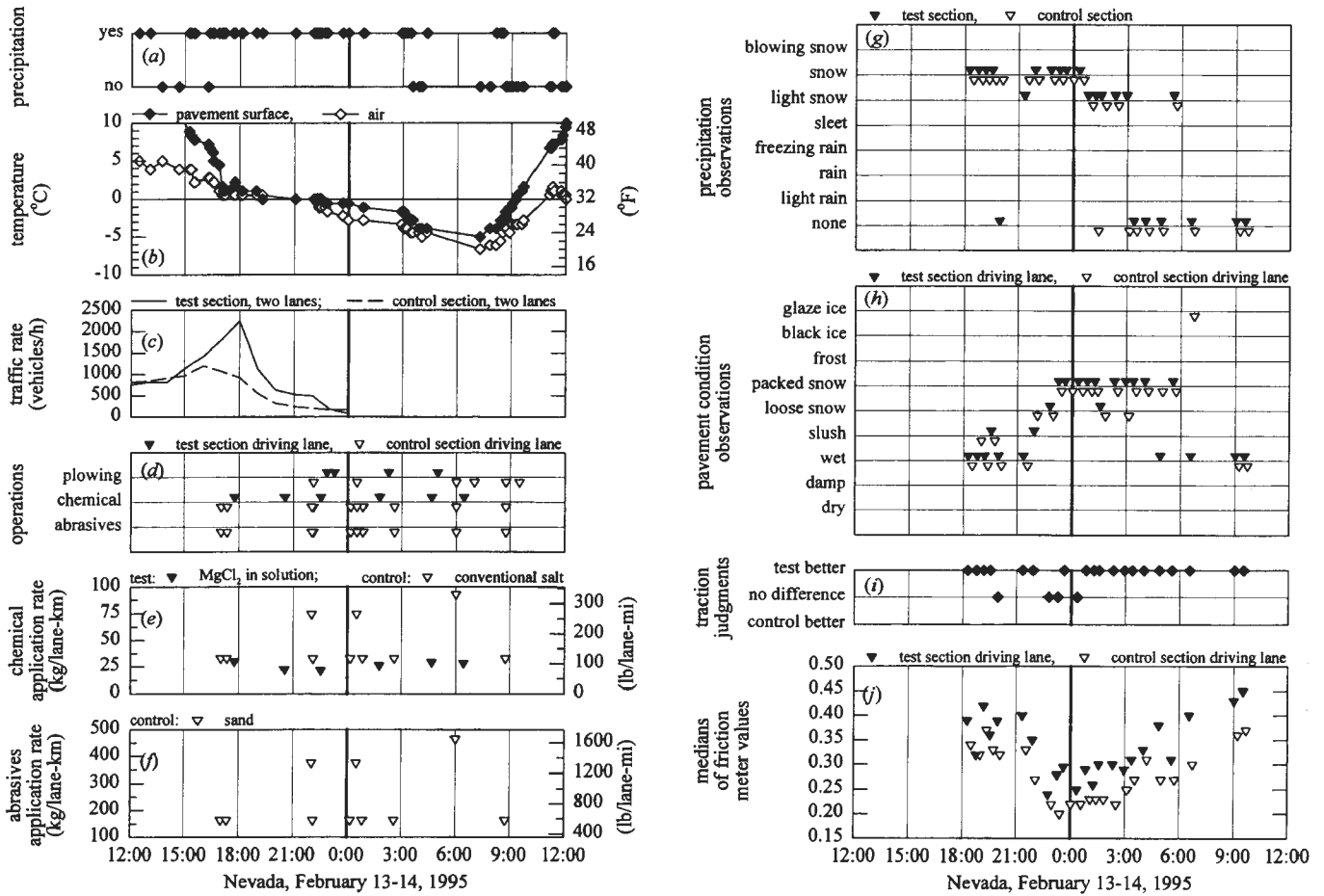
FIGURE 2 Data histories of storm of February 13–14, 1995, Nevada site: (a) precipitation, (b) temperature, (c) traffic rate, (d) operations, (e) chemical application rate, (f) abrasives application rate, (g) precipitation observations, (h) pavement condition observations, (i) traction judgments, (j) medians of friction meter values.

Lake Ontario in the city of Webster, and Figure 2 contains data histories from the February 13–14, 1995, storm at the Reno, Nevada, site.

Figures 1 and 2 each contain 10 graphs. The left columns are histories of (a) precipitation from the RWIS data—that is, the precipitation rate in Figure 1 and a yes-or-no indication of precipitation in Figure 2; (b) pavement surface and air temperatures, also from the RWIS data; (c) traffic rates on the test and control sections; (d) the plowing, chemical, and abrasives operations on the test and control section driving lanes; (e) the chemical application rates; and (f) the abrasives application rates. The right columns present histories of (g) the precipitation observations, (h) the pavement condition observations, (i) the traction judgments, and (j) the friction meter values, all of which were recorded by the driver or passenger in the measurement vehicle. The observation graphs display categories of precipitation and pavement condition that could be selected during the on-road data collection.

All data histories developed for the project included many features of the graphs in Figures 1 and 2:

- The time scale appears at the bottom of each column. It is shown with grid lines at 3-hr increments and a heavier grid line at midnight or 0:00.
- Only driving lane operations are shown.
- All operations, observations, traction judgments, and friction data are plotted at the time of the beginning of the pass.
- The number of lanes used to calculate the application rates is the integer number of lanes over which material is spread.
- All application rates of chemical solutions, whether for prewetting of solids or straight liquid applications, present the rate of the solute, or dry chemical, in the solution.
- On the operations and observations graphs, test section data points are indicated slightly above control section points.

TABLE 1   Summary of Driving Lane Operations, New York, January 23–25, 1995

| | Section | |
	Test	Control
Total number of passes:	7	7
Number of passes with plowing:	0	0
Number of passes with fine salt application:	7	0
Total application of fine salt, kg/lane-km (lb/lane-mi):	199 (707)	0
Number of passes with conventional salt application:	0	7
Total application of conventional salt, kg/lane-km (lb/lane-mi):	0	497 (1763)
Number of passes with application of calcium chloride prewetting solution:	7	0
Total application of calcium chloride, kg/lane-km (lb/lane-mi):	13 (45)	0
Number of passes with abrasives application:	0	0
Total application of abrasives, kg/lane-km (lb/lane-mi):	0	0

- Precipitation and observation data points represent the mode—the most frequent observation—of the multiple observations made during a pass.
- The friction value data point plotted is the median—the 50th percentile—of the multiple friction measurements made during a pass. The friction values are those of maximum braking action, of either conventional or antilock braking systems.

Summaries of the driving lane operations during the two storms are presented in Tables 1 and 2. Each table lists the total number of passes as well as the number of passes with plowing, chemical, and abrasives operations. The total applications of the various materials are given as well, presented per unit lane-kilometer (lane-mile). If a pass included more than one task, for example, if plowing and chemical operations were conducted simultaneously, or if a mix of abrasives and chemicals was applied, the tables list separately the component tasks or applications.

Storm Data Interpretations

The storms depicted in Figures 1 and 2 were chosen to illustrate the diversity of operations in the project and

the depth of data interpretation conducted for the project. Comments based on the full data analysis for each storm are presented in the following sections.

New York, January 23–25, 1995

At the New York site the test and control sections were 11-km (7-mi) sections of NY-104. The eastbound lanes were the test section and the westbound lanes were the control. Throughout the season the chemical operations on the test section were primarily applications of fine salt prewetted with a calcium chloride ($CaCl_2$) solution, while dry conventional rock salt was used mainly in the control section operations. The operations and data collection were conducted by New York State Department of Transportation (NYSDOT) maintenance personnel.

The January 23–25 storm was a light snow storm with one period of heavier snow. Before the event, lake effect snow flurries and showers were forecast to begin in the afternoon hours on January 23 and continue into the next day. Accumulations of up to 50 mm (2 in.) were predicted. The pavement temperature was forecast to drop to and below freezing after 9:00 p.m. and remain below freezing until the morning peak hour. The pavement temperature indicated in Figure 1(b) reflects this prediction, hovering just below freezing during the ear-

TABLE 2   Summary of Driving Lane Operations, Nevada, February 13–14, 1995

| | Section | |
	Test	Control
Total number of passes:	11	12
Number of passes with plowing:	5	6
Number of passes with application of magnesium chloride solution:	6	0
Total application of magnesium chloride, kg/lane-km (lb/lane-mi):	159 (565)	0
Number of passes with conventional salt application:	0	10
Total application of conventional salt, kg/lane-km (lb/lane-mi):	0	474 (1682)
Number of passes with abrasives application:	0	10
Total application of abrasives, kg/lane-km (lb/lane-mi):	0	2367 (8398)

lier part of the operations and rising slightly above freezing after the morning peak period on January 24 to well above freezing during the midday hours. In the evening hours of January 24 the temperature dropped again toward freezing. Traffic counts were not available for the storm, but workday traffic on the test section driving lane typically reaches 1,000 vehicles per hour (vph) in the morning peak period, fluctuates between 500 and 1,000 vph midday, and increases to 1,500 vph in the afternoon peak period.

As indicated in Figure 1(d) and Table 1, test section applications of the prewetted fine salt, and control section applications of conventional rock salt, were the only operations conducted during the January 23–25 storm. No abrasives were applied, and because conditions did not warrant them, plowing operations were not conducted. The initial fine salt–$CaCl_2$ solution application was made about 2 hr after the pavement temperature dropped to freezing and snowfall began. Snow covered the highway at the time of the application, according to storm records. Although observations and friction measurements were not made until more than 4 hr after the beginning of the storm, the supervisor's log and other data suggest that earlier operations were not warranted and the initial operation was indeed preventive. Control section salt applications were begun soon after the test operations. Throughout the storm there was similar timing of the chemical applications on both test and control. This timing was not unusual at the New York site and indicates that preventive anti-icing practices are built into conventional operations. In the same number of passes, however, more than twice as much chemical was used on the control section driving lane as on the test section driving lane (Table 1).

As indicated by the predominantly wet pavement conditions in Figure 1(h) and the fact that bonded snow and ice was clearly prevented, both the test and the control operations were successful anti-icing operations. Although these were developmental anti-icing operations, very little obscures their success. A January 24 late-morning increase in snowfall resulted in a temporary drop in friction on both sections, although the drop was greater on the test section, perhaps reflecting the lower chemical rate used there. A subsequent rise in pavement temperature above freezing resulted in a rapid increase in friction. A miscommunication resulted in the application of chemicals on both the test section and control section driving lanes after this rise in pavement temperature, although the supervisor had recognized that the application was not necessary and had sent trucks only to plow shoulders.

Although more than twice as much chemical was used on the control section driving lane as on the test section, the observation, traction, and friction data do not indicate significantly greater control section effec-

tiveness, suggesting that the test section fine salt application rate at an average of approximately 28 kg/lane-km (100 lb/lane-mi) is more appropriate for light snow and relatively high pavement temperature than the control section conventional rock salt application rate at an average of 70 kg/lane-km (250 lb/lane-mi).

Nevada, February 13–14, 1995

The Nevada test and control sections were 10-km (6-mi) sections of US-395 in the northbound and southbound directions, respectively. For the season the chemical operations on the test section were mostly applications of a magnesium chloride ($MgCl_2$) solution, and a conventional 1:5 rock salt–sand mixture was used on the control section. The operations and data collection were conducted by Nevada Department of Transportation (NDOT) maintenance crews.

The precipitation observations in Figure 2(g) show that this storm consisted of several hours of moderate and heavy snowfall followed by light snow. Maintenance crews referred to the storm as the "St. Valentine's Day Massacre." Forecasts called for light rain changing to a snow-rain mix at 5:00 p.m. on February 13 and pavement temperatures dropping to freezing at 6:00 p.m. The mix was predicted to change to all snow during the evening and last into the following day with accumulations up to 150 mm (6 in.), and freezing or below-freezing pavement temperatures were predicted to remain until after daylight the next morning. The forecasts were accurate.

The traffic rate data in Figure 2(c), although not complete, reflect peak hour directional variations of the afternoon of February 13. On the basis of traffic records from other days, data from February 14 would probably have shown a morning peak period with two-lane control section rates peaking at close to 2,500 vph and two-lane test section rates close to 1,000 vph.

On the test section the $MgCl_2$ solution was initially applied after light snow had begun and the road was wet. The timing was based on rapidly falling pavement temperature, which was expected, and provided a good demonstration of the use of RWIS data and RWIS-based forecasts for timing decisions. Subsequent $MgCl_2$ applications were made on the basis of observations of conditions and RWIS pavement temperature and chemical concentration data. Control section sand and salt applications were begun just before the test operations. Like the timing of the initial New York operations, this timing was not unusual and illustrates the preventive nature of the Nevada conventional operations and their reliance on RWIS and other information sources. Table 2 shows that throughout the storm three times as much chemical was used on the control section driving lane as on the test section driving lane. No abrasives were used on the test section, whereas 2367 kg/lane-km (8,398

lb/lane-mi) of sand was used on the control section driving lane.

The percentage breakdown of all test section pavement condition observations was 42 percent packed snow, 37 percent wet, 9 percent slush, 8 percent loose snow, and 3 percent damp. On the control section the breakdown was 44 percent packed snow, 22 percent wet, 16 percent loose snow, 14 percent slush, and 4 percent glaze ice. The chi-square statistical test (4) showed a significant difference between the test and control observations. This difference is probably because although both operations resulted in the development of undesirable sustained packed snow conditions, the test section operations resulted in more wet and fewer loose snow or slush observations, which is desirable.

Figure 3 depicts the friction distributions for the February 13–14 storm and for the 1994–1995 season. Figure 3(a) is a graph showing Tukey box plots of test section and control section friction data from the storm, which are distributions of all measured friction values of the sections during the storm. The top of a box indicates the 75th percentile (i.e., 75 percent of the observations were at or below that friction value on the left scale), and the bottom indicates the 25th percentile. The line inside a box is the median, or the 50th percentile. The single line above a box is the 90th percentile and that below a box the 10th percentile. The distributions provide a graphical comparison of the test and control section data. A further comparison was provided by results of the Mann-Whitney rank sum statistical test (4), which reveals whether the medians of the test and control friction are significantly different. As indicated in Figure 3(a), the test found a significant difference. Both the distribution and the median were higher for the test section friction data, re-

flecting the Figure 2(j) data showing that the test section friction was higher throughout the storm.

Figure 3(b) shows box plot distributions from the combined friction and observation data of 14 storms of the season. The variation of the distributions with pavement condition category is reasonable and provides confidence in both the friction and pavement condition data as independent effectiveness measures. By comparison of the storm distributions of Figure 3(a) and Figure 3(b), the test section median value of the storm was typical of a slush pavement condition, whereas the control section median friction was typical of loose snow or packed snow conditions. Although more chemical was used on the control section, and sand was used only on the control section, the overall storm test section friction was higher, reflecting a better pavement condition. In addition to the friction and observation data showing better test section conditions, the measurement vehicle operator's judgments graphed in Figure 2(i) suggest that the test section usually had better traction.

The development of packed snow on both test section and control section driving lanes occurred during a period of heavy snow and low nighttime traffic. At 10:30 p.m. on February 13, a test section application of the $MgCl_2$ solution was made onto loose snow just before the development of pack. The operator noted that the road was "covered" and snowfall was "heavy." Plowing did not precede this application, however.

During the period of packed snow on both sections, much more chemical was used on the control section driving lane than on the test section driving lane, and a large quantity of sand was placed on the control section driving lane. The greater chemical amounts and use of abrasives during this time did not lead to better friction or traction, or an earlier breakup of the pack,
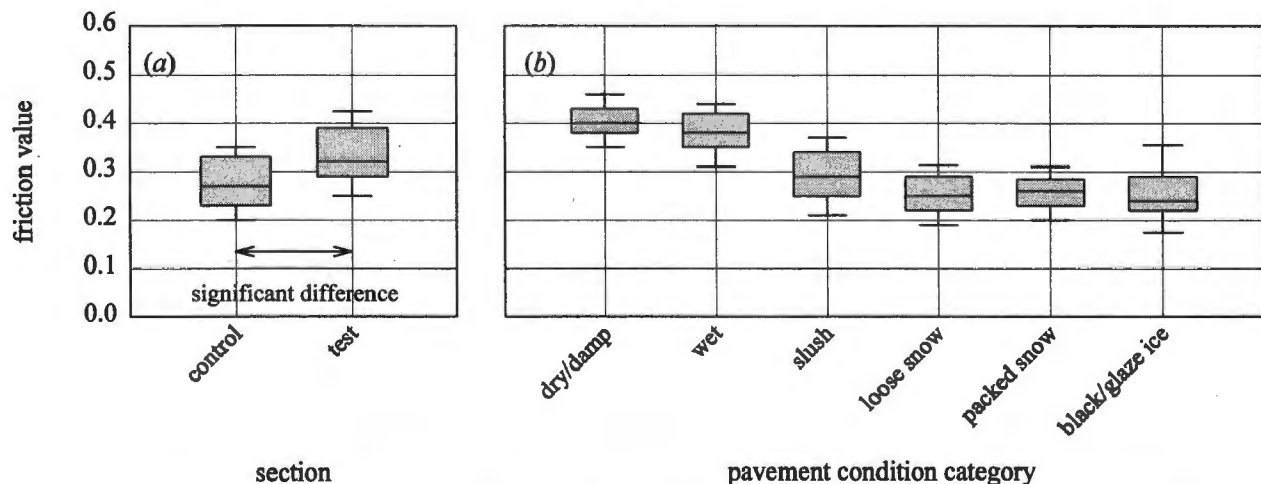

FIGURE 3   Nevada friction distributions: (a) as function of section for February 13–14, 1995, storm, and (b) as function of pavement condition category for 1994–1995 season.

however. In fact, the packed snow broke sooner on the test section. Regular plowing operations, moderate applications of the MgCl₂ solution, and precipitation changing from moderate snow to light snow to no snow led to the test section breakup *before* peak hour traffic. For the test section, traffic was not a factor. The later breakup of the control section snowpack coincided with a rise in pavement temperature and peak hour traffic.

The Figure 2 data indicate that the application rates of the $MgCl_2$ solution were too low or the number of passes before the development of the packed snow were too few to prevent a bonded snowpack with the snowfall, temperature, snow moisture, and traffic conditions of the storm. Plowing ahead of liquid applications appears essential when snowfall is heavy and with conditions of loose snow on the pavement. Even so, the test section operations resulted in an apparently weaker and easier-to-clear compacted snow–pavement bond than did the control section operations. For the control section abrasives applications, no evidence in Figure 2(*j*) indicates a short- or long-term increase in test section or control section friction caused by their use. In fact, during the storm the measurement vehicle operator described a friction test after an abrasives application as "sliding on sand," suggesting that the abrasives application had a detrimental effect on friction.

Discussion of Results

Beyond the specifics of the individual events, the two storms reveal much about the nature of the project and how the results could be used to develop recommendations for practice. As typified by the New York and Nevada operations, very few of the conventional operations of the project were traditional deicing operations in which, typically, plowing and chemical applications are initiated to remove already bonded snow or ice. In fact, several of the conventional operations were high service level operations that in many ways were preventive in nature and yielded insight into the anti-icing process. This is probably because of prior implementation by state and site personnel of technology such as RWIS and site-specific weather and pavement forecasts, anti-icing practices developed during SHRP H-208 (2), and other preventive techniques over the course of several years. Nonetheless, relative to the operations specified in the manual of practice (1), even the anti-icing operations of the project represent development phase operations. This is precisely because the results of the field evaluation provided the basis for the development of comprehensive guidance for imple-

menting the anti-icing process at efficient chemical application rates.

The nature of the project is further reflected by the timing of the initial operations of the two storms. Although prestorm chemical applications can certainly be effective, anti-icing has previously been associated wholly with this timing of the initial treatment. In neither storm example was the initial test section chemical application made in advance of precipitation. This was the intentional strategy of the supervisors, and both operations were successful—the first by preventing the formation of the bond and the second by preventing the development of a strong bond. By relying on local personnel to develop their own anti-icing strategies, the project was able to demonstrate the range of application timings that can either prevent the bond altogether or reduce its severity. More important, by the design of the experiments the project was able to build such field-demonstrated lessons into the manual of practice.

Beyond timing of the initial chemical application, further indication of the diversity of successful operations is provided by classifying the various chemical treatments. In the two storms presented, four general chemical treatment types were used: a dry solid chemical, a prewetted solid chemical, a dry solid chemical in a mix with abrasives, and a chemical solution. Together with a prewetted chemical–abrasives mix, these were the types used in the project. Three of these—solid chemical, liquid chemical, and prewetted solid chemical, as they are classified in the manual of practice (1)— were demonstrated to be efficient anti-icing treatments under a variety of conditions and are covered in the manual's guidance. However, as the results did not show any consistent advantage to the use of abrasives with chemicals, there are no grounds for recommending their use, and therefore no guidance is given.

CONCLUSIONS

Improvements in snow and ice control have long been made by winter maintenance forces by shifting toward preventive instead of reactive practices. Recognizing this, the anti-icing field evaluation conducted under FHWA T&E 28 accommodated both conventional and modern preventive practices and, by analysis of the operations and their effectiveness, identified the diversity of operations that can support the bond-prevention objective of anti-icing. The result is a field-derived manual of practice that provides comprehensive guidance for implementing efficient anti-icing practices. Although information sources, technology, and education are required to use the guidance—particularly site-specific forecast information and pavement temperature, effi-

cient spreaders to apply chemicals at desired rates, and anti-icing training for maintenance crews—the guidance can readily be implemented to provide a high level of service. For managers involved in implementing anti-icing practices, it is well to recognize that both conventional and high-technology preventive practices, intelligently applied, can be the foundation on which to build a successful program.

ACKNOWLEDGEMENTS

REFERENCES

1. Ketcham, S. A., L. D. Minsk, R. R. Blackburn, and E. J. Fleege. *Manual of Practice for an Effective Anti-Icing Program: A Guide for Highway Winter Maintenance Personnel.* Report FHWA-RD-95-202. FHWA, U.S. Department of Transportation, Washington, D.C., 1996.
2. Blackburn, R. R., E. J. McGrane, C. C. Chappelow, D. W. Harwood, and E. J. Fleege. *Development of Anti-Icing Technology.* Report SHRP-H-385. National Research Council, Washington, D.C., 1994.
3. Ketcham, S. A., and L. D. Minsk. *Test and Evaluation Project 28, Anti-Icing Technology, Field Evaluation Report.* FHWA, U.S. Department of Transportation, Washington, D.C. (in preparation).
4. *SigmaStat™ Statistical Software for Windows™ User's Manual.* Revision SSW 1.0. Jandel Scientific, San Rafael, Calif., 1994.

Test and Evaluation of Calcium Magnesium Acetate–Sodium Chloride Mixtures in Sweden

Anita Ihs and Kent Gustafson, *Swedish National Road and Transport Institute*

Together with plowing and sanding, chemical deicing and deicing agents are important tools for highway snow and ice control. The most commonly used deicing agent is sodium chloride (NaCl), which is effective, easy to handle, and inexpensive. Many negative and often costly side effects, have, however, been recognized over the years. Extensive research has therefore been conducted to find alternatives. Calcium magnesium acetate (CMA) is an alternative deicing agent that has given very promising results in laboratory and field tests. The most significant impediment to its use is its high price, which is more than 20 times that of NaCl. To reduce the cost but maintain the benefits of CMA, tests have been conducted with CMA-NaCl mixtures. In 1993 the Swedish National Road and Transport Research Institute initiated a research project to test and evaluate a mixture of 20 percent CMA and 80 percent NaCl. The field evaluation was conducted on Highway E4 and included both friction measurements and corrosion tests. The laboratory testing, mainly done at the Swedish National Testing and Research Institute, included corrosion tests and freeze-thaw testing on cement concrete. The laboratory tests showed that the addition of CMA to NaCl does reduce the corrosion of steel and the scaling of concrete. The field tests also indicated reduced corrosion of steel, but not to the same extent as the laboratory tests. Furthermore, the same deicing could be obtained with the CMA-NaCl mixture as with NaCl.

The Swedish National Road and Transport Research Institute (VTI), in cooperation with the Swedish National Road Administration, has conducted research projects to test and evaluate salting methods and alternative deicing agents for many years. From 1985 to 1990 the Swedish MINSALT program, "minimizing the adverse effects of salt," was carried out with the aim of finding more effective ways to improve skid resistance without the negative effects of salt (NaCl). The results from the MINSALT projects have been reported in various reports and summarized in a final report (1).

Chemical deicing (salting) spreading methods have progressed from the earlier use of dry salt to the use of prewetted salt and saline solutions. The results from the MINSALT projects have led to a proposed strategy to reduce salt consumption and make salting more effective. This has been accomplished by working more with anti-icing measures, before the icy conditions occur, and less with deicing. Prewetted salt or brine is used.

A number of different chemical alternatives to NaCl have been tested. In particular, calcium magnesium acetate (CMA) has been studied closely for ice-melting capacity, corrosiveness, and effect on concrete. Studies of alternatives have also included chemicals suitable for runway purposes. Potassium acetate, a liquid deicer, has been tested and is now used at some Swedish airports (2,3).

Since CMA is very expensive, more than 20 times more costly than NaCl, tests have been conducted with CMA-NaCl mixtures. In the United States very promising results regarding the corrosive effect have been obtained by mixing NaCl and CMA. Tests conducted in Minnesota with a mixture of 20 percent CMA and 80 percent NaCl by weight showed that this mixture can give a significant reduction of the corrosion rate (4).

In 1993 the Swedish National Road Administration commissioned VTI to start a research project to test and evaluate a mixture of 20 percent CMA and 80 percent NaCl by weight. The evaluation included a field study of the operational effects under varying weather and road surface conditions and laboratory testing of deicing properties, corrosive effects, and the effect on cement concrete. The latter two tests were made by the Swedish National Testing and Research Institute (SP). The corrosion tests were conducted with steel plates in a climate chamber under simulated field conditions, and the effect of various mixtures of CMA and NaCl on cement concrete was investigated by freeze-thaw testing.

METHOD

Laboratory Tests

Ice Melting Rate

The melting capacity of the 20/80 CMA-NaCl mixture was tested on blocks of ice at three temperatures, −2, −6, and −10°C. For comparison, pure NaCl and CMA also were included in the test. The deicer was evenly spread over the surface of the 114-cm^2 ice block in two amounts, 10 and 20 g. The melted ice or brine that formed on the surface of the block of ice was decanted at specified time intervals and weighed.

Corrosion

The corrosive effect of the CMA-NaCl mixture on steel plates was investigated by SP (5). A spray test was performed in a climate chamber under simulated field conditions. The chamber is divided into two sections to allow two deicers to be tested at the same time under identical conditions. In one of the sections a 3 percent aqueous solution of the 20/80 CMA-NaCl mixture was sprayed onto the steel plates, and for comparison a 3 percent aqueous solution of NaCl was used in the other section.

Freeze-Thaw Test on Cement Concrete

Freeze-thaw tests were conducted by SP to determine the effect of various CMA-NaCl mixtures on cement concrete (6). The method used was based on the Swedish Standard SS 13 72 44 according to which a sawed concrete surface is exposed to a 3 percent NaCl solution during 56 freeze-thaw cycles. Four proportions of CMA-NaCl were included in the test: 0/100, 20/80, 40/60, and 100/0, and cement concrete of three qualities was used: (A) an old type of concrete, made before air-entraining agents came into use, (B) a modern type of concrete with air-entraining agents added, and (C) a very dense concrete of high quality, which is used only in certain structures but which is expected to be more common in the future; this concrete is air-entrained and also contains 5 percent silicon dust. An investigation of the effect of higher concentrations of CMA on cement concrete was also conducted.

Field Tests of CMA-NaCl Mixture on Highway E4

Deicing Performance

Field studies were undertaken during the winters of 1993–1994 and 1994–1995 on a section of Highway E4, which is a four-lane divided highway with bituminous surfacing. To compare the performance of the CMA-NaCl mixture and NaCl as deicing agents, skid resistance measurements and pavement surface observations were conducted on a test (CMA-NaCl) section and a control (NaCl) section. Each section was about 20 km long and included both north- and southbound lanes. Within the test and control sections were a number of 400-m-long sampling sections, in both the driving and the passing lanes, in which the skid resistance measurements were conducted. The sampling sections were selected to be uniform for pavement cross section, flatness, traffic, and other conditions. This segment of Highway E4 does not experience the effects of peak hour or commuting traffic.

Friction measurements and pavement surface observations were made at each of the sampling sections during a number of situations with slippery conditions. The friction measurements were made using a SAAB Friction Tester. The skid resistance monitoring and pavement surface observations were usually made before the spreading operation, 10 to 30 min after spreading, and then at intervals of 45 to 60 min until a stable or bare pavement condition was reached. In addition, the atmospheric conditions and pavement temperatures were monitored by using two road weather information system stations, which were located in the test and control sections. The time of application and the application rate were reported by the operators of the spreading vehicles.

The mixture used in the field testing was 20 percent CMA and 80 percent NaCl by weight. The mixture was prepared by using a small double hopper with a conveyor belt (Figure 1). The accuracy of the mixture was checked

FIGURE 1   Mixing CMA-NaCl by using a small double hopper with conveyor belt.

by taking a sample of the mixture and then separating and weighing the salt and CMA compounds.

Corrosion

To study the corrosive effect of the CMA-NaCl mixture under more realistic and varying conditions, field experiments were conducted by placing steel plates in the median of the road between the northbound and southbound lanes (5). Five painted and five unpainted steel plates were mounted on a stand (Figure 2). The painted steel plates were provided with a scratch to be used for evaluating the formation of cracks and scaling caused by corrosion. Two stands were placed at the test and control sections, one stand facing the northbound lane and the other facing the southbound lane (Figure 3). The atmospheric corrosion rate was monitored with five unpainted plates placed far from the road at each section (Figure 4). By subtracting the atmospheric corrosion from that of the specimens at the road side, the corrosive influence from the road environment could be evaluated.

FIGURE 3   Panel with steel plates for corrosion test, placed between northbound and southbound lanes of Highway E4.

After the first winter the steel plates were taken down, the rust was removed, and the weight loss of the plates was determined. The test was repeated with new steel plates the second winter.

RESULTS

Laboratory Tests

The ice-melting rates at –6°C for NaCl, CMA, a 20/80 mixture of CMA and NaCl, and sodium acetate (NaAc) are shown in Figure 5. It can be noted that CMA has a considerably lower melting rate than NaCl. Especially, CMA has a very slow initial melting effect compared with NaCl. The melting rate for the CMA-NaCl mixture is, however, not very much lower than that for NaCl. The same relationships are found at lower temperatures, but under those conditions the slower melting effect of CMA is even more pronounced.

According to the results of the corrosion test in the climate chamber, the CMA-NaCl mixture reduced the

FIGURE 2   Steel plates, five painted and five unpainted, for corrosion test.

FIGURE 4   Steel plates for monitoring atmospheric corrosion.

Meltwater (g)
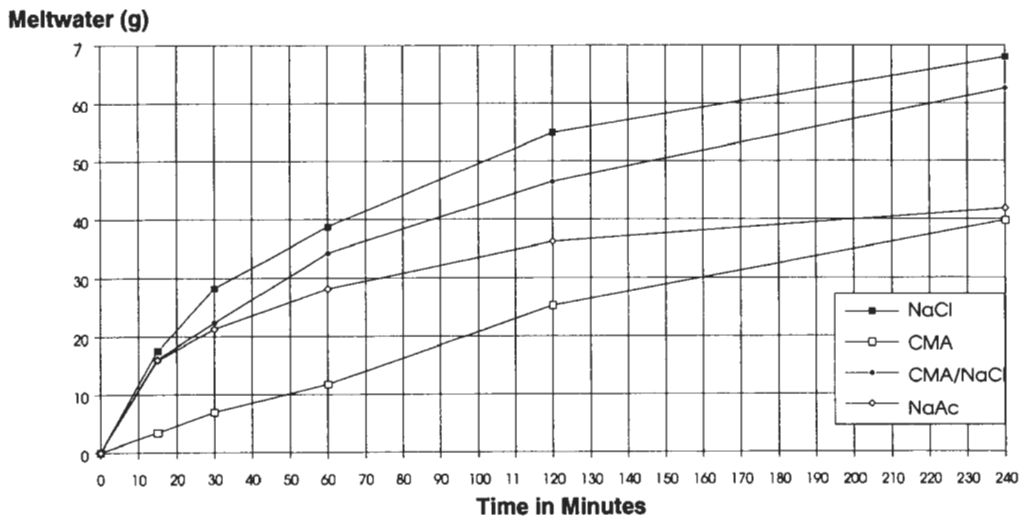
Note: 10 g deicer spread on blocks of ice.

FIGURE 5   Ice-melting rate at −6°C for various deicers.

corrosion rate of steel by 45 percent compared with NaCl. The results from the laboratory tests are presented in Figures 6 and 7, together with the results from the field corrosion tests.

The concrete scaling obtained after 56 cycles of freezing and thawing is shown in Table 1. As expected, the scaling of the old type of concrete (A) caused by NaCl is very extensive. The concentration of the solutions used in the test was chosen to be 3 percent since earlier experiments had shown that the degradation caused by NaCl has a peak at this concentration (7). When NaCl is partly replaced by CMA in the solution,

the scaling is significantly reduced. The scaling caused by NaCl on modern, air-entrained concrete (B) is very small, but even here a reduction can be observed when NaCl is partly or fully replaced by CMA.

Field Tests

During winter 1993–1994 approximately 10 percent more applications of deicing agent were made and about 17 percent more material was spread on the control section with NaCl than on the test section with CMA-NaCl.

Weightloss (g/m²)
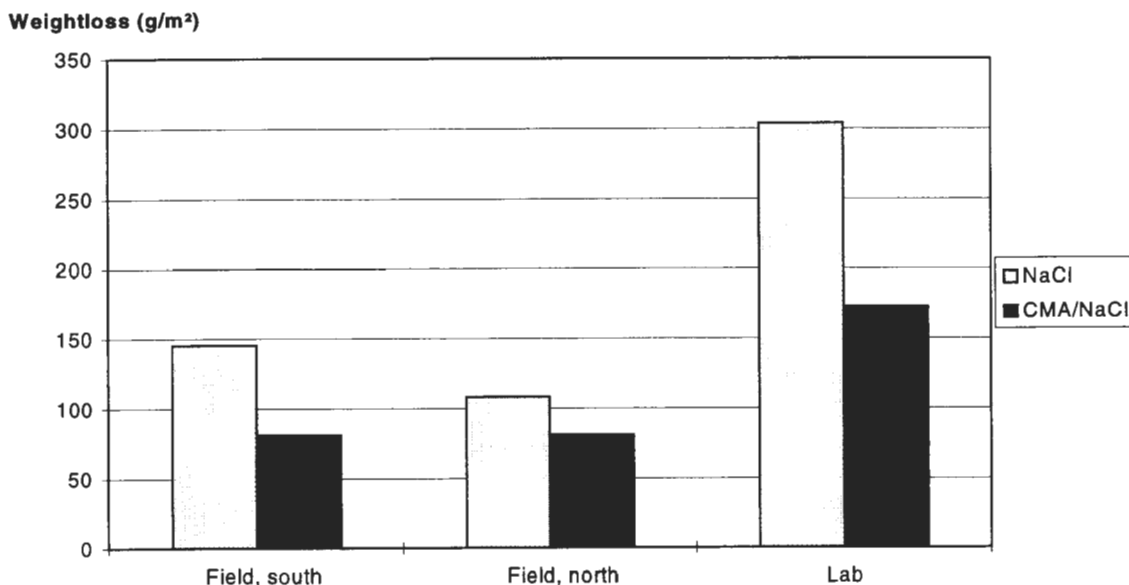
FIGURE 6   Corrosion tests performed during winter of 1993–1994. Histogram shows results from field exposures at both southbound and northbound lanes. For comparison, results from laboratory experiments performed in climate chamber are presented.

Weightloss (g/m²)
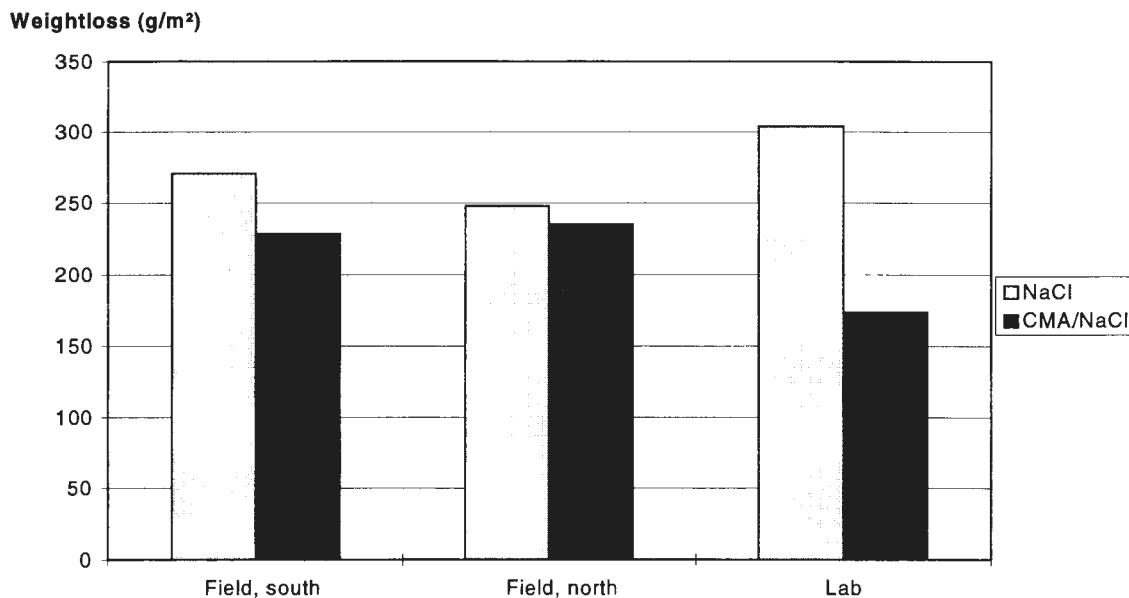
FIGURE 7   Corrosion tests performed during winter of 1994–1995. Histogram shows results from field exposures at both southbound and northbound lanes. For comparison, results from laboratory experiments performed in climate chamber are presented.

Maintenance personnel explained the difference by saying that when they applied NaCl to the control section, they sometimes judged that compared with the NaCl, the CMA-NaCl was having a longer-lasting effect and did not need to be applied again to the test section. Nine storms and approximately three times as many applications of chemicals were followed closely by monitoring the skid resistance. According to the friction measurements, the CMA-NaCl mixture worked as well as, and in some cases even better than, NaCl in situations with slippery conditions. There were also situations in which NaCl worked better but these were not as frequent.

For the winter of 1994–1995 the locations of the test and control sections were switched and results almost opposite to those of the first winter were obtained. Approximately 10 percent more applications were made and as much as 28 percent more material was spread on the test section. This result led to the conclusion that the difference in application rate and amount of chemicals on the test and control sections was due

mainly to different local climates along the sections. In 1994–1995 the operational effects were studied during six storms, and the friction measurements also showed that it was possible to obtain the same deicing with the CMA-NaCl mixture as with NaCl. As an example, the skid resistance monitoring performed during one storm in March 1995 is shown in Figure 8.

The results for corrosion from the field test the first winter pointed in the same direction as the results from the laboratory test, indicating that the corrosion rate is reduced by adding CMA to NaCl (Figure 6). The reduction was not as large as in the laboratory test, however. There was also a difference between the northbound and the southbound directions. The reduction of the corrosion rate for the CMA-NaCl mixture was approximately 45 percent on the plates facing the southbound lanes and 20 percent on the plates facing the northbound lanes. The difference in the two directions may have been caused by wind direction or traffic influence. The difference in corrosion rate for the CMA-NaCl mixture and NaCl not only is explained by the materials, but depends also to some extent on the difference in number of applications and amount of material spread. During the first winter more applications were made and a larger amount of material was spread on the control section where the highest corrosion rate was also obtained.

During the second winter, when the test and control sections had been switched, the situation for the number of applications and amount of material was reversed. Although more chemicals were spread on the test section, the corrosion rate was lower than at the control section (Figure 7). The reduction of the corro-

TABLE 1   Scaling of Three Qualities of Concrete After 56 Freeze-Thaw Cycles

Alt.	Solution	Scaling (kg/m²)		
		A	B	C
1	NaCl 3 %	13.78	0.03	
2	CMA/NaCl 20/80 weight-%	10.84	0.01	0.03
3	CMA/NaCl 40/60 weight-%	3.79	0.01	0.01
4	CMA 3 %		0.01	0.01
5	CMA 10 %		0.01	
6	CMA 20 %		0.01	

Note: A is an old type of concrete, B and C are two different modern types of concrete with air-entraining agents added.
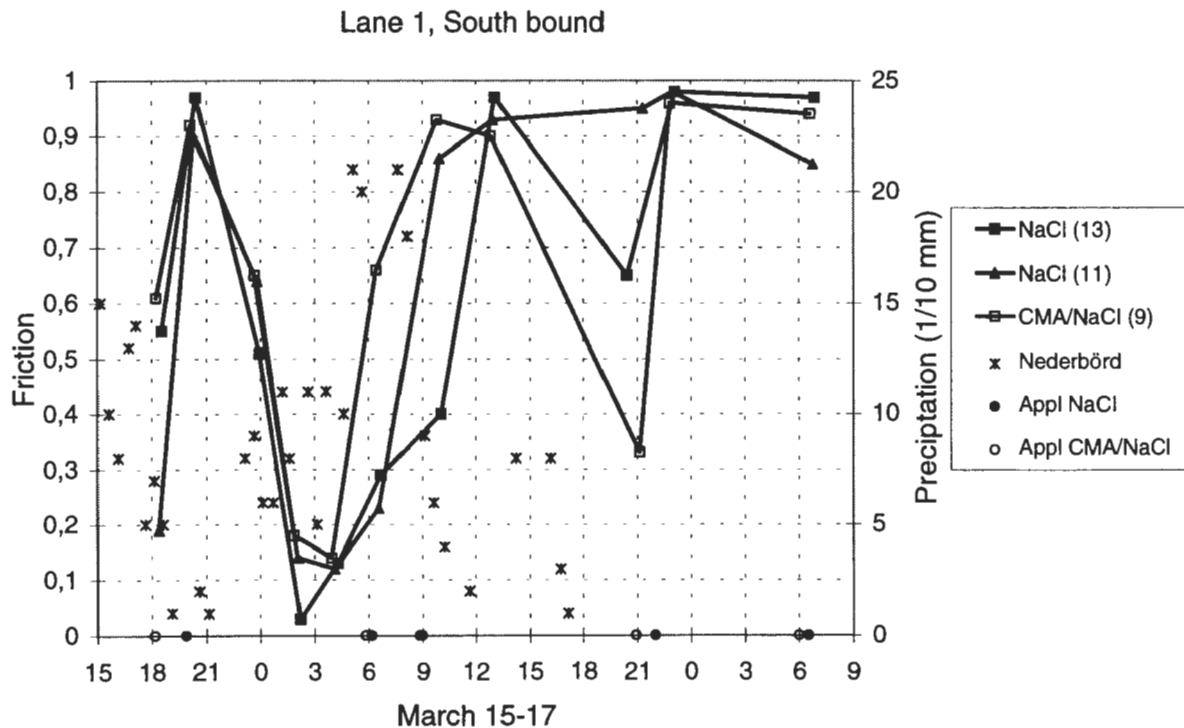
FIGURE 8 Friction measurements conducted in northbound driving lane during snow storm in March 1995. Numbers in parenthesis refer to sampling sections within test and control sections.

sion rate for the CMA-NaCl mixture was, however, considerably smaller than that of the first winter. The reduction was approximately 16 percent on the plates facing the southbound lanes and 5 percent on the plates facing the northbound lanes.

CONCLUSIONS

During the period 1993–1995 a mixture of 20 percent CMA and 80 percent NaCl by weight was evaluated in laboratory and field tests. The results from the tests are summarized here.

- Deicing properties
    - Laboratory tests showed that the 20/80 CMA-NaCl mixture has an ice melting capacity similar to, but somewhat less than, that of salt.
    - Friction measurements showed that the 20/80 CMA-NaCl mixture works as well as NaCl in most situations with slippery conditions.
    - The effect of the 20/80 CMA-NaCl mixture was not observed to last longer than that of NaCl.
- Corrosion
    - Corrosion tests in a climate chamber resulted in a reduction of the corrosion rate by 45 percent for the CMa-NaCl mixture compared with NaCl.

- In the field tests, the 20/80 weight-% CMA-NaCl mixture also gave a certain reduction in corrosion rate as compared with NaCl. The reduction was, however, not as large as that in the laboratory tests.
- Concrete
    - On concrete of poor quality, a very large scaling was observed for NaCl in freeze-thaw tests. The scaling was considerably reduced by replacing some of the NaCl with CMA.
    - On modern, air-entrained concrete of good quality, the scaling was very small even for NaCl. A reduction of the damage was observed for the 20/80 CMA-NaCl mixture.

The price for CMA is about 20 times the price for NaCl, which means that the 20/80 CMA-NaCl mixture is about 5 to 6 times more expensive than NaCl. Although a cost-benefit analysis has not been done, it is doubtful if the benefit from the reduced corrosion, in particular, is large enough to compensate for the high price of the CMA-NaCl mixture. Furthermore, the environmental effects of CMA have not been considered in this study. Many studies have shown that CMA is less harmful to the environment than is NaCl. However, when CMA is decomposed, oxygen is consumed.

The decomposition rate is strongly temperature dependent, and low temperatures may lead to the accumulation of nondecomposed acetate in soil and water. A very restrictive use of CMA was recommended in a Finnish study after it had been observed that the infiltration of nondecomposed acetate into deep soil can be rather significant (8).

ACKNOWLEDGEMENT

REFERENCES

1. Oberg, G., K, Gustafson, and L. Axelson. *More Effective De-Icing with Less Salt: Final Report of the MINSALT Project.* VTI Report 369 SA. Swedish National Road and Transport Institute, Linköping, 1991.

2. Gustafson, K. *Test with Clearway 1 on Örnsköldsvik Airport 1988-04-05-08* (in Swedish). VTI Notat V 63. Swedish National Road and Transport Institute, Linköping, 1988.

3. Gustafson, K. *Test with Potassium Acetate (Clearway 1) for Deicing of Runways* (in Swedish). VTI Notat 11/93. Swedish National Road and Transport Institute, Linköping, 1993.

4. Bohlmann, B. W. *1990-92 Salt Additives and Alternatives Lab Study.* Minnesota Department of Transportation, St. Paul, 1993.

5. Jutengren, K. *Evaluation of Salt (NaCl) with CMA-Additive Regarding the Corrosivity by Field Trials in the Nyköping area* (in Swedish). SP AR 1995:26. Swedish National Testing and Research Institute, 1995.

6. Lundgren, M., and A. Andalen. *A Study of the Influence of Different Deicing Agents on the Freeze/Thaw resistance of Concrete* (in Swedish). SP AR 95B4 3905. Swedish National Testing and Research Institute, 1995.

7. Vebeck, G. J., and P. Klieger. Studies of "Salt" Scaling of Concrete. *Bulletin 150*, HRB, National Research Council, Washington, D.C., 1957, pp. 1–13.

8. Yli-Kuivila, J. *Infiltration Studies of CMA by Finnish National Road Administration in Winter 1993–1994.* Internal Publication 34/1994. Finnish National Road Administration, Helsinki, Finland.

Production of Low-Cost Acetate Deicers from Biomass and Industrial Wastes

Shang-Tian Yang and Zuwei Jin, *The Ohio State University*
Brian H. Chollar, *Federal Highway Administration*

Calcium magnesium acetate (CMA), a mixture of calcium acetate and magnesium acetate, is used as an environmentally benign roadway deicer. The present commercial CMA deicer made from glacial acetic acid and dolomitic lime or limestone is more expensive than salt and other deicers. Also, a liquid potassium acetate deicer is used to replace urea and glycol in airport runway deicing. Two alternative low-cost methods to produce these acetate deicers from cheap feedstocks, such as biomass and industrial wastes, were studied. CMA deicers produced from cheese whey by fermentation and extraction were tested for their acetate content and deicing property. The CMA solid sample obtained from extraction of the acetic acid present in a dilute aqueous solution and then back-extracted with dolomitic lime to form CMA had about the same acetate content (70 percent acetic acid or 90 percent CMA) as the commercial CMA deicer. The sample from dried whey fermentation broth contained 50 percent acetic acid or 63 percent CMA, with the remaining solids being other organics and salts present in whey. Deicing tests showed that CMA samples from fermentation and extraction had an ice penetration rate equal to or slightly better than the commercial CMA. Cost analysis showed that CMA can be produced at a product cost of $204 to $328/ton, less than 30 percent of the current market price for the commercial CMA, for a plant size of 8,400 tons CMA per year. The lower CMA cost should dramatically increase CMA use in the deicing market.

From 10 million to 14 million tons of road salt are used annually in the United States and Canada. Salt is an extremely effective snow and ice control agent and is relatively inexpensive. However, a study in New York State showed that although 1 ton of road salt cost only $25, it caused more than $1,400 in damage (1). Salt is corrosive to concrete and metals used in the nation's infrastructure, is harmful to roadside vegetation, and poses serious threats to environment and ground-water quality in some regions (2). FHWA spends about $12.5 billion annually, a substantial portion of which is used to rebuild and resurface highways and bridges damaged by salt corrosion. FHWA has long recognized this problem and has identified calcium magnesium acetate (CMA) as one alternative road deicer (3).

CMA is a mixture of calcium acetate and magnesium acetate. It is currently manufactured by reacting glacial acetic acid with dolomitic lime (CaO-MgO) or limestone (Ca/MgCO$_3$). CMA has a deicing ability comparable to salt but is noncorrosive and harmless to vehicles, highway concrete, bridges, and vegetation. It is biodegradable and associated with no identified environmental concerns (2). CMA is not simply noncorrosive; it inhibits corrosion (2). Thus, CMA can be used in mixture with salt to reduce corrosion caused by salt. The use of CMA for highway deicing should save millions of dollars each year just in highway and automobile main-

tenance costs. Detailed discussions of the comparison between salt and CMA for highway deicing can be found elsewhere (4,5).

At the present cost of $1,000/ton, versus $35/ton for salt, CMA is too expensive for widespread use, although some studies have shown that all its material costs may be offset by the savings in infrastructure replacement costs (1). Consequently, CMA is used only in limited areas where corrosion control is required or in environmentally sensitive areas to protect vegetation and ground water from salt contamination (6). The use of CMA as a deicer, however, will be cost-effective and better accepted if its price can be reduced to $300 to $400/ton (7). It is thus desirable to produce low-cost CMA deicers from alternative feedstocks such as biomass and industrial wastes (8).

Several alternative methods to produce acetic acid and CMA by fermentation of biomass and extraction of acetic acid from dilute aqueous solutions are reviewed. An anaerobic fermentation process to produce CMA from cheese whey, a dairy waste, is examined in detail. Deicing performance and cost analyses of this new, alternative CMA deicer from whey were also studied and are discussed.

PRODUCTION OF ACETIC ACID AND CMA

Acetic acid is an important raw material in the chemical industry. In the last several years, the yearly production of acetic acid in the United States has continuously increased to 1.8 million tons in 1995. Current commercial glacial acetic acid is exclusively produced from petrochemical routes (9,10) and costs $0.7/kg. The high price of glacial acetic acid contributes to the major cost of CMA deicer. Thus, there has long been an interest in producing low-cost acetic acid and acetate from fermentation (11).

Production by Fermentation

Several fermentation routes have been widely studied for their potential to produce acetic acid or acetate from biomass. A comparison of various fermentation routes is given in Table 1.

Aerobic Acetic Acid Fermentation

Acetic acid (vinegar) traditionally has been produced from ethanol derived from sugar fermentation. This process generally involves two steps: (a) fermentation of sugar to ethanol by yeasts such as *Saccharomyces cerevisiae* and *Kluyveromyces fragilis*, and (b) oxidation of ethanol to acetic acid by species of *Acetobacter*. The reactions are as follows:

$$C_6H_{12}O_6 \rightarrow 2\ CO_2 \uparrow + 2\ C_2H_5OH \overset{O_2}{\rightarrow} 2\ CH_3COOH$$

This process has two major disadvantages. First, the acetic acid yield is, at most, only two-thirds of the sugar source, since up to one-third of the organic carbon is lost as carbon dioxide (CO_2) during the ethanol fermentation. In practice, the yields of ethanol and acetic acid are rarely more than 90 percent and 85 percent of the theoretical value, respectively. With an overall efficiency of 75 percent, only 0.5 g of acetic acid can be produced per gram of sugar used. Second, strict aeration is required for the growth of *Acetobacter* to convert ethanol to acetic acid. Improper aeration may cause serious damage to the acetic acid bacteria or result in overoxidation of acetic acid to CO_2 and water. As a result, the conventional aerobic vinegar fermentation process suffers from low yield and high production cost, and thus cannot compete well with the natural gas-based synthetic process (9).

Earlier studies conducted by Stanford Research Institute concluded that CMA production via aerobic vinegar fermentation of glucose or hydrolyzed corn

TABLE 1 Comparison of Various Fermentation Routes for Producing Acetate from Biomass

	Aerobic Vinegar Fermentation[1]	Anaerobic Homoacetic Fermentation		Anaerobic Digestion[3]
		C. thermoaceticum	C. formicoaceticum[2]	
Substrate	Glucose / Ethanol	Glucose	Lactate	Cellulosics
Acetate yield	<60%	>80%	>95%	30% ~ 80%
Acetate conc. (w/v)	6% ~ 10%	2% ~ 10%	3% ~ 7.5%	<3%
Fermentation time	1 ~3 days	1 ~ 7 days	2 ~ 7 days	6 ~ 15 days
Energy requirement	high in fermentation	medium	low	high in product recovery

[1]requires ethanol fermentation of glucose first; ethanol is the substrate for acetic acid fermentation.
[2]lactate can be obtained from carbohydrates through homolactic acid fermentation.
[3]methanogenic activities are suppressed to allow acetate accumulation.

starch was not economically competitive and did not warrant further consideration (12). This prompted the search for anaerobic homoacetogens for acetic acid and CMA production.

Anaerobic Homoacetogenic Fermentation

There has been increasing interest in producing acetic acid from renewable resources by using anaerobic homoacetogens because of the high product yield from anaerobic fermentation. In contrast to the aerobic vinegar process, nearly 100 percent of the substrate carbon can be recovered in the product, acetic acid, by anaerobic fermentation. The reaction is as follows:

$$C_6H_{12}O_6 \rightarrow 3\ CH_3COOH$$
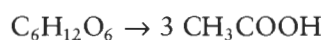
The actual acetic acid yield from glucose is usually greater than 80 percent (weight per weight). With a few exceptions, the final concentration of acetic acid produced from the anaerobic process is usually low, only about 2 percent, as compared with 6 to 10 percent obtained from the aerobic process. This low product concentration leads to a prohibitively high energy requirement for the recovery of the acetic acid produced in the anaerobic process (13), although the overall energy consumption is still lower than that for the aerobic process. To attain a viable, economical production, acetate concentration must exceed 4 percent and a low-cost feedstock should be used.

Table 2 presents some anaerobic bacteria that can convert carbohydrates and other carbon sources to acetic acid via homofermentation. C. thermoaceticum has been extensively studied for its ability to convert glucose, xylose, and cellulose to acetic acid at 60°C (11,14). Other known anaerobic homoacetogens include C. formicoaceticum, C. aceticum, C. thermoautotrophicum, C. magnum, Acetobacterium woodii, A. carbinolicum, and Acetogenium kivui. Ljungdahl et al. (15) studied three thermophilic acetogens—C. thermoaceticum, C. thermoautotrophicum, and A. kivui—for their abilities to produce CMA from glucose. It was concluded that although C. thermoaceticum was the most desirable, none would have successful industrial applications.

Recently, Parekh and Cheryan (16) reported a mutant strain of C. thermoaceticum that could produce acetate concentration as high as 10 percent (weight per volume) in a fedbatch fermentation with cell recycle. The reactor productivity was 0.8 g/L/hr and the acetate yield from glucose was 80 percent. However, the results were obtained with a synthetic medium with a high yeast extract content. Efforts to use inexpensive industrial feedstocks for acetate production by using this strain have not been as successful.

None of the homoacetogenic bacteria can ferment lactose; however, several of them can readily convert lactate to an equal amount of acetate. Among all the homoacetogens, only A. woodii, A. carbinolicum, and C. formicoaceticum can ferment lactate to acetate. A. woodii can grow at temperatures below 32°C and at a pH between 4.5 and 6.8. C. formicoaceticum can grow at a temperature around 35°C and a pH between 6.6 and 9.6 (17). Both organisms are inhibited by acetic acid, but C. formicoaceticum can tolerate a higher concentration than can A. woodii. C. formicoaceticum is also more active than A. woodii when grown on lactate at neutral pH and mesophilic temperatures. A. carbinolicum is a new isolate similar to A. woodii. C. formicoaceticum is the most promising to convert lactate to acetate. Recent study with this organism obtained a high acetate concentration of 7.5 percent (weight per volume) in a fibrous bed bioreactor.

Homolactic fermentation has been widely applied in the dairy industry for producing lactic acid from lactose. It is feasible to produce acetic acid from whey permeate by converting lactose to lactic acid, and then to

TABLE 2　Optimal Growth Conditions and Substrates for Various Anaerobic Homoacetogens

Organism	Temp	pH	Growth Substrate
Clostridium aceticum	30°C	8.3	Fructose, Pyruvate, CO_2/H_2, CO/H_2
C. formicoaceticum	37°C	7.6	Fructose, Pyruvate, Pectin, Lactate, Galacturonate
C. thermoaceticum	60°C	7.0	Fructose, Pyruvate, Glucose, Xylose, (Lactate)*
C. thermoautotrophicum	60°C	5.7	Fructose, Glucose, Galactose, Glycerate, Methanol, Formate, CO_2/H_2, CO/H_2, (Lactate)*
C. magnum	30°C	7.0	Fructose, Glucose, Sucrose, Xylose, Citrate, Malate
Acetobacterium woodii	30°C	6.7	Fructose, Glycerate, Glucose, Lactate, CO_2/H_2, Formate
A. carbinolicum	27°C	7.0	Fructose, Glucose, Pyruvate, Lactate, Formate, Aliphatic alcohols C_1-C_5, CO_2/H_2
Acetogenium kivui	66°C	6.4	Fructose, Pyruvate, Formate, Mannose, Glucose, CO/H_2

*only a few strains can utilize lactate for growth.

acetic acid by using homolactic and homoacetic bacteria, respectively (18). Since both lactate and lactose are abundant in many industrial waste streams (lactate in corn steep liquor from the corn wet milling process and lactose in whey from the cheese industry), it is promising to produce low-cost acetate from lactate and lactose fermentations (19,20).

Anaerobic Digestion

Anaerobic digestion of biomass as a means of producing CMA in a mixture of organic-acid salts was recently studied by Trantolo and others (21–23). In their processes, growth of methanogens was suppressed to allow acetate accumulation. Sewage sludge, woody biomass, and, in principle, any low-grade biomass such as cheese whey can be used in this process. However, the reaction rate is low and acetate yield is only 30 percent to 80 percent, depending on the fermentation condition. The acetate concentration obtained from this process was also very low, only 0.8 percent, although theoretically 3 percent is possible. Other organic acids present in the product stream include propionic and butyric acids. The major problem with this process is that the reactor performance is not stable because many undefined mixed cultures are involved and are difficult to control.

Other Bioprocesses

As shown in Table 2, some homoacetogens may use hydrogen gas and single-carbon compounds, such as carbon monoxide (CO), CO_2, methanol, and formate, to produce acetic acid. This provides a biological method to convert syn-gas (CO, CO_2, and H_2) to acetic acid, although the low solubilities and large volume associated with the gaseous feedstocks might limit their industrial applications. Engineering Resources, Inc. (Fayetteville, Ark.), is currently developing a process to produce acetic acid from biomass and industrial wastes through gasification followed with fermentation of the syn-gas.

Acetate Production from Whey Lactose

Whey is a byproduct from the manufacture of cheese and casein. It contains about 5 percent lactose, 1 percent protein, 1 percent salts, and 0.1–0.8 percent lactic acid. The biological oxygen demand of whey is high—40,000 mg/L. Currently, less than 50 percent of the total whey solids produced in the United States is used in human food or animal feed (24). The surplus whey must find a new use or be treated as a pollutant. Whey can be used for acetic acid production via fermentation.

There is no homoacetogen that can directly convert lactose to acetate. However, acetate can be produced efficiently from lactose via two anaerobic fermentation processes. The first is to use propionic bacteria to ferment lactose to propionate and acetate (25). Acetate is not the major product, but it may be economically recovered as a byproduct from this process. The second process is to use a coculture consisting of homolactic and homoacetic bacteria, which sequentially converts lactose to lactate and then to acetate. The feasibility of producing acetate from whey fermentation by using such a coculture has been studied in both free cell batch cultures and immobilized cell continuous cultures (19,20). The overall acetate yield from lactose was greater than 90 percent (weight per weight), and a high acetate concentration of up to 7.5 percent was obtained in recycle fedbatch fermentation by using immobilized cells and a fibrous bed bioreactor.

Acetic Acid Recovery from Fermentation Broth and Wastewater

Fermentatively produced acetic acid usually is recovered by solvent extraction or azeotropic dehydration. However, the acetic acid produced in the anaerobic fermentation at pH 7 is in the form of acetate salt. Conventional solvents can extract only free acid from the fermentation broth. Previous attempts to adapt the microbes to acidic pH and to acidify the broth before extraction failed to reduce production costs to a competitive level. Separation of acetic acid by adsorption with ion exchange resins is not feasible at present. Steam or gas stripping of the volatile acetic acid present in a dilute aqueous solution is not economically feasible, either. An energy-efficient steam stripper with caustic solution to improve stripping efficiency has been described recently (U.S. Patent 4,917,769, 1990). However, because of the low relative volatility of acetic acid to water (0.69), a large number of trays or equilibrium stages are required to obtain 90 percent recovery. Also, the tray design in this stripping tower is quite complicated. It is difficult to use high concentrations of lime slurry as the caustic in this stripper.

Recently, extractive recovery of carboxylic acids, including acetic acid, from dilute, aqueous solutions, such as fermentation broth and wastewater, having an acid concentration of 1 to 4 percent, has received increasing attention (26–28). The highest concentration of acetic acid that most anaerobic homoacetogens can tolerate is usually lower than 3 percent. Conventional extraction solvents require a concentration of acetic acid higher than 10 percent and, therefore, an evaporation process is usually recommended before solvent extraction. Nevertheless, if a highly efficient extractant is available, the

heating process can be reduced to a level sufficient only for killing the microbes in the liquor. Solvents with a high distribution coefficient can be used to extract acetic acid from a low concentration solution. These solvents include trioctylphosphine oxide (TOPO) and long-chain aliphatic amines (27).

In general, only the undissociated acid can be extracted by the solvent (28). Under basic conditions (pH > 7), the acetic acid is present as acetate salt and cannot be extracted. Therefore, the extraction is usually conducted at a pH value lower than 5 and the extractant can be regenerated by back-extraction with an alkaline solution at pH > 10. A two-step extraction process thus can be used to produce concentrated organic salts from a dilute acid solution. In this process, a solvent with a high distribution coefficient is used to extract organic acids from a fermentation broth with a pH value below 6 (preferably at 3). Back-extraction with an alkaline solution (with pH above 10) is then followed to regenerate the extractant and to form an organic salt in a concentrated solution. This two-step extraction method would provide an energy-efficient way to recover, separate, and concentrate organic acids from a dilute fermentation broth.

PROCESSES FOR CMA PRODUCTION FROM WHEY

Two potential processes to produce acetate and CMA from cheese whey based on the fermentation and extraction technologies discussed earlier are shown in Figure 1. The technical feasibilities of the fermentation and extraction to be used in the processes have been discussed in the previous sections and demonstrated in a recent laboratory study (19). Several CMA samples were prepared from whey following the process steps shown in Figure 1. They were then tested for their likeness to the present commercial CMA in their chemical composition and deicing performance. The purpose of this work was to evaluate the qualities and deicing ability of the CMA produced from cheese whey.

CMA Sample Preparation

CMA Samples from Process 1

The first sample (Sample 1) was prepared as follows. Three L synthetic media containing 4 percent lactate were fermented in a batch fermentor [37°C, pH 7.6,
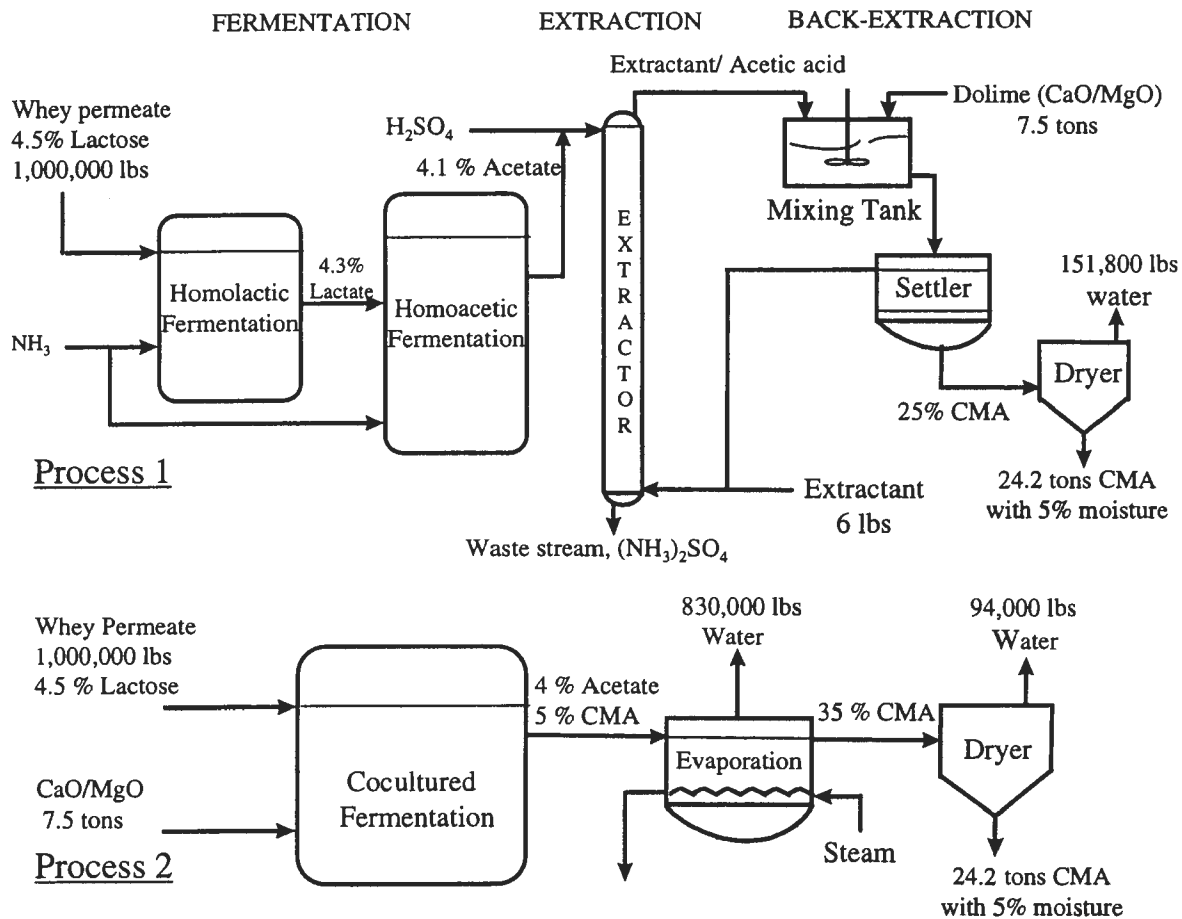

FIGURE 1   Two processes for CMA production from whey permeate.

with sodium hydroxide (NaOH)] for about 5 days. The broth containing 3.5 percent acetate was acidified to pH 3 with sulfuric acid, extracted with an amine extractant, and then back-extracted with CaO-MgO slurry. The CMA-containing solution was then dried and the solids were crushed to powder.

A second sample (Sample 2) was prepared from acid whey in a similar way. The acid whey was first fermented in a homolactic bioreactor to convert lactose to lactate. The broth was then added with some yeast extract and trypticase, autoclaved, and then fermented again in a homoacetic bioreactor to convert lactate to acetate. The final broth containing sodium acetate was then acidified with sulfuric acid, extracted with the amine extractant, and back-extracted with dolomitic limestone slurry. The three phases—organic, aqueous, and solid (unreacted dolime)—were then separated by centrifugation; the aqueous phase containing CMA was dried and crushed to obtain the powder product.

It was found later that these two CMA samples contained significant amounts of sulfate. Improved extraction methods were therefore used to prepare two more CMA samples. These two CMA samples were prepared from whey broth containing calcium acetate as follows. The broth containing 4 percent acetate was acidified to pH 3 with sulfuric acid. After the precipitate was removed, the broth was extracted with the amine extractant and then back-extracted with CaO-MgO slurry. One sample (Sample 3) was obtained from continuous extraction process by using the packed column extractor described previously and the other sample (Sample 4) was prepared from batch extraction. After the unreacted dolime was removed by centrifugation, the CMA-containing solution was dried and the solids were crushed to powder. These samples were then tested for acetate content and ice penetrating ability.

CMA Sample from Glacial Acetic Acid

For comparison purposes, a CMA sample (Sample 5) was prepared by directly reacting acetic acid with dolomitic lime (this is the present commercial production method for CMA deicer). After the unreacted solids were removed, the solution was dried and the solids were crushed to powder.

CMA Sample from Process 2

Another CMA sample (Sample 6) was prepared from the fermentation broth without extraction. Sweet whey permeate was fermented in a bioreactor containing both homolactic and homoacetic bacteria to convert lactose to acetate. CaO and MgO were used to neutralize the acetic acid during the fermentation. The initial lactose concentration in the whey medium was 3.5 percent and the final acetic acid concentration was 3 percent. After

cells and unreacted CaO and MgO were removed by sedimentation, the whole broth was dried to obtain an unrefined (crude) CMA sample.

CMA Sample Analysis and Testing

Composition Analysis

The first two CMA samples were tested for their CMA and insoluble contents and deicing ability. Weighted samples were dissolved in water. The solution was filtered to remove any insoluble and the filtrate was analyzed with high-performance liquid chromatography to determine acetate content. The filter paper used in filtration was washed and then dried. The dry weight difference of the filter paper before and after filtration was measured to determine the amount of insoluble in the CMA samples. Sample 1 had 60 percent CMA and 30 percent insoluble, Sample 2 had 75 percent CMA and 0 percent insoluble, and the commercial CMA product had 90 percent CMA and 7 percent insoluble. The large amount of insoluble in Sample 1 is believed to be CaO and MgO residues that were not reacted during back-extraction. This insoluble can be easily removed by filtration or centrifugation as evidenced in Sample 2, which does not have any insoluble. However, about 10 percent of Sample 1 and 25 percent of Sample 2 are believed to be magnesium sulfate ($MgSO_4$). This impurity was carried into the final CMA product by the sulfuric acid used to acidify the acetate broth during extraction. The product purity from the extraction process was later improved by avoiding sulfate contamination in the acetate broth.

Deicing Test

The ice penetration test described in SHRP H-205.3 was carried out to test the deicing ability of various CMA samples. The experiment was done at 0°C and –15°C. Salt and dolime were also tested for comparison purposes. A water-soluble blue dye and a deicer (in powder form) were spread to cover the surface of the ice formed in a well. The same weight of each deicer sample was used in this experiment. The color penetrating depth as a function of time after applying the deicer was recorded. Each sample test was duplicated and the average was plotted (Figure 2). Salt clearly is the fastest deicer and dolime does not work as a deicer. Sample 2 and commercial CMA have about the same deicing performance, and Sample 1 is slightly inferior because of its large insoluble content.

Comparison with Commercial CMA

The other four CMA samples were also tested for their acetate content and deicing ability. The ice penetrating
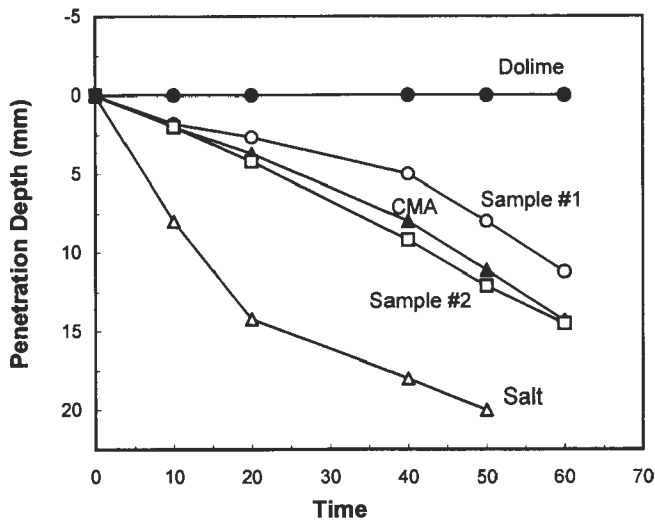
FIGURE 2   Ice penetration performance of various deicers at 0°C.

rate for each deicer was estimated from the ice penetration data, and the relative rate (with commercial CMA = 1) is reported in Table 3. Sample 3 has about the same acetate content as the commercial CMA deicer. The slightly lower acetic acid content per gram of the solid sample can be attributed to the higher calcium-magnesium ratio in this sample (the commercial CMA has a 3:7 ratio). The ice penetration experiment showed that this sample is at least as good as the commercial CMA deicer. Sample 4 is slightly inferior in its deicing ability. It is not clear why this sample did not perform as well as the other sample. There may have been some

procedural errors in preparing this sample by using batch extraction. Sample 6 is slightly better in its ice penetrating performance, probably because of the presence of other small molecular weight salts. Its acetate content is only 70 percent of the pure CMA sample. This is not unexpected since lactose makes up 70 percent of the total solids in whey. In summary, CMA samples from both processes showed an ice penetration rate similar to that of the commercial CMA. The CMA made from cheese whey should perform as well as the current CMA deicer made from glacial acetic acid.

ECONOMIC AND COST ANALYSES

An earlier study conducted by Stanford Research Institute (12) estimated that the CMA production costs from corn using *C. thermoaceticum* to ferment glucose to acetate were $0.266/lb for a 100 ton/day plant and $0.188/lb for a 1,000 ton/day plant. Depending on the plant size, the raw material costs associated with the feedstock used in the fermentations accounted for 30 to 50 percent of the total production costs. Any costs associated with the raw materials will presumably be transferred to the product cost on a one-to-one basis. It is thus compelling to use low-cost waste materials to produce CMA. Also, the CMA production costs were found to be more sensitive to the operating costs than to the capital costs. Increasing the acetate concentration from fermentation is especially important for reducing the operating costs when energy-intensive evaporation and distillation are used in product recovery. Similar conclusions were obtained in a more recent study (29).

TABLE 3   Comparison of Acetate Content and Ice-Penetrating Rate of Various CMA Samples

Sample	Composition (w/w %)			Relative Ice Penetrating Rate
	Acetate	Ca	Mg	
Commercial CMA deicer	67.2	8.38	10.62	1.0
Sample #1 synthetic medium	44.8	-	-	0.81 ± 0.11
Sample #2 acid whey	56.0	-	-	1.04 ± 0.02
Sample #3 continuous extraction	64.8	14.41	2.62	0.99 ± 0.01
Sample #4 batch extraction	70.1	21.34	0.095	0.88 ± 0.02
Sample #5 direct reaction	70.2	14.55	7.04	0.97 ± 0.03
Sample #6 whole fermentation broth	50.0	13.04	3.31	1.03 ± 0.02

Sample #1 also contained ~30% insolubles (mainly CaO and MgO)
Sample #2 also contained ~25% $MgSO_4$

Another recent study using either sewage sludge or woody biomass to produce CMA showed that the production costs would be $0.117/lb if the residue biomass cost $50/ton, or $0.092/lb if the biomass were free (22). Anaerobic digestion with 6.5-day fermentation time to reach 3 percent acetate was assumed in this process evaluation. The product yield from fermentation was assumed to be 50 percent, and extraction with TOPO was used for acetate recovery and reaction with lime (CaO) to make calcium acetate. The plant capacity in this analysis was 500 tons/day CMA.

On the basis of cost relationships and financial analyses provided by these previous studies, the CMA production costs could be easily reduced to $0.09 to $0.15/lb or less by using zero-cost raw material such as sweet whey permeate and acid whey. Because the fermentation of whey performed either as well as or better than that in all the previous studies, it is conceivable that a low-cost CMA deicer could be produced from whey. The economics of the two CMA processes shown in Figure 1 were evaluated. Cost analysis for CMA production from whey permeate was based on a plant scale of processing 1 million lb whey permeate (4.5 percent lactose) per day, which is equivalent to a CMA production capacity of about 24 tons/day or 8,400 tons/year. This plant scale was chosen on the basis of present and immediate future market size for the CMA deicer and available cheese whey supplies from typical dairy plants. The product cost was estimated at $328/ton for Process 1 and $290/ton for Process 2. These costs are significantly lower than the present market price of $1,000/ton. However, the CMA product from Process 2 also contains large amounts of other materials (30 percent in weight), which contribute to deicing performance. Thus, on a total solid basis, this product cost is only $204/ton.

For these two CMA processes, the total direct production costs consist of 60 percent of the product cost. It is noted that CMA product costs would increase dramatically if the process scale were less than 25 percent of the one studied here. The economical process scale for CMA production from whey is ￼ tons/day (2,200 tons/year) or more. This corresponds to a daily supply of 250,000 lb whey to the CMA plant. A cheese plant usually produces 250,000 to 1,000,000 lb whey per day. Therefore, producing CMA from whey should work well for both CMA manufacturing and whey disposal.

MARKET ANALYSIS

Comparison of CMA and Other Deicers

Although CMA has been proven to be as effective as rock salt in road deicing and is an effective anti-icing

agent, it is currently used only in limited areas because of its high price. A lower-cost CMA deicer (from cheese whey) should allow CMA to compete better with other chemical deicers (salt, calcium chloride, Cargill CG-90, and urea) and increase CMA use in deicing. It is noted that the demand for chemical deicers is very sensitive to winter weather and may vary by as much as a factor of two or three from year to year.

All solid chemical deicers, except salt, cost $150/ton or more, but CMA at $1,000/ton is the most expensive at present. However, all of these lower-cost deicers are more corrosive than CMA. Also, CMA is a corrosion inhibitor. The 20 percent CMA–80 percent salt mixture in solution has been shown to be almost as noncorrosive as the CMA solution. Thus, it is possible to make a deicer consisting of 20 percent CMA and 80 percent salt with a competitive price of $150/ton. In addition, the federal government pays states for 80 percent of the CMA cost used in deicing new bridges and highways in environmentally sensitive areas. The costs for CMA users in these applications thus are only 20 percent of the purchasing price. When the low-cost CMA deicer from cheese whey is available, at a projected price of $400/ton or lower, the CMA deicer will be much cheaper to use than most other low-corrosion deicers. However, federal cost sharing alone has not yet increased CMA use.

CMA Market Survey

Current Use of CMA in Highway Deicing

To determine CMA market size and price effects on its market acceptance, a CMA market survey of 10 state transportation departments was conducted in 1993. Only state transportation departments were surveyed because they are the major potential users of CMA and most current CMA use is for highway deicing. Of the 10 states surveyed, 8 had used CMA deicer in the past, but only 3 used CMA in the 1992–1993 winter season. Five states were planning to use CMA again in the 1997–1998 winter season. The amount of CMA used (or to be used) by each state ranged from 50 to 400 tons, depending on weather conditions. State transportation departments had used CMA in the past (a) to prevent corrosion (six responses), (b) to prevent environmental damage (two responses), (c) to support SHRP research (one response), and (d) to comply with laws banning the use of salt on new bridges (one response). The price of CMA was the most important factor affecting its future use. Other factors were deicing performance (six responses), followed by corrosion (two responses) and laws (one response). Environmental damage by salt was not considered as important to future decisions to use a CMA deicer.

Factors Affecting CMA Use

According to a 1991 report, the cost of salt use associated with infrastructure and automobile damage was $555/ton (4). However, this information apparently did not encourage CMA use in highway deicing (four *no* responses, six *maybe* responses), especially at the CMA price of $650/ton in 1993. Again, no respondents gave much attention to the environmental benefit of CMA use. The Intermodal Surface Transportation Efficiency Act of 1991, which provided states with 80 percent CMA costs, did not have a significant effect on CMA use either (eight *no* responses, one *yes*, one *maybe*), because federal funds were needed for highway reconstruction and rehabilitation. Also, the possible use of a 20 percent CMA and 80 percent salt mixture as a deicer to reduce both costs and corrosion did not appear to affect CMA use (six *maybe* responses, three *no*, one previous user). Only 50 percent of the respondents were interested in anti-icing using CMA (five *yes* responses, five *no*). However, this anti-icing application is likely to increase CMA use by 63 percent, based on the estimated CMA uses in anti-icing and in deicing.

The low-level interest in these potentially cost-effective applications may be attributed to a lack of education on the cost benefits of a CMA deicer, and a lack of a driving force for change. The high CMA price again was the major obstacle to CMA use in highway deicing. Price resistance may be much lower in the consumer product market if the CMA/salt blend works as effectively as salt. Laws banning salt use on new bridges and in environmentally sensitive areas have helped increase CMA use, but the effect is relatively small. It is clear that a much-lower-priced CMA is the only hope for increasing CMA use in highway deicing now and in the foreseeable future.

Effect of CMA Price on Market Size

Eight respondents provided their estimated CMA use at various price levels. Only one respondent indicated that price would have a slight effect for the range between $400 and $650. The price for CMA to start to break into the highway deicing market is most likely $300/ton (six responses) or lower ($200/ton, one response; $100/ton, one response). Two respondents indicated that at the break-in price, the amount of CMA used could increase from zero or 200 tons to 50,000 to 100,000 tons. It is thus clear that the price effect on CMA use will not be significant until the price is $300/ton or lower. On the basis of responses from this survey, CMA market size as affected by its price was estimated. Figure 3 illustrates the effect of CMA price on CMA market size normalized on either usage (tonnage) or market value ($MM) with the $650/ton price in 1993 at 1. Figure 3(a) gives a more conservative view
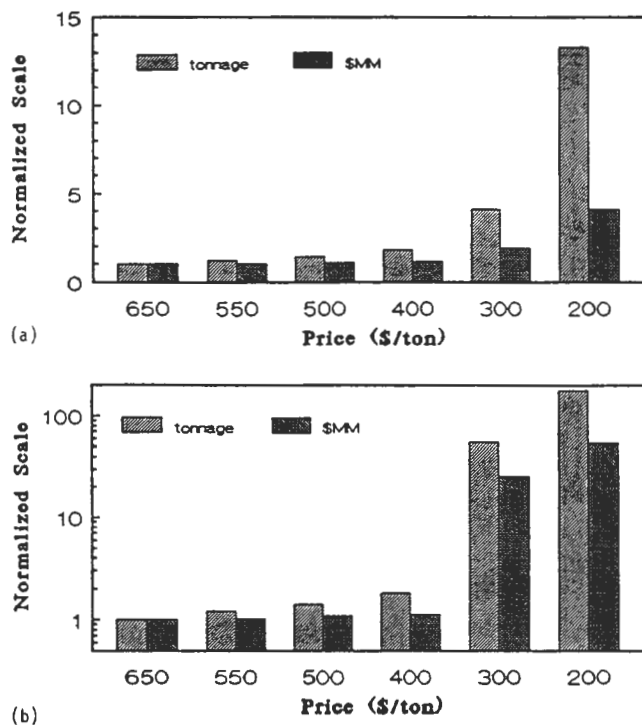
FIGURE 3 Effect of CMA price on projected market size: (a) conservative view; (b) aggressive view.

whereas Figure 3(b) provides a more aggressive view (based on a quantum jump in CMA use at the break-in price). It is clear that there is no commercial benefit to lowering the CMA price to $400/ton, especially in the highway deicing market. This market survey did not cover other potential uses for CMA, such as for private property, airport, and municipality deicing, which may have a greater acceptance for a higher-priced CMA. These markets may provide better opportunities for small, local CMA producers.

CONCLUSIONS

Low-cost CMA deicers can be produced from cheese whey via anaerobic fermentation and extraction by using long-chain aliphatic amines. The CMA deicers produced from the two processes have deicing performance similar to that of the present commercial CMA deicer made from glacial acetic acid. The lowered CMA costs could dramatically increase CMA use in the deicing market.

ACKNOWLEDGEMENT

REFERENCES

1. Hudson, L. R. Calcium Magnesium Acetate (CMA) from Low Grade Biomass. Presented at IGT conference on Energy from Biomass and Wastes XI, Orlando, Fla., 1987.
2. Fritzsche, C. J. Nonpoint Source Pollution, Calcium Magnesium Acetate Deicer an Effective Alternative for Salt-Sensitive Areas. *Water Environment & Technology*, Jan. 1992, 44–51.
3. Chollar, B. H. Federal Highway Administration Research on Calcium Magnesium Acetate—an Alternative Deicer. *Public Roads*, Vol. 47, 1984, p. 113.
4. *Special Report 235: Highway Deicing, Comparing Salt and Calcium Magnesium Acetate*. TRB, National Research Council, Washington, D.C., 1991.
5. D'Itri, F. M. *Chemical Deicers and the Environment*. Lewis Publishers, Boca Raton, Fla., 1992.
6. Harrach, N., and J. Watt. Fine Tuning CMA for Corrosion Control. *Public Works*, July 1990, pp. 40–41.
7. Ministry of Transportation of Ontario. CMA—A Practical Alternative to Salt? Ontario R & D Report, 1(1), 1989, pp. 1–4.
8. Bryan, W. L. Research To Reduce the Cost of Calcium Magnesium Acetate. In *Chemical Deicers and the Environment* (F. M. D'Itri, ed.), Lewis Publishers, Boca Raton, Fla., 1992.
9. Ebner, H., and H. Follmann. Acetic Acid. In *Biotechnology*, Vol. 3 (H. J. Rehm and G. Reed eds.), Verlay Chemie GmbH, Weinheim, Germany, 1983.
10. Ghose, T. K., and A. Bhadra. Acetic Acid. In *Comprehensive Biotechnology*, Vol. 3 (M. Moo-Young, ed.), Pergamon Press, New York, 1985.
11. Ljungdahl, L. G. Formation of Acetate Using Homoacetate Fermenting Anaerobic Bacteria. In *Organic Chemicals from Biomass* (D. L. Wise, ed.), Benjamin/Cummings Publishing Co., London, 1983, pp. 219–248.
12. Marynowski, C. W., J. L. Jones, D. Tuse, and R. L. Boughton. Fermentation as an Advantageous Route for the Production of an Acetate Salt for Roadway Deicing. *Industrial and Engineering Chemistry, Product Research and Development*, Vol. 24, 1985, pp. 457–465.
13. Busche, R. M., E. J. Shimshick, and R. A. Yates. Recovery of Acetic Acid from Dilute Acetate Solution. *Biotechnology and Bioengineering Symposium*, Vol. 12, 1982, pp. 249–262.
14. Parekh, S. R., and M. Cheryan. Acetate Production from Glucose by *Clostridium thermoaceticum*. *Process Biochemistry International* Vol. 25, 1990, pp. 117–121.
15. Ljungdahl, L. G., L. H. Carreira, R. J. Garrison, N. E. Rabek, and J. Weigel. Comparison of Three Thermophilic Acetogenic Bacteria for Production of Calcium-Magnesium Acetate. *Biotechnology and Bioengineering Symposium*, Vol. 15, 1985, pp. 207–223.
16. Parekh, S. R., and M. Cheryan. Continuous Production of Acetate by *Clostridium thermoaceticum* in a Cell-Recycle Membrane Bioreactor. *Enzyme Microbiology Technology*, Vol. 16, 1994, pp. 104–109.

17. Yang, S. T., I. C. Tang, and M. R. Okos. Kinetics of Homoacetic Fermentation of Lactate by *Clostridium formicoaceticum*. *Applied Environmental Microbiology*, Vol. 53, 1987, pp. 823–827.
18. Tang, I. C., S. T. Yang, and M. R. Okos. Acetic acid production from whey lactose by the Coculture of *Streptococcus lactis* and *Clostridium formicoaceticum*. *Applied Microbiology and Biotechnology*, Vol. 28, 1988, pp. 138–143.
19. Yang, S. T., I. C. Tang, and H. Zhu. A Novel Fermentation Process for Calcium Magnesium Acetate (CMA) Production from Cheese Whey. *Applied Biochemistry and Biotechnology*, Vol. 34/35, 1992, pp. 569–583.
20. Yang, S. T., H. Zhu, V. P. Lewis, and I. C. Tang. Calcium Magnesium Acetate (CMA) Production from Whey Permeate: Process and Economic Analysis. *Resources Conservation and Recycling*, Vol. 7, 1992, pp. 181–200.
21. Trantolo, D. J., J. D. Gresser, D. C. Augenstein, and D. L. Wise. Calcium Magnesium Acetate from the Bioconversion of Residue Biomass. In *Calcium Magnesium Acetate, An Emerging Bulk Chemical for Environmental Applications* (D. L. Wise, Y. A. Levendis, and M. Metghalchi, eds.), Elsevier, Amsterdam, Netherlands, 1991.
22. Trantolo, D. J., J. D. Gresser, D. C. Augenstein, and D. L. Wise. The Feasibility of a Residue Biomass Bioconversion Process To Prepare Calcium Magnesium Acetate Deicing Salt. *Resources Conservation and Recycling*, Vol. 4, 1990, pp. 215–232.
23. Wise, D. L., and D. C. Augenstein. An Evaluation of the Bioconversion of Woody Biomass to Calcium Acetate Deicing Salt. *Solar Energy*, Vol. 41, 1988, pp. 453–463.
24. Yang, S. T., and E. M. Silva. Novel Products and New Technologies for Use of a Familiar Carbohydrate, Milk Lactose. *Journal of Dairy Science*, Vol. 78, 1995, pp. 2563–2583.
25. Lewis, V. P., and S. T. Yang. Continuous Propionic Acid Fermentation by Using Immobilized *Propionibacterium acidipropionici* in a Novel Packed-Bed Bioreactor. *Biotechnology and Bioengineering*, Vol. 40, 1992, pp. 465–474.
26. Althouse, J. W., and L. L. Tavlarides. Analysis of Organic Extractant Systems for Acetic Acid Removal for Calcium Magnesium Acetate Production. *Industrial and Engineering Chemistry, Research and Development*, Vol. 31, 1992, pp. 1971–1981.
27. Kertes, A. S., and C. J. King. Extraction Chemistry of Fermentation Product Carboxylic Acids. *Biotechnology and Bioengineering*, Vol. 28, 1986, pp. 269–282.
28. Yang, S. T., S. A. White, and S. T. Hsu. Extraction of Carboxylic Acids with Tertiary and Quaternary Amines: Effect of pH. *Industrial and Engineering Chemistry, Research and Development*, Vol. 30, 1991, pp. 1355–1342.
29. Wiegel, J., L. H. Carreira, R. J. Garrison, N. E. Rabek, and L. G. Ljungdahl. Calcium Magnesium Acetate (CMA) Manufacture from Glucose by Fermentation with Thermophilic Homoacetogenic Bacteria. In *Calcium Magnesium Acetate, An Emerging Bulk Chemical for Environmental Applications* (D. L. Wise, Y. A. Levendis, and M. Metghalchi, eds.), Elsevier, Amsterdam, Netherlands, 1991.

PART 4
TRAVEL SURFACE
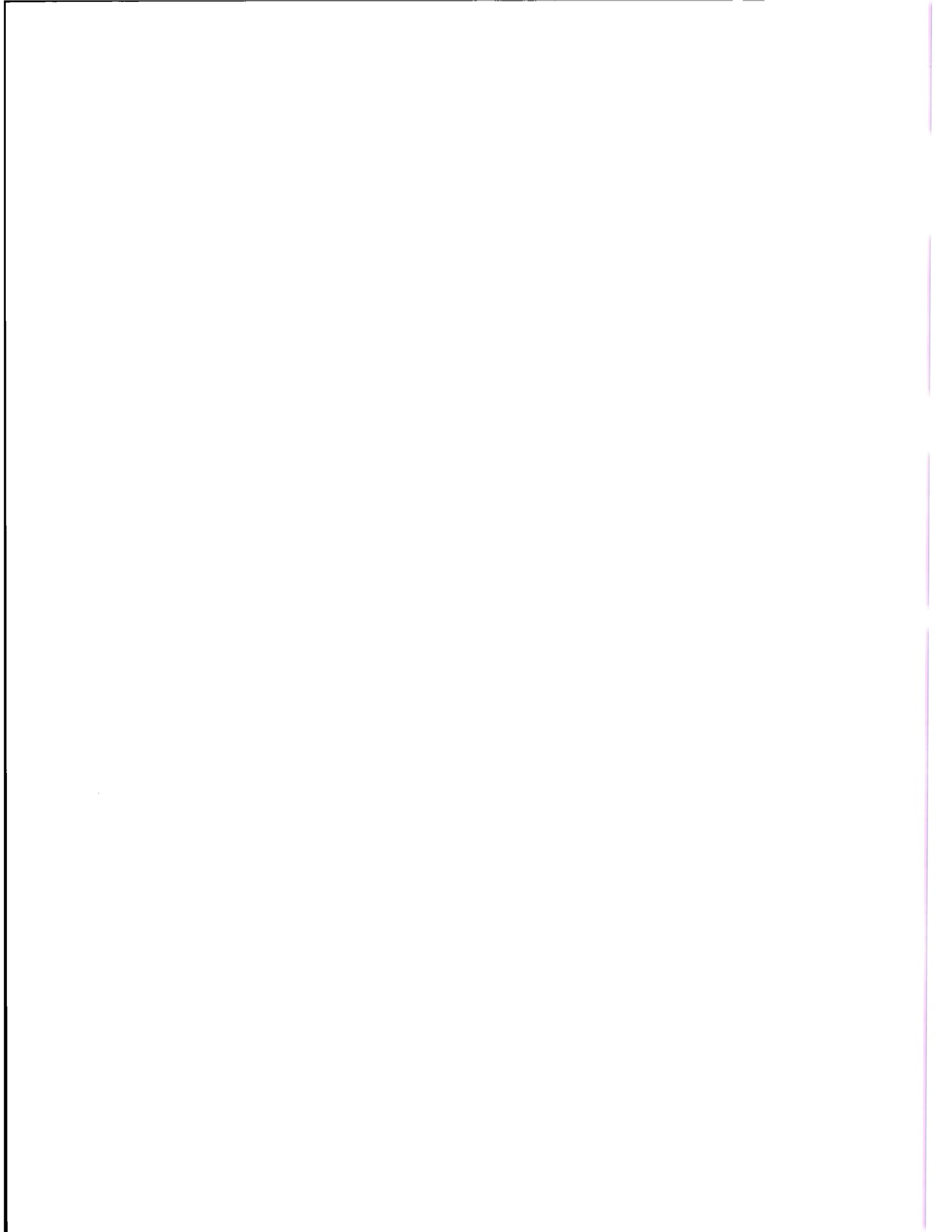
Active Microwave Remote Sensing of Road Surface Conditions

Baskin I. Tapkan, Suzanne Yoakum-Stover, and Robert F. Kubichek,
University of Wyoming

An active microwave sensing system is investigated to provide real-time information about road surface conditions. Microwave radiation is very sensitive to the presence of water in the medium through which it passes. Thus, the amplitude and phase of a wave reflected from a road contains information about water, snow, and ice accumulation. Computer simulations of surface reflectivity based on the dielectric constant of various media were completed as a preliminary feasibility study. An experimental detection system was then constructed along with a liquid nitrogen–cooled asphalt test bed to simulate the road surface. Preliminary tests were conducted in the frequency range of 26.5 to 40 GHz. Microwave signals were directed to the asphalt surface by using a horn antenna, and the reflected signal was received by a microwave antenna feeding a diode detector. The resulting signal was then analyzed to extract the road surface information. Tests indicated that wet snow and ice can easily be distinguished, although it is difficult to discriminate among dry snow, dry ice, and dry pavement conditions. This problem is addressed by sensing the road with two separate transmitter frequencies. A simple maximum likelihood classifier algorithm was applied to the measured data to automatically identify the surface conditions.

I nformation about road surface conditions during winter is important for travelers as well as for highway patrol and maintenance personnel. Because accumulations of ice and snow create dangerous driving conditions, obtaining timely and accurate data is an important task for highway departments and requires frequent patrolling (1). A more effective and less expensive alternative is the use of automatic sensors deployed along the road. The most prominent current technology involves the use of in-pavement sensors that measure pavement temperature, the presence of water, and the presence of deicing chemicals. The main disadvantage of such in-pavement sensors is their high installation and maintenance costs. Also, they are sensitive to only a small area of the surface, which may cause erroneous results when partial icing exists on the road.

Remote sensing approaches based on either active or passive microwave techniques have been investigated by several researchers. In an active system, a microwave transmitter generates a signal to probe the road surface (2–5), whereas in a passive microwave system only the black body radiation of the surface is detected (6).

In this paper, the technical feasibility of an active microwave sensing system using multiple frequencies is investigated. Microwaves in the range of 26.5 to 40 GHz are directed to the road surface, and the reflected microwaves are received and analyzed. Since the magnitude of the received signal for various surface conditions is measurably different because of moisture content, the received signal can be analyzed to provide an estimate of surface conditions.

Computer simulations based on various surface covers with different thicknesses were performed. The reflection coefficients were computed by using Fresnel's formulas of

reflection for plane waves. The results indicate that many conditions are distinguishable if multiple frequencies are used. Monte Carlo simulations were also completed to model real-world variations of the physical parameters such as temperature and surface cover thickness.

A prototype detection system covering the Ka-band of the microwave spectrum (26.5 to 40 GHz) and an artificial road test bed were constructed. Surface scans were made for different conditions including various thicknesses of water, snow, slush, and ice. For the analysis, specific frequencies were chosen for which distinctive features appeared in the received signal. The variations of surface conditions over time were also monitored. Typical data from this experiment are presented. Finally, a simple classification scheme was developed that could provide an automatic assessment of the surface cover.

THEORY

The dielectric constant of a material determines the scattering characteristic of microwaves by the material. By observing the propagation of microwaves in the medium, one can derive information about the dielectric constant, which in turn gives insight into the physical properties of the material, such as its moisture content, density, and temperature. The following notation is used for the complex dielectric constant:

$$\varepsilon = \varepsilon' - j\varepsilon''$$

where ε' is the permittivity and ε'' is the dielectric loss factor.

The differences in the dielectric constant among the various media cause the wavefront to bend, reflect, or refract at an interface. Snell's law of refraction determines the angle or direction of transmitted and reflected electromagnetic waves, as shown in Figure 1.
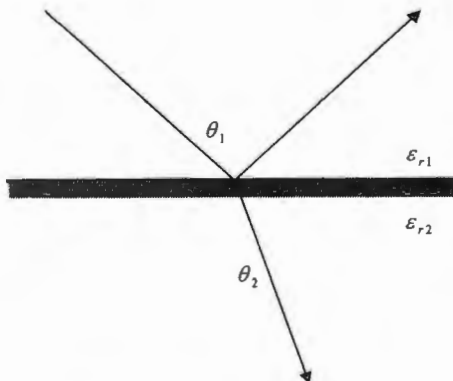
Snell's law in the case of nonmagnetic media is

$$\frac{\sin \theta_1}{\sin \theta_2} = \sqrt{\frac{\varepsilon_{r2}}{\varepsilon_{r1}}}$$

where θ_1 and θ_2 are the angles of the incident and transmitted waves, and ε_{r1} and ε_{r2} are the relative dielectric constant values of the corresponding media.

By employing Maxwell's equations and applying the boundary conditions at an interface, the Fresnel's reflection coefficients can be calculated (7). The change in the amplitude and phase of the reflected wave is given by the reflection coefficient.

For a wave polarized perpendicular to the scattering plane, the reflection coefficient is given by

$$R_{12}^{\perp} = \frac{\sqrt{\mu_{r2}/\varepsilon_{r2}}\cos\theta_1 - \sqrt{\mu_{r1}/\varepsilon_{r1}}\cos\theta_2}{\sqrt{\mu_{r2}/\varepsilon_{r2}}\cos\theta_1 + \sqrt{\mu_{r1}/\varepsilon_{r1}}\cos\theta_2}$$

and for a parallel polarized wave it is

$$R_{12}^{\parallel} = \frac{\sqrt{\mu_{r1}/\varepsilon_{r1}}\cos\theta_1 - \sqrt{\mu_{r2}/\varepsilon_{r2}}\cos\theta_2}{\sqrt{\mu_{r1}/\varepsilon_{r1}}\cos\theta_1 + \sqrt{\mu_{r2}/\varepsilon_{r2}}\cos\theta_2}$$

The medium is assumed to be nonmagnetic; therefore, the permeability values (μ_r) are unity (8,9).

For a three-layer medium, shown in Figure 2, the overall reflection coefficient is given by

$$R = \frac{R_{01} + R_{12}\exp\left(-j2k_{1z}d_1\right)}{1 + R_{01}R_{12}\exp\left(-j2k_{1z}d_1\right)}$$

where

$$k_{1z} = \left(\omega^2\mu_{r1}\varepsilon_{r1} - \omega^2\mu_{r0}\varepsilon_{r0}\sin^2\theta_0\right)^{1/2}$$
$$= \omega\sqrt{\mu_{r1}\varepsilon_{r1}}\cos\theta_1$$

is the propagation factor, and d_1 is the thickness of the middle layer. The total reflectivity is given by $\Gamma = |R|^2$.

FIGURE 1   Refraction and reflection in a two-layer medium.
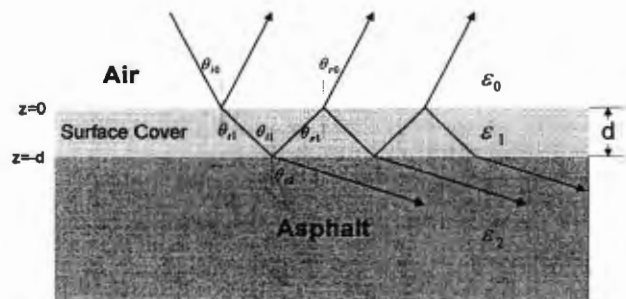

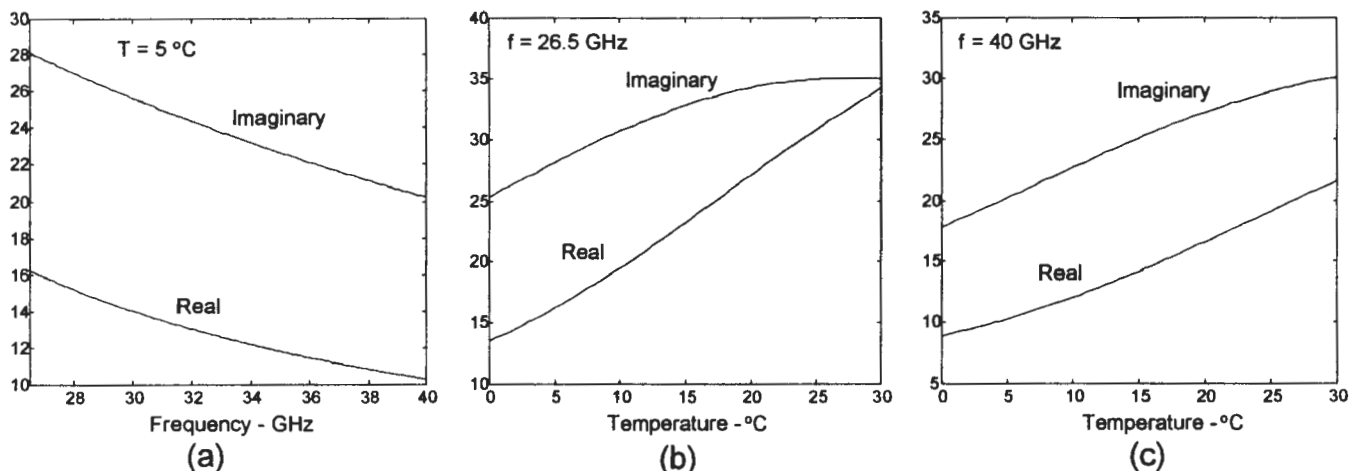FIGURE 2   Three-layer surface model used in computer simulations.

FIGURE 3 Dielectric constant of water as function of frequency and temperature, calculated with Debye formula.

COMPUTER SIMULATIONS

By using these equations, the reflectivities of three-layer surfaces were computed as a function of frequency, thickness of the middle layer, polarization, and angle. The following values of relative material dielectric constants are used in the simulations (5,7).

The dielectric constant of water is both frequency and temperature dependent. As shown in Figure 3(a), at 5°C it varies monotonically from about $16 \pm j28$ at 26.5 GHz to $10 \pm j22$ at 40 GHz. The dependence on temperature is shown in Figures 3(b) and 3(c) for two representative frequencies. The permittivity of ice is independent of frequency with a value of 3.15, and the loss factor is three to four orders of magnitude smaller than that of liquid water. The dielectric constant of snow depends on its density and water content (7). For these calculations the values corresponding to a density of 0.25 g/cm³ were used.
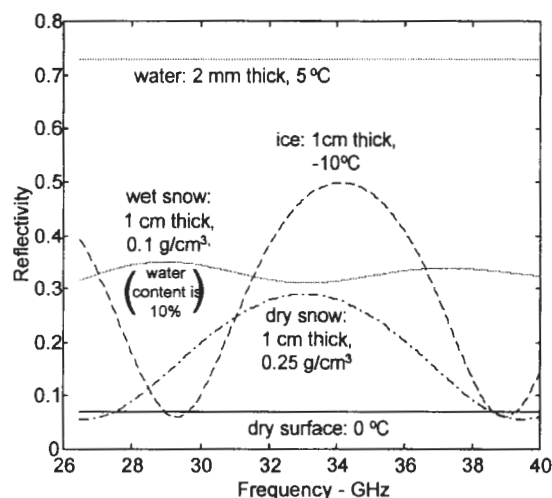

FIGURE 4 Reflectivity of surface conditions for plane wave parallel to scattering plane.

Figure 4 displays the general behavior of reflectivity versus frequency for an incident angle of 60° using plane waves polarized parallel to the scattering plane. The surfaces, with the exception of the dry surface condition, are assumed to have covers for 2 mm water, 1 cm ice, wet snow, and dry snow. Although the real situation is far more complex than this simplified theory, the results indicate that the surface conditions should be distinguishable at certain frequencies.

Monte Carlo simulations were conducted to model the full range of likely real-world variations in the parameters. In this approach, the values of dielectric constants and thicknesses for each condition were uniformly randomized over the range given in Table 1 (10). Utilizing reflectivities at two frequencies creates a variable space, as shown in Figure 5. Curved decision boundaries can be used to distinguish between wet snow and ice covers. Water is easily distinguished because its reflectivity values are around 0.7 for each frequency.

METHODOLOGY

The prototype system comprises a 486-based computer with data acquisition board, a microwave oscillator, wave guides, microwave horn antennas, lock-in ampli-

TABLE 1 Approximate Dielectric Constant Values for Ka-Band of Microwave Spectrum

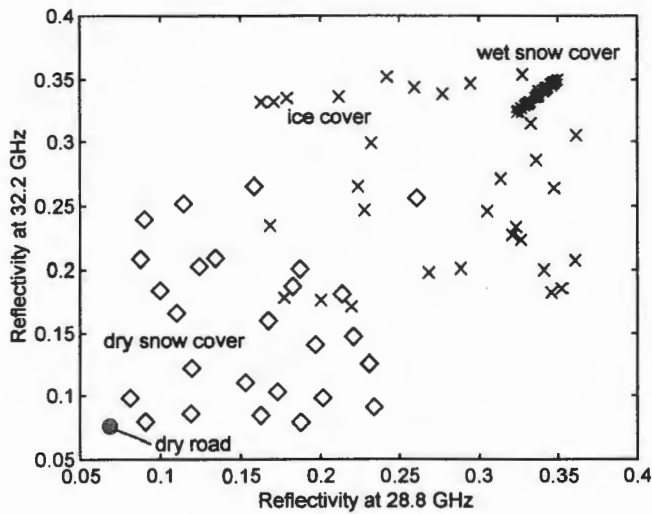| Material	Permittivity (ε')	Dielectric loss factor (ε'')
water	13 ± 3	24 ± 4
wet snow	4 ± 0.5	0.75 ± 0.25
ice	3.15 ± 0.1	$2 \times 10^{-3} \pm 5 \times 10^{-4}$
dry snow	2.1 ± 0.2	$4 \times 10^{-4} \pm 5 \times 10^{-5}$
road (dry)	1.43	0.21

FIGURE 5   Reflectivities for important surface conditions at two frequencies as the dielectric constants and surface cover thickness (1 to 2 cm) are varied.

fiers, a reference oscillator, adjustable test stands to support the equipment, and a liquid nitrogen–cooled model road surface. A high-level diagram of the system is shown in Figure 6.

The data acquisition board generates an output voltage between 0 and 10 volts as set by software. This voltage controls the YIG-tuned GaAs microwave oscillator to produce microwaves in the range from 26.5 to 40 GHz. The microwaves travel through waveguides, an isolator, and two directional couplers. The first coupler is used for voltage-to-frequency calibration. The second coupler is used to monitor the source power, which was not leveled. Next, microwaves are modulated by the PIN diode attenuator, which is driven by the local oscillator's reference signal.

For most measurements, the modulated microwave signal is directed with a horn antenna onto the center of road surface at an incidence angle of 60° from a height of 40 cm. A second horn antenna receives the reflected microwave signal, and a crystal diode detector converts it to a direct current that is proportional to power. This current is dropped across a load resistor to provide an appropriate voltage input signal to the lock-in amplifier. The input voltage is mixed with the reference signal supplied from the local oscillator. The output voltages from the lock-in amplifiers are sent to input channels of the data acquisition board and recorded.

Road surface covers that were simulated include wet surfaces with various amounts of water, wet snow, dry snow, and ice with thicknesses varying from 0.1 to 2 cm. The road surface was covered with Styrofoam to maintain low surface temperatures over longer periods.

RESULTS AND ANALYSIS

The first step in the procedure is to normalize the reflection data to account for variations in transmitter power and path attenuation as a function of frequency. A reference signal was created by measuring reflection from a copper sheet placed over the road surface to act as a near-perfect reflector. Subsequent scans of actual surface conditions were then normalized by dividing the received signal with the reference signal. Reflectivity of surface condition is then given by

$$R_i = \frac{V_i}{V_{ref}}$$

where V_{ref} is the corresponding reference signal.
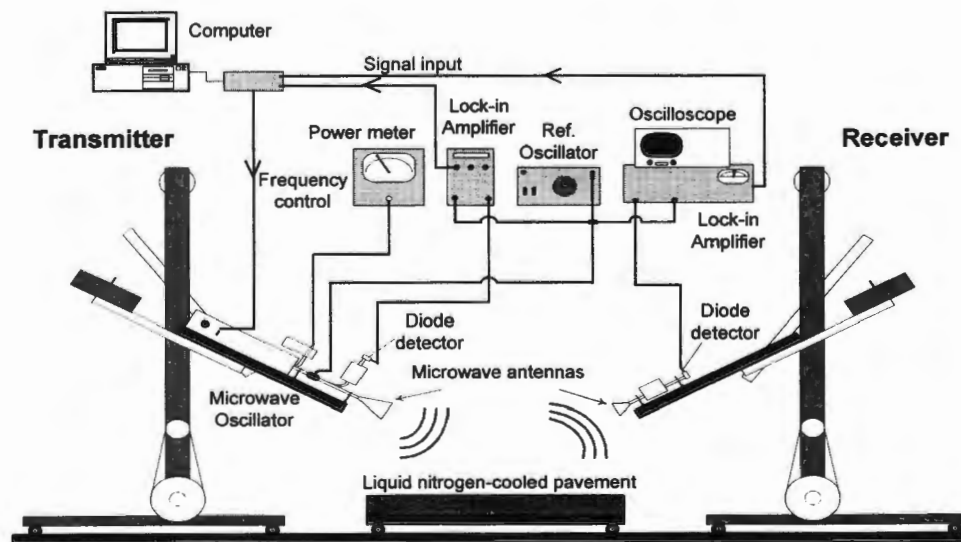

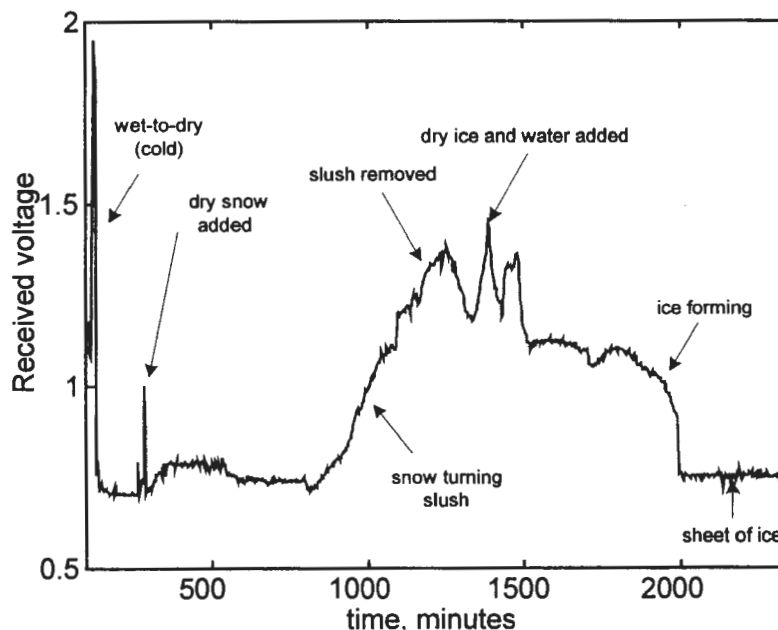FIGURE 6   High-level diagram of active microwave remote sensing system.

FIGURE 7   Reflectivity versus time for changing surface covers at
32.2 GHz.

Typical data are shown in Figure 7. The thicknesses of water, slush, ice, and dry snow covers were 0.2 cm, 0.5 cm, 1 cm, and 0.5 cm, respectively. The large peaks are caused by mismatches in the microwave apparatus and peculiarities of the source whose power is unleveled.

The results indicate that the ability to distinguish various surface covers on the basis of reflectivity data is dependent on the frequency used. For example, all conditions appear to be distinguishable for frequencies centered at 33.2 GHz, whereas at 32.9 GHz dry snow, ice, and dry surface reflection overlap each other.

The time to acquire the surface scans as a function of frequency was about 3 min. Because conditions on the road surface change very slowly, these scans can be viewed as snapshots of the surface reflectivity at a given instant of time. In contrast, monitoring the surface as a function of time indicates how reflectivity changes as the surface undergoes a transition from one condition to the next. Figure 8 shows a continuous record of reflectivity for changing road surface cover over a 2-day period, with transmitter frequency fixed at 32.2 GHz. Water, dry snow, and dry ice were added and liquid nitrogen was used for cooling to achieve various surface states. Details of the experiment are given in Table 2.

It is interesting to note that the reflectivity of the dry surface changes with temperature. Figure 9 shows a significant increase in reflectivity as the surface temperature increases from 15°C to 22°C. Figure 9 also shows results for snow cover superimposed on the same graph. As can be seen, the reflection amplitudes for snow and warm, dry surfaces overlap significantly, making it difficult to differentiate the surface states on the basis of reflectivity alone. However, if surface temperatures were known, the surface condition could be classified correctly.

SIMPLE MAXIMUM LIKELIHOOD CLASSIFIER

The results indicate that unambiguous estimates of the surface cover will require multiple measurements including reflectivity at two or more frequencies, surface temperatures, and perhaps phase information. Combin-

FIGURE 8   Normalized reflected signal from various surfaces.

TABLE 2   Details of Experiment

Time	Action	Comments
3 minutes	1 liter of water added while surface is cooled by liquid nitrogen.	absorbed quickly due to porosity of asphalt.
210 minutes	2 buckets of dry snow is added to the chilled surface and leveled by hand using a metal shovel.	spikes in the reflectivity are caused by the presence of metal shovel.
700 minutes	None	snow is becoming slushy due to relatively warm temperatures.
1250 minutes	Slush is removed with the metal pan.	surface is being cooled by circulating liquid nitrogen through the coil.
1500 minutes	3 kilograms of dry snow and 0.5 liters of water are added.	wet and icy surface when temperature plunges below zero ($^\circ$C).
1900 minutes	None	ice is forming.

ing this information to form an optimal estimate can be done most efficiently by using pattern recognition, neural networks, or other adaptive strategies. These autonomous schemes would eliminate dependence on human interpretation and increase decision speed significantly. A simple experiment was conducted to see how a rudimentary pattern recognition scheme could be implemented. The input parameters comprise reflectivity values at only two frequencies to make it simple and easy to visualize. Other parameters can be added to improve system accuracy.

The surface detection scheme was based on a maximum likelihood classifier. Several simplifying assumptions were required. First, the data for each condition (class) were assumed to have a Gaussian distribution. This assumption did not turn out to be valid for all classes, but it allowed a simple classifier to be built and studied. Second, the road conditions were assumed to belong to a finite number of discrete classes. This is not physically correct, because gradual transitions can be expected from one condition to another. This problem could be addressed by using a more sophisticated algorithm such as a fuzzy classification approach.

The probability density function (pdf) for reflectivity vector $\mathbf{x}$ given that the signal belongs to surface class s_i is

$$p\!\left(\frac{x}{s_i}\right) = \frac{1}{(2\pi)^n |\mathbf{C}|^{1/2}} \, \exp\!\left[-\frac{1}{2}(\mathbf{x} - \mathbf{m}_i)' \, \mathbf{C}_i^{-1}(\mathbf{x} - \mathbf{m}_i)\right]$$

where $\mathbf{C}_i$ is the covariance matrix and $\mathbf{m}_i$ is the mean vector of surface class s_i (11).

To test the road surface when the condition state is concealed, the unknown reflectivity vector $\mathbf{x}$ is input into the density function. The class with the largest pdf value is chosen as the assigned class for that particular input.

The maximum likelihood decision surface is shown in Figure 10. Note that the graph was generated by using a contour-type plot, which unfortunately results in multiple lines for each boundary. More properly, a single line would be used to represent the boundary. Figure 10 shows that the classifier works well for separating slush cover from dry surface and ice cover. Water reflectivity (not shown) would be very high (around 4), and thus

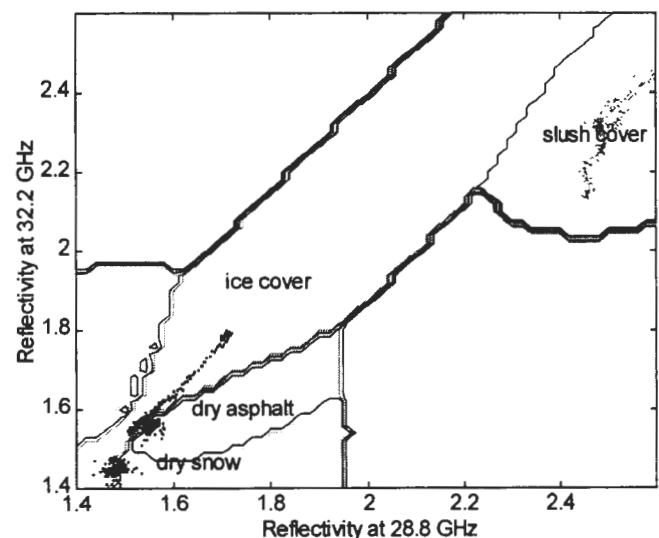FIGURE 9   Ambiguity in surface detection, emphasizing the need for surface temperature.

FIGURE 10   Decision boundaries and measured data points at two frequencies.
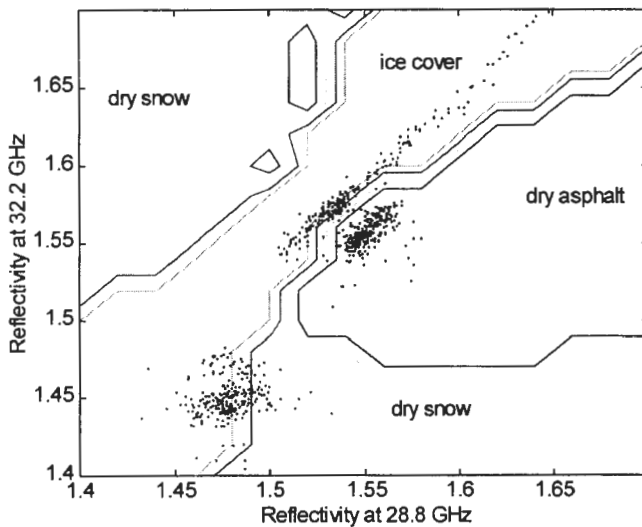
FIGURE 11 Zoomed decision boundaries with measured data points for several surface conditions.

would be easily distinguishable from the other surfaces. A zoomed plot of Figure 10 is given in Figure 11 to emphasize the region containing the snow cover, ice cover, and dry surface data points.

Figure 11 indicates that the distinctly non-Gaussian distribution of ice cover reflectivity causes approximately half of the snow cover data points to be misclassified into the ice class. This is caused by the non-Gaussian distribution of ice cover. It should be noted that these data points are not separable if either frequency is used alone but are distinct when two of them are combined.

For visualization and simplicity, this classification was limited to two input parameters, but it could easily be extended to more than two input parameters, such as additional frequencies, phase information, or surface temperature. Also, better pdf estimates could be used to provide better performance for non-Gaussian conditions.

PRACTICAL CONSIDERATIONS

System Implementation

The complexity, size, and cost (about $5,000) of a fully implemented system would be comparable to that of a police radar gun. The sensor could be implemented as a small pole-mounted transceiver unit installed adjacent to the roadway, with passive reflectors located on the opposite side of the road. At the receiver, a microprocessor would process the received signals to estimate signature values. A second set of algorithms would provide real-time estimates of surface moisture, snow, ice, slush, and multiple-layer conditions such as a thin sheet of water overlying an ice layer. On the basis of the preced-

ing analyses, a dual-frequency system, which would operate at two well-separated microwave frequencies to provide independent information about surface conditions, is proposed. Additionally, the proposed system would employ both a reflected path, in which the principal radio beam would reflect off the road surface, and a direct path, in which the beam would travel directly from transmitter to receiver antennas without intercepting the road surface. Unwanted variations common to both signals, such as antenna icing, atmospheric effects, and power supply fluctuations, could be eliminated by comparing the direct and reflected signals. This system design is being investigated as an NCHRP Innovations Deserving Exploratory Analysis (IDEA) Program project (NCHRP 31).

The proposed active microwave sensing technique offers many technical advantages over embedded sensors and passive microwave systems:

• The active microwave system should provide a more representative measure of actual pavement conditions than do point estimates of moisture from embedded sensors. Microwave measurements are based on reflections from the entire surface illuminated by the transmitter antenna.

• Unlike embedded sensors that detect moisture accumulations indirectly, the microwave system directly senses road ice and snow conditions, and trained personnel are not needed to interpret the data. The estimates are made by computer and are available to the public and maintenance personnel in real time.

• Use of both a direct signal and a reflected signal provides immunity to antenna icing and other time-varying effects, making this system much more robust and reliable than a passive system.

• The proposed microwave system would cost a small fraction of an embedded sensor installation while providing accurate condition reports and more detailed information about ice and snow accumulation. Moreover, as compared with embedded sensors, microwave systems can be relocated easily to new positions as required by highway managers, and are not damaged by snowplowing operations.

Application

Increasingly, state and local highway departments must maintain more roads with fewer personnel, older equipment, and declining budgets. Low-cost winter road condition sensors would provide a means to leverage limited human resources by concentrating maintenance efforts where they are most needed. High-resolution real-time road information removes much of the guesswork and

allows optimum assignment of personnel and equipment to developing trouble spots.

Because of low unit cost and small size, the proposed system sensors could be installed at regular intervals along less-traveled rural highways, on bridges and mountain passes, along hazardous curves, and along highway stretches prone to icing or drifting snow. Microwave sensors would instantly detect worsening road conditions caused by rapidly evolving weather systems and thus eliminate inherent delays associated with eyewitness reporting methods. This detailed road information could be delivered to users by way of telephone and radio broadcasts, as well as other formats such as a World Wide Web page.

CONCLUSIONS

The feasibility of active microwave remote sensing of road surface conditions was investigated. A prototype system was constructed and tested. Microwave reflectivity data were collected for a variety of conditions including accumulations of ice, snow, and slush produced in the laboratory. Two types of surface reflectivity scans were done, reflectivity versus frequency and reflectivity versus time. The following conclusions were drawn:

• Differing surface conditions generate distinguishable signatures in the microwave reflection data, establishing the feasibility of an active microwave system.

• Reflection characteristics vary as a function of frequency. Radiation at more than one frequency could be used to identify the road surface condition.

• Computer simulations were consistent with the actual measurements.

• Knowledge of surface temperature would be a desirable parameter for a detection system to help avoid misclassification of the road surface for dry snow cover, hard-frozen ice cover, or warmer, dry surface conditions.

REFERENCES

1. Boselly, S. E. Road Weather Information Systems: What Are They and What Can They Do for You? In *Transportation Research Record 1387*, TRB, National Research Council, Washington, D.C., 1993, pp. 191–195.
2. Magerl, G., and W. Pritzl. Microwave Remote Sensing of Road Surface During Winter Time. *Proc., International Microwave Conference*, Ksiaz, Poland, Vol. 3, 1994, pp. 173–181.
3. Magerl, G., W. Pritzl, and P. Frohling. A Road Condition Sensing Microwave Radar. *Proc., International Symposium on Recent Advances in Microwave Technology (ISRAMT'91)*, Reno, Nev., 1991, pp. 376–381.
4. Frohling, P., G. Magerl, and W. Pritzl. Detection of Weather Induced Road Conditions. *Proc., International Symposium on Snow Removal and Ice Control Technology*, Vol. 2, Preprint 34, 1992.
5. Hertl, S., G. Schaffar, and H. Stori. Contactless Determination of the Properties of Water Films on Road. In *Journal of Physics. E: Scientific Instruments*, Vol. 21, Oct. 1988, pp. 955–958.
6. Berinsky, S., H. K. Hong, T. H. Lee, and W. T. Schrader. *The Development of a Microwave Radiometer for Use as a Highway Ice Detector*. FHWA-RD-78-223. FHWA, U.S. Department of Transportation, 1978.
7. Ulaby, F. T. *Microwave Remote Sensing: Active and Passive*. Artech House, London, England, 1981.
8. Matzler, C. Application of the Interaction of Microwaves with the Natural Snow Cover. In *Remote Sensing Reviews*, Vol. 2, Issue 2, 1987.
9. Balanis, C. *Advanced Engineering Electromagnetics*. Wiley Publishing, West Sussex, U.K., 1989.
10. Kong, J. A., L. A. Tsang, and R. T. Shin. *Theory of Microwave Remote Sensing*. Wiley Interscience, West Sussex, U.K., 1985.
11. Tou, J. T., and R. C. Gonzales. *Pattern Recognition Principles*. Addison-Wesley, Reading, Mass., 1974.

Theoretical Background for Use of a Road Weather Information System

Jörgen Bogren, *Göteborgs University, Sweden*

Background factors must be considered in the adaptation of a road weather information system for a maintenance area. These factors may be climatological, meteorological, or related to the structure of the road infrastructure. The methodology used in Sweden involves analyses of thermal mapping along the actual road stretches, climatological statistics such as precipitation patterns and average temperature, and so forth. Other important components are the variation in topography and vegetation. These factors are integrated into a decision procedure for which the output is a proper location based on climatology of the field stations within the system.

The possibility of maintaining a high and effective level of winter road maintenance has increased dramatically through the use of road weather information systems (RWISs). Records of climatological parameters such as air temperature, air humidity, precipitation, and wind, together with pavement temperature, make it possible to detect risk of icy conditions in an early stage and to take action against them. However, to gain optimum benefits from this type of automatic system, several background factors must be considered during the planning and establishment of a system in a new area. Accuracy and reliability are to a great extent determined by the capabilities and accuracy of the specific sensors, but without knowledge of the local and microclimatological situation information provided by the sensors will be misleading and difficult to interpret. The topoclimatological conditions are also very important when the RWIS is used along with tools such as forecast models, stretchwise information, and winter indexes (1). An overview of the climatological background that must be considered in the establishment of an RWIS is presented here.

The road surface temperature (RST) is determined by several factors. To an extent determined by the prevailing weather, the local topography causes a more or less pronounced effect on the temperature pattern, along with factors such as altitude and surface construction. In the analysis of the climatology of a certain area or region and its need for field stations, it is important to consider local and regional temperature differences. Locally induced temperature variations are best detected and studied by direct measurements, that is, thermal mapping. Temperature variations on the regional scale are determined by analysis of synoptic weather data and topographical maps. These analyses form the basis for determining the most appropriate locations of field stations in an RWIS.

TOPOCLIMATOLOGY

The combination of a varied topography and variations in the weather in a landscape causes a diversified temperature distribution that has great impact on the risk of winter slipperiness. The main topographical factors controlling temperature variations are valleys, elevated areas, and screened areas. Bridges, road materials, and vegetation are also factors that alone or in combination with the topoclimate must be regarded for analyses of the temperature variations.

Valleys

Accumulation of cold air in valleys during clear, calm nights results in a varying air temperature pattern along road stretches. Bogren and Gustavsson (2) demonstrated that the variation in temperature between valley

bottoms and summits can be related to such factors as the valley geometry, that is, the width and depth of the valley. Another factor of great importance is the wind exposure of the valleys. The return period of the occurrence of the cold air pool, as well as the magnitude of the temperature difference, increased if the valley location was sheltered from the wind by, for example, trees. Pooling of cold air in valleys causes a reduction of the RST compared to that of nearby neutral areas. As shown by Gustavsson (3) and Bogren and Gustavsson (2), the lowering of the RST is linearly related to the lowering of the air temperature, which is termed the intensity of the pooling of cold air. An air temperature difference of 6°C results in a lowering of the RST by approximately 2.5°C. By use of the relationship between the geometric factors and variation in air temperature, it is possible to calculate the variation in RST.

Elevated Areas

The local topography has a small effect on temperature variations during cloudy, windy weather. Counter-radiation from clouds and turbulence caused by wind reduce local temperature variations, which otherwise develop under more stable conditions. Under cloudy, windy conditions variations in temperature are largely caused by changes in altitude, and the influence of local topography is most reduced. Under fully mixed conditions the temperature falls by approximately 1°C per 100 m. This general tendency can be applied to both night and day.

Screening

The effect of screening as a factor causing large RST variations is connected to clear day conditions. The largest influence of screening, which can affect the risk of slipperiness, occurs during late autumn and early spring. A study by Bogren (4) demonstrated that the factors of greatest importance to screening effects are the position of the sun in relation to the site (time of day and season) and the type of screening object and its orientation in relation to the road. The intensity of the temperature difference that develops between the screened and exposed sites is also affected by the amount of cloud cover. That the orientation and geometrical configuration of the screening object are the most important factors controlling the variation in surface temperature during days with sunshine has also been documented in a study by Gustavsson and Bogren (5). Figure 1 shows the temperature pattern of the RST during a clear day in February. It is obvious how distinctly and regularly the RST reacts on the screening objects along the road stretch.

Bridges

Analyses of bridges is important because they often have a different temperature development than adjacent roads, caused by different qualities of heat storage and conductance. The importance of these temperature differences is most pronounced during changes in the weather during both cooling and warming trends. Factors controlling the surface temperature of bridges include the type of bridge
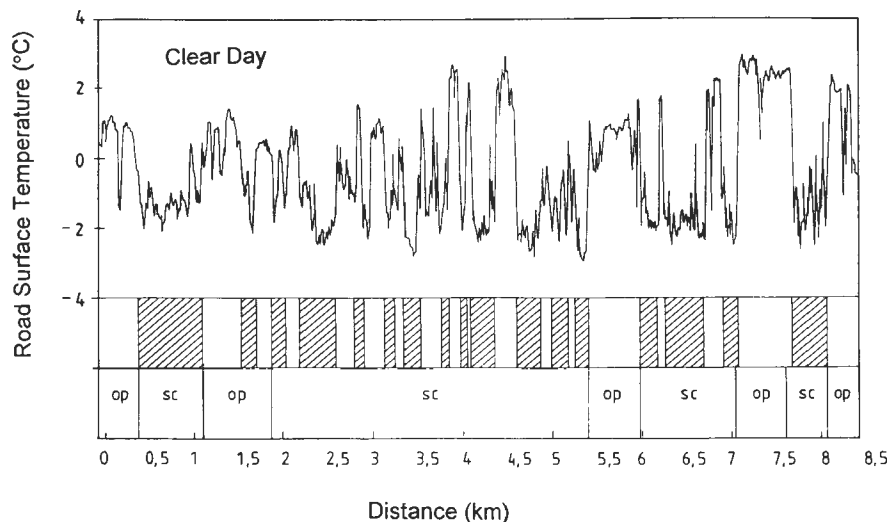

FIGURE 1   Thermal mapping showing effect of screening objects (gray) on road surface temperature on clear day (op—open, well-exposed; sc—screened).

crossing (over water or other roads), bridge composition, bridge thickness, and weather. Another factor that can affect the temperature pattern at bridges is the surrounding terrain characteristics. In analysis of climate and topoclimatological characteristics in an area, regional climate must be considered. When large areas with variations in latitudes and altitudes are analyzed, factors such as distance to the sea or to large lakes must be considered along with spatial differences in the distribution of precipitation. The variation in regional climate must be considered in all types of weather because these differences could be of the same magnitude as the variations caused by topoclimatological factors.

THERMAL MAPPING

Temperature variations within a small area are the result of several factors. By use of the thermal mapping technique, the total result of these factors is detected as the temperature variation. When these measurements are combined with field analyses of topography and weather parameters, the relative importance of the different factors can be determined.

Studies of thermal mappings and climatological records from field stations within the RWIS has made it possible to evaluate the effect of different terrain factors on the temperature pattern. The factors that must be covered and analyzed to determine the locations of road weather sensors are radiation, advection, and construction of the road.

Radiation

Heating and cooling rates of the road surface are largely determined by radiative processes. During the day incoming solar radiation heats exposed areas while screened areas are shaded, creating large temperature variations within a short distance. A clear sky allows solar radiation to heat the road during the day. Solar radiation is disturbed by road rock cuts and vegetation, which form shadow patterns on the road.

It is possible to consider the potential for radiative input and screening by combining the thermal maps with a study of the field conditions along the roads where the potential for screening can be determined. The relative input of radiative cooling can be determined. This can be done by use of video recording through which the sky view is calculated according to the degree of obstruction of the sky. It is also possible to use a radiometer for direct measurements of the radiation conditions. A mobile-mounted radiometer can also be used for the stretches of road. Information from nearby field stations may also be used in the investigation of a new area.

Advection

The horizontal transport of air from nearby areas has a marked effect on RST. Air transported from an adjacent area may have properties that differ from those of the road. A typical example occurs when cool air produced on an open area is drained from its production area toward the lower-lying road. The wind may also play a significant role in bringing air with different properties, such as temperature and humidity, over the road.

The advective factor is registered by measuring the air temperature at two levels. By performing thermal mapping along the same route at different times, it is possible to analyze the relative change in temperature during a period, revealing the relative importance of the advective term. Moisture from adjacent lakes or other wet areas can also play an important role in affecting the risk of slipperiness on the roads. During midwinter, when the lakes and bogs are ground frozen, these areas may produce very cold air that can be advected to the road.

Construction of Roads

Differences in road construction materials and types of surface coating will provide variations in thermal properties. Surface temperature measurements made with infrared recording equipment take these factors into account. To take the thermal properties into account, thermal mapping may be performed in two ways. One method is to make the measurements after midnight, to allow the minimum temperature to be reached. Another method is to perform two measurements along the same route at different times so that the differences in cooling rates at different locations may be analyzed. To cover the different components that give rise to temperature variations and risk of slipperiness, thermal mapping is performed under various weather conditions, including cloudiness, wind, and time of day or night.

Clear situations are divided into day and night situations. Nocturnal thermal mapping missions should be performed during calm weather conditions because the goal is to detect the temperature pattern created by the gathering of cold air and radiative loss. Thermal mapping carried out during the day is performed to detect the temperature anomalies associated with screening from topography and vegetation. These measurements are not dependent on wind conditions.

Cloudy conditions are divided into partly cloudy and overcast situations. For cloudy conditions the best results are achieved when there is a prevailing wind. The measurements can be carried out independently of the time of day.

SITING OF FIELD STATIONS

To site the field stations in the most appropriate locations a thorough climatological analysis must be carried out. The fundamental tool for achieving knowledge of the climatological variability within an area is a thermal mapping. The field stations should be located at road sites that are frequently struck by slipperiness and where an early warning is given during different weather conditions. Typical locations are valleys, high areas, bridges, and road rock cuts. At the field stations air temperature and humidity are traditionally measured at the 2-m height and the RST is measured by pavement sensors in the top layer of the road coating. Several of the stations have extra equipment, such as sensors for wind speed, wind direction, and precipitation.

Research has shown that the specific location of the sensors at each station is important for the timing of ice detection. Because of local factors the development of the internal boundary layer influences the temperature stratification at a site. This indicates that air temperature and humidity sensors should be located according to site-specific conditions. Future research will show if various levels must be used or if a software transformation can be used.

Interpretation of the temperature recordings from a certain site requires awareness of the RST variations that can occur in different lanes or at different locations within the lane. Such differences may occur because of differences in traffic density or various surface coatings.

It is also important to be aware that sensors for measuring precipitation and wind are very sensitive to obstruction. A major mistake is to underestimate the impact of vegetation or other objects, which may disturb the recording and give false information about the risk of slipperiness.

REFERENCES

1. Gustavsson, T. Application of a Road Weather Information System. *Proc., 4th International Symposium on Snow Removal and Ice Technology*, Reno, Nev., Aug. 11–16, 1996.
2. Bogren, J., and T. Gustavsson. Nocturnal Air and Road Surface Temperature Variations in Complex Terrain. *International Journal of Climatology*, Vol. 11, 1991, pp. 443–455.
3. Gustavsson, T. Variation in Road Surface Temperature Due to Topography and Wind. In *Theoretical and Applied Climatology*, Vol. 41, 1990, pp. 227–236.
4. Bogren, J. Screening Effects on Road Surface Temperature and Road Slipperiness. *Theoretical and Applied Climatology*, Vol. 43, 1991, pp. 91–99.
5. Gustavsson, T., and J. Bogren. Infrared Thermography in Applied Road Climatological Studies. In *International Journal of Remote Sensing*, Vol. 12, 1991, pp. 1811–1828.

Predicting Slipperiness of Road Surface in Winter with a Neural-Kalman Filter

Takashi Fujiwara, Takashi Nakatsuji, Yuki Onodera, and Toru Hagiwara,
Hokkaido University, Japan

An artificial intelligence method was developed to predict the slipperiness of a road surface in winter by emulating the prediction process of experienced drivers. To realize this method, a neural network model was integrated into the Kalman filter. First, the state equation that defines how the slipperiness varies with time and the observation equation that relates the slipperiness to the road surface temperature were described by using a multilayered neural model. Then, a prediction procedure similar to the conventional Kalman filter was developed. The introduction of the neural network model made it possible to formulate complicated phenomena mathematically, and the Kalman filter made it possible to predict slipperiness indirectly through the road surface temperature. Precision of the new method was examined through a comparison with actual measurement data. The kind of weather data needed to predict road surface slipperiness was also investigated.

R oad surface conditions in winter undergo complex changes. They are strongly affected by many factors, such as weather, traffic, and other peripheral factors. They also vary greatly with time and space. Therefore, mathematical formulation and precise prediction of changes in road surface conditions are difficult. Several attempts have been made to predict ice formation and temperature on the road surface. Some approaches are analytical, based on energy balance theory (1,2), and others are statistical, based on regression analysis (2–6). However, none of these methods deals with slipperiness of the road surface.

Although several indexes represent road surface slipperiness, a friction coefficient is considered to be the best index because it directly indicates the degree of slipperiness. Precise predictions of the degree of road surface slipperiness would provide useful information not only to road maintenance officers but also to drivers. However, although the coefficient is not difficult to measure, special equipment, such as a skid-resistance tester, is required. Also, many testers or much time is necessary to measure the degree of slipperiness over a given road section because a friction coefficient greatly varies with time and space.

Drivers who live in a snowy region and have experience driving on snow- or ice-covered roads are very sensitive to changes in road conditions. Such drivers can often predict the slipperiness precisely by combining their past experience with the weather forecast information data, although they have no information concerning the friction coefficient. To emulate this forecasting process of experienced drivers, a new prediction method was developed by integrating a neural network model into the Kalman filter. First, indirect estimation of the degree of slipperiness through the use of a weather condition variable was considered. Air temperature is easy to measure but is not always correlated to the degree of slipperiness. Road surface temperature is more difficult to measure but is more closely related to the degree of slipperiness than is air temperature. Therefore, road surface temperature was used as the indirect variable. The Kalman filter is a mathematical technique for estimating unmeasurable state variables indirectly through some measurable observation variables. However, to apply the Kalman filter, both the state equation that describes how the state variables vary with time and the observation equation that relates the state variables to the observation variables must be defined analytically. Unfortunately, variations of road surface are too complex to be used to define

these equations mathematically. To deal with this difficulty, a multilayer neural network model was introduced. To establish the relationship between the state and the observation variables, another neural network model was used. Both neural network models were integrated into the Kalman filter to establish a new prediction method, the neural-Kalman filter. The effectiveness of the neural network model in predicting the slipperiness on a road surface is discussed in this report.

NEURAL-KALMAN FILTER

Kalman Filter

The Kalman filter is a technique for indirectly estimating some state variables (7,8) that cannot be directly measured through the measurement of the other variables. It consists of two equations: the state equation and the observation equation. The former defines how state variables vary with time:

$$\mathbf{x}_{k+1} = A_k \cdot \mathbf{x}_k + \mathbf{v}_k \tag{1}$$

where $\mathbf{x}_k$ denotes the state variable vector at time k, and $\mathbf{v}_k$ denotes the white noise vector. The observation equation describes how state variables are related to observation variables:

$$\mathbf{y}_k = C_k \cdot \mathbf{x}_k + \mathbf{w}_k \tag{2}$$

where $\mathbf{y}_k$ is the observation variable vector at time k and $\mathbf{w}_k$ is also the white noise vector. When the new values of the vector $\mathbf{y}_k$ at time k are obtained, the state vector $\mathbf{x}_k$ at time k can be estimated according to the theory of the Kalman filter:

$$\hat{\mathbf{x}}_k = \tilde{\mathbf{x}}_k + K_k(\mathbf{y}_k - \tilde{\mathbf{y}}_k) \tag{3}$$

$\tilde{\mathbf{x}}_k$ and $\tilde{\mathbf{y}}_k$ are the one-step predictors of $\mathbf{x}_k$ and $\mathbf{y}_k$, respectively, and $\hat{\mathbf{x}}_k$ is the estimator of $\mathbf{x}_k$ at time k:

$$\tilde{\mathbf{x}}_k = A_{k-1}\hat{\mathbf{x}}_{k-1}$$
$$\tilde{\mathbf{y}}_k = C_k\tilde{\mathbf{x}}_k \tag{4}$$

where K_k is termed the Kalman gain, which is a function of both coefficient matrices A_k and C_k and also the covariance matrices of noise vectors $\mathbf{v}_k$ and $\mathbf{w}_k$. Equation 3 corrects the estimate $\tilde{\mathbf{x}}_k$, which was predicted without the observed data $\mathbf{y}_k$ at time k, in proportion to the error between the actual vector $\mathbf{y}_k$ and the predicted vector $\tilde{\mathbf{y}}_k$.

Extended Kalman Filter

The preceding filtering technique is applicable only to linear systems. In many dynamic problems, the state and the observation equations are often described nonlinearly:

$$\mathbf{x}(k+1) = f[\mathbf{x}(k)] + \boldsymbol{\varphi}(k) \tag{5}$$

$$\mathbf{y}(k) = g[\mathbf{x}(k)] + \boldsymbol{\zeta}(k) \tag{6}$$

where $\boldsymbol{\varphi}(k)$ and $\boldsymbol{\zeta}(k)$ are noise vectors. Expanding the right sides of Equations 5 and 6 in the vicinity of $\tilde{\mathbf{x}}(k)$ and neglecting the higher-order terms yields

$$\mathbf{x}(k+1) = A(k) \cdot \mathbf{x}(k) + \mathbf{b}(k) + \boldsymbol{\varphi}(k) \tag{7}$$

$$\mathbf{y}(k) = C(k) \cdot \mathbf{x}(k) + \mathbf{d}(k) + \boldsymbol{\zeta}(k) \tag{8}$$

where

$$\mathbf{b}(k) = f[\hat{\mathbf{x}}(k)] - A(k) \cdot \hat{\mathbf{x}}(k) \tag{9}$$

$$\mathbf{d}(k) = g[\hat{\mathbf{x}}(k)] - C(k) \cdot \hat{\mathbf{x}}(k) \tag{10}$$

$$A(k) = \frac{\partial f}{\partial \mathbf{x}} \quad C(k) = \frac{\partial g}{\partial \mathbf{x}} \tag{11}$$

Now we can estimate the state variable $\mathbf{x}(k)$ in the same manner as linear systems.

Neural Network Model

Figure 1 shows the multilayer neural network model used in the present analysis (9,10). It consists of five layers: an input layer, three intermediate layers, and an output layer. Neurons in each layer are mutually connected to neurons in adjacent layers, except for those in the input layer. The strength of the connections is called synaptic weight. The synaptic weights for both intermediate and output layers are adjusted. The input layer serves only as a normalizer. First, the synaptic weights are initialized randomly. The raw variables x_i^A are input into the input layer and normalized. If the normalized signals are transmitted in sequence from the input layer to the output layer, the output signals may be obtained during the neural operations:

$$y_m^E = h\left(\sum_k w_{km}^{DE} h\left\{\sum_j w_k^{CD} h\left[\sum_i w_{ij}^{BC} h(x_i^B)\right]\right\}\right) \tag{12}$$

where h is an activation function that represents the input-output relationship for each neuron. The sigmoid function is used as the activation function. The ability of neural network models to describe nonlinear behavior comes from this nonlinear function. This represents the foreword signal process in Figure 1. Next, the synaptic
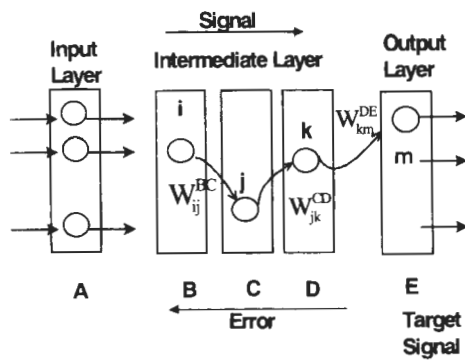
FIGURE 1   Mutilayer neural network model for describing state and observation equations.

FIGURE 2   Basic concept of neural-Kalman filter for estimating slipperiness on a winter road surface.

weights are adjusted so that the error between the output signals and the target signals is minimized. The back-propagation method is used to adjust the synaptic weights. The errors are corrected and the weights are modified backward from the output layer to the input layer. Iterative adjustment of synaptic weights by using many training patterns produces a stable input-output relationship between input and output signals, even for a nonlinear system. In other words, the neural network model is very effective in accurately describing nonlinear phenomena.

Neural-Kalman Filter

Because of the difficulty of measuring slipperiness of road surfaces in winter, an attempt was made to estimate slipperiness indirectly through other variables that are closely related to slipperiness but are easily measurable, such as road surface temperature. Air temperature was another promising variable because it is very easy to measure, but it was not used because it is not as closely correlated to slipperiness as is road surface temperature. Application of the Kalman filter theory is possible with prior knowledge of how slipperiness varies with time and how closely it is correlated with road surface temperature. As shown in Figure 2, slipperiness varies according to weather and traffic conditions. This transition process is too complex to formulate analytically, that is, it is too difficult to physically or mathematically define the state equation. Therefore, the process is described as using a multilayer neural network model, which inputs the slipperiness as well as data on weather and traffic conditions at time k, and outputs the slipperiness at time $k + 1$. The relationship between slipperiness and road surface temperature is also very complex, and is almost impossible to describe analytically. Thus, another multilayered neural network
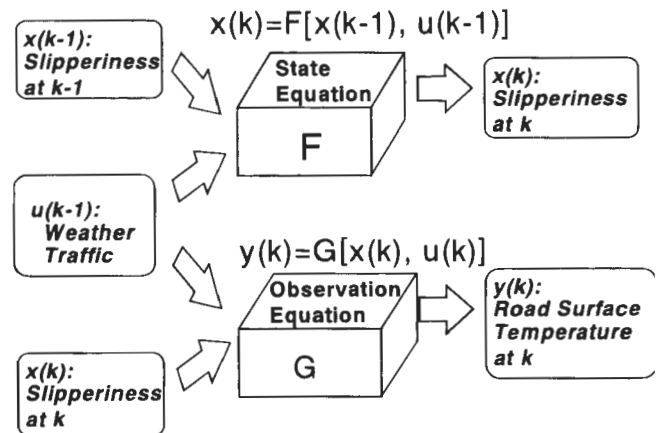
model is introduced for establishing a steady nonlinear relationship between them. The input signals are the same as those of the state equation, and the output signal is the road surface temperature. Thus, an estimation method was developed by incorporating the neural network model into the Kalman filter. This artificial intelligence method was named the neural-Kalman filter. Figure 2 shows a conceptual representation of this method.

Since the proposed method is essentially a Kalman filtering technique, it consists of two equations: the state equation that defines how the slipperiness varies with time, and the observation equation that describes how the slipperiness is related to the road surface temperature. First, each equation is identified by using a multilayer neural network model. This simply requires the preparation of a large volume of measurement data on slipperiness, weather, and traffic conditions. The synaptic weights are then adjusted. This is the training phase in establishing the neural networks. The completion of the training makes it possible to estimate or predict the degree of slipperiness for unknown weather and traffic situations. The fundamental algorithm is identical to that of the conventional Kalman filter. First, on the basis of the estimate at the previous time k, the slipperiness $\tilde{x}(k + 1)$ at time $k + 1$ is predicted by using the neural function F. Then the road surface temperature $\tilde{y}(k + 1)$ is estimated by using the neural function G, before the actual temperature $y(k + 1)$ at time $k + 1$ is measured. At the same time, the derivative matrices $A(k)$ and $C(k)$ given by Equation 12 are calculated and the Kalman gain is evaluated. Finally, the slipperiness $\hat{x}(k)$ may be estimated from Equation 3 after the actual temperature $y(k)$ is measured. By repeating these procedures, the degree of slipperiness in real time may be estimated and predicted successively.

FIELD MEASUREMENTS

To obtain fundamental data on road conditions in winter, field measurements were carried out at an intersection in a suburb of Sapporo over several days in December 1994, 1995, and 1996. Weather conditions such as air temperature, total solar radiation, and net radiation also were measured as were traffic conditions, such as traffic volume. Table 1 shows the items measured. The measurements were carried out from early in the morning to late in the evening because road conditions changed greatly during the daytime. To evaluate the degree of slipperiness on the road surface, the friction coefficient (skid number) was measured by using a bus-type skid tester with a test wheel mounted in the center. The effect of sunshine was evaluated through both total solar radiation and net radiation, cumulated every 30 min. Road surface temperature was measured on the surface of two tire ruts in the road that were covered with snow or ice by using a portable thermistor. Humidity data were not used here because they had little influence on prediction precision. Traffic volume was measured by counting the number of vehicles passing by the intersection every 30 min.

NUMERICAL EXPERIMENTS

Structure of Neural Network Model

By using the measurement data, the neural network models for both state and observation equations were determined. Table 2 presents the input and the output signals for neural networks F and G in Figure 2. For the neural State Equation F, the skid number at time k was input together with weather conditions and traffic volume at time k, and the skid number at time $k + 1$ was output. Similarly, for the neural Observation Equation G, the same data as those used in the state equation were input, and the road surface temperature at time k was output.

To clarify the weather data necessary for precise estimation of the degree of slipperiness, the weather data were classified into two groups: ordinary data that can be measured without any special equipment, and special data that require special equipment (Table 3). Ordinary weather data were obtained through the SNET system, which is a weather information system in Sapporo. However, some items of weather data required special equipment for measuring, because the SNET system does not measure total solar radiation or net radiation. Two cases were simulated, one using only ordinary weather data and the other including the special weather data. The number of neurons in the input layer was eight for Case 1, in which solar radiation data were used, and six for Case 2, in which these data were not used. The number of neurons in the intermediate layers was empirically determined—the same number of neurons for the first intermediate layer, and half that number of neurons for the second intermediate layer. Naturally, the number of neurons in the output layer was one for both equations in this analysis.

Training of Neural Networks

To determine the neural networks precisely for both equations, measurement data for extensive road and weather conditions are needed. Also, to examine the validity of the models, checking data for which the neural models are not yet trained are needed. Unfortunately, the number of measurement data sets here is restricted. Excluding the incomplete data caused by the failure in the measurement, the measurement data for 8 days were used as the training data. The training procedure was simple. First, the initial synaptic weights were set. Then the input signals into the input layer were set, and the output signals were calculated. These signals were then compared with the actual measured signals (target signals), and the synaptic weights were adjusted to minimize the difference between the output signals and target signals. This procedure was repeated until the error

TABLE 1   Field Measurements of Winter Road Conditions

Date	December 1994	19(Mon), 20(Tue), 21(Wed), 22(Thu), 23(Fri)	7:00 to 20:00
	December 1995	14(Thu), 18(Mon), 20(Tue), 27(Wed)	15:00 to 20:00
		15(Fri), 19(Tue), 21(Thu), 28(Thu)	6:00 to 20:00
	December 1996	18(Wed), 19(Thu), 20(Fri), 21(Sat), 22(Sun)	6:00 to 20:00
Items	Weather Conditions	Air Temperature, Snowfall Intensity, Snowfall Depth, Total Solar Radiation, Net Radiation, Humidity	every 30 minutes
	Road Conditions	Skid Number, Road Surface Temperature Pavement Surface Temperature	every 30 minutes
	Traffic Conditions	Traffic Volume, Heavy Traffic Volume	every 30 minutes

TABLE 2   Input and Output Signals of Neural Network Models for State and Observation Equations

	State Equation	Observation Equation
Input Signals	Skid number at time k Weather condition data Traffic volume Pavement surface temperature	Skid number at time k Weather condition data Traffic volume Pavement surface temperature
Output Signals	Skid number at time k+1	Road surface temperature

became sufficiently small for all the training patterns. In general, the estimation ability of a neural network model can be evaluated by the estimation precision for checking data that are not trained yet. The measurement data for 3 days were used as the checking data. After the completion of training, the input signals of the checking data were set, and the corresponding output signals were calculated by using Equation 12. These signals were then compared with the actual measured signals.

Figure 3 shows the root mean square (RMS) errors for both the training and the checking data sets for each case. The errors for Case 1 in Figure 3(a), for which the solar radiation data as well as the ordinary weather data were used, were around 5 percent for both state and observation equations except for a few data sets. The errors for the checking data were larger than those for the training data. In particular, the errors of the state equation for the data sets on December 22, 1994, and December 19, 1995, exceeded 15 percent. This means that the number of training data sets is not sufficient yet. That is, the neural model did not experience weather and road conditions similar to those of the checking data in the training process. The errors for the data set on December 21, 1996, were less than 10 percent for both equations.

The errors for Case 2 shown in Figure 3(b), for which the solar radiation data were not used, were larger than those for Case 1 for both state and observation equations. The errors of the state equation were more than 10 percent for half of the training data sets. This means that there is no definite relationship between the input and output signals. In other words, any other weather condition data, such as solar radiation data in Case 1, may be needed to accurately describe the degree of slipperiness on roads in winter. The errors of the checking data for Case 2 were better than those for Case 1. However, the errors of the state equation were more than 10 percent for all checking data sets.

Prediction Precision

Training Process

To determine how precisely the neural network model represented the state and the observation equations, the skid numbers predicted by the neural-Kalman filter were compared with the actual measured skid numbers. For this purpose, the skid numbers were calculated by following the procedure of the neural-Kalman filter already explained. Figure 4 shows variations in skid number with time for the training data on December 19, 1996. The skid number was predicted 30 min in advance at 30-min intervals. It can be seen that the values predicted with solar radiation data trace the measured values better than do the values predicted without solar radiation data. This reflects the results of the training process for both cases shown in Figure 3. Similar results were obtained for the other training data.

Checking Process

The results in Figure 4 can be expected because the synaptic weights had been adjusted so that the estimated variables agreed with the measured variables. As mentioned, the true estimation ability of the new method can be evaluated by the estimation precision for checking data. Figure 5 shows a comparison of the skid number predicted for the checking data on December 21, 1996, with the measured skid numbers. As shown in Figure 5(a), the level of prediction precision obtained by using the neural-Kalman filtering method was not bad for Case 1, except for the initial period from 7:00 to 9:00 a.m. This outcome reflects the effect of solar radiation data in both state and observation equations. If the initial skid number were estimated more precisely at the beginning of the prediction, the errors could be decreased for the initial period. On the other hand, the

TABLE 3   Weather Condition Data

CASE	Ordinary Weather Data	Special Weather Data
1	Air temperature, Moisture, Snowfall depth	Total solar radiation, Net radiation
2	Same as Case 1	None

(a) with Solar Radiation Data

(b) without Solar Radiation Data

FIGURE 3   RMS errors for training and checking data.

(a) with Solar Radiation Data

(b) without Solar Radiation Data

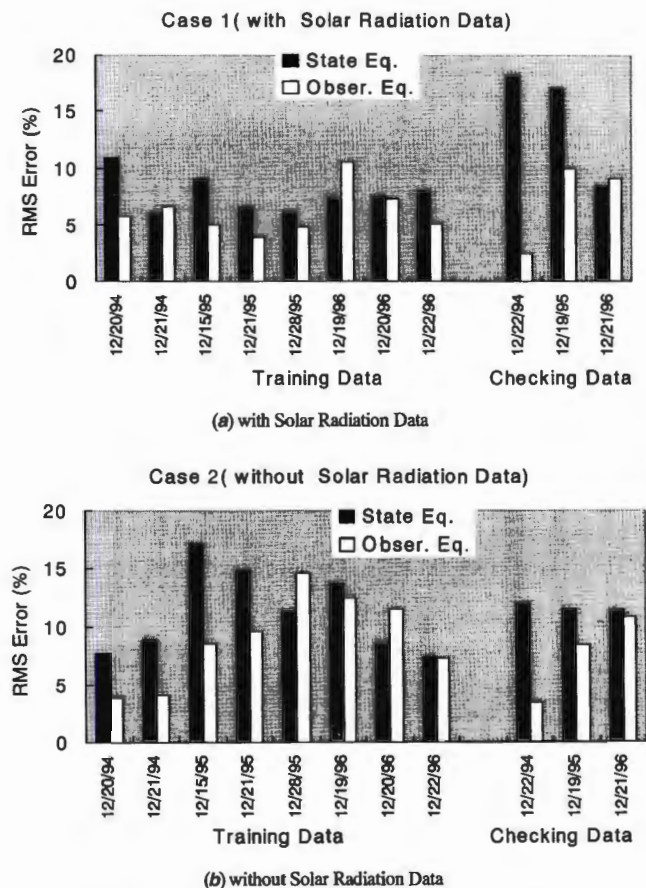FIGURE 4   Skid numbers predicted by neural-Kalman filter in comparison with measured numbers for training data.

prediction in Case 2, in which solar radiation data were not used, gave very poor results. This is partly because of insufficient training of the neural networks as well as the lack of solar radiation data. Because a neural network model has the promising characteristic of being able to flexibly adjust synaptic weights regardless of the number of training data sets, the neural-Kalman filter could predict more precisely by training the neural networks with more measurement data sets.

CONCLUSIONS

Information on the degree of slipperiness on road surfaces is very important for efficient snow and ice control. It is also useful for drivers using unfamiliar roads in winter. However, the transition of slipperiness is too complex to formulate mathematically. Slipperiness is difficult to measure because it varies greatly with time and space. To emulate the prediction process of experienced drivers, an artificial intelligence method for predicting the degree of slipperiness was developed. The major findings were as follows.
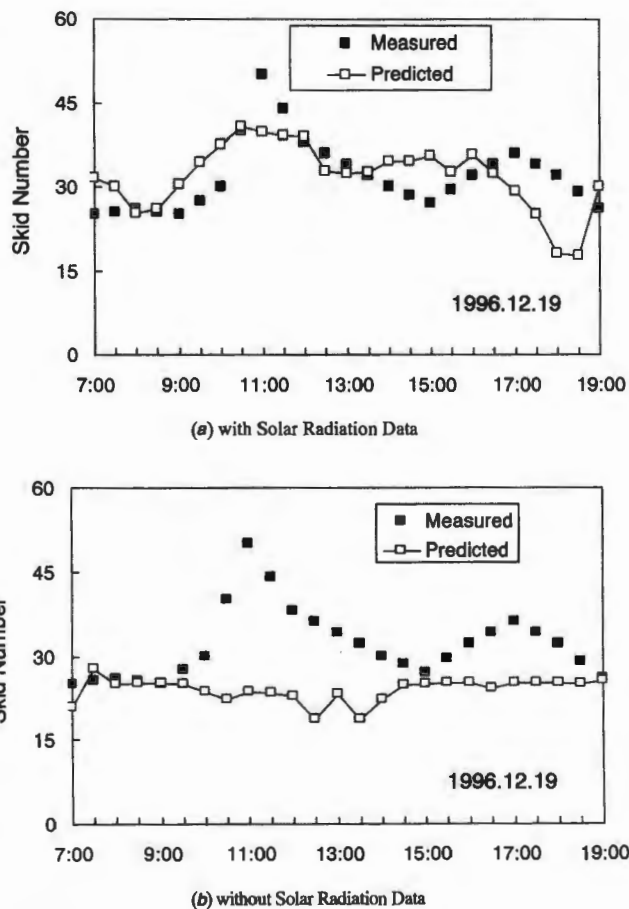
1. A multilayer neural network model was proposed to describe the nonlinear behavior of how slipperiness varied with time and how it was related to road surface temperature and weather conditions.

2. A method that could indirectly predict the skid number through road surface temperature was developed by integrating a neural network model into the Kalman filter.

3. The weather data that represent solar radiation activities were effective in constructing the neural network system and predicting the skid number.

4. The road surface temperature may not be sufficient to accurately represent the observation equation. Other weather condition variables may be needed.

This study is only the first step to predicting the slipperiness of road surfaces in winter. Many problems remain to be resolved. First, training precision of the neural network models must be improved. The estimation precision for checking data is not yet satisfactory. Also, what input signals are influential in the transition of road conditions in winter must be assessed
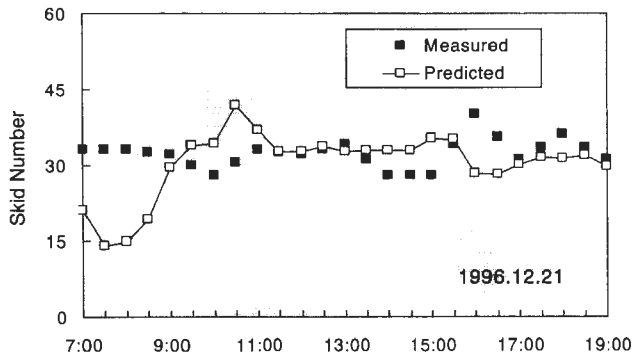
(a) with Solar Radiation Data
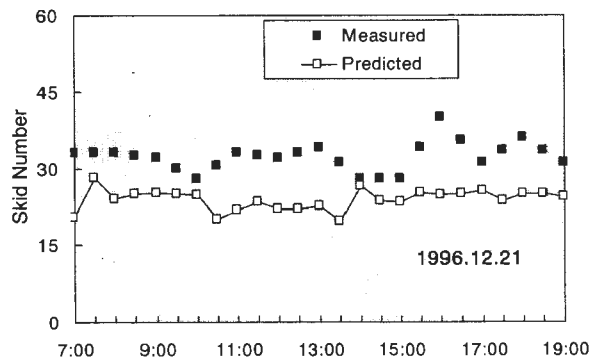
(b) without Solar Radiation Data

FIGURE 5   Skid numbers predicted by neural-Kalman filter in comparison with measured numbers for checking data.

quantitatively. Fortunately, because it is easy to differentiate the output signal y_m^E of Equation 12 with respect to any input signal x_i^B, the effect of each input signal is easily evaluated. Although comparison with other statistical approaches is another problem, it is too early to evaluate the new method because much has yet to be improved.

REFERENCES

1. Thornes, J. E. *The Prediction of Ice Formation on Motorways in Britain*. Ph.D. Dissertation. University of London, England, 1984.
2. Borgen, J. *A Combined Statistical and Energy Balance Model for Prediction of Road Surface Temperature*. Technical Report of IXth PIARC International Winter Road Congress, Seefeld, Austria, 1994, pp. 68–76.
3. Frohling, P. W. *A Neural Network for Short Term Temperature Forecast on Roads*. Technical Report of IXth PIARC International Winter Road Congress, Seefeld, Austria, 1994, pp. 601–608.
4. Suzuki, T, et al. Study on Prediction Methods of Road Surface Freezing. In *Yuki*, Vol. 11, 1993, pp. 69–77.
5. Takeichi, K. Studies on Pavement Freezing Predictions. In *Journal of Infrastructure Planning and Management*, No. 470, IV-20, 1993, pp. 175–184.
6. Wada, A., et al. Study on Level of Winter Maintenance. In *Traffic Engineering*, Vol. 21, No. 1, 1986, pp. 25–35.
7. Arimoto, T. *Kalman Filter*. Sangyo-Tosho, Tokyo, Japan, 1979.
8. Katayama, T. *Advanced Kalman Filter*. Asakura Press, Tokyo, Japan, 1980.
9. Nielsen, R. H. *Neurocomputing*. Addison-Wesley, New York, 1990.
10. Wasserman, P. *Neural Computing*. Van Nostrand Reinhold, New York, 1989.

Variable Slip Friction Measurement Techniques for Snow and Ice Operations

E. J. Fleege, *Minnesota Department of Transportation*
J. C. Wambold, *CDRM, Inc.*
Zoltán Radó, *Norsemeter, Norway*

Maintenance agencies seek a relatively inexpensive device that can measure roadway friction under winter conditions and tell the operator in real time whether friction is present. This method would assist the operator in determining when and where abrasives or chemicals should be applied during snow and ice control operations under all conditions. Past studies have used braking action friction measurements as an indicator, but this method cannot be used under high-traffic-volume conditions. Field studies have been conducted in Minnesota and Norway using Norsemeter's road analyzer and recorder to determine the applicability of the equipment to snow and ice operations and its reliability and durability. The measuring device, mounted on a smaller trailer, uses an industry-standard pavement friction measuring tire. The measurement is made by employing wheel braking on the road surface and measuring the braking friction force that the road surface exerts against the braking wheel. Each measurement uses a variable slip speed measurement and records peak friction, slip at peak friction, and the friction versus slip shape factor. Data were collected for precipitation, pavement condition, pavement temperature, air temperature, speed of the measuring device, and friction values. The equipment, measurement procedures, and findings are described in detail. This preliminary research study shows that the contaminant conditions can be separated and the friction level can be evaluated to determine whether to salt and whether to salt lightly or heavily. Also, with this method a supervisor can evaluate the effectiveness of applied abrasives and chemicals.

A joint project on winter road friction measurement with Norsemeter, the Norwegian Road Administration, the Norwegian Director, and the Norwegian Road Research Laboratory was carried out in 1994 and 1995 (1). The study mapped maintenance guidelines and looked at current technology in friction measurements and the friction and texture research project of the Permanent International Association of Road Congresses (PIARC). On the basis of this study, Norsemeter developed its road analyzer and recorder (ROAR). The unit was designed to be used as a stand-alone tester mounted on a trailer, or to be mounted on a salt spreader truck. Field studies were conducted in Norway and Minnesota during the 1995–1996 winter season in a joint Norsemeter–Minnesota Department of Transportation (MinnDOT) project. This report summarizes these field studies; describes the equipment, measuring procedures, and findings of the preliminary research study; and includes some of the data from the Norwegian study as well.

TEST SITE

The roadway selected for the test site is a western segment of the beltway around the twin cities of Minneapolis and St. Paul (I-494) (Figure 1). This segment of I-494 (both the southbound and the northbound roadways) is located between Trunk Highway 7 and Trunk Highway 55. The site consisted of four test areas: two concrete surfaces, south-
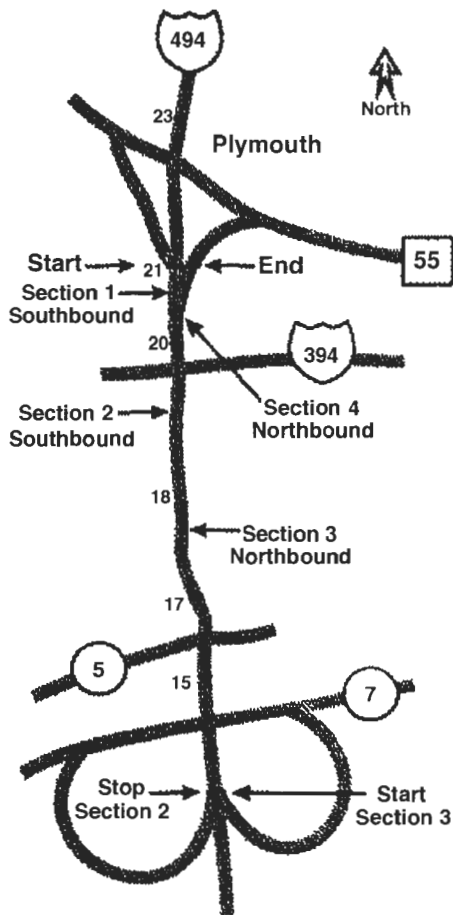
FIGURE 1   Test sections, west of Minneapolis–St. Paul.

bound and northbound, and two bituminous surfaces, southbound and northbound. This segment of I-494 is approximately 9.6 km (6 mi) long and has three bridges that cross another Interstate route, a county road, and railroad tracks. The hourly average weekday and weekend traffic for each roadway is 43,015 and 31,953 vehicles in the southbound lane, respectively, and 43,447 and 30,575 in the northbound lane, respectively. Located near the county road overpass is a road weather information system site that monitors atmospheric parameters and pavement temperatures every 15 min; wind speed and direction, relative humidity, air temperature, and precipitation are measured. The pavement sensor is located in the southbound roadway of I-494, in the bituminous section.

The test site was entered on the southbound roadway of I-494 at the ramp for Route 55. The friction measurements were begun at the nose of the on-ramp and continued to the nose of the off-loop to eastbound Route 7. The friction measurements were suspended, the vehicle continued through the interchange loop, and measurements were begun again on northbound I-494 at the nose of the entrance loop from the Route 7 eastbound roadway. The measurements were continued to the nose of the off-ramp for Route 55 and then were stopped.

TEST APPARATUS

ROAR is a continuous measuring device with a variable slip test wheel. It was mounted on a two-wheel trailer and towed by a host vehicle. The test wheel was located in the left wheel track and mounted directly on the axle of a hydraulic wheel slip controller, which was programmed to perform a desired braking action on the test wheel. The braking action was a linearly decreasing rotational wheel speed from free-rolling to locked wheel. During this action the torque on the wheel axle was measured and converted to a friction coefficient by the digital computer of the device. A vertical static load of 1.5 kN (300 lbf) was applied on the test wheel, which had a four-bar suspension with no spring and no shock absorber. ASTM E1551 was used as the test tire with an inflation pressure of 207 kPa (30 psi). The instrumentation could measure the torque acting on the test wheel, which was converted to friction coefficients in a digital computer, and the rotational speed of the test wheel, which was converted to a distance and a distance-traveled-per-unit time. The computer was programmed to calculate several friction process parameters including peak friction co-efficient, the slip speed at which the peak friction occurred, the slope of the friction coefficient curve as a variable of slip speed, and others. The computer program used the Radó friction model for deriving these parameters (2). Friction coefficients for all slip speeds could be computed from each braking action, including friction at lower slip ratios like 15 or 18.5 percent and at traveling speeds other than the one at which measurements were taken. The measured values were stored in the computer and output as a strip chart and data files on diskette.

TEST PROCEDURES

A baseline test was made of the test sections when bare and dry and when bare and wet. The actual tests were made whenever there was a significant snow or ice storm. The test procedure was to measure right after the first salting, 30 min after salting, and just before salting a second time. For the same period, the weather conditions (precipitation type, pavement condition and contaminate, time since plowed, and chemical type used) were recorded by the driver. From the remote weather station, an office report was created for the time period including the time, air and pavement temperature, pavement condition, dew point and relative humidity, and beginning and end of precipitation.

DATA REDUCTION AND ANALYSIS

The ROAR measures variable slip as shown in Figure 2, which gives an example from the baseline dry tests and
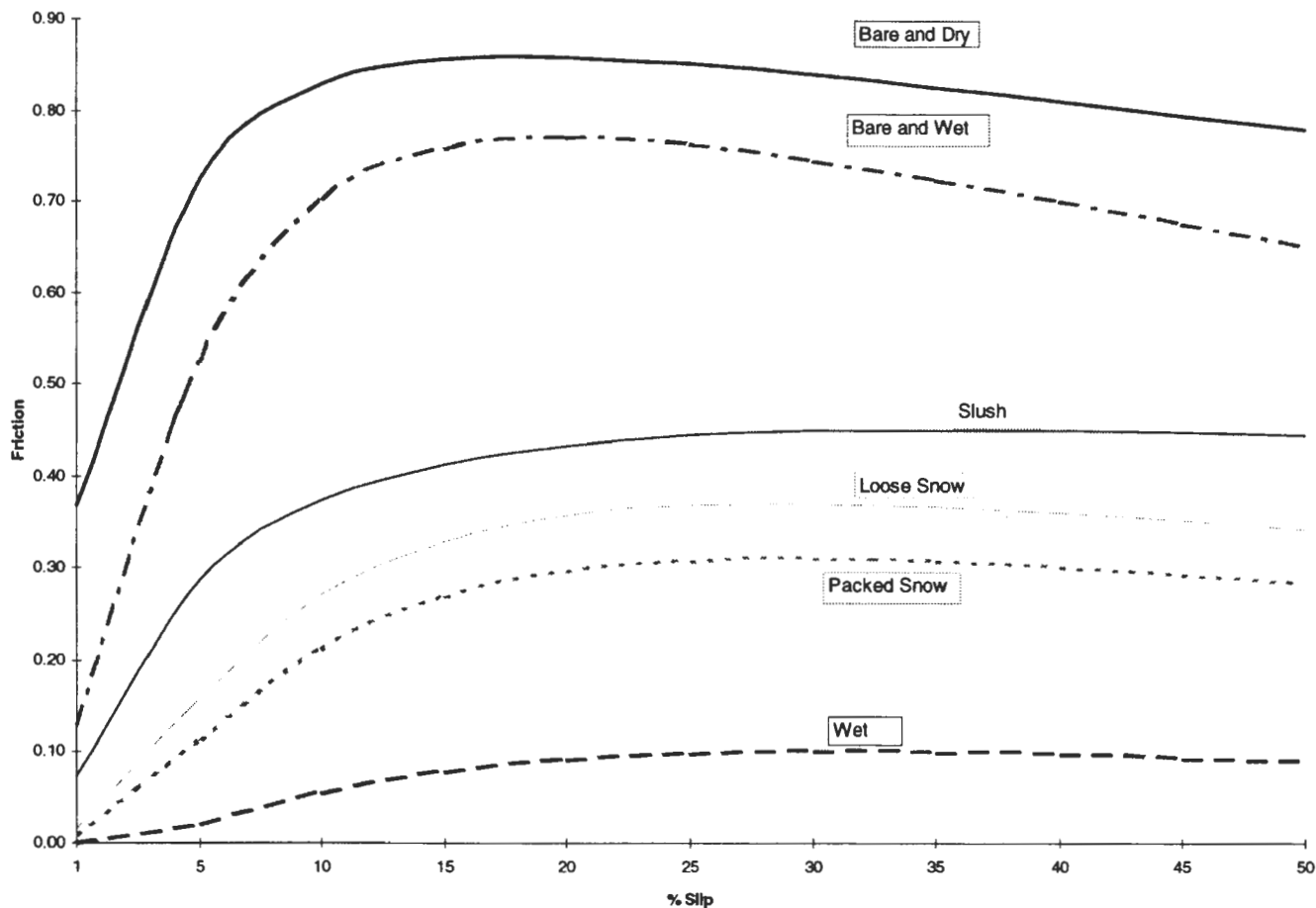
FIGURE 2 Sample friction versus percent slip for six conditions.

an example for wet, slush, loose, and packed snow from the MinnDOT tests, as well as an example on ice from the Norwegian tests. The data are fitted to the Radó model to provide the three coefficients required to produce the friction-slip speed curve. The three coefficients are μ_{peak} (value of the peak friction), S_{peak} (value of slip speed at which the peak friction occurred), and C (a value that gives the shape of the curve, called the shape factor). These values are studied to determine the type of contamination and whether salting is needed. Figure 2 shows that the wet friction drops faster with speed, and this has been shown to be correlated to macrotexture (3). The slip at which the peak value occurs is around 18 percent on dry, 20 percent on wet, and nearly 30 percent on the winter contaminated surfaces. This, along with the drop in the peak value, appears to be a clear sign. The shape factor also separates the loose snow and slush from the packed snow and ice, and the ice is separated from the packed snow by the low friction.

Peak Slip Distributions

Figure 3 is a continuous plot of the peak friction verses position for the baseline (dry) of the test site. Real-time

Bayesian statistics are applied to the μ_{peak} values. A research goal was to determine proper Bayesian values so that the data could be used for decision making. In these plots of peak friction, the dots are the individual data points and the line represents the applied second-generation Bayesian statistics applied. Figure 4 shows the average peak value for each section as well as the most frequent peak friction value. There is a difference between the average and most frequent values although less for the dry baseline than for later plots for winter conditions. All sections run between .84 and .87 in the dry condition. Figure 5 gives the baseline values for the test site under wet conditions. Both the peak friction and the friction at a slip velocity of 60 kmh (37.5 mph) (FR60) of the PIARC international friction index are reported. FR60 is near the value of a locked wheel test per ASTM E274 with a blank tire.

Figure 6 is a sample plot of the peak friction value on packed snow, and Figure 7 shows the average and most frequent peak values for the different sections. The sections are fairly uniform near 0.3, and there is more difference between the average and most frequent values. Figure 8 shows the peak variations for each section for four periods on January 28 and 29. The first period de-
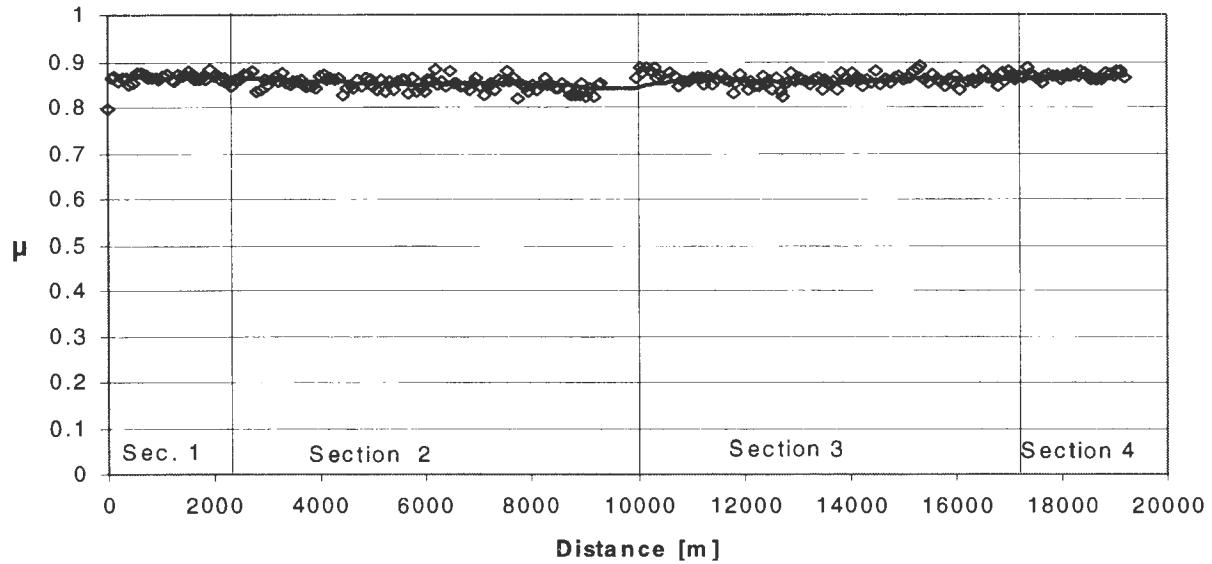
FIGURE 3   Peak friction on dry pavement.

picted is for black pavement showing (bare); and the second, 30 min later after sanding of the bridges, shows that all sections are now even. The next period, 18 hr later, shows that the friction level drops from .6 to .4 when drifting snow spots the roadway. The last period is 30 min later while following a plow truck; although there is some improvement, it is not significant. During this time the temperature dropped from $-10°C$ to $-20°C$ ($15°F$ to $-5°F$).

Figure 9, which depicts results for slush and wet pavement, is of more interest. It is apparent that parts of the site have a good friction value compared with the dry and wet baseline. However, other sections within the site have very poor showings. Clearly, a protocol could have been
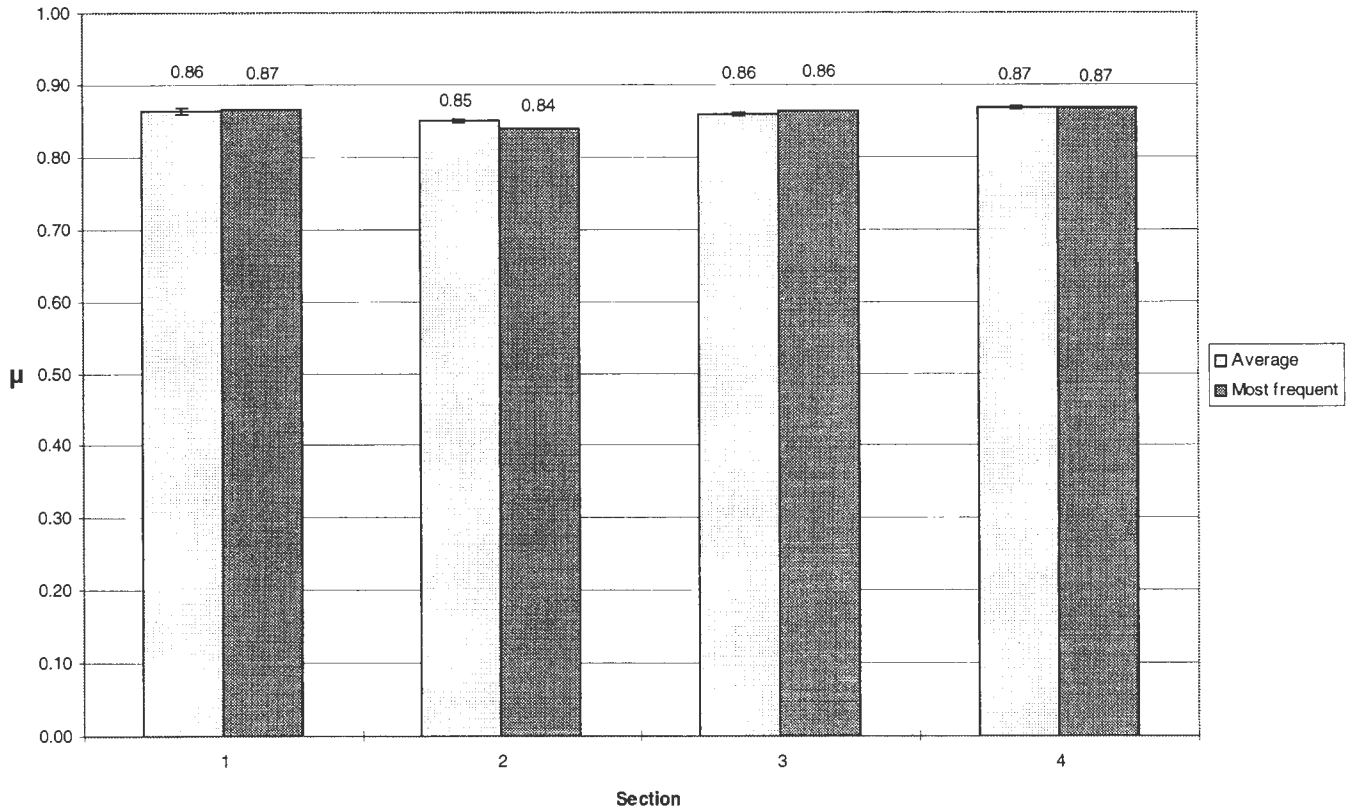
FIGURE 4   Peak average and most frequent for dry pavement.
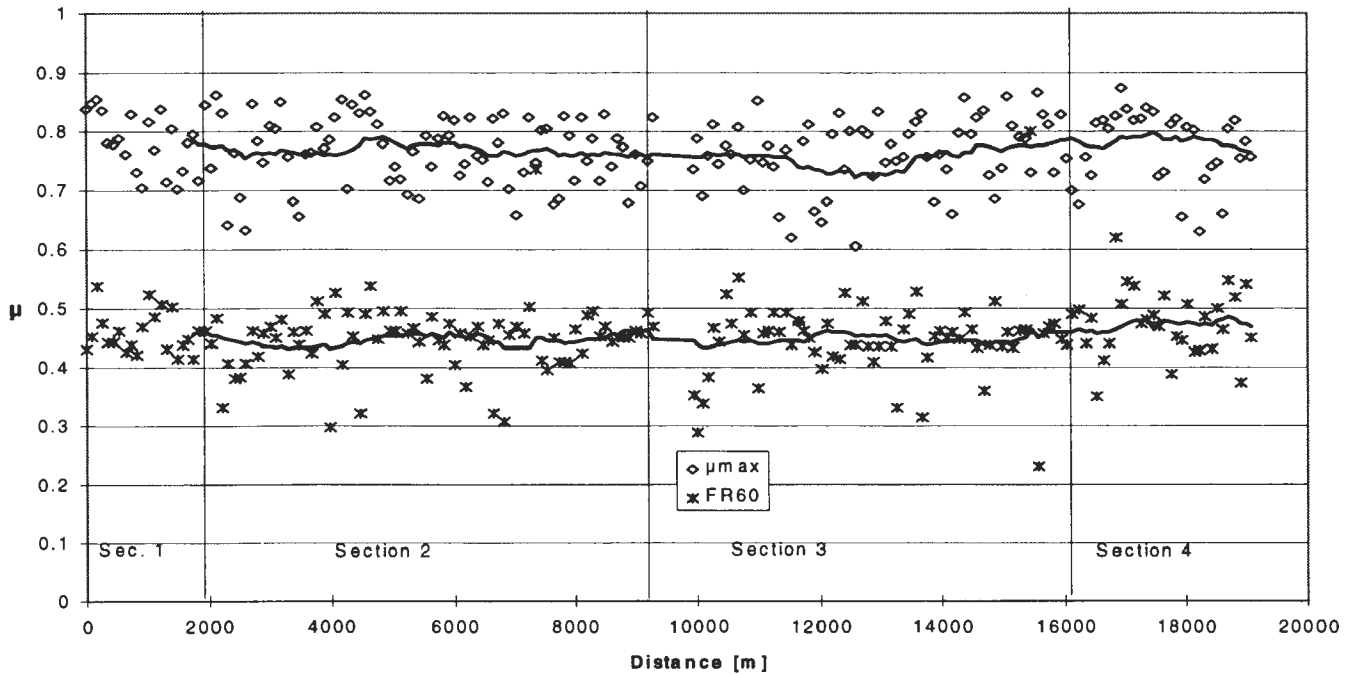
FIGURE 5   Peak friction and FR60 for wet pavement.

set requiring no salting for some parts, light salting for others, and heavy salting for still others. Suggested levels are given, but these would be subject to the roadway's baseline values, the average daily traffic, and the type of roadway, and should also consider whether the temperature is rising, falling, or holding steady. On this day the temperature had dropped from above freezing to below and had later risen again. Figure 9 also shows the improvement of the newer Bayesian values now being used

as a result of this study. Because ROAR is under computer control, all of these factors can be programmed for control of salting. Figure 10 shows the distribution for Section 1. Although this would not be useful in real time for salting control, it is useful to the field engineer for evaluating the effectiveness of salting or sanding by comparing conditions before and after maintenance is performed. Note that in Section 1 most of the friction points are satisfactory and only a few need salting in this section.
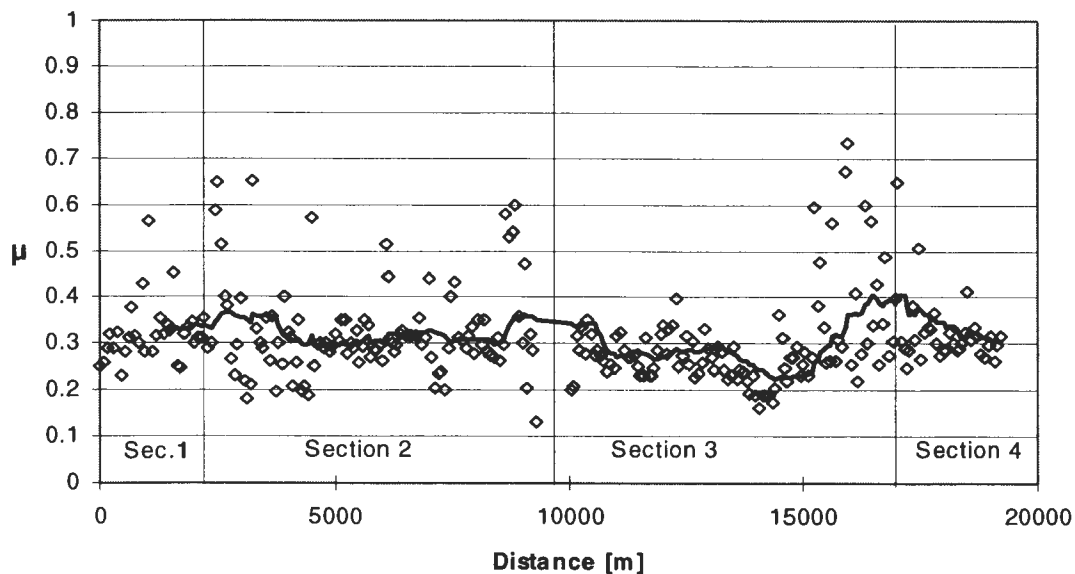

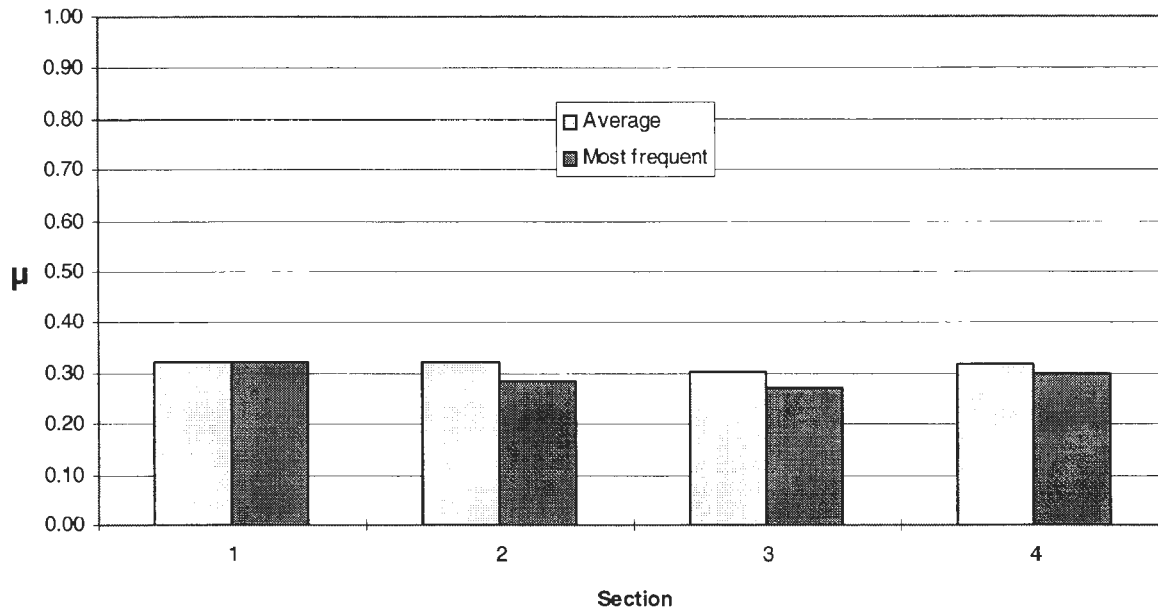FIGURE 6   Peak friction for packed snow.

FIGURE 7   Average and most frequent for packed snow.
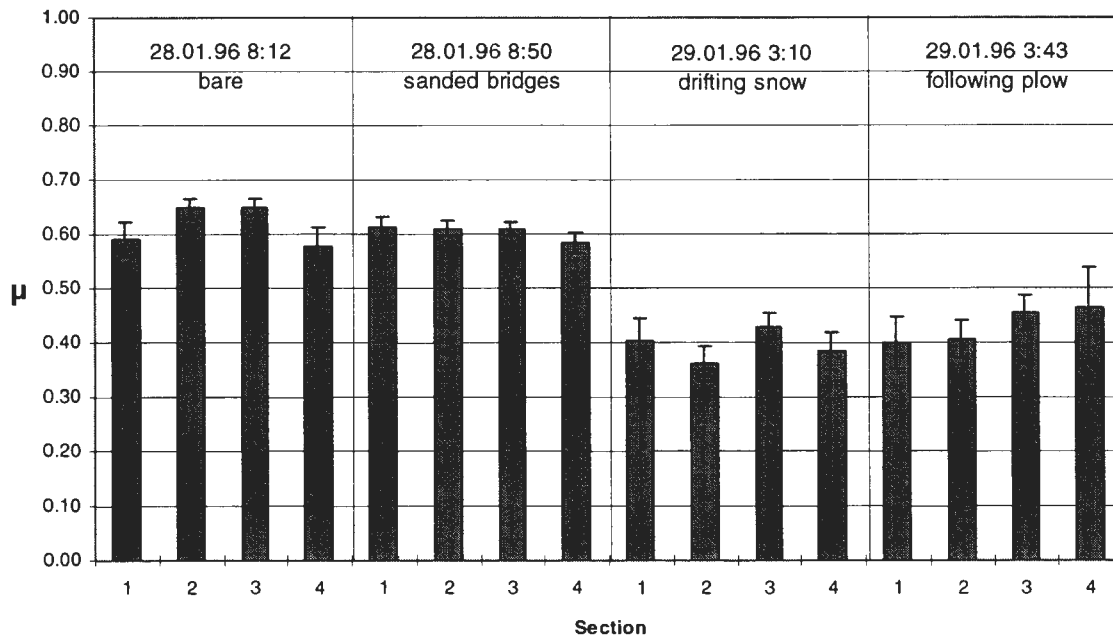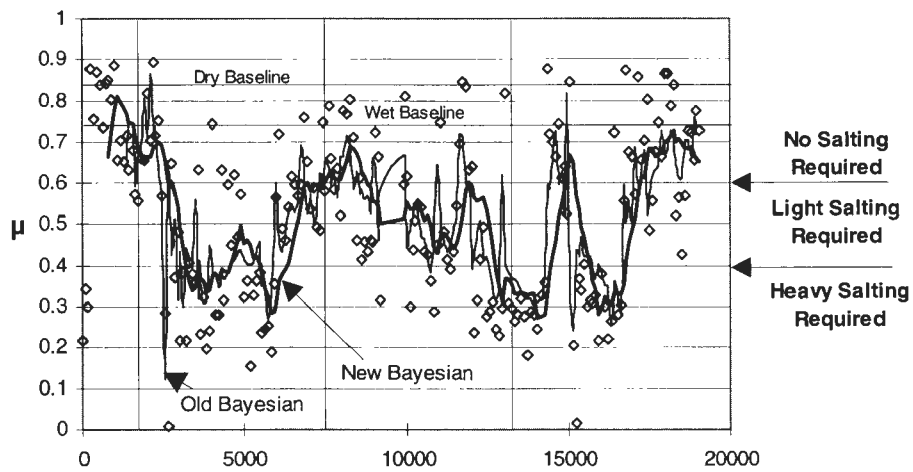

FIGURE 8   Distribution of peak friction on loose snow.

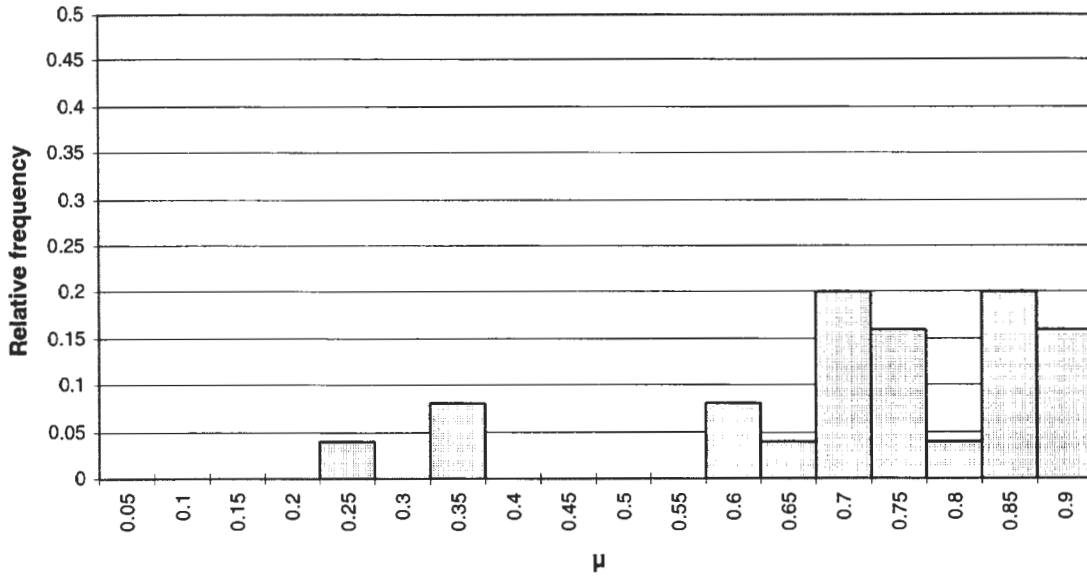FIGURE 9   Peak friction in slush and wet pavement.

FIGURE 10   Relative frequency of peak values for Section 1 on slush and wet pavement.

Norwegian Data

The remaining figures present Norwegian data. Figure 11 shows the effect of speed on hard-packed snow; friction appears to increase with increased speed. However, it has been found that most of this increase is due to increased rolling resistance caused by snow plowing in front of the tire. Figure 12 shows the time effect of sanding for four periods—before sanding, 30 min after sanding, 2.5 hr after sanding, and 4.5 hr after sanding. As found in other studies, there is an initial 15 to 25 percent improvement, but much of this is then lost with time and traffic, and sand must be reapplied if salt is not also applied.

Figure 13 shows the time effect after salting on five sites. In each case improvement occurs as the salt has time to work; the increasing temperature also helps. Figure 14 shows the values for loose snow and hard-packed snow on ice. These are followed by values just before salting, then 30 min, 2.5 hr, and 4.5 hr later. At 30 min slush is forming; at 2.5 hr there is slush and
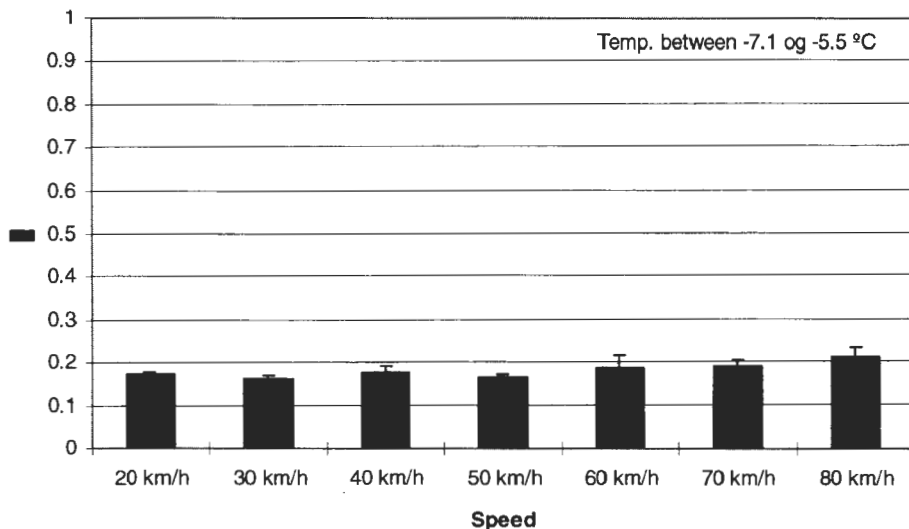

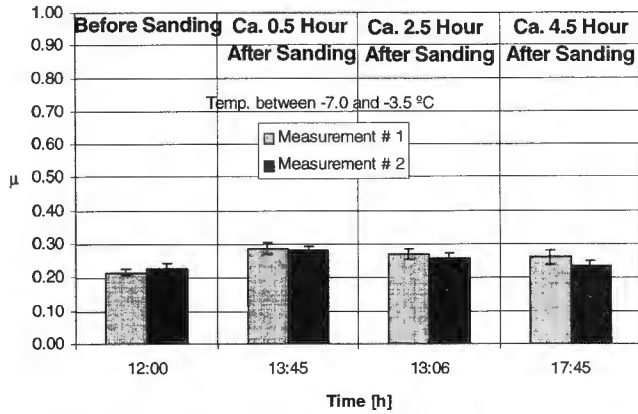FIGURE 11   Effect of speed on hard snow and ice.

FIGURE 12 Effect of sanding on hard-packed snow.

wet; at 4.5 hr ice again starts to form and the recovery is lost.

CONCLUSIONS

This preliminary study was successful in establishing better Bayesian values, and it showed that the Radó model constants can be used to differentiate contaminates. The peak friction and the slip speed at the peak separates the ice and snow from dry or wet. The shape factor then separates loose snow and slush from packed snow and ice. The study showed that friction levels can
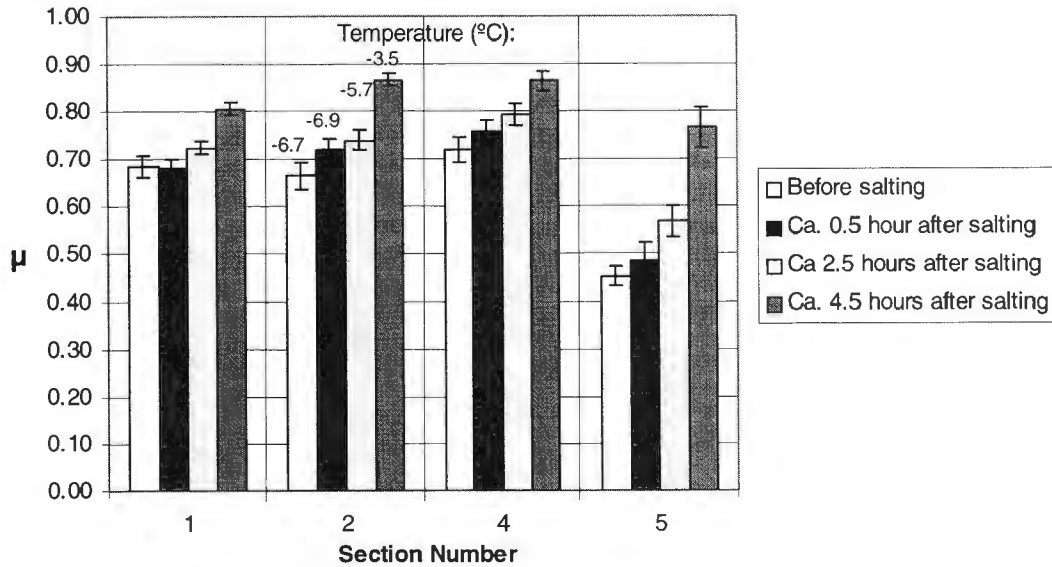

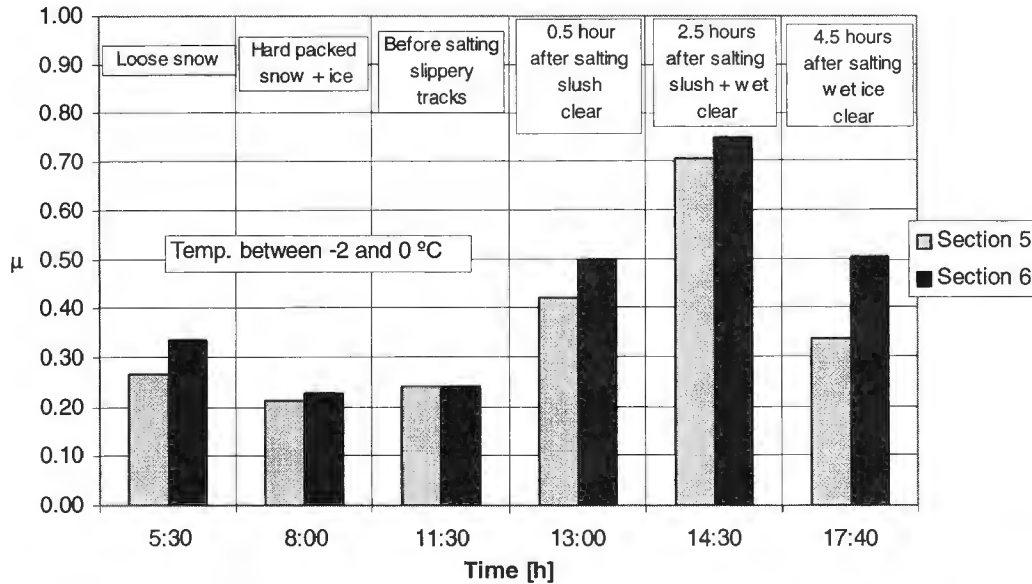FIGURE 13 Time effect of salting on four sections.

FIGURE 14 Time effect of salting on two sections.

be monitored in real time and salting control does appear to be feasible, either with a go–no-go approach or perhaps with varying levels of salting.

More sites should be tested next season to finalize how the three Radó constants can be used to differentiate the contaminate. Also, because salting control appears to be feasible, continued study in the United States and Norway with more experiments is planned. MinnDOT plans to mount a unit on a salting truck and will evaluate its use during the coming winter season.

REFERENCES

1. Norsemeter. *Winter Testing Reports*. Norwegian Road Administration, 1995.
2. Radó, Z. *A Study of Road Surface Texture and Its Relationship to Friction*. Ph.D. dissertation. Pennsylvania State University, University Park, 1994.
3. Navin, F., M. Macnabb, and C. Nicolleti. *Vehicle Traction Experiments on Snow and Ice*. SAE 960652.2-96, SAE, Warrendale, Pa.

PART 5
ENVIRONMENT AND HEALTH
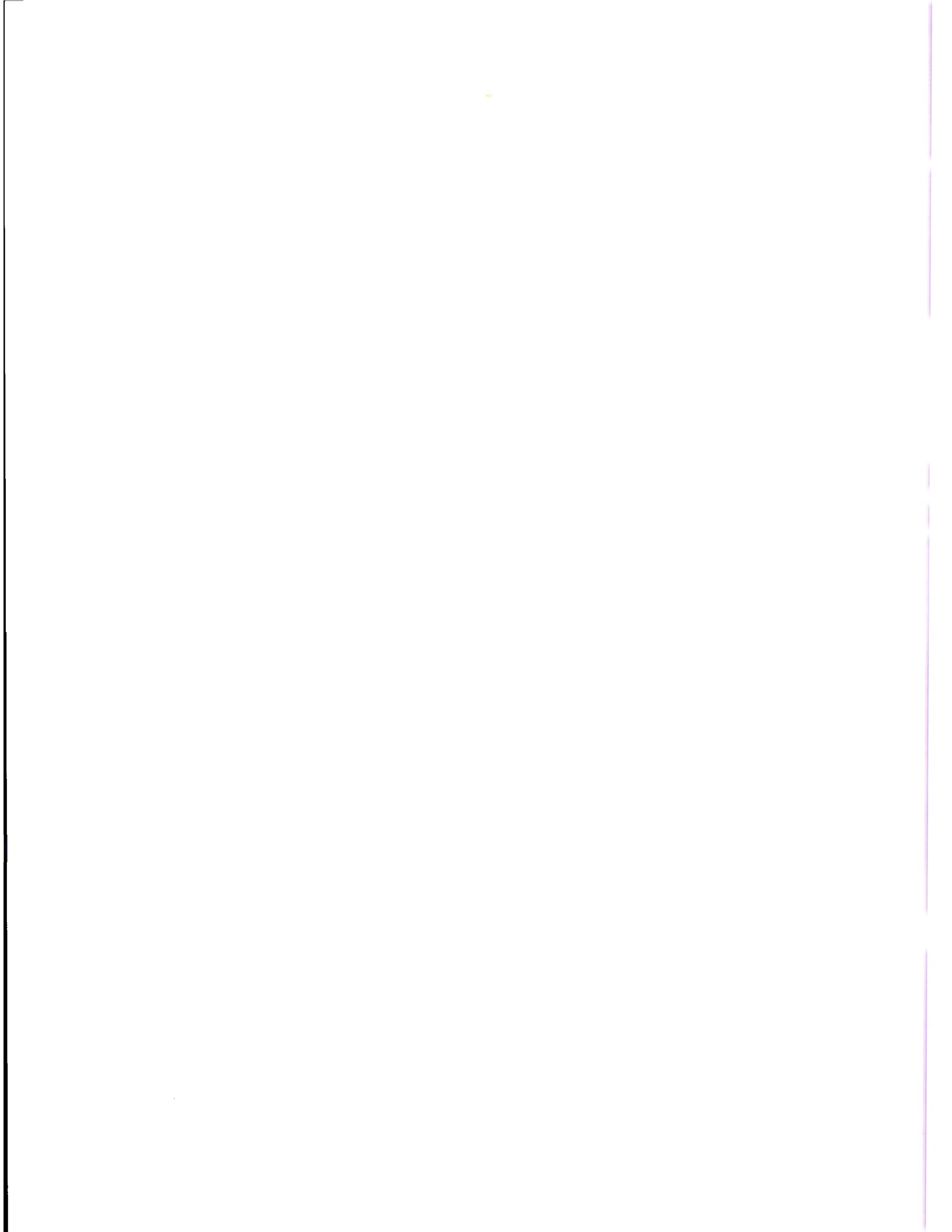
Effects of Studded Tire Regulation on Road Environments and Traffic Conditions in Hokkaido

Hideki Takagi, Hidetsugu Onuma, and Akihiro Shimojo,
Hokkaido Development Bureau, Civil Engineering Research Institute, Japan

To prevent dust pollution generated by studded tires in Japan, the use of such tires was first regulated in the winter of fiscal year 1991 in accordance with the law on the prevention of road dust caused by studded tires, which took effect in June 1990. For the last several years, the rate of vehicles equipped with studded tires has decreased from 0.9 to almost zero in Hokkaido. The ban on the use of studded tires helped considerably to decrease the environmental pollution caused by airborne particles. On the other hand, several new road traffic problems have arisen, including an increase in traffic accidents and congestion caused by changing conditions on roads covered with snow and ice. The past problem of studded tires causing wear of paved surfaces was replaced with a new problem of studless tires polishing surfaces covered with snow and ice. In recognition of this, road environmental effects, snow- and ice-covered road surfaces in the age of studless tires, road maintenance using antifreezing or antislipping agents, and traffic accidents are examined, and present and future problems are discussed.

The use of studded tires rapidly spread beginning around 1970 in Hokkaido. Five years later, almost 100 percent of passenger cars were equipped with such tires in the winter. The tires began to generate controversy in 1977 or 1978, however, because road abrasion and falling dust generated by studded tires were feared to be polluting roadsides and the air, to the detriment of public health. Subsequently, a grassroots anti-studded-tire movement gained momentum. As a consequence, studded tire regulations went into effect in 1990, followed by the enactment of penal provisions in the winter of 1992.

The process of applying the studded tires regulation in Hokkaido was divided into three phases, as shown in Figure 1. At present, 85 percent of the total population and 85 percent of automobiles are subject to such regulation. Because the sale of studded tires stopped in 1991, the percentage of cars using studded tires has been decreasing, as shown in Figure 2. The data show that studded tires nearly disappeared in 1992 in the primary designation area of Sapporo and that the percentage of cars using studded tires dropped to almost 0 in 1993 in the secondary designation areas. In the tertiary designation areas and other areas that are not yet designated, less than 10 percent of cars used studded tires in 1994. Studded tires are disappearing from Hokkaido.

ENVIRONMENTAL SURVEY RESULTS

Density of Suspended Particulate Matter

Suspended particulate matter, which makes up about half the dust generated by studded tires and is feared to affect the human body, consists of microparticles
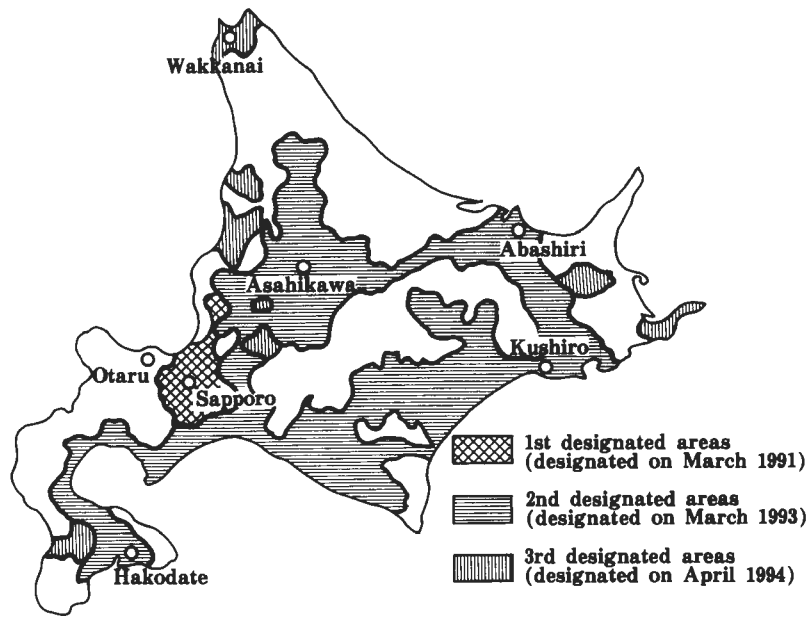
FIGURE 1   Designated areas in Hokkaido.

smaller than 10 µm in diameter. The microparticles are invisible, and when inhaled they enter the windpipe and the lung directly, without being stopped at the nose or the throat. Japan's Environment Agency conducted a survey of the effect of such dust on the human body and reported that although no carcinogenicity was identified, the dust may cause pneumoconiosis. Figure 3 shows the yearly change in the maximum density of suspended particulate matter in Sapporo. In 1984, when the equipping rate of studded tires was greater than 95 percent, the density was 171 µg/m^3, exceeding the environmental standard of 100 µg/m^3. After 1989, however, the density dropped below the environmental standard and has remained there. The density was 49 µg/m^3 in 1993, 30 percent of the 1984 value. Figure 4 shows the change in density of suspended particulate matter in late winter, when such density peaks. Figure 4 indicates that there were 3 days in March 1984 on which the density ex-

ceeded the environmental standard; at such times the air is considered to be badly polluted. Subsequently, however, the density of suspended particulate matter has decreased yearly and now there are no days on which the density exceeds the environmental standard, proof that clean air is returning.

Amount of Falling Dust

"Amount of falling dust" (often consisting of particles more than 10 µm in diameter) is a measurement of the dust falling on the ground because of gravity or rain. The majority of such dust in the winter consists of the dust of asphalt abraded by studded tires. The amount of falling
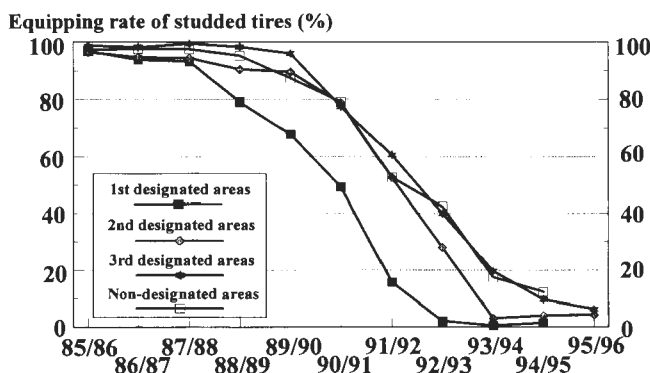

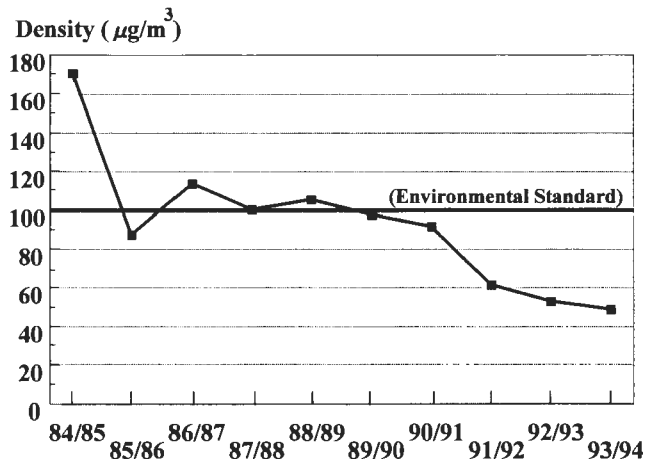FIGURE 2   Studded tire equipping rate, by designated area.

FIGURE 3   Annual changes in maximum density of suspended particulate matter (1).
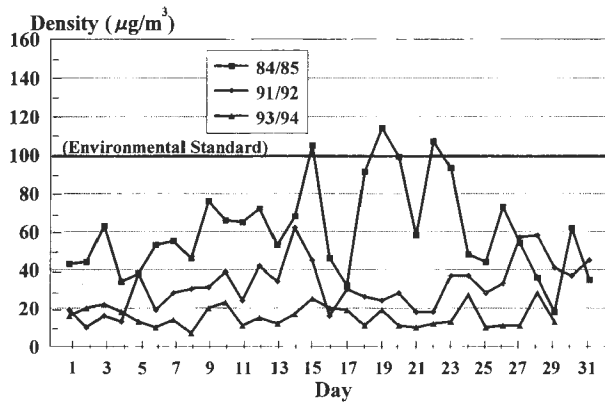
FIGURE 4 Changes in density of suspended particulate matter in March (1).

dust in the air tends to increase in early spring when snow melts and in early winter when snowfall begins. Figure 5 shows the monthly change in the amount of falling dust in Sapporo. As indicated, March always has the highest value for the year, 131.8 t/km²/month in 1988, 7 times the amount of each summer month. The amount was 63.5 t/km²/month in 1991. However, in 1993, when the equipping rate of studded tires approached zero, the amount of falling dust decreased to 22.1 t/km²/month. Also, 1993 not only showed a low value each month but also showed no great seasonal differences, indicating that the Sapporo area regained a "white winter" with the decline in the use of studded tires.

Road Abrasion

For the survey, a lane of National Route 12 in Sapporo where no special measures for wear resistance or plastic flow resistance are employed was chosen. Standard pins were buried perpendicular to the road from one roadside to the other, and abrasion was measured with a cross road profile meter with an accuracy of 0.1 mm at 10-cm inter-
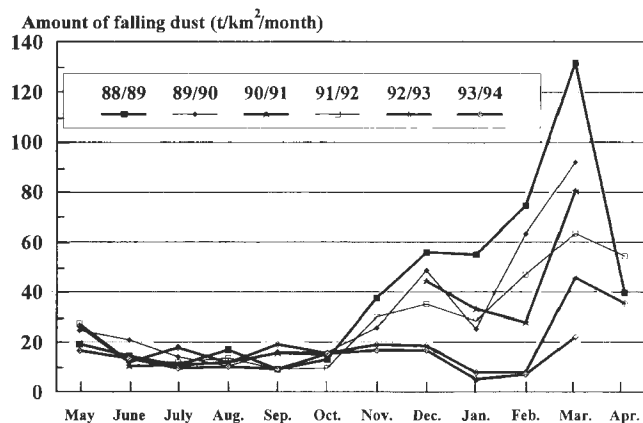

FIGURE 5 Monthly changes in amount of falling dust in Sapporo (1).

vals. The average amount of abrasion for each year and the equipping rate of studded tires are shown in Figure 6. As indicated, the value in 1989 was 6.1 mm with an equipping rate of studded tires of 63 percent. The value in 1992 fell to 1.1 mm when the equipping rate of studded tires approached 0 percent. Figure 6 shows that the decrease in the equipping rate of studded tires directly leads to a decrease in road abrasion. This is also reflected in the decline in the amount of falling dust, which was 92 t/km²/month in March 1989 but fell to 45.7 t/km²/month in 1992, or about half the 1989 level.

CHANGES IN NATURE OF SURFACES COVERED WITH SNOW AND ICE

Studless tires have been gradually popularized in the last several years, as shown in Figure 2. The use of studless tires had been promoted in a relatively smooth way until 1991 despite a variety of opinions and criticisms. In the winter of 1992, however, extremely slippery surfaces (Figure 7) appeared suddenly, which created a stir in the smooth transition. As people in Hokkaido had never experienced roads covered with snow and ice to be slippery so frequently, this problem gave rise to sensational controversy. Criticism against road administrators was strong, and technically more-sophisticated measures of road management in winter were required because skidding accidents increased and traffic congestion in urban areas was aggravated.

Slippery roads are categorized into frozen road surfaces, surfaces with black ice, and those covered with compacted snow. Compacted snow–covered surfaces that have been affected by climate and traffic conditions caused by studless tires are much more slippery than they were before the elimination of studded tires. These can be considered new and fundamental characteristics of winter road surfaces. As an example of the structure of slippery roads, Figure 8 (prepared by the Disaster Prevention and Snow Engineering Section, Civil Engineering Research Institute) shows that the traffic of cars with studless tires affects the surface of compacted snow to form a thin top layer of ice, about 1 mm thick, with a crystal structure different from the middle and bottom layers.

When studded tires were still used, drivers using studless tires presumably must have had very few opportunities to drive on extremely slippery roads, whether frozen surfaces, black ice, or surfaces covered with compacted snow, because studs of other cars created adequately coarse surfaces.

Although braking and other types of performance of winter tires, especially studless tires, on road surfaces covered with snow and ice have been improving through the efforts of manufacturers, there has been little serious discussion about the problem of slippery surfaces result-
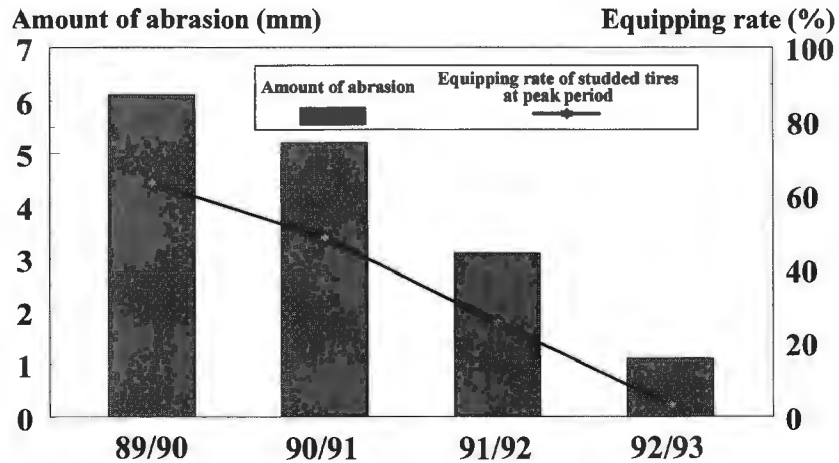
FIGURE 6   Equipping rate of studded tires and amount of abrasion (2).

ing from the use of studless tires and the elimination of studded tires. The changes in the nature of road surfaces covered with snow and ice are actually a new problem for road traffic in winter, because the slipperiness of roads depends on both the performance of tires and the condition of the road surfaces.

Extremely slippery roads are now problems all over Hokkaido, but the problem is most apparent in the area centering in Sapporo in which snow falls on many days and the average daily temperature is between 0 and −5°C from December to February. Road administrators in this area have been trying to use correct measures, relying mainly on deicers or other physical measures such as sand, to improve the conditions of surfaces covered with snow and ice in critical areas.

Among all the snowy and cold regions in Japan, Hokkaido is characterized by heavy snowfall and low temperatures, and in many places snow and ice on roads rarely melts naturally even after snow clearing operations. Because Hokkaido's climate does not allow complete

snow removal from road surfaces, studless tires affect the condition of roads covered with snow and ice more markedly than they do on the main island of Honshu.

CHARACTERISTICS OF WINTER TRAFFIC ACCIDENTS

The use of studless tires has been greatly promoted in Hokkaido in recent years, and a major characteristic is

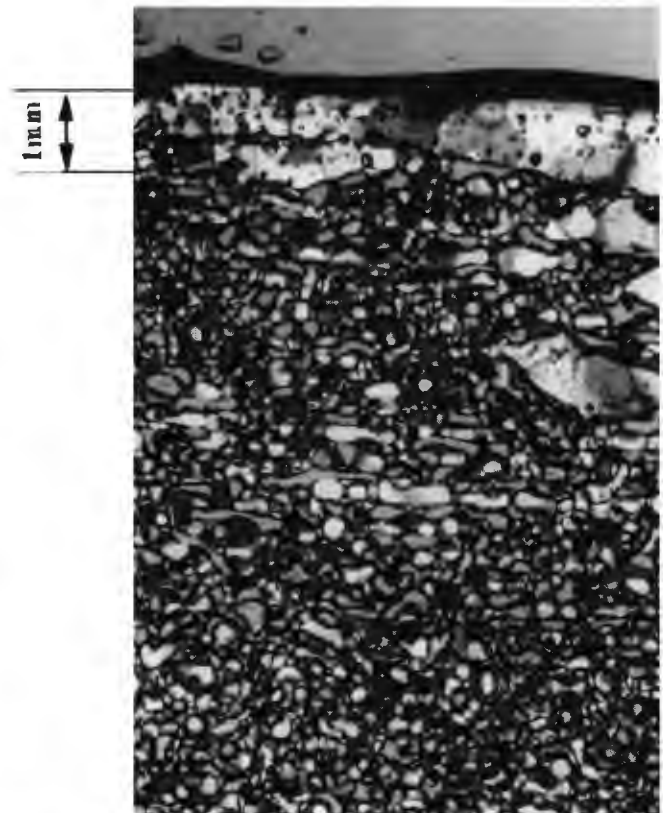FIGURE 7   Extremely slippery road covered with snow and ice.

FIGURE 8   Thin layer of compacted snow from extremely slippery road observed through a polarizing microscope.
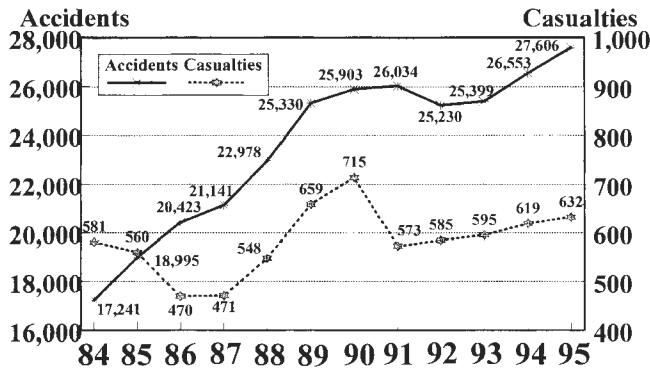
FIGURE 9   Change in number of traffic accidents in
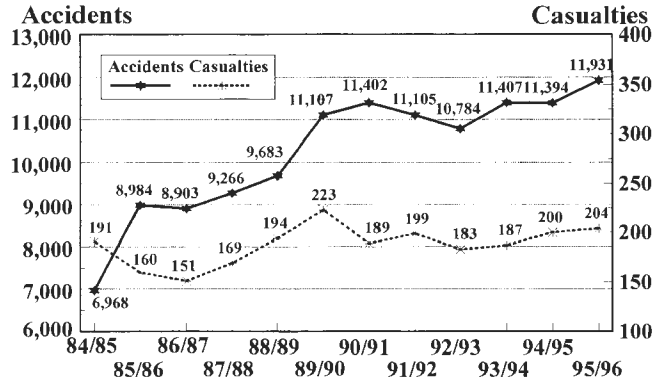Hokkaido (all roads included, by year).

FIGURE 10   Change in number of traffic accidents in winter
in Hokkaido (all roads included).

noticeable in winter traffic accidents. Figures 9 and 10
show the changes in the number of traffic accidents per
year and per winter (November to March), respec-
tively. The number of the accidents resulting in injury
or death did not change greatly between 1989, when
drivers began to use studless tires, and 1994, when al-
most all studded tires disappeared, although the num-
bers fluctuate slightly year by year and winter by
winter.

On the other hand, analysis of accidents in winter in
Figure 11 shows that one particular type of accident pe-
culiar to winter has increased rapidly with the increased
use of studless tires. Most of the accidents were caused
by skidding, and others were caused by reduced visibil-
ity and ruts. Additionally, the number of casualties in se-
rious accidents has been leveling off. For Hokkaido in
general, the number of accidents caused by skidding that
have resulted in injury or death reached a peak in 1993,
when almost all cars in Hokkaido used studless tires,

and the number decreased gradually and slightly in 1994
and 1995.

Figure 12 shows that annual changes in the number
of skidding accidents are much greater on municipal
roads than on trunk roads, such as national roads. Ini-
tially, it was expected that the traffic accidents would in-
crease significantly on trunk roads with heavy traffic,
but the analysis shows the opposite. As mentioned, it is
difficult to completely remove snow and ice from roads
in such a cold and snowy region as Hokkaido, and the
snow and ice remaining on the surface tends to be af-
fected by weather and studless tires. Consequently, it is
possible that a difference in road management is largely
reflected in the increase in skidding accidents.

Figure 13 shows that the number of accidents in-
creases in the beginning and in the depth of winter,
namely in December and January, and that it is greatly
influenced by weather conditions in winter. Figures 14,
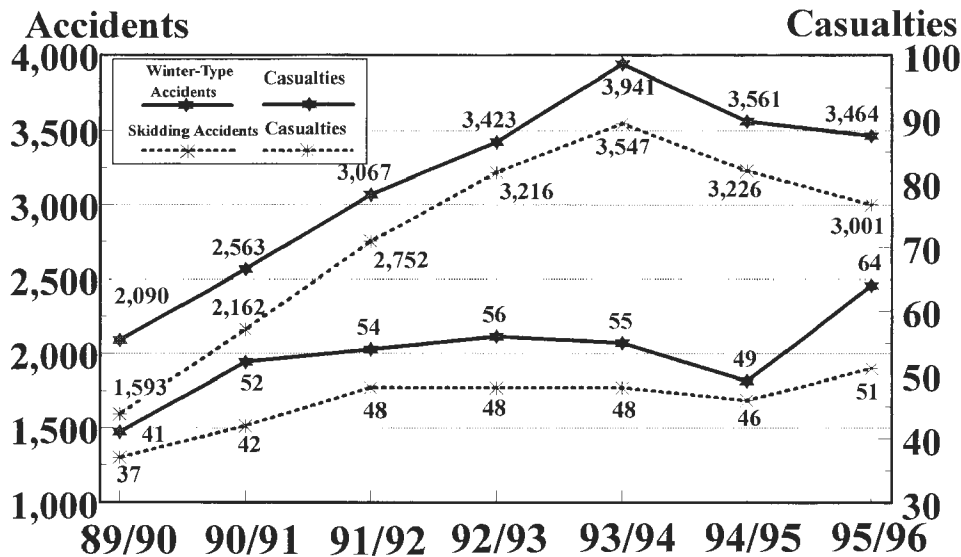15, and 16 indicate that rear-end colliding accidents in

FIGURE 11   Change in number of winter traffic accidents and skidding accidents in
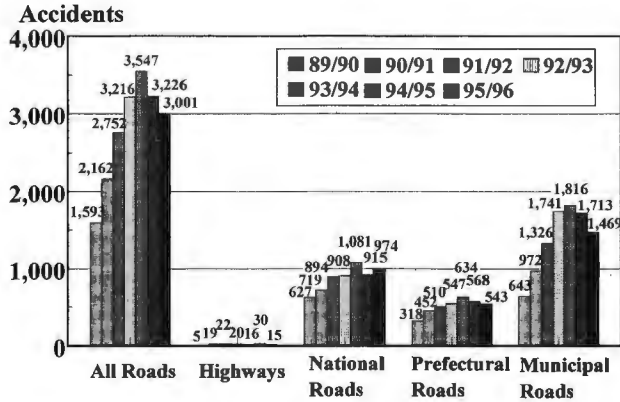Hokkaido (all roads included).

FIGURE 12   Number of skidding accidents classified by road category.

FIGURE 14   Number of skidding accidents classified by geographic features (all roads included, winter).

intersections in urban areas are rapidly increasing with the popularization of studless tires. In other words, accidents on roads covered with snow and ice increase conspicuously in the places where drivers must start and stop their cars frequently, which is likely to cause unexpected behavior such as skidding. This must be kept in mind by both road administrators and drivers. Road administrators must improve their management standard regarding not only trunk roads but also wider areas. This means that road administrators, especially local governments in cold and snowy regions must overcome difficulties in systems and budgets for road management. This situation also suggests that drivers must be more careful and drive according to surface conditions when driving both on streets with relatively little traffic and on trunk roads.

Because the total length of national, prefectural, and municipal roads combined is tremendous, it is impossible to apply an ideal, real-time management system to each individual road subject to harsh climatic conditions and changes in winter. Therefore, drivers are required to drive with deliberation and appropriate

consideration, and road administrators must continue to look for the most efficient ways of management based on analyses of past traffic accident data as well as on limited financial resources and existing systems.

WINTER ROAD MANAGEMENT

In Japan, particularly in Hokkaido, antifreezing or antislipping agents had not been used in road management except for in special areas such as mountain passes, because of the large amount of snow in winter and the use of studded tires by most vehicles. However, the spread in the use of studless tires, promoted by the regulation of studded tires, has led to very slippery frozen road surfaces, and it has become important to upgrade road management. During the last several years, therefore, road administrators improved machine snow removal and gradually promoted the use of antifreezing and antislipping agents, especially on major roads.

Using the results of analyses of traffic accidents, road administrators have selectively and intensively con-
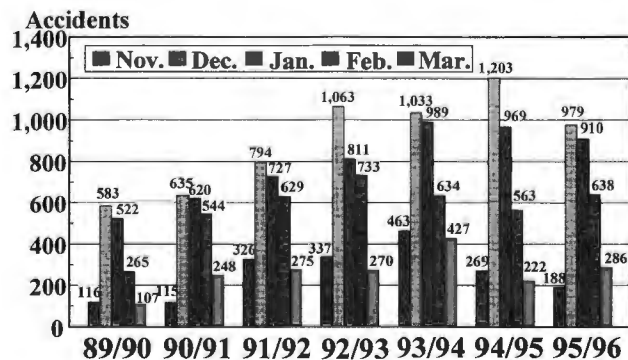

FIGURE 13   Number of skidding accidents by month (all roads included, winter).

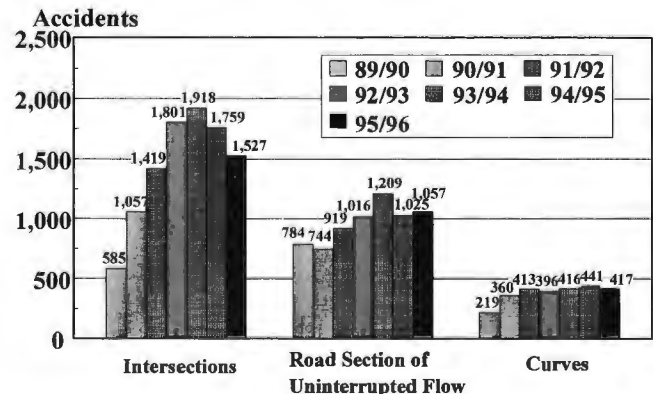FIGURE 15   Number of skidding accidents classified by road feature (all roads included, winter).
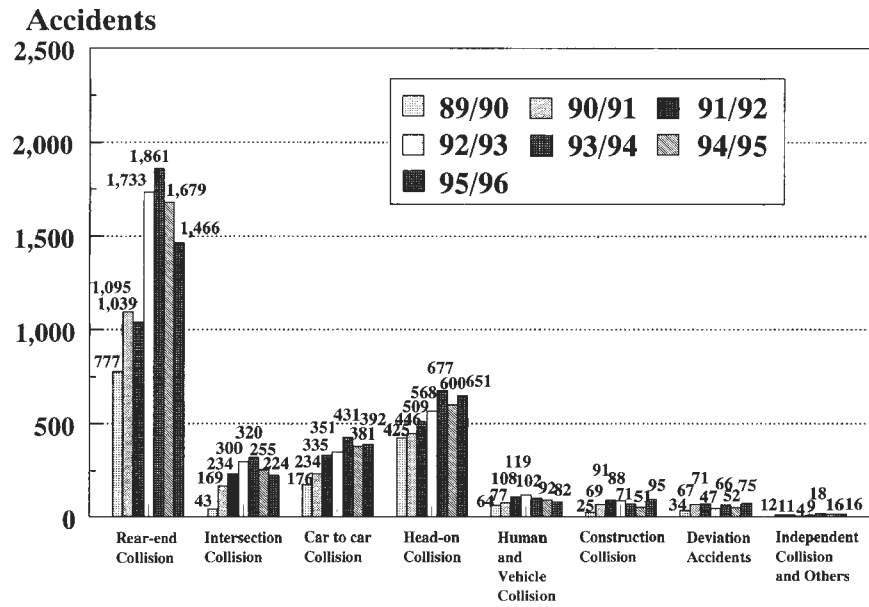
Accidents

FIGURE 16   Number of skidding accidents classified by type of accidents (all roads included, winter).

ducted road management for, among other sites, sections with poor alignment such as mountain passes, shaded sections of road, sections near structures such as bridges and tunnels, and urban intersections. Road management for these sections of road has been conducted not only to improve the safety and smoothness of road traffic, but also to minimize secondary effects of antifreezing agents used in winter road management. Figure 17 shows changes in quantities of various agents used, including antifreezing ones, on national roads, and Figure 18 gives skid resistance coefficients for frozen road surfaces (measured values on National Route 230, in the suburbs of Sapporo, during 20 days between late December 1994 and late February 1995 on which frozen road surfaces occurred). Skid resistance coefficients have been improved for sections of road (especially at intersections in urban areas) over which the various agents

are intensively distributed. Road administrators are considering to what extent these agents should be used, based on the relationship between road management levels and road user needs.

SUMMARY AND CONCLUSIONS

With regulation of studded tires, the spread of dust was greatly reduced and a "white winter" was regained, but with the spread of studless tire use, extremely slippery frozen road surfaces occurred, resulting in an increase of skidding accidents. Skidding accidents occurred more frequently in urban areas than in suburban areas. Rear-end collisions at intersections, where vehicles apply their brakes, particularly, occurred more frequently than on other sections of road. Furthermore, accidents
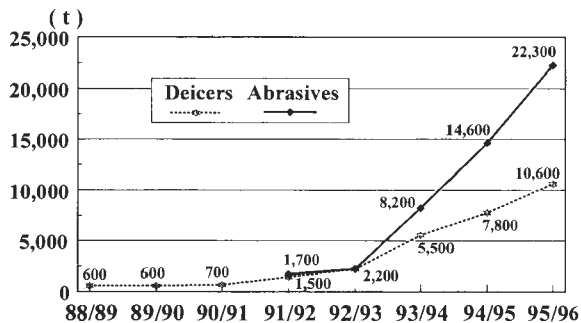

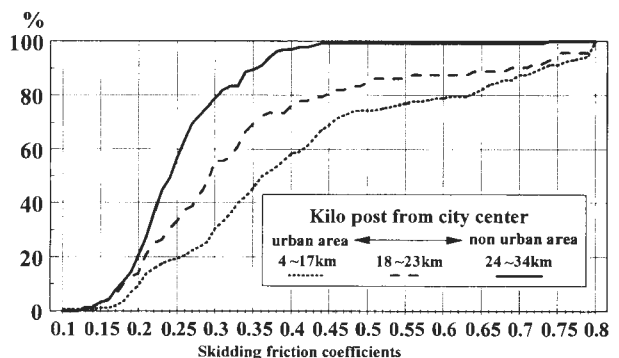FIGURE 17   Use of deicers and abrasives on national roads in Hokkaido.

FIGURE 18   Cumulative curve of skidding friction coefficients on Route 230 (3).

occurred more frequently on nonmajor roads, where snow was always compacted, than on major roads. It is believed that this was because of differences in road management levels. To improve management for major roads, road administrators conducted various measures, including the improvement of machine snow removal and the use of antifreezing and antislipping agents. On sections of road over which antifreezing and antislipping agents are intensively distributed, skid resistance has been improved. The next challenge is to expand the use of these agents to, among other areas, suburban sections of road.

Comprehensive examination of recent changes in various types of data on road environment problems, traffic accidents, and winter road surface countermeasures, all of which are associated with the regulation of the use of studded tires in Hokkaido, indicates that to ensure safer, smoother winter road traffic in cold, snowy regions, rational measures and improved road management based on the winter pattern seen in Hokkaido in 1991 are effective. In areas in which climate make it difficult to completely remove snow and ice from road surfaces, the occurrence of extremely slippery frozen road surfaces can be prevented by allowing, for example, 20 percent of vehicles to use studded tires, because these vehicles make frozen road surfaces appropriately rough. The use of studded tires in this proportion would not create serious dust problems. In early and late winter, it is imperative to thoroughly clean road surfaces. Road management can be improved through the combination of upgraded machine snow removal and, as conducted in past road management practices, prudent use of combined antifreezing and antislipping agents. The road weather forecast system can be used to improve road management and the information provided to road users.

REFERENCES

1. *Results of Air Pollution Measurement in Sapporo City* (in Japanese). Environmental Management Department of the Health and Sanitation Bureau, Sapporo, Japan, 1993.
2. Takagi, H., et al. Influences and Problems of Studded-Tire Regulation in Hokkaido (in Japanese). In *Civil Engineering Research Institute Monthly Report*, Vol. 483, Aug. 1993.
3. Takagi, H. Road Surface Covered with Snow and Ice and Traffic Accidents in Hokkaido (in Japanese). In *Journal of the Japanese Society of Snow and Ice SEPPYO*, Vol. 57, No. 4, Nov. 1995.

Influence of Deicing Salt on Vegetation, Groundwater, and Soil Along Two Highways in Sweden

Lars Bäckman and Lennart Folkeson, *Swedish National Road and Transport Research Institute*

During spring 1994, vegetation damage to a remarkable and previously unknown extent was observed along many heavily used roads in southern Sweden. An investigation was conducted to determine the cause of vegetation damage along Highways E20 and 48 by performing a damage survey and measurement of sodium and chloride concentrations in pine and spruce needles, groundwater, and soil. At the same time, changes in salt concentration in groundwater and soil in two previously studied areas close to E20 were documented. The extensive damage to vegetation probably can be attributed to three interacting factors: the large amount of deicing salt applied during the winter of 1993–1994, the lateness of the last salting, and the hot, dry weather during the budding season. This conclusion is supported by the damage observations and the very high sodium and chloride concentrations in pine and spruce needles along the roads. In extreme cases, the sodium concentration was >1,000 ppm (dry weight) in current-year needles and >5,000 ppm in needles from the previous year. The concentrations decreased rapidly with increasing distance from the road and, similarly, the needles in branches turned toward the road had higher salt concentrations than needles in branches turned in other directions. The groundwater and soil from an area along E20 showed greatly increased sodium and chloride concentrations, especially next to the road, compared with previous measurements. The increased concentration can be explained only by the increase in road salting.

During early summer 1994, extensive damage to vegetation was observed along heavily used roads in large parts of southern and central Sweden, including clear signs of damage along Highways E20 and 48 in Skaraborg County. It was suspected even at an early stage that the damage was the result of road salting.

During the late 1970s, the Swedish National Road and Transport Research Institute (VTI) had carried out a study of the environmental influence of road salt based on seven observation areas in Skaraborg County where samples of soil, groundwater, and vegetation were taken. The areas were followed from spring 1978 to autumn 1979. The results showed increased salt concentrations in several areas resulting from the use of road salt (1).

To study the long-term effects of winter road salting, VTI performed further sampling of groundwater and soil in 1988 in three of the observation areas but limited the samples to groundwater and soil. The results indicated that one area continued to be largely unaffected by salting, another showed a further increase in already high salt concentrations, and the third had an unchanged high level of salt concentrations (2).

The purpose of the present investigation was to identify the causes of vegetation damage along Highways E20 and 48 in Skaraborg County by using damage inspections and sodium and chloride analysis of conifer needles, groundwater, and soil. In addition, changes in salt con-

centrations in groundwater and soil in two previously investigated areas along E20 were documented (3).

WINTER SALTING AND METEOROLOGICAL AND HYDROLOGICAL CONDITIONS

In comparison with earlier years, road salt consumption by the Swedish National Road Administration (SNRA) was very high in winter 1992–1993 and especially in winter 1993–1994, both in Skaraborg County and in Sweden as a whole (Table 1). In spring 1994, the last salt applications on E20 took place relatively late, March 25 and April 3.

E20 has an average daily traffic of 5,000 to 8,500 vehicles, with a large proportion of heavy vehicles (15 to 20 percent). In the particular area, the period April through May 1994 was dry and precipitation was 47 to 55 percent of normal. The temperature was unusually high for 4 to 5 weeks beginning on April 22. During April, the groundwater level in the county was almost normal, unlike in areas to the north and south, where the groundwater level was higher than normal. In May, the groundwater level was lower than normal.

FIELD METHODS

Needle Sampling

The extent and character of the vegetation damage along Highways E20 and 48 were inspected in the beginning of June 1994. The damage was discussed with SNRA personnel and several university experts. In June samples of current-year needles and the previous year's needles on Scotch pine and Norway spruce twigs were collected. This included sampling at two earlier VTI sampling areas, R4 and R6. The samples were taken at various distances from the road, various heights above the ground, and various orientations to the trunk. Sampling also was performed on two spruce hedges, one parallel to Highway E20 and one perpendicular to it.

The distance from the road was measured from the edge of the asphalt. Unless otherwise specified, samples were taken from twigs about 2 to 3 m above the ground.

TABLE 1   Salt Consumption (Tonnes) by the Swedish National Road Administration

	Skaraborg County	All Sweden
Winter 1991/92	24,000	210,000
Winter 1992/93	26,000	330,000
Winter 1993/94	31,000	420,000

Groundwater and Soil Sampling

Sampling of groundwater and soil was performed in two previously established observation areas on E20 between Götene and Mariestad.

At one of the areas (R4), the road is built on a low embankment and consequently there are no proper ditches. The area is bordered to the east by a stream. The clay in the area is covered by a comparatively thin (1.0 to 1.5 m) layer of fine-medium sand. The groundwater level is mostly high, although during dry periods it may fall below the level of the sand layer. The groundwater flows slowly toward the northeast, parallel to the road. Since the road's longitudinal profile also slopes toward the northeast, the area receives water from a relatively long stretch of the road immediately to the southwest.

The other area (R6) is level with the road, from which it is separated only by a normal ditch. Geologically, the area resembles Area R4, with a relatively thin layer of fine-medium sand overlying clay. Unlike Area R4, however, the sand layer contains more medium sand, which probably makes the layer somewhat more permeable to water. During spring and autumn, the groundwater level is high, about 0.5 m below the ground surface. In dry periods during the summer, however, the groundwater level may fall below the level of the sand layer. The groundwater flows in a westerly direction from the road.

During spring 1978, groundwater pipes were installed in the two areas. The perforation in the pipes was 0.5 to 1.5 m below the ground level, in the sand layer. Sampling of the groundwater was performed in the beginning of June 1994. The groundwater levels were then very low, and sampling was therefore not possible in all pipes. Soil sampling was performed in the beginning of July 1994. Samples were taken from two to four levels down to 165 cm below ground level close to each groundwater pipe. Samples were taken only in the sand layer because it was likely that fossil water, which originated in the early development of the Baltic Sea, could occur in the underlying clay.

RESULTS

General Damage in Area

A majority of the trees and bushes along both E20 and 48 in Skaraborg County showed clear signs of damage. The damage appeared on most species of trees and bushes, both in gardens and in agricultural and forested areas. It took the form of bare or dead branches, twigs, or shoots; lack of emerging shoots during the late spring; red-brown pine needles from the

previous year; and generally sparse foliage. The damage was by far the most pronounced in the immediate vicinity of the road. Trees and bushes nearest the road showed the most severe damage. There was no difference in vegetation damage on the two sides of the road. In the woods, the damage decreased rapidly with increasing distance from the road, particularly in dense stands. At sites with sparse stands or isolated trees or bushes, or where insufficient shelter was provided by other trees, the damage also appeared at greater distances from the road (at least 50 m). The damage thus was closely related to exposure to the road. Similarly, noise barriers appeared to provide good protection; often, the part of the tree exposed above the barrier showed clear signs of damage while the sheltered part of the tree was relatively undamaged.

Visible Damage to Coniferous Trees

On small pine trees very close to the road, all the foliage was often red-brown, sometimes with the exception of the top shoot. On somewhat less-exposed pines and on older pines, damage usually occurred only on branches facing the road. Similarly, lower branches were often more damaged than upper branches, the top shoot being completely unaffected.

On exposed pine branches, the current-year shoots had often completely failed to emerge, especially where the previous year's needles were red-brown. However, it was not unusual for shoot formation to have taken place from branches whose previous year's needles were completely red-brown and which had no older needles.

Remarkably enough, the spruce showed a different damage image. Close to the road, small spruces and exposed branches of larger trees generally lacked needles from previous years, but these branches had to a large extent succeeded in producing shoots in 1994. On fresh spruce shoots from the current year, the young needles had a healthy, bright green color. Because of these bright green current-year shoots, the spruces near the road left a relatively healthy impression on a superficial inspection. It should be noted that the striking bright green color of the growing needles distinguished the spruce from the pine, whose new shoots had a dark green color from the beginning. Another factor that strongly influenced the difference in visual impression between the species was that the red-brown needles from the previous year were still in place on the pine trees, while the spruce trees had already shed their dead needles.

Introduced coniferous species such as cypress, arborvitae, and others also had been damaged. However, damage in gardens was not registered systematically.

Visible Damage to Deciduous Trees and Bushes

In gardens and elsewhere along the roads, extensive damage was observed in nearly all species of deciduous trees and bushes. The damage appeared mainly as sparse foliage, dried-up twigs, twigs that had produced no buds, and failure to flower.

Salt Concentrations in Needles

In every case, needles from the previous year had many-times-higher sodium concentrations than needles from the current year, in both high and low salt loading. The chloride concentrations were, however, more similar between the different year growths of needles; often, the previous year's needles showed higher concentrations than the current year's needles, although seldom more than twice as high.

Samples taken close to the road showed heavily increased sodium and chloride concentrations both in needles from the current year and in those from the previous year (Figures 1 and 2). The chloride concentration was greatly increased within about 10 to 30 m of the road, but the concentration was on the same level at a distance of 48 m as at 98 m. Even at 98 m, the chloride concentration showed a certain increase compared with normal concentrations according to the literature. However, it should be added that the studied area lies only 120 to 180 km from the sea and that salt can be transported long distances by the wind.

A tall spruce tree showed a large increase in concentration of both sodium and chloride in the lowermost branch and a certain increase in sodium concentration in the previous year's needles up to a height of 9 m.

With few exceptions, the needles on branches facing the road had many-times-higher concentrations of both sodium and chloride compared with branches facing
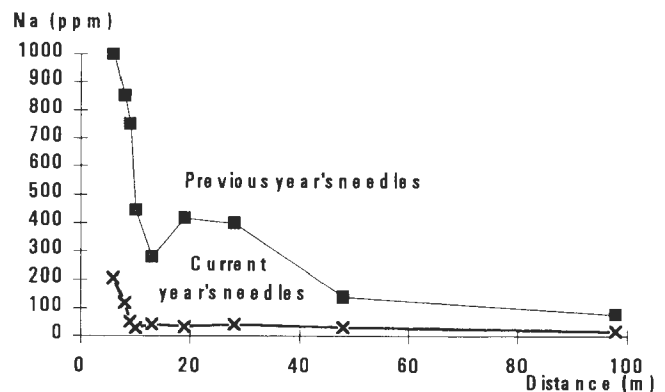

FIGURE 1 Concentrations of sodium in needles from pine trees at various distances from Highway E20, ppm = μg (g dry weight)$^{-1}$.
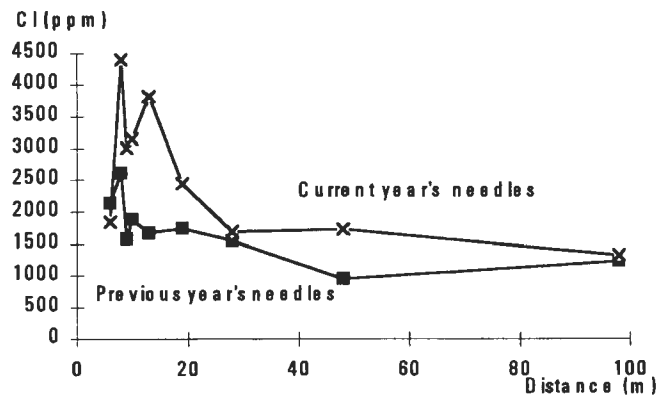
FIGURE 2   Concentrations of chloride in needles from pine trees at various distances from Highway E20, ppm = μg (g dry weight)$^{-1}$.

away from the road. That a dense spruce hedge along the road can offer effective protection is shown by the low sodium and chloride concentrations in needles on the lee side of the hedge compared with the high concentrations in needles on twigs facing the road, which showed extensive damage (Table 2).

In needles from extremely exposed trees, very high concentrations were recorded: for sodium sometimes more than 1,000 ppm in the current year's needles and 5,000 ppm in the previous year's needles, and for chloride sometimes more than 8,000 ppm in both years' needles. In previous-year brown needles of a dying pine, the sodium concentration was 1.7 percent and the chloride concentration, 2 percent.

Salt Concentrations in Groundwater and Soil

Compared with the earlier samplings, the sodium and chloride concentrations in Area R4 were greatly increased in 1994 both in the groundwater and in the soil samples (Figure 3). The concentrations were increased at all sampling points, but the greatest increases were measured in those points nearest the road. The concentrations also showed a clear relationship to distance from the road.

The sodium and chloride concentrations in Area R6 in 1994 mainly remained at the relatively high levels

measured earlier—no significant increase in concentrations was observed (Figure 4). At the two sampling points nearest the road, the concentrations were highest at a level 0.5 m below the ground surface.

DISCUSSION

Vegetation

Vegetation Damage Along Roads

Nearest the road, the vegetation generally is exposed to severe conditions as a result of several interacting stress factors. In many cases, this may lead to a generally weakened condition, predisposing the vegetation close to the road to damage from exhaust emissions, road salt, and other pollutants, as well as to attack by pathogens (fungi) of various types.

Damage to Coniferous Trees

The observed damage to the conifers was clearly of a physiological nature. The red-brown color, often of the whole needle but initially at its tip, is typical of drying out as a result of salt. Salt accumulation can produce rapid discoloration and die-back of needles.

On the other hand, it is probable that the pollution load in combination with unfavorable meteorological conditions causing frost drought or water stress during previous years may have weakened those trees that showed damage in 1994. During spring and early summer 1993, the spruce trees were exposed to severe frost drought on a large scale in southern Sweden, including Skaraborg county. In many cases, the lack of previous year's needles observed during early summer 1994 may be attributed to frost drought during spring 1993.

Sodium and Chloride Concentrations in Needles

According to the literature, the sodium concentration in pine and spruce needles is normally between 50 and 200 ppm (microgram per gram dry weight) and some-

TABLE 2   Sodium and Chloride Concentrations in Needles from a Spruce Hedge on E20, μg (g Dry Weight)$^{-1}$

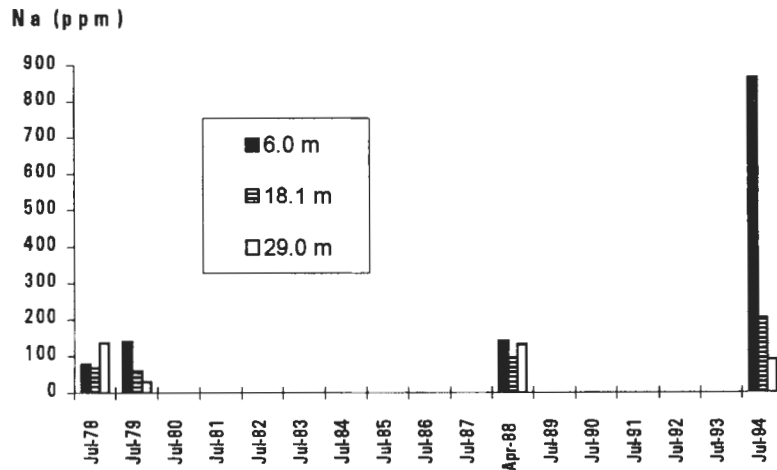| Side of the hedge	Na Previous year's needles	Na Current year's needles	Cl Previous year's needles	Cl Current year's needles
Facing road	744	62	4280	2200
Facing garden	358	28	2470	1370

Na (ppm)

FIGURE 3   Sodium concentrations in soil (0 to 15 cm depth) sampled at various distances from edge of pavement, Area R4 on Highway E20.

times up to 1,000 ppm (4). This probably applies to needles from the previous year and before. In the samples of previous year's needles analyzed here, sodium concentrations lower than 200 ppm were observed only in a spruce tree 98 m from the road, in the spruce hedge at a distance of 38 m from the road, in two pine trees 48 m and 98 m from the road, respectively, and in a pine branch 19 m above the ground. In the investigations carried out in 1978 and 1979 along the particular section of E20, the background concentration in the previous year's needles was about 60 to 80 ppm (1). The highest concentrations recorded in the present investigation, several thousand parts per million, must be considered very high. Needles on small, dying trees had concentrations of more than 4,000 ppm and in completely brown pine needles 17,000 ppm was recorded. In the investigations carried out in 1978 and 1979, it was found that trees with sodium concentrations of more than 5,000 ppm in needles regularly showed damage in the form of dying needles and branches (1).

In the case of salt damage, the chloride ion is considered more indicative than the sodium ion. The extent of visible vegetation damage is often stated to be closely related to the chloride concentration in the tissues. In the literature, needles (probably the previous year's needles and older needles) are stated normally to have chloride concentrations of 500 to 800 (to 1,300) ppm. Concentrations greater than about 2,500 to 3,500 ppm are considered toxic. Other information indicates 4,000 to 6,000 ppm as a lower limit for the occurrence of damage. In one investigation, the needles on dying spruce trees proved to have chloride concentrations of 4,500 to 10,000 ppm. An investigation of coniferous trees influenced by salt in highway storm water revealed chloride concentrations of 13,000 to 15,000 ppm in damaged spruce trees, while undamaged spruce trees had concentrations below 1,500 ppm. For current year's needles on spruce trees, a long-term investigation gives 3,000 ppm as the lower limit for the occurrence of road salt damage. Spruce is stated to be somewhat more sensitive to
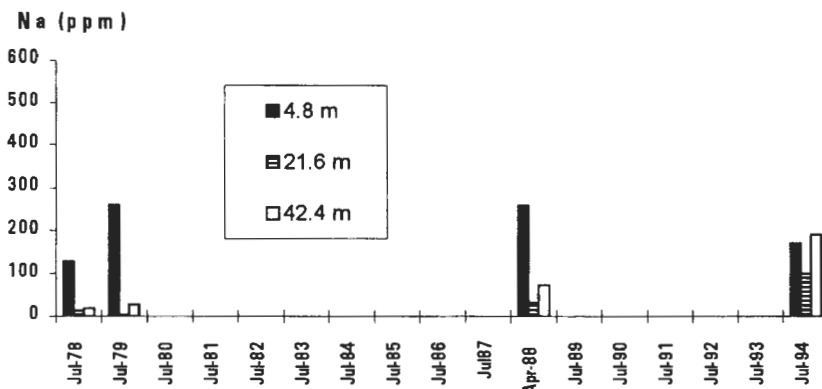
Na (ppm)

FIGURE 4   Sodium concentrations in soil (0 to 15 cm depth) sampled at various distances from edge of pavement, Area R6 on Highway E20.

salt than pine. Similarly, coniferous trees, which are evergreen, are generally stated to be more sensitive to salt damage than are deciduous trees (4).

Damage to Deciduous Trees

Damage to deciduous trees in the survey area was to a remarkable and previously unknown extent. The damage to deciduous trees that appeared in 1994 was, as in the conifers, probably the result of a combination of salt load and other stress factors over a series of years. Birch trees were probably weakened by drought stress following very hot, dry weather during spring and early summer of 1993 and particularly 1992.

Foliar Uptake or Root Absorption

The sodium and chloride ions in salt can reach the leaves or needles both by foliar uptake and by root absorption. The fact that needle discoloration and lack of shoot formation in the present study were clearly limited to the most exposed branches and twigs indicates that transport took place mainly through direct spray and aerosol deposition on the foliage, and that root absorption did not play a major part, at least in the rapid damage. In root absorption, the damage would not have been so clearly limited to the directly exposed branches and twigs.

Even if the observed damage is probably more attributable to direct deposition on the foliage than to root absorption, it cannot be excluded that unfavorable soil conditions, such as salt stress and drought, during earlier periods may have weakened the vegetation and made it predisposed to damage. Salt influence via the roots during a long series of years may thus have contributed to a deterioration of the tree's growth conditions.

Road Salting and Weather

In addition to the quantity of salt applied, the timing and the weather conditions are stated to be among the most important factors controlling the occurrence of salt damage along roads (4). It is likely that one of the main causes of vegetation damage was both that salt application in the area during the winter of 1993–1994 was high and that salting was carried out relatively late in the season. The hot, dry weather during the period of bud swelling, bud unfolding, and shoot formation probably contributed greatly to the occurrence of damage, or at least aggravated it.

Groundwater and Soil

A conclusion from the earlier investigations in the area (1) was that there is no clear and unambiguous relationship between the salt quantities spread on the road and the salt concentrations occurring in the surrounding natural environment. A certain quantity of salt thus may give rise to high concentrations in soil and groundwater in one area, while the same quantity of salt would lead to no observable salt increase in another area. The geological and hydrological conditions determine the extent to which an area is affected by salt pollution.

Both investigated sites on E20 (R4 and R6) are considered to have unfavourable hydrogeological conditions with permeable surface soil layers, high groundwater levels, and very poor water renewal rates (flat topography). This is confirmed by the raised salt concentrations in soil and groundwater throughout the follow-up period (1978 to 1994).

It is difficult to determine with certainty why Area R4 appeared to be considerably more influenced than Area R6 in 1994. A contributory cause is that Area R4 receives salt from a considerably longer section of road. The somewhat more permeable soil layers in Area R6 may also contribute to transporting the incoming quantities of salt away more quickly. Another possible explanation is differences between the two areas in the salt quantities applied over the years.

It is worth noting that both R4 and R6 are located in a low-lying area that was covered by sea water after the latest deglaciation. The fine-grained sediments (principally clays) deposited in this salt water still contain considerable quantities of salt. As a result, the area has a relatively large number of salt-polluted wells. However, the salt concentrations in soil and groundwater reported here are not considered to be influenced by these conditions because sampling, both of groundwater and soil, was performed only in the sand layers overlying the clay. Because of the permeability and the water renewal rate, it is unlikely that any fossil water of marine origin remains in this layer.

CONCLUSIONS AND RECOMMENDATIONS

The extent of the vegetation damage clearly shows that damage is related to the road and its traffic. The very high concentrations of sodium and chloride in the needles indicate that road salt plays a decisive, or at least dominating, role in the occurrence of the damage. Direct foliar uptake probably plays a more important role than root absorption in salt transport to the needles. This is supported by two observations—the damage to

branches with varying exposure to the road, and the difference in the salt concentration in the needles with varying exposure and height above the ground. That the damage is so great is probably because of three interacting factors: the large quantity of salt applied during the salting season in 1993–1994, the lateness of the last salt application, and the very hot, dry weather during bud unfolding. The large quantity of salt applied during the winter of 1992–1993 probably contributed to the damage that occurred during the spring of 1994. The unusual weather conditions during 1993 may also have had an influence. Growth conditions for the vegetation nearest roads with heavy traffic are often unfavorable. Groundwater and soil showed clearly increased salt concentrations in the two areas studied on E20. The large increase in concentration in one of the areas during the summer of 1994 cannot be explained in any way other than by a large increase in road salting.

To reduce the influence on vegetation, groundwater, and soil nearest the roads, it is important both to mini-mize total salt consumption and to avoid salting late in the season, that is, during the last few weeks before bud unfolding.

REFERENCES

1. Bäckman, L. *Vintervägsaltets miljöpåverkan.* VTI Rapport 197. Swedish National Road and Transport Research Institute, 1980.
2. Bäckman, L. *Vintervägsaltets miljöpåverkan—Uppföljning av miljöundersökningar i Skaraborgs län.* VTI Notat V 102. Swedish National Road and Transport Research Institute, 1989.
3. Bäckman, L., and Folkeson, L. *The Influence of Deicing Salt on Vegetation, Groundwater and Soil Along Highways E20 and 48 in Skaraborg County During 1994.* VTI Meddelande 775A. Swedish National Road and Transport Research Institute, 1996.
4. Brod, H.-G. *Langzeitwirkung von Streusalz auf die Umwelt.* Berichte der Bundesanstalt für Straßenwesen, Verkehrstechnik, V 2. Bergisch Gladbach, 1993.
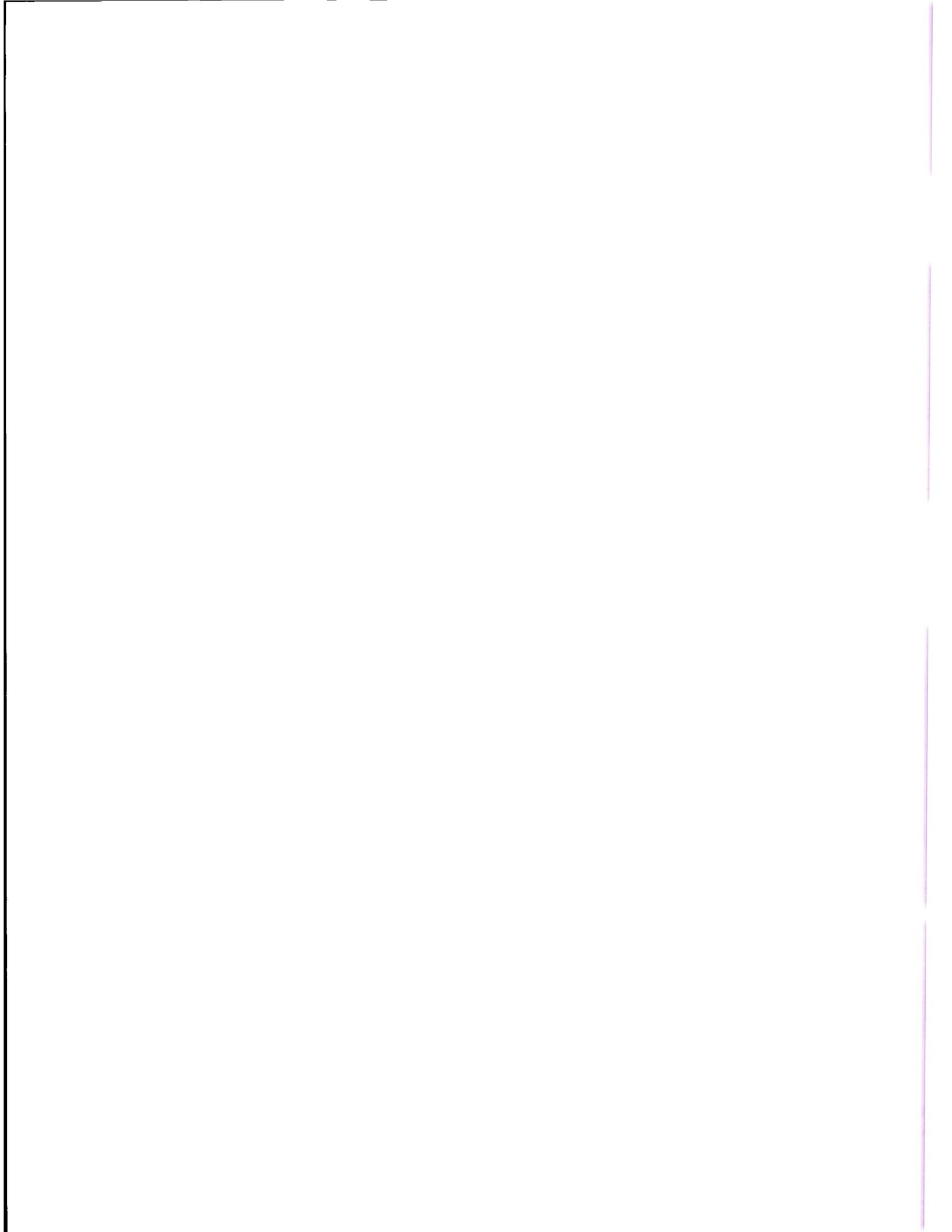
PART 6
ROADWAY WEATHER INFORMATION SYSTEMS AND FORECASTING
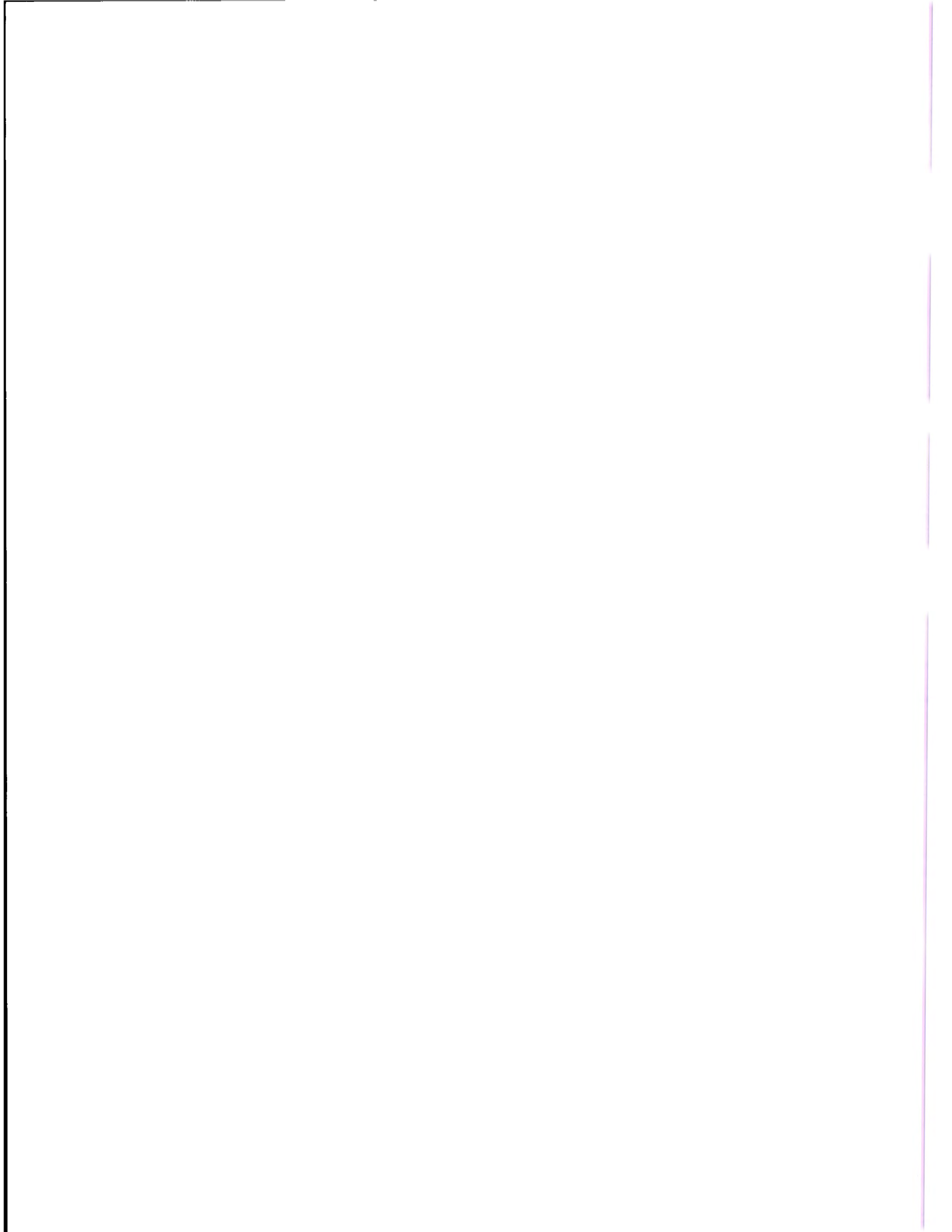
Application of a Road Weather Information System

Torbjörn Gustavsson, *Göteborgs University, Sweden*

Data from road weather information systems (RWISs) are used to plan winter maintenance activities. RWISs provide measurements of air and road surface temperature, air humidity, and precipitation. Models are available and in practical use in Sweden for both obtaining temperature information over stretches of road and forecasting road surface temperatures. The temperature information is calculated by using a local climatological model, which is run on a topoclimatological basis. Through a division of the road stretches into segments according to variation in topography, vegetation, construction material, and weather, different temperature patterns are calculated. The input for the model is temperature data from the field stations. The forecast model is based on a combination of statistics and energy balance calculations. The prognosis is calculated individually for each station so that local effects may be considered. The input to the model is given from the RWIS and a cloud forecast is also needed. A presentation of a winter index model, which can be used to calculate the need for maintenance activity in an area, is included.

T he idea behind a road weather information system (RWIS) is that field stations measuring air and road surface temperature (RST), humidity, and precipitation should be located so as to allow early warning of road icing. Various topographical areas and road sections with varying road construction must be covered by the system. Weather conditions produce varying temperatures; for example, during clear, calm nights the lowest surface temperatures are found in valleys, but during clear days screening effects are the most important consideration. The relationships among topography, weather, and temperature variation have been a subject of intense research carried out at the Department of Physical Geography in Göteborg, Sweden. Knowledge gained in this research has in several ways helped in the development of today's RWIS in Sweden. This paper focuses on three of these applications.

First, the forecast of temperatures and slipperiness risk, to assist maintenance personnel in their decisions concerning winter road activities, is described. Also important is valid extrapolation of the temperatures given by field stations to entire road stretches. This can be done with a computerized model described in this paper. Third, how winter statistics can be calculated by using the stored data from the field stations in the RWIS is described. The theoretical background of the RWIS is described by Bogren elsewhere in these proceedings.

RST FORECAST

In Sweden a combined energy balance and statistical model is used to calculate RST for the coming 1 to 4 hr. The relatively short forecast time is useful in guiding road maintenance personnel in decisions regarding salt-

ing actions and other operations. Other advantages of such a short forecast time are that the accuracy of the calculation can be high and that the model is thus more sensitive to rapid weather changes.

By use of a combination of energy balance modeling and a statistical model, all major factors controlling the RST can be determined. The radiation components are covered by the energy balance model and, in combination with an external input of the cloudiness, an effective radiation is calculated. The statistical part allows the local topography to be taken into account, along with the road construction materials, surface coating, and so forth used at each station site.

The cloud forecast, which is fed into the model, is a prognosis of the effective cloud cover, that is, cloud height and type in combination. The grid-net resolution is 4000 m, in accord with the requirement to consider the local conditions at each station site.

The forecast model has been tested against measured data from field stations located in various environments. An example is shown in Figure 1. The 2-hr RST forecast is plotted against the observed RST value. The straight line in the diagram shows the 1:1 relationship and the dotted line is the 1°C deviation. A total of 1,344 observations was used for this month. The test showed that the model is well suited for the type of information needed by the local maintenance personnel and that the correlation is high between observed and forecast temperatures. An advantage of this model is the low costs for both adapting and running it. The forecast model takes advantage of the measured parameters at the actual field stations and the only external input parameter is cloudiness. Current research by the Swedish Meteorological Office will automate this process with computerized intrepretations of satellite pictures and other information.
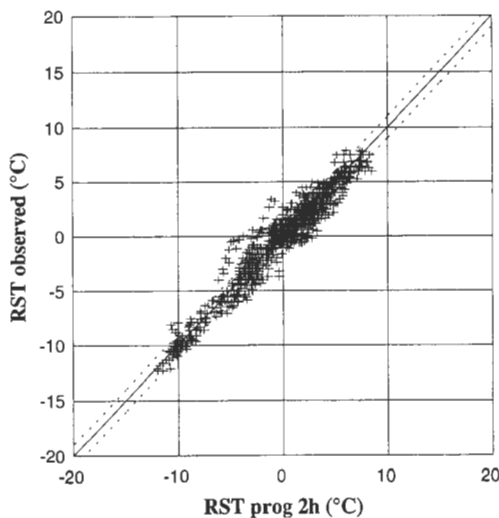
Compared with this semiautomatic model, other models require many more input parameters, including those measured at meteorological stations—precipitation, clouds, wind speed and direction, and air and surface temperature (1). This limits the models' ability to make forecasts for various areas. Also, running costs are high.

Further development of the RST forecast model includes a model for forecasting the dew point temperature and interaction with a regional model to improve correlation between the regional weather and the forecast for each station site.

LOCAL CLIMATOLOGICAL MODEL

The idea behind an information system with field stations is, as previously described, that the stations should be located in various local climatological environments. Extrapolation of the data for large areas is not possible without consideration of topography, weather, and so forth.

By using historical data from the field stations and mobile temperature recordings along the major road stretches, a computerized model has been developed by the Department of Physical Geography (2). This local climatological model (LCM) uses topoclimatological principles to calculate temperatures between field stations. Road stretches are subdivided into segments according to the local climatological parameters that are the most important for a fixed combination of time of day, time of year, and prevailing weather conditions. Calculation algorithms are further linked to the segments.

During the winter of 1995–1996 a combination with a cloud forecast was tested as input data to the model. This information allows the area to be subdivided according to prevailing weather. Previously, the variation in temperature between the field stations was used to determine what type of algorithm to use for the extrapolation of data. With the development of the LCM, a more complete coverage of the weather parameters is achieved. Analyses and tests carried out during the 1995–1996 winter season showed that accuracy had increased and that the cloud forecast could be most helpful in decisions regarding the local variations in weather.

During the operational run of the model, questionnaires were delivered to model users. Users were asked to give their views of the model's usefulness, accuracy, presentation, and so forth. Their responses, along with analyses of stored data and detailed measurements carried out in the test area, will be most helpful in the development of the model.

The questionnaires indicated that maintenance personnel using the model found correspondence between the LCM and the field station was good, that the LCM added information concerning the susceptibility of various road stretches to icing, and that the LCM was espe-

FIGURE 1 Plot of forecast versus observed RST for Station 1403, February 1993.

cially useful during slipperiness due to sublimation. This is because a varying temperature pattern causes the risk of slipperiness to vary a great deal.

WINTER INDEX

Studies of the geographical variation in road icing (3,4) have shown that the most diversified pattern can be found over an area the size of an average county. Topography and road construction are two of the most important parameters that account for this variation.

Through analyses of stored data from RWIS stations, it has become possible to conduct detailed studies of winter weather and the associated maintenance needed to keep roads free from ice, snow, and the like. Use of winter indexes, along with historical RWIS data, is one way to gain information about the winter season as it relates to the number of road icing conditions. The indexes can be used to calculate both the spatial variation in the need for maintenance activity and the severity of a specific winter. This approach is especially useful for calculating different types of slippery conditions and associated maintenance needs.

The GAB index sums the occasions with snow, frost, and black ice. According to the description of different types of road icing, these three represent the categories of road slipperiness that may be detected by an RWIS. This index was developed in Sweden to meet the demands of maintenance personnel concerning a separa-

tion of the needs for winter activity in different areas. The formula is as follows:

$$GAB = \sum A*\text{snow} + B*\text{frost} + C*\text{black ice}$$

Snow (or rain, provided the surface temperature is below 0°C) can be divided into subgroups depending on the amount of snow. The smallest increment to increase the index value is 20 mm. Frost is the number of occasions with risk of frost formation, at least a 2-hr duration with a time interval of at least 4 hr. Black ice is the number of occasions on which temperature drops from above 0°C to below 0°C and the surface does not dry (checked against humidity and occurrences of precipitation). The temperature drop must be from at least +0.5°C to −0.5°C.

All parameters in the index are given the value 1 if the criteria are fulfilled; otherwise they are 0. The summation is carried out daily and could be given for the whole winter season or a shorter time period if required. A, B, and C are weight functions that can be related to the cost of maintenance activity. It is also possible to change the influence of the three parameters to reflect their importance in a specific area or road stretch. For example, large roads with much traffic require faster action than smaller roads, and therefore the need for maintenance activity may be much higher.

The time interval for frost and black ice occasions is set to 4 hr. This is based on studies that show how long salt-
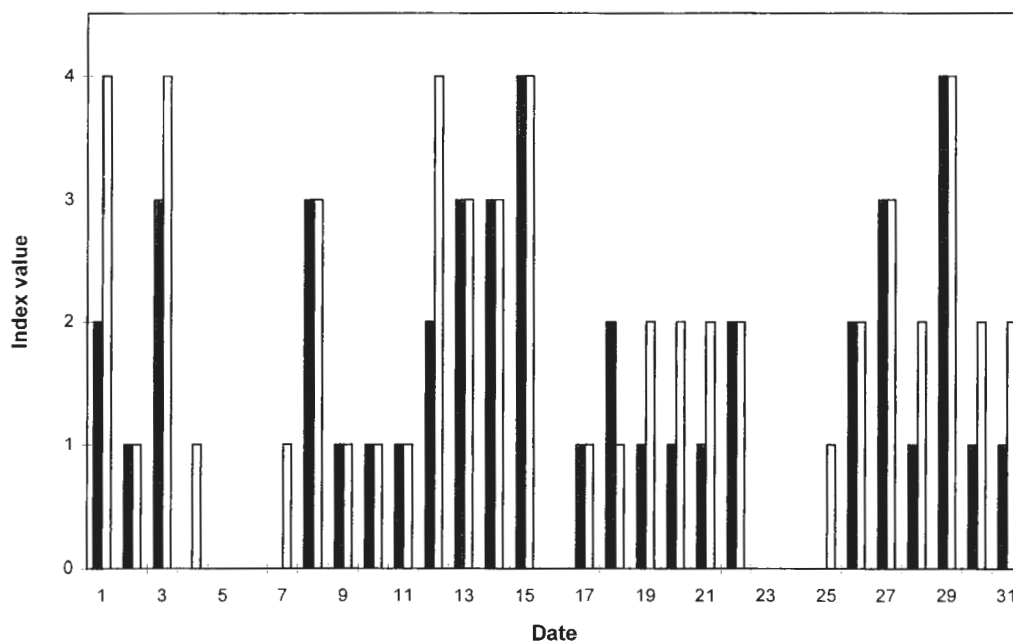

FIGURE 2   Calculated GAB index values for two field stations, showing variations in maintenance needs.

ing effects may last on a road. The decline of salt amounts on the road has been shown to be related to weather, state of the road surface, traffic, and so forth. In theory, four different frost situations may occur in a 24-hr period, with a total of six temperature drops from above to below freezing. The snow criterion relates to the amount of snow; at least 20 mm must be recorded before action must be taken. As a result, the snow parameter may occur several times during each day. Snowfall often requires a number of salting and plowing operations to keep the roads free from snow and this must be accounted for in a fully developed index. This can be achieved, for example, by giving the snow event a higher ranking than the other events.

Figure 2 shows how the GAB index may be used. The number of slippery events is summarized for each day during December 1994 for two stations. In the example the index value differs for the two stations because of their local climatological siting. Performance of calculations like this allows the need for salting activities in different areas to be compared.

In a study by Gustavsson (5), it was concluded that a winter index that can be used in relation to winter maintenance activities should

• Show a relation between the summation of different parameters related to slipperiness and the need for maintenance activity;

• Give a number that allows interpretation on physical grounds, in addition to comparison with other time periods;

• Have a proper time resolution so that only occasions and that call for action are included in the summation;

• Relate a weight function, if used, to either the cost or the need for activity during the specific occasion.

REFERENCES

1. Rayer, R. J. The Meteorological Office Forecast Road Surface Temperature Model. *Meteorological Magazine*, Vol. 116, 1987, pp. 180–191.
2. Gustavsson, T. and J. Bogren. *Use of a Local Climatological Model for the Prediction of Air and Road Surface Temperatures Along Road Stretches*. Guni Rapport 29, Department of Physical Geography, Göteborgs University, Göteborg, Sweden, 1990.
3. Gustavsson, T., and J. Bogren. Road Slipperiness During Warm-Air Advections. *Meteorological Magazine*, Vol. 119, 1990, pp. 267–270.
4. Gustavsson, T. Analyses of Local Climatological Factors Controlling Risk of Slipperiness during Warm-Air Advections. *International Journal of Climatology*, Vol. 11, 1991, pp. 443–455.
5. Gustavsson, T. Test of Three Indices for Classification of Winter Climate. *Meteorological Applications 3*, 1996, pp. 215–222.

Field Test of Road Weather Information Systems and Improvement of Winter Road Maintenance in Hokkaido

Masaru Matsuzawa, Yasuhiko Kajiya, and Keishi Ishimoto,
  *Hokkaido Development Bureau, Civil Engineering Research
  Institute, Japan*
Masao Takeuchi, *Japan Weather Association*

After the studded tire regulation law came into effect, extremely slippery frozen road surfaces occurred in the Sapporo area. The Hokkaido Development Bureau (HDB) has been conducting Hokkaido-wide surveys of road surface conditions with other road administrators since February 1993. The purpose of the surveys is to determine frozen road surface occurrence and regional road surface conditions in Hokkaido. In addition, in the winter of 1993–1994, HDB introduced the Finnish ice prediction systems to downtown Sapporo. HDB examined the accuracy of the system and clarified its limits of application. It was confirmed that the system has some limits because of errors in detection, which frequently occurred in cases of much snow, compacted snow, and frozen road surfaces. In the winter of 1994–1995, a new road surface classification method, which can identify extremely slippery frozen road surfaces and is easily used in winter maintenance operation, was developed. The Hokkaido-wide winter road surface condition survey was conducted with the use of the new classification method. In addition, an investigation was begun to develop ice prediction methods by using the road weather information system (RWIS) for the greater Sapporo area in the winter of 1995–1996. In this investigation, use of the radar snowfall forecasting system was also considered, as was the use of forecast information for efficient winter road maintenance. Furthermore, the ideal RWIS of the next generation and the way to exchange and share the information with other organizations are now under discussion.

Since the winter of 1992–1993, when the studded tire regulation law came into effect, very slippery frozen road surfaces have occurred in the Sapporo area. The Hokkaido Development Bureau (HDB), with other road administrators, has been conducting Hokkaido-wide surveys of road surface conditions since February 1993. The purpose of the surveys is to examine frozen road surface occurrence and to establish countermeasures against it. Because the original road surface classification used in the survey was not sufficient to identify very slippery frozen road surfaces, a new, improved classification system was introduced.

Furthermore, HDB has introduced the use of Vaisala's ice prediction system in downtown Sapporo and examined the accuracy of the system since the winter of 1993–1994. Through the surveys over two winters, points for improvement were confirmed. On the basis of the results, investigations to develop new road condition forecasting methods for the greater Sapporo area have been conducted since the winter of 1995–1996.

SURVEYS OF ROAD SURFACE CONDITIONS

New Road Surface Classification

Snow plowing is the main method of winter road maintenance in Japan. No standards of winter road maintenance consider slipperiness. Formerly used road surface classifi-

cations were insufficient to suitably identify the very slippery frozen road surfaces that began to appear after the studded tire regulation law came into effect. In the meantime, Akitaya and Yamada (1) reported a classification method for snow and ice on roads from the viewpoint of snow scientists. By using their classification methods, it is possible to judge road surface slipperiness by appearance. Their method was improved and a new road surface classification method, which can identify the very slippery frozen road surfaces described, was suggested (Figure 1).

The new road surface classification method was based on "road surface condition," which describes the characteristics of snow and ice on roads, and snow deposit shape, which describes the shapes of snow and ice deposits. Road surface condition consists of "reflection on the surface," "snow property," and "latent slippery ice under the surface," and the "snow deposit shape" consists of "Bump" and "rutting." Terms in this new road surface classification method are as follows:

1. Slipperiness is judged by reflection on the road surface. In cases in which the surface reflects sunlight or a headlight beam well, "very slippery" precedes snow property.

2. Snow property is classified into "compacted snow," "ice crust," "ice film," "slush," "powder snow," and "grain snow." A flow chart allows easy assessment of snow property (Figure 2).

3. If a slippery ice is covered with powder or grain snow, "on ice" follows snow property. In this situation, the subsurface ice has a much greater effect on vehicles than does the powder or grain snow on the surface, and it is important to discriminate between this situation and another.

4. A bump is described by size. Observed bumps less than 5 cm high are called "small bump," and those 5 cm or more are called "big bump."

5. Rutting is described by depth. Rutting less than 5 cm deep is called "shallow rutting," and that 5 cm or deeper is called "deep rutting."

6. Dry and wet (bare pavement) are considered types of road surface conditions.

With this new classification method, 13 states of road surface condition may be described.

Analysis of Survey

HDB surveyed road surface conditions using the new classification system at 41 locations in Hokkaido starting in December 1994. Snowplowing and the spreading of deicing agents and abrasives were also considered in the survey.

Figure 3 presents the relationship between days of snow removal and days of spreading of deicing agents and abrasives. Figure 3 shows that spreading of deicing agents and abrasives was as popular as snowplowing at some locations (Group A), whereas mainly snowplowing was conducted at others (Group B). Table 1 shows that the ratio of very slippery road conditions in Group B was higher than that in Group A. This indicates that deicing agents and abrasives are becoming more important as winter road maintenance methods under the studded tire regulation law.

INSPECTIONS FOR ICE PREDICTION SYSTEM

Introduction of Ice Prediction Systems

HDB has used Vaisala's Icecast system in downtown Sapporo since the winter of 1993–1994 and has examined the accuracy of the system and clarified its limits of application.
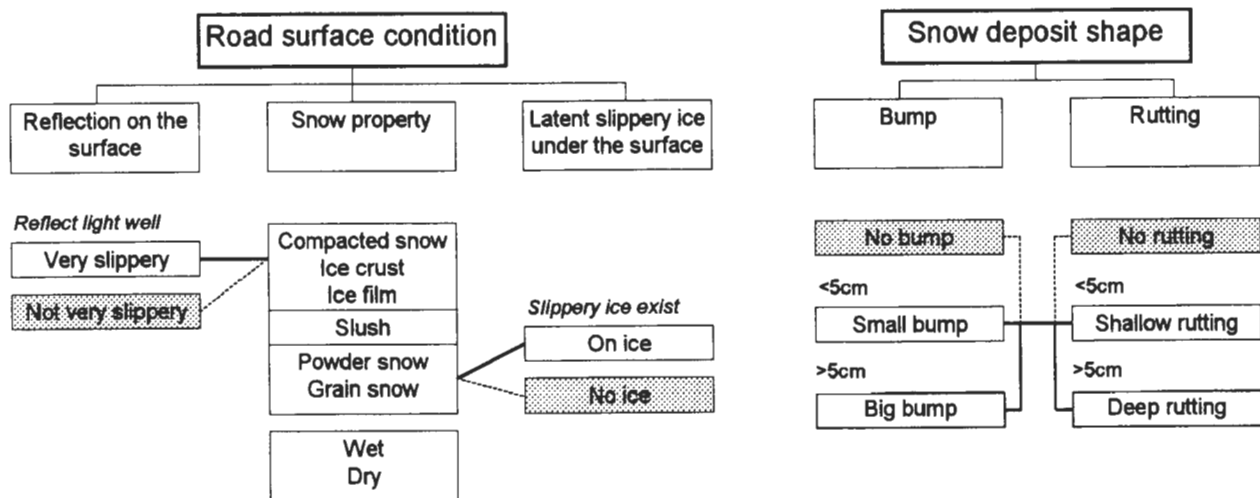

FIGURE 1   New classification method (shaded words are not classification terms).
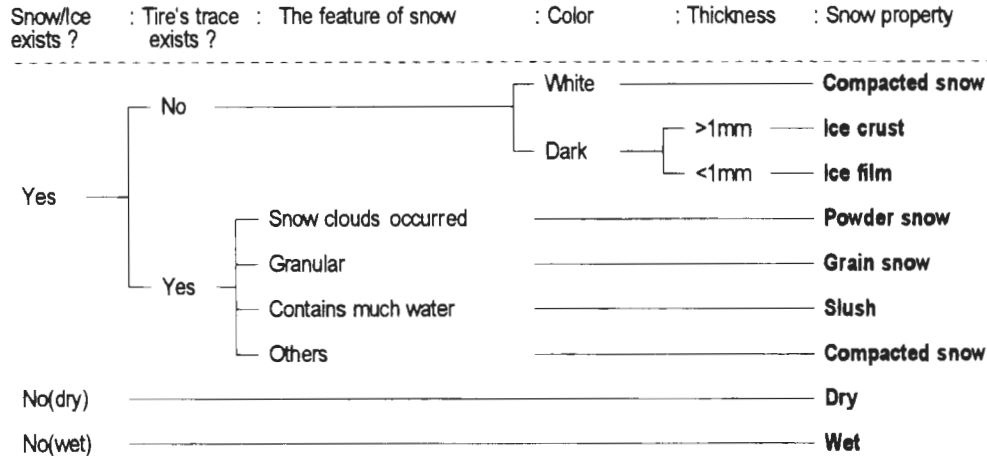
FIGURE 2   Flow chart of "snow property" decision.

Weather observation stations were installed at sites in two environments. Site 1 was surrounded by buildings and Site 2 had only one tall building, to the southeast. Air temperature, relative humidity, road surface temperature, and rainfall were measured by the original sensors. In addition, the amount of precipitation was measured by a precipitation gauge and road conditions were observed and recorded by video camera.

Road Sensor Inspection

The road sensor DRS12 (Vaisala) can measure road surface conditions, remaining chemicals, road surface temperatures, and ground temperatures. The sensors describe eight types of road surface conditions. The conditions obtained by the sensor were compared with a video camera's observations classified into four types: dry, wet, snow, and ice (Figure 4). The correspondence ratio was defined as the number of cases in a given shadowed area divided by the total number of cases recorded.

Table 2 shows the average correspondence ratio of each month in the winters of 1993–1994 and 1994–1995. The average correspondence ratio was 50 to 60 percent, but was lower in January and higher in March. These inconsistencies were then investigated. Table 3 shows the results of the investigation conducted at Site 1 during the winter of 1994–1995. The investigation showed that 48 percent of ice, 28 percent of wet, and 23 percent of snow indicates treatment by the sensor. Site 2 showed the same tendency.

Accuracy of Ice Prediction System

To forecast road conditions by using the Icecast model, weather forecast data (air temperature, dew point, cloud amount, cloud type, and precipitation) were
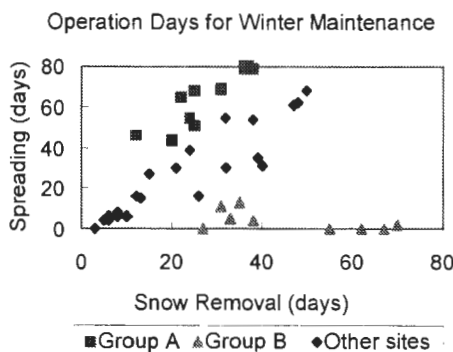

FIGURE 3   Comparison of days with salt or sand spreading and those with snow removal.

TABLE 1   Ratio of "Very Slippery Road" Appearance

Group A		Group B	
Site	Ratio (%)	Site	Ratio (%)
A-1	2.5	B-1	35.5
A-2	3.3	B-2*	0.8
A-3	12.4	B-3	14.0
A-4	9.9	B-4	9.1
A-5	0.0	B-5	38.8
A-6	2.5	B-6	14.9
A-7	5.0	B-7	22.3
A-8	5.8	B-8	21.5
A-9	5.0	B-9	33.9
A-10	5.0		
A-11	9.9		
A-12	0.0		
Average	5.1	Average	21.2
		(except B-2)	31.2

(* Use of studded tire was admitted around site B-2)

DRS12's Indication			Video's observation			
Symbol	Meaning	Road conditions	Dry	Wet	Snow	Ice
DR	Dry	Road surface is dry				
TR	Treatment	There is salt on the road surface and dry				
WE	Wet	There is free water on the surface				
WT	Wet/Treatment	There is salty free water on the surface				
MO	Moist	There is moisture on the surface				
FR	Frost	Frost is forming				
SN	Snow	There is snow or white ice on the surface				
IC	Ice	There is transparent ice on the surface				

FIGURE 4   Matrix of correspondence between DRS12 indication and video observation.

entered as meteorological parameters for the system. To confirm the accuracy of the model, the retrospective verification results obtained from actual measured data were compared with the video observations. Table 4 shows that the correspondence ratio at both sites was approximately 60 percent. The accuracy of the forecasting meteorological parameters is increasing, but improvements in road condition predictions are limited. It is impossible to explain the reason because the algorithm of the model has not been revealed, but ignoring snowfall depth as a meteorological parameter may be unwise.

Suggestions for Improvement

Suggestions for improvement of the ice prediction systems are as follows.

1. Because there are many errors in the treatment indications by the road surface sensor, another method is needed to obtain actual road conditions.
2. Snowfall depth must be considered in road condition predictions.

TABLE 2   Ratio of DRS12 Indication Considered Same as Video Observation (Percentage)

	Site 1		Site 2	
	1993/94	1994/95	1993/94	1994/95
DEC.		56.0		51.2
JAN.	29.2	52.2	30.2	50.9
FEB.	52.3	51.8	46.7	66.7
MAR.	66.4	77.7	70.8	80.7
AVE.	49.8	59.6	51.0	62.2

3. Whether ice forms on roads is sufficient for winter road maintenance in a country with a "bare pavement" policy. Snow and ice often are found on roads because of the heavy snow in Japan. Therefore, the ice prediction system must account for the formation of very slippery roads in winter road maintenance.

DEVELOPMENT AND INVESTIGATION OF NEW PREDICTION SYSTEM

Investigations into Ice Prediction

Investigations to develop new ice prediction methods for the greater Sapporo area were begun in the winter of 1995–1996. The meteorological office was responsible

TABLE 3   Comparison of DRS12 Indication and Video Observation at Site 1

DRS12's Indication	Video's Observation				Total
	Dry	Wet	Snow	Ice	
DR	1031	145	35	35	1246
TR	147	448	221	738	1554
WE	61	547	28	12	648
WT	0	159	9	8	176
MO	187	62	8	2	259
FR	0	7	11	11	29
SN	23	232	613	686	1554
IC	21	13	23	45	102
Total	1470	1613	948	1537	5568

NOTE: DR = Dry, TR = Treatment, WE = Wet, WT = Wet/Treatment, MO = Moist, FR = Frost, SN = Snow, IC = Ice.

TABLE 4 Ratio of Predicted to Observed Forecast Data (Percentage)

Time	18	21	00	03	06	09	11	Average
Site 1	54.2	59.4	61.7	61.7	64.5	63.6	55.1	60.0
Site 2	56.1	66.4	72.0	70.1	67.3	57.0	56.1	63.6

for investigation of ice prediction. Two stretches of highway, from Sapporo-Miyanosawa to Otaru-Irifune on National Route 5 (Route A), and from Sapporo-Toyohira to Sapporo-Kiyota on National Route 36 (Route B), were chosen for study, and representative points on those highways were selected. The ice prediction period was from December 24, 1995, to February 17, 1996. By 18:00 every evening the meteorological office predicted road conditions for 0:00 and 8:00 the next day. The predictions were sent by fax at 18:00 to the Civil Engineering Research Institute, Sapporo Road Office, and winter road maintenance operator's offices. Thirteen types of road surface condition in the new classification method were used in these predictions of road conditions.

The winter road operator's office is responsible for making observations of road conditions and maintaining records of winter road operations. Observations of road conditions were conducted at the representative points every day at 0:00, 8:00, and 16:00. The results were reported by fax to the meteorological office by 17:00. Road conditions at 16:00 were used in the predictions, and conditions at 0:00 and 8:00 provided data for the later investigations of the accuracy of the predictions. In addition, the records of winter road operation were also re-
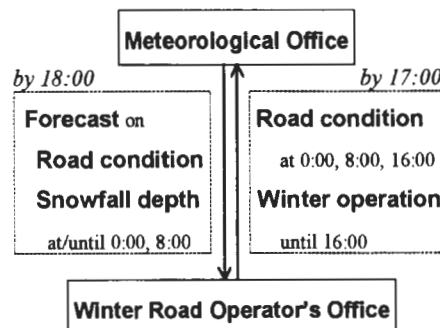

FIGURE 5 Flow of information.

ported to the meteorological office along with the faxed information on road observations. These results were used later when the accuracy of the prediction system was examined (Figure 5).

Results of Predictions

Actual measured data or road and weather conditions were analyzed, and flow charts on road conditions were developed (Figure 6).

The prediction points along Routes A and B were referred to as Sites A1 through A5 and Sites B1 through B4, respectively. Table 5 shows the ratio of correspondence between the predictions and observed road conditions at each site, based on 13 types of road surface condition. Table 5 clearly shows that this prediction method has yet to reach a practicable stage of development.
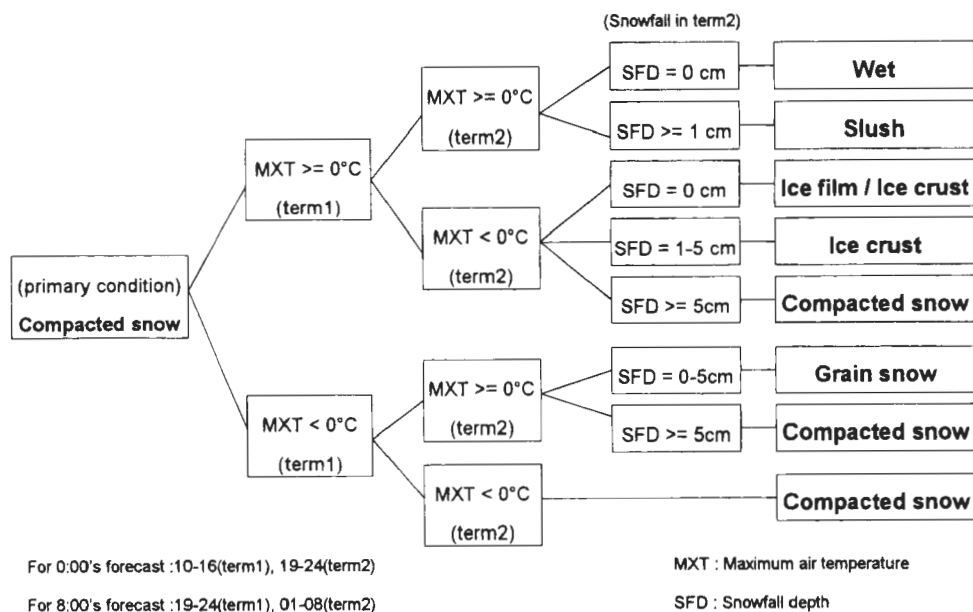

FIGURE 6 Example of forecast flow chart.

TABLE 5 Ratio of Predicted to Observed Forecast Data

Sites	Time		Sites	Time	
	0:00	8:00		0:00	8:00
Site A1	0.35	0.29	Site B1	0.28	0.14
Site A2	0.32	0.32	Site B2	0.26	0.16
Site A3	0.32	0.31	Site B3	0.26	0.16
Site A4	0.20	0.21	Site B4	0.25	0.19
Site A5	0.27	0.36			

CONCLUSIONS

The introduction of the European ice prediction system to Japan has had some problems because of the amount of snowfall in Japan and the differences in winter maintenance levels. However, developing an ice prediction method for snowy areas that is unique to Japan also is not easy. Nevertheless, improvement in winter road maintenance is expected of road administrators and is a subject that cannot be avoided. In addition to conducting the surveys, HDB has conducted improvements of the snowfall forecast system through the integrated use of other administrations' weather radars, and an analysis of the cost and benefit of ice predictions. Furthermore, a working group consisting of concerned representatives has met and discussed ways to exchange and share information with other organizations and the ideal RWIS for the next generation. Through these surveys, winter road maintenance will be improved.

REFERENCES

1. Akitaya, E., and T. Yamada. Classification of Snow and Ice on Roads (in Japanese). *Proc., Cold Region Technology Conference*, 1994, pp. 63–69.

Real-Time Road Ice Prediction and Its Improvement in Accuracy Through a Self-Learning Process

J. Shao and P. J. Lister, *Vaisala TMI, United Kingdom*

In winter road maintenance, it is important for highway engineers and authorities to know where and when road surface temperature is to fall below freezing and whether road surfaces will remain dry or icy. To provide this information, several numerical models have been developed in the last decade. However, the accuracy of model prediction in real-time application largely depends on the accuracy of forecast inputs (such as air temperature, dew point, wind speed, cloud type, and cloud amount), which are typically supplied by meteorologists. The experience and skills of the meteorologists are critical in some circumstances for the models to provide useful and reliable output. There is little doubt that such experience and skills vary individually within a group of meteorologists. To remedy model prediction errors resulting from input errors, a self-learning process is developed. The magnitude of error in real-time model input is investigated by comparing forecast input to actual measurements and observations, and the effect of input error on model prediction is demonstrated. A variety of methods, including self-adjustment and self-quality-control mechanisms, are introduced in this paper to show improvements of a numerical model in 24-hr forecasts and 3-to-6-hr nowcasts of road surface temperature.

Since the early 1980s, numerical prediction of road surface temperature for winter road maintenance has become more and more popular and has been accepted as a useful tool to determine where and when ice or frost is likely to occur (1–5). Such information enables highway engineers or authorities to salt or grit potentially freezing roads at the right time to minimize the cost of salting/gritting operations and possible damage to the environment. To achieve maximum benefits, the accuracy and reliability of temperature prediction is vitally important.

It has been known that nearly all input for a site-specific road ice prediction, produced by either human forecasters or mesoscale models, unavoidably has large or small departures from real conditions. As a consequence, the error in the input causes systematic or non-systematic distortion in road ice predication. Even in the case of automatic nowcasting (5), self-generated input by the model contains a degree of error. Although many statistical and dynamic ways (e.g., Kalman filter) exist to diagnose and adjust the error of numerical predictions, the principle of "simplicity is beauty" should be adopted in road ice prediction. This view is supported by three considerations. First, computing time and space are often limited for a local user of a model. Second, fast updating of prediction is desired in certain circumstances (e.g., when weather conditions are charging significantly). Third, only a few fundamental meteorological variables are measured at an automatic roadside weather station. These limitations or requirements mean that using some sophisticated error-correction schemes (e.g., Kalman filter) for this particular problem may not be practicable. A desirable method of road ice prediction is one that requires less computing time, computer storage space, and human intervention; one that is better understood by users; and one that is effective in removing errors in real time.

In the past, a method of simple template has been proved to be useful to remove systematic errors (6,7).

However, the effectiveness of the method is restricted in some circumstances (e.g., when the error is systematic or weather conditions do not change rapidly). To overcome this drawback, a new attempt is made in this paper to search for simple and effective methods to reduce model prediction errors in real time.

DATA COLLECTION

24-hr Forecast

Real-time input (in 24 hr) is usually provided on-line by local meteorologists and stored in archives. Therefore, a number of stations and days of real-time or realistic inputs (together with measurements of road surface temperature) have been successfully collected and extracted. The largest data set was obtained at Chapman's Hill (site code: WN001) on the M5 near Birmingham, England, from December 1, 1988, to March 12, 1989, and was derived from hard copy (printout). This site has been used as a model and sensor testing site since 1988. It is also a typical motorway forecast site. The data cover 65 days with forecasts of air temperature, dew point, wind speed, cloud amount, cloud type, and precipitation in 3-hr intervals, and sensor measurements of surface temperature in 1-hr intervals.

It is understandable that forecast input at one site may contain human errors by the group of forecast providers responsible for the site. Such errors in real-time input are likely to differ from one group (or site) to another in both magnitude and style. Therefore, an error-correcting method that is valid for one site may not work at another site. For this reason, efforts have been made to recover data from sites other than Chapman's Hill. In the Netherlands, 2 to 9 days' data were reestablished at four sites (GM004, GN001, HB008, and NW021). Another 2 to 3 days' data were recovered at three sites (RL002, RL004, and RL006) in Norway. These sites are located in different geographical and climatic regions with different topography and road construction, meteorologists' skills and experience also differ from site to site. The sites are considered to provide a reasonable database for the validation of methods developed in this paper.

Nowcasts

It has been shown elsewhere (5) that the accuracy of a self-integrated and automatic road ice nowcasting model deteriorates when weather conditions change dramatically. It is expected that the model should be able to monitor the change and make necessary adjustment to subsequent nowcasts without human intervention. For testing of the nowcasting model, a series of data was collected at an Austrian site (NO001) on the A21 near Vienna for the period

from January 10, 1996, to April 20, 1996 (72 days). As a by-validation, another site (SM001) on a flat plain in northern Italy between Bologna and Ferrara was also used for the study. Its data cover 53 days, from January 18, 1994, to March 17, 1994.

MIDNIGHT ADJUSTMENT

In the so-called template method (6,7), hourly model predictions in a specific day are corrected by the mean hourly error of predictions in previous days. Because weather conditions and a human forecasters' errors are unlikely to be the same or even similar for more than 1 day, this method is only useful to remove systematic or regular errors when weather conditions remain unchanged and input is provided by the same forecaster. In reality, forecaster error and weather condition change can become significant within a 12-hr period, usually starting at noon. In these cases, the template method contains too much old and useless information from some days ago; new and fresher information about model prediction error becomes increasingly important. On the other hand, accurate prediction of minimum temperature, which usually occurs at or shortly before dawn, is one of the most important parameters for winter road maintenance. For these reasons, a method called midnight adjustment is developed.

In this method, the model is fed original real-time input and run for 24 hr until noon of the next day. After 12 hr model performance is checked at midnight and the original forecasts are adjusted from 0100 to 1200. The algorithm of the method can be simply described by two equations:

$$\overline{E}_m = \frac{1}{n}\sum_{i=1}^{n}\left(F_i - A_i\right) \tag{1}$$

and

$$\hat{F}_j = F_j - \overline{E}_m, \quad j = 1, 2, \ldots, 12 \,(\text{hour}) \tag{2}$$

where

$\overline{E}_m$ = averaged model error in the previous n hours before 0100,

F_i and A_i = respectively forecast and actual road surface temperatures at hour i,

F_j = original model forecast for the period from 0100 to 1200, and

$\hat{F}_j$ = the forecast after midnight adjustment.

To get rid of "memory" that may be too old and may have a negative influence on the effectiveness of the adjustment, n is determined to be 3, that is, the error is averaged from 2200 to 0000.

TABLE 1   Comparison of Adjusted and Nonadjusted Forecasts of All
Nights (Chapman's Hill, 1988–1989, 65 days)

| | Noon to noon (24 hours) | | | | After mid-night (12 hours) | | | |
| | Overall | | Minimum | | Overall | | Minimum | |
	Bias	RMS	Bias	RMS	Bias	RMS	Bias	RMS
Adjusted	0.12	1.39	-0.08	1.34	-0.01	1.39	-0.10	1.32
Not adjusted	0.05	1.47	-0.16	1.50	-0.14	1.54	-0.16	1.49
Improvement	-0.07	0.08	0.08	0.16	0.13	0.15	0.06	0.17

TABLE 2   Comparison of Adjusted and Nonadjusted Forecasts of Marginal
Nights (Chapman's Hill, 1988–1989, 15 days)

| | Noon to noon (24 hours) | | | | After mid-night (12 hours) | | | |
| | Overall | | Minimum | | Overall | | Minimum | |
	Bias	RMS	Bias	RMS	Bias	RMS	Bias	RMS
Adjusted	0.09	1.45	0.05	0.90	0.20	1.48	0.05	0.90
Not adjusted	-0.08	1.45	-0.21	1.11	-0.13	1.48	-0.18	1.15
Improvement	-0.01	0.0	0.16	0.21	-0.07	0.0	0.13	0.25

In Table 1, the results of the application of the method to all nights at Chapman's Hill are compared with the results of unadjusted forecasts. The comparison was made on every hour available in all days and minimum temperature forecasts in two periods: noon to noon and midnight to noon. In the table, a positive sign shows the reduction of error by the adjustment and a negative sign shows its increase of error. The table shows that for a 24-hr comparison, the adjustment's slight reduction of overall root mean square (RMS) error is accompanied by a small increase in its bias. Apart from this, an improvement of around 0.1°C is generally seen in the comparison. Results of similar comparisons of

marginal nights when minimum surface temperature was in the range of –1°C to +1°C are shown in Table 2. As the table indicates, the error of minimum temperature forecast with midnight error adjustment was significantly reduced by 0.13°C to 0.25°C for the marginal nights.

The improvements in accuracy of overall and minimum temperature predictions are also seen at sites in Holland (GM004, GN001, HB008, and NW021) and Norway (RL002, RL004, and RL006). Tables 3 and 4 show the improvement of minimum temperature prediction at these sites. The reduction of RMS error in minimum temperature forecast by the method is generally

TABLE 3   Comparison of Adjusted and Nonadjusted Minimum
Temperature Predictions (Holland)

| | GM004 | | GN001 | | HB008 | | NW021 | |
	Bias	RMS	Bias	RMS	Bias	RMS	Bias	RMS
Adjusted	0.28	1.43	0.04	1.39	-0.25	1.59	0.35	0.49
Not adjusted	0.13	1.81	-0.47	1.86	-0.57	2.13	0.45	0.64
Improvement	-0.15	0.38	0.43	0.47	0.32	0.54	0.10	0.15

TABLE 4   Comparison of Adjusted and Nonadjusted Minimum
Temperature Predictions (Norway)

| | RL002 | | RL004 | | RL006 | |
	Bias	RMS	Bias	RMS	Bias	RMS
Adjusted	0.85	0.85	0.95	1.10	0.63	0.69
Not adjusted	0.95	0.96	1.40	1.40	0.57	0.65
Improvement	0.10	0.09	0.05	0.30	-0.06	-0.04

seen at these sites. The largest reduction is 0.54°C at HB008. Although the number of samples (or days) at each site is limited, the results are encouraging, and the average improvement at these sites is 0.2°C in bias and 0.36°C in RMS error.

Although the results are positive, the application of midnight adjustment does not mean that improvement can be made on every night and under all conditions. Figure 1 displays the daily variation of improvement by the technique for all hours over during 65 days at Chapman's Hill. The same variation for marginal nights is demonstrated in Figure 2. In these figures, positive (above zero bar) means improvement of forecast accuracy, while whereas negative means deterioration. It is seen from the figures that although positive improvement dominates, a much worse forecast can be made with the adjustment in some circumstances. One example is day 48 or December 12, 1989, in Figure 1, and day 11 or December 12, 1989, in Figure 2. Analysis of the first example reveals that in the input data, both air temperature (1.5°C) and cloud amount (0 octa) forecasts were significantly underestimated at 2100, compared with actual (4.0°C and 4 octas). In contrast, both air temperature and cloud amount were then overestimated after midnight. The consequence of this mistake in the input is a large negative error (and thus positive adjustment) of road surface temperature prediction. This error, caused by underestimation of air temperature and cloud amount in the period of 2200 to 0000, was passed on and added to the erroneous predictions resulting

from overestimation in the period after midnight. Therefore, the prediction after midnight deteriorated substantially. This example shows the principal limitation of the midnight adjustment technique.

SELF-LEARNING IN NOWCASTING

One of the most important features of automated and accurate nowcasting is the generation of short-term forecasts without human intervention. In such nowcasting, the input of air temperature, dew point, wind speed, cloud type and amount, and precipitation are all generated within the model itself. This feature can save costs by minimizing provision of human forecasts and has the potential to provide "cheap, cheerful and accurate" (8) forecasts in meteorological applications. To check and improve the quality of road ice nowcasting and to retain this important feature of automation, a scheme of self-quality-control is introduced into the icebreak model.

Air temperature is one of the most dominant factors controlling the variation in (and prediction of) road surface temperature. Therefore, model-generated forecasts of air temperature become a natural target for improvement. In the scheme, the model learns from historical data consisting of sensor measurements and nowcasts. Combined with its knowledge of current time, sunshine, and humidity, the model decides if an error correction is necessary. The fundamental decision rules are presented
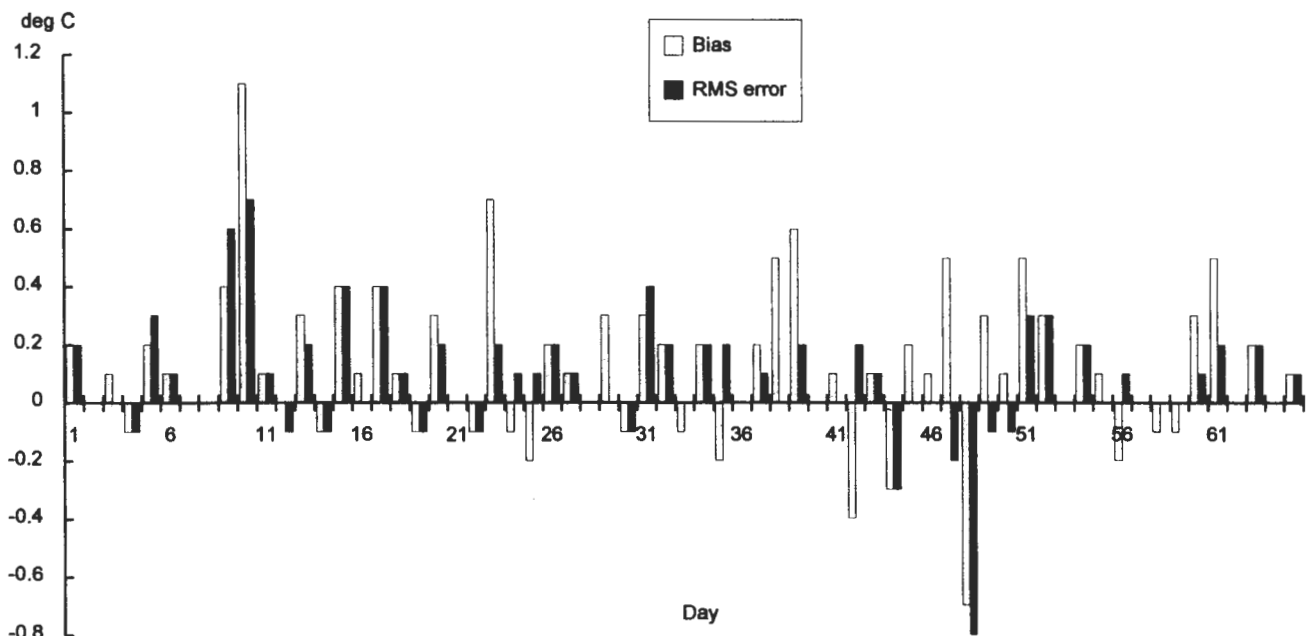

FIGURE 1   Comparison of real-time forecasts with and without midnight adjustment (Chapman's Hill, January 12, 1988, to December 3, 1989).
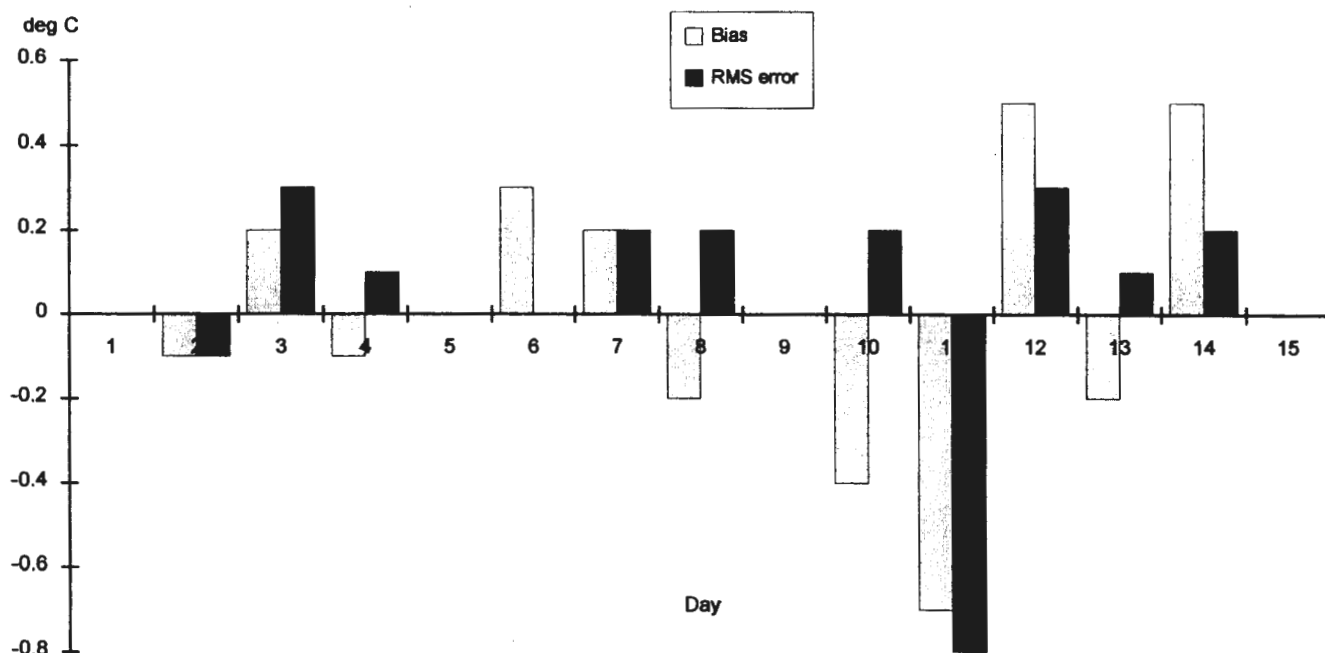
FIGURE 2   Comparison of real-time forecasts with and without midnight adjustment (Chapman's Hill, marginal nights).

in Table 5. The scale of correction depends on the magnitude of the latest actual tendency of air temperature, the calculated intensity of solar radiation, and the value of the forecast itself.

The results of nowcasts of air temperature with and without this self-learning scheme are listed in Table 6. Generally, there is a small reduction in RMS error, accompanied by a small increase in bias, for 2-, 4-, and 6-hr nowcasts by the scheme. The results of site SM001 appear more positive than those of site NO001, especially for overall temperature nowcasts. It is noticed in the study that in some circumstances the method can be very helpful. Figure 3 shows an example of 4-hr nowcasts of air temperature at site SM001 with and without self-learning and correction. The figure indicates that the

method enables the model nowcasts to closely track variation in actual temperature, especially after sunset and sunrise.

DISCUSSION

In this study, two simple methods are explored to improve 24-hr forecasts and 2- to 6-hr nowcasts of road surface temperature in real-time application through deduction of midnight error of model prediction from the after-midnight predictions and through trend correction of air temperature, respectively. A comparison of 24-hr forecasts with and without midnight adjustment shows that the method is effective in most cases, with a

TABLE 5   Rules for Correction of Air Temperature Forecasts in Nowcasting

Rule 1:	IF(forecast trend is not consistent with the latest actual trend), and IF(it is day time), and IF(relative humidity < 90%), and IF(forecast declines) -------> Positive correction.
Rule 2:	IF(forecast trend is not consistent with the latest actual trend), and IF(it is night time), and IF(relative humidity < 90%), and IF(forecast climbs) -------> Negative correction.
Default:	Zero correction.

TABLE 6 Comparison of Nowcasts With and Without Self-Error-Correction

	NO001				SM001			
	Overall		Minimum		Overall		Minimum	
	Bias	RMS	Bias	RMS	Bias	RMS	Bias	RMS
2 hour:								
Corrected	0.08	0.96	-0.06	0.31	0.17	1.02	0.04	0.33
Not corrected	0.04	0.99	-0.04	0.32	0.09	1.12	0.01	0.36
Improvement	-0.04	0.03	-0.02	0.01	-0.08	0.10	-0.03	0.03
4 hour:								
Corrected	0.14	1.31	-0.14	0.64	0.28	1.54	0.18	0.74
Not corrected	0.12	1.31	-0.07	0.64	0.26	1.68	0.33	0.78
Improvement	-0.02	0.0	-0.07	0.0	-0.02	0.14	0.15	0.04
6 hour:								
Corrected	0.07	1.86	-0.19	0.82	0.49	2.03	-0.10	0.95
Not corrected	0.06	1.94	-0.06	0.82	0.31	2.20	0.16	0.96
Improvement	-0.01	0.08	-0.13	0.0	-0.18	0.17	0.06	0.10

general reduction of bias and RMS error of about 0.1°C to 0.2°C. The method is an especially useful tool for improving minimum temperature forecasts. The trend correction method, however, does not significantly and consistently improve nowcasts, although it has demonstrated its effectiveness in some cases. It could be useful at some sites but may be useless at others. Generally, both methods show positive results in this study.

The main drawback of the methods, as shown in the paper, is that there is no general rule to predict when they will succeed or fail. This is particularly true when weather conditions on one day are largely different from those of the previous day. To overcome this drawback, detailed historical information about tendency and variation of the error in forecast input is required. More sophisticated methods (e.g., neural network analysis) are needed to analyze and recognize error patterns. This will improve the accuracy of road ice prediction but will also inevitably require a large quantity of computing power and space. To achieve a more fundamental and consistent improvement, further study is needed.

ACKNOWLEDGMENT
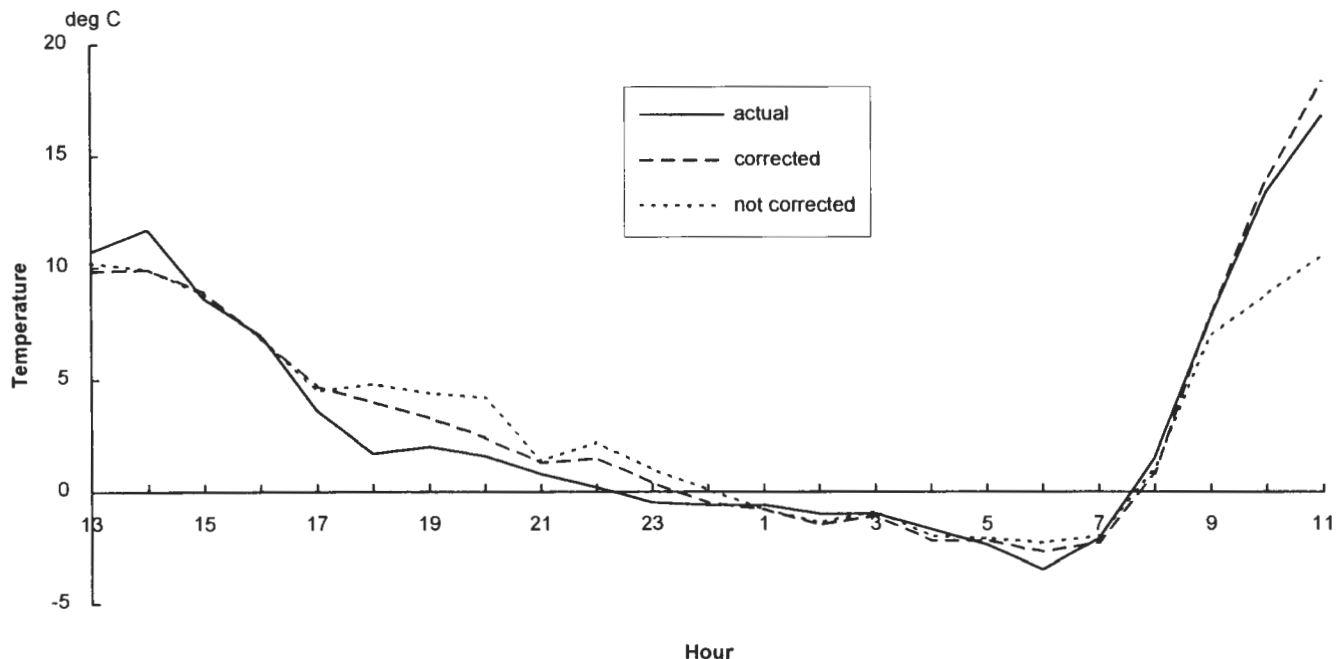
FIGURE 3 Comparison of 3-hour nowcasts with and without correction of air temperature forecast (SM001, January 26, 1994).

REFERENCES

1. Nysten, E. *Determination and Forecasting of Road Surface Temperature in the COST 30 Automatic Road Station (CARS)*. Technical Report No. 23. Finnish Meteorological Institute, Helsinki, 1980.
2. Thornes, J. E. *The Prediction of Ice on Motorways*. Ph.D. dissertation. University College, London, 1984.
3. Rayer, P. J. The Meteorological Office Forecast Road Surface Temperature Model. *The Meteorology Magazine*, Vol. 116, 1989, pp. 80–190.
4. Shao, J. *A Winter Road Surface Temperature Prediction Model with Comparison to Others*. Ph.D. dissertation. University of Birmingham, 1990, 245 pp.
5. Shao, J., and P. J. Lister. An Automated Nowcasting Model of Road Surface Temperature and State for Winter Road Maintenance. *Journal of Applied Meteorology*, Vol. 38, 1996, pp. 1352–1361.
6. Thornes, J. E., and J. Shao. Objective Methods for Improving the Operational Performance of a Road Ice Prediction Model Using Interpolated Mesoscale Output and a Templet for Correcting Systematic Error. *The Meteorology Magazine*, Vol. 121, 1992, pp. 197–204.
7. Astbury, A. Removal of nonmeteorological errors from ice prediction models by use of a statistical templet. Vol. 2, *Preprints of Third International Symposium on Snow Removal and Ice Control Technology*, Sept. 14–18, 1992, Minneapolis, 1992.
8. Thornes, J. E. The Quality and Accuracy of a Sample of Public and Commercial Weather Forecasts in the UK. *Meteorological Applications*, Vol. 3, 1996, pp. 63–74.
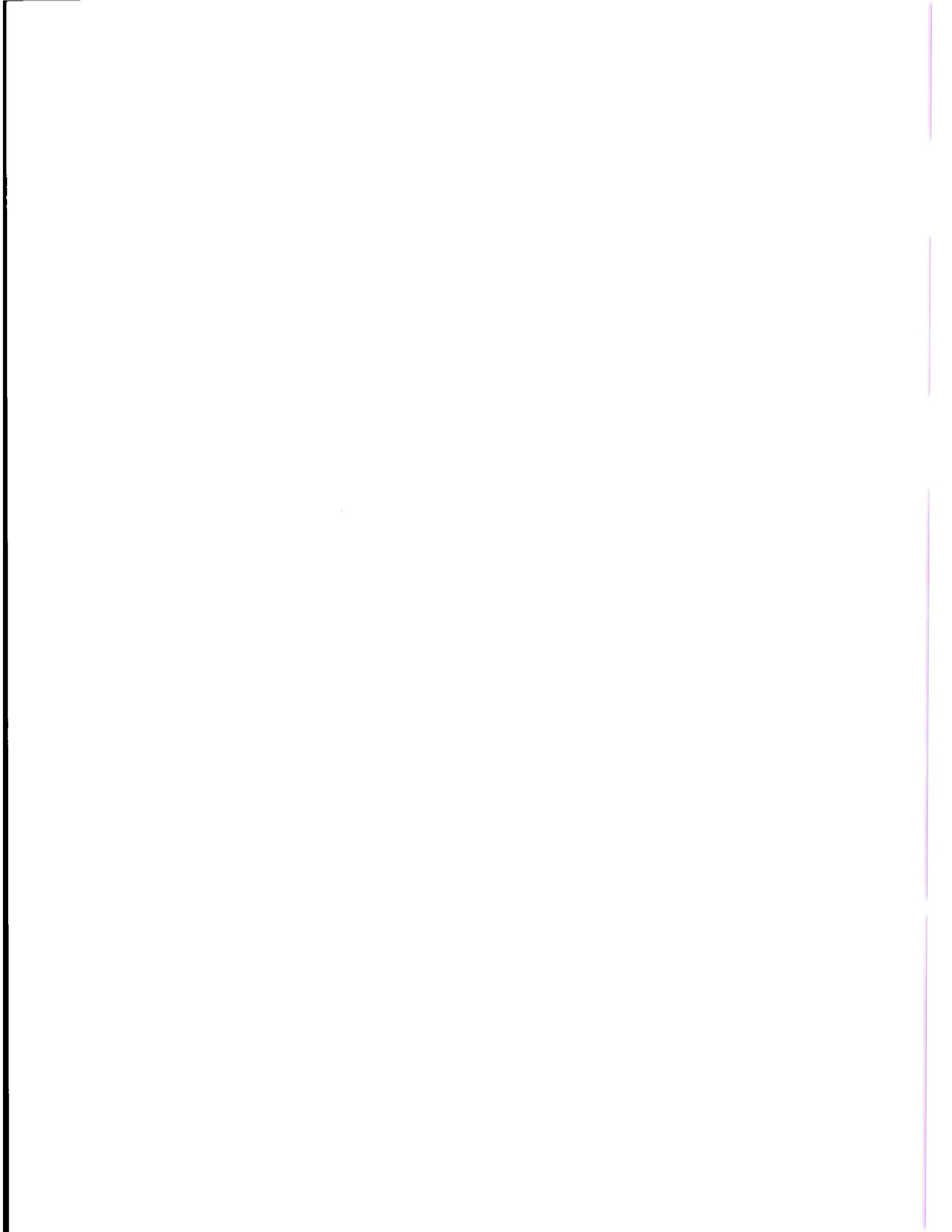
PART 7
SAFETY AND VISIBILITY
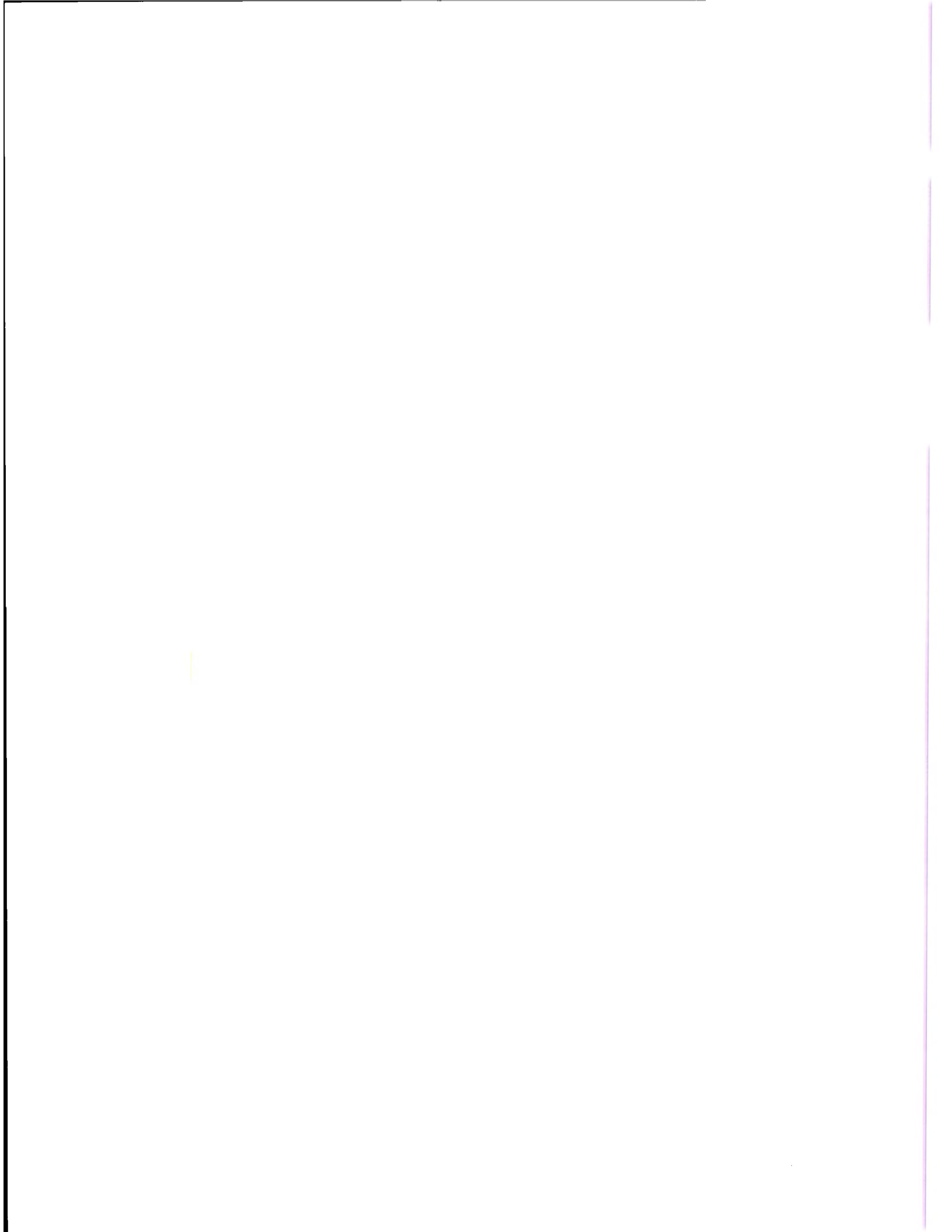
Benefit-Cost Comparison of Salt-Only Versus Salt-Abrasive Mixtures Used in Winter Highway Maintenance in the United States

David A. Kuemmel and Quazi Bari, *Marquette University*

A study at Marquette University examined accident rates and benefit-cost estimates of winter maintenance operations by state agencies that use primarily salt-abrasive mixtures as deicers. The study methodology was patterned after a prior study at Marquette with state agencies that used primarily salt alone as a deicer. The recent study included 788.8 km of two-lane highway and 92.8 km of freeway in five maintenance districts in four states. The study was conducted during the winters of 1992–1993 and 1993–1994. Field data, which were collected by the state departments of transportation, included event and weather information and the amount of salt and abrasives used for more than 781 events. Traffic volumes were adjusted for seasonal, daily, hourly, and snow-reduction variations. Before and after accident rates were calculated, and benefit-cost estimations were made for both two-lane highways and freeways. Accident rate reductions were calculated and benefits were measured. Standard benefit analysis was performed for increased fuel savings and reduced travel time. Accident reductions for two-lane highways on which salt-abrasive mixtures were used were less than those of the prior study of salt-only use. Accident reductions for freeways were much less and took much longer to occur when salt-abrasive mixtures were used, compared with the reductions with salt only. Benefit-cost calculations showed that the application of salt-abrasive mixtures did not recover winter maintenance costs on two-lane highways during the 12-hr analysis period. This finding is affected by the low number of accidents. Benefit-cost calculations showed that freeway operations recovered costs in 6 hr, substantially longer than with salt only. Comparisons are made between the results of accidents and benefit-cost data between the two studies (salt-only and salt-abrasive mixtures).

T he benefits of winter maintenance can be categorized as direct and indirect. Direct benefits include improved travel time, reduced travel costs, and reduced accidents and can be estimated or are measurable (1). Indirect benefits are those on a socio-economic level and include reduction in lost wages, maintenance of business opportunities and social activities, and provision of close-to-normal fire, police, ambulance, and paramedic services.

The costs of winter maintenance can likewise be categorized as direct and indirect (1). Direct costs are agency costs to perform winter maintenance activities. They include the costs of labor, material, and equipment to plow snow and apply ice control chemicals, as well as the costs of equipment repair, snow fence installation, abrasive cleanup, and supervision (1). Indirect costs include environmental costs associated with the use of ice control chemicals and abrasives and those related to corrosion of highway components and vehicles. The most complete study of indirect costs of deicing is one by the Transportation Research Board (TRB) in 1991 (2). Also, a 1991 study by the Denver Council of Regional Government reported the problems with air quality following heavy use of abrasives (3). This study deals with rural highways and direct benefits and costs.

The Marquette University study goals were to compare winter maintenance results achieved by agencies

that generally use salt only to reach bare pavement as quickly as is practical, with results achieved by agencies that generally use salt-abrasive mixtures to produce a given level of service. Specifically, the study measured:

- Differences in accident rates before and after treatment,
  - Differences in benefit-cost ratios of operations, and
  - Differences in accident rates as the percent of salt varied from minimal (5 to 10 percent) up to 50 percent.

METHODOLOGY

Data Gathering

Highway Selection

The research was conducted between 1992 and 1995 by personnel at Marquette University. The states involved in the study were Iowa, Minnesota, New York, and Pennsylvania. Only highways under the states' jurisdiction were included. Within five maintenance districts in the four states, highways were selected jointly by the states and the research team without regard to geometry or their accident potential. The goal was to pick lengths of highway similar to those in the earlier Marquette University salt-only study. The following lengths of highway were used as test sections:

State	Two-Lane Highways (km)	Freeways (km)
Iowa (Mason City)	160	17.6
Minnesota (Rochester, Owatonna)	318.4	44.8
New York	144	30.4
Pennsylvania	166.4	0.0
Total length	788.8	92.8

General geometric characteristics of the two-lane test sections were 3.33-m or 3.63-m lanes and 0.91-m to 3.03-m paved or gravel shoulders. Divided highways had four 3.63-m-wide lanes and 3.03-m paved shoulders.

State Winter Maintenance Policies

Iowa generally uses 50 percent rock salt (hereafter referred to as salt) and 50 percent abrasives (4). On lower-volume highways Iowa uses minimal salt but any blend may be used, depending on conditions.

In Minnesota, the percent of salt in the salt-abrasive mixture is varied depending on storm conditions but generally falls in the 5 to 60 percent range on rural highways and can be 100 percent if dictated by winter conditions (5).

In New York, the policy is to discourage general abrasive use, and most of the state uses 100 percent salt only (6). The Watertown district policy is to use an approximately 25 percent salt-abrasive mixture because of the district's location at the end of Lake Ontario and adjacent to the St. Lawrence River.

In Pennsylvania's policy (7), priority, classification, time of day, and snow accumulation determine the amount of salt. On freeways, which have the highest priority, 100 percent salt is used. On second-priority highways, either salt only or salt-antiskid (abrasive) material is used, depending on temperature. On third-priority highways, a salt-abrasive mixture from minimal to 25 percent salt is generally used, depending on temperature.

Winter Event Data

Data collection occurred in the winters of 1992–1993 and 1993–1994. Because the winter maintenance policies varied, and because each storm had the potential to change the amount of salt used, an event reporting form was designed to provide the information required in each district. A key data gathering point, stressed in on-site meetings with the supervisors involved in each district, was to accurately determine the quantity of salt and abrasives in each application.

Traffic Volumes

All states provided average annual daily traffic (AADT) for the test sections. They also provided factors (or information) to adjust AADT for seasonal, daily, and hourly variations. Automatic traffic recorder (ATR) stations were used to develop an additional factor, known as the snow reduction factor. This is described in the data analysis section and is based on previous work by Marquette University (8–10).

When traffic volumes along a given test section (snow maintenance route) varied and were separately counted, these sections were broken into subsections and volume adjustments were calculated separately to derive million kilometers of travel (MKT).

Direct Benefit Data

Fuel savings related to winter maintenance were based on work by Claffey (11). Actual operating costs were not gathered, but the procedures from Claffey's work were used. The differences between gasoline consumed on snow covered or icy pavement and bare pavement in gallons per kilometer traveled, adjusted for travel speed and multiplied by MKT, were used to calculate excess fuel savings through winter maintenance. By

using Claffey's methodology, the excess fuel for two-lane roads was determined to be 20 percent and the excess fuel consumed for freeways was 10 percent. The value of fuel savings for all events was then multiplied by the current price of gasoline in that region during the months of testing and averaged over all regions for the benefit calculation. It should be noted that the assumption in Claffey's work calls for bare pavements, and not all events resulted in bare pavement because service standards varied. This assumption tends to overstate any benefits from using salt-abrasive mixtures.

The American Association of State Highway Officials user benefit analysis methodology (12) was followed for savings in travel time. A 16-kph reduction in normal average travel speed of 64 kph (25 percent reduction) on two-lane highways and a 16-kph reduction of normal average travel speed of 96 kph (17 percent reduction) on freeways were assumed. These are more conservative than speed reductions reported in other work (13). The value of travel time of $3/hr was updated by using the implicit price deflator for the gross national product index (more conservative than the consumer price index), to $7.68 per travel hour in 1993 dollars.

In all states, the researchers worked with staffs to determine references for locating accidents by section and subsection to ensure that accidents were logged in the appropriate hour before or after the hour when the level of service was achieved with a final application (zero hour).

Accident cost data were reviewed from a variety of sources, including the National Safety Council (14) and a 1991 Federal Highway Administration report (15). The latter was used because it is more appropriate for benefit-cost calculations. The following values [adjusted to 1994 as recommended (15)] were used for the cost of each broad category of accidents: fatal accident, $2,722,548; injury accident, $69,592; and property damage only, $4,489. (Injury Categories A, B, and C were disregarded for uniformity purposes.)

Winter Maintenance Direct Costs

The winter maintenance costs for the entire season for each maintenance district were obtained following the close of the season for the second year of data gathering. These included labor, material, equipment, and supervision where applicable. Some states included substantial administrative costs and others included none. This does not significantly affect results, however, because the same procedure was followed in the salt-only study. Unit costs per event were averaged for the entire season by dividing the season's costs by the estimated number of events, and costs per event were averaged for all agencies.

Data Analysis

Winter Events

For purposes of this research, a winter event is described as the occurrence of winter maintenance on an entire length of test section because of freezing rain, formation of ice, or accumulation of snow. The section may have been treated with a mixture with or without plowing.

When an event form was received, it was reviewed by the researchers for completeness and to determine if it was a usable event, depending on the number of applications. Because multiple applications closely spaced in time could actually result in applying more salt to the roadway than salt-only treatment, it was agreed initially to limit selection of events to those with no more than three applications and not more than 50 percent salt mixed with abrasives per application. This was done to allow comparison with 100 percent salt applications.

When forms were reviewed, a zero hour was selected to be most representative of the middle of the last hour of application before achievement of level of service.

As data began to arrive, the researchers realized that many events had more applications, particularly in New York, where the area on the east end of Lake Ontario could have an event that lasted 4 days and could have 35 applications of a 25 percent salt mixture. To expand the database, it was decided to classify the events into regular and special events. The limit for the number of applications for regular events was raised to four in New York only and remained at three in the other states. Events with four or more applications in other states and five or more in New York were identified as special events for separate analysis. They are addressed in another report (16).

This change increased the number of included events, but the change was not tested for statistical significance. It also lessened the difference between agencies using salt only and those using multiple applications of salt-abrasive mixtures. This meant that differences in accidents would be potentially more conclusive.

If a section of highway for which an event occurred had a variation in traffic volumes, a subsection of highway was created in the database and an event became a subevent. There were 551 regular events in the 1992–1993 winter, and 230 regular events in the winter of 1993–1994. A total of 3,045 regular subevents for both winters was analyzed.

Traffic Volume Analysis

For purposes of a before-and-after accident analysis for each of the 12 hr before and after the zero hour, it was necessary to select the proper hourly traffic count for each of the appropriate 24 hr for each subevent to

calculate MKT. The following formula was used for this conversion:

$$HTV_{nH} = AADT \times MF_M \times DF_D \times HF_H \qquad (1)$$

where

HTV_{nH} = hourly traffic volume, normal day, for hour H,

MF_M = monthly factor for month M,

DF_D = day of week factor for day D, and

HF_H = hourly factor for hour H of the day.

MKT was then calculated by using the length of the subsection multiplied by HTV_{nH}.

A detailed description of the databases and the calculations is provided elsewhere (16,17). The methodology was also described elsewhere (8–10).

Daily Traffic Adjustment Factor

An analysis of daily factors was made by using the actual days and times of each event to determine if a daily factor was needed. The four scenarios from the earlier study were used to determine the impact on results if a day-of-the-week factor were not used. There are 198 events with underestimation of accidents and 194 with overestimation. Therefore, as in the earlier study, a day-of-the-week factor was not used.

Snow Reduction Adjustment Factor

It is conceivable that when it snows, traffic volumes may change by hour or by day. How much they can change was explained in work performed by Hanbali and Kuemmel (9). That approach was used in this study, and data from nearby ATR stations were used to adjust volumes on the basis of variations from a normal traffic day to arrive at the factors for either reduction of or increases in traffic during an event (16,17). Adjustments to reduce or increase volumes were applied to all hours to avoid any use of assumptions.

Accident Analysis

Each accident was identified to determine a match between the date and hour of the accident and the 24 hr surrounding the zero hour of any event. Accidents were tabulated in accidents per MKT, as used in similar studies in Europe (18) and the United States (1,8–10) for each test section and subsection. MKT also was accumulated for all subevents, for each of the 12 hr before and after zero hour, by using databases described previously. Separate tabulations were made for two-lane highways and freeways for regular events. The computerized database performed approximately 75,000 calculations of MKT. After MKT was established, accident rates were calculated by hand for each hour.

Accident rate reductions (or increases) were calculated for each cumulative hour following zero hour for both two-lane highways and freeways, for both injury and property-damage-only accident rates (there were no fatalities). These rate reductions were multiplied by the appropriate cost and type of accident to arrive at total savings due to reduction in accidents.

Treatment of Variables

In a study of this type, many variables were not accounted for simply because they are nearly impossible to account for. Human factors, roadway geometry, maintenance policies, and weather all varied. The use of control sections was not possible. More than 1,000 events with a variety of traffic, geometry, and weather conditions were analyzed, and it was believed that these events would be representative of a cross section of possibilities that would reduce the impact of any one variable.

Statistical Analyses of Accident Data

Following calculation of the accident rates for each of the 12 hr before and after the zero hour, the percent rate of change in accident rates was calculated for each of the cumulative pair of hours (conjugate hours). For example, in a comparison of the 4 hr before and after the zero hour, the percent rate of change was the difference between the cumulative accident rates for the 4 hr before (Hours −3 to 0) and the 4 hr after (hours 1 to 5) divided by 100.

Three separate statistical analyses were applied to the differences in these changes in accidents for each conjugate pair of hours. The Poisson and revised decision criteria were applied to the change in accident frequencies, and the paired t-test was applied to the percent rate of change of accident rates. The revised decision criterion test was developed by Weed (19) to meet some of the disadvantages of the Poisson test.

Finally, the paired t-test was used to draw inference of parameters between two populations. The data from this study use two dependent variables in the conjugate hours before and after zero hour. This will constitute two dependent samples from two populations (before and after accident rates), and in this case is the most appropriate test.

RESEARCH RESULTS

Accident Results

Accident rates before and after (B/A) zero hour are shown in Figure 1 for two-lane highways and Figure 2
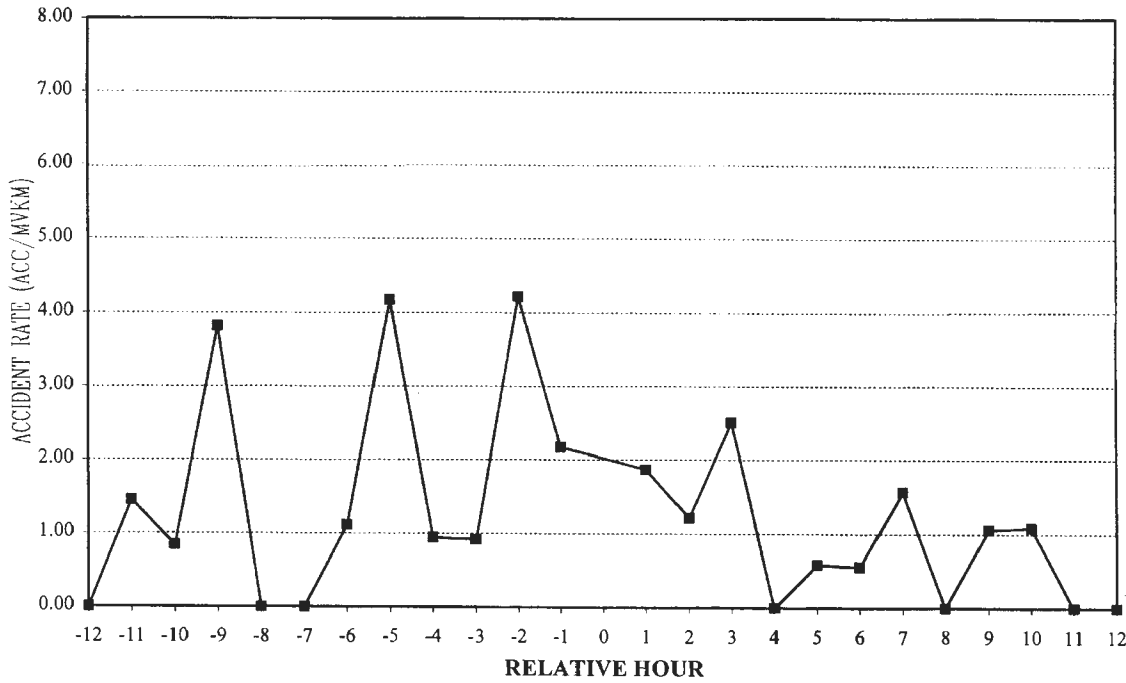
FIGURE 1 Accident rates for regular events, two-lane highways.

for freeways for all regular events in all states. Accidents and MKT were combined for two-lane and freeway test sections and the B/A accident rates were calculated for various groupings of percent salt in the salt-abrasive mixture. The results were inconclusive because of the insufficient accident data. A full discussion and results are presented elsewhere (15,16).

Results of Benefit-Cost Analysis

Winter Maintenance Costs

The direct costs of winter maintenance in each of the maintenance districts ranged from $9 to $63/lane-km/event. The average cost for all agencies was approximately

FIGURE 2 Accident rates for regular events, freeways.
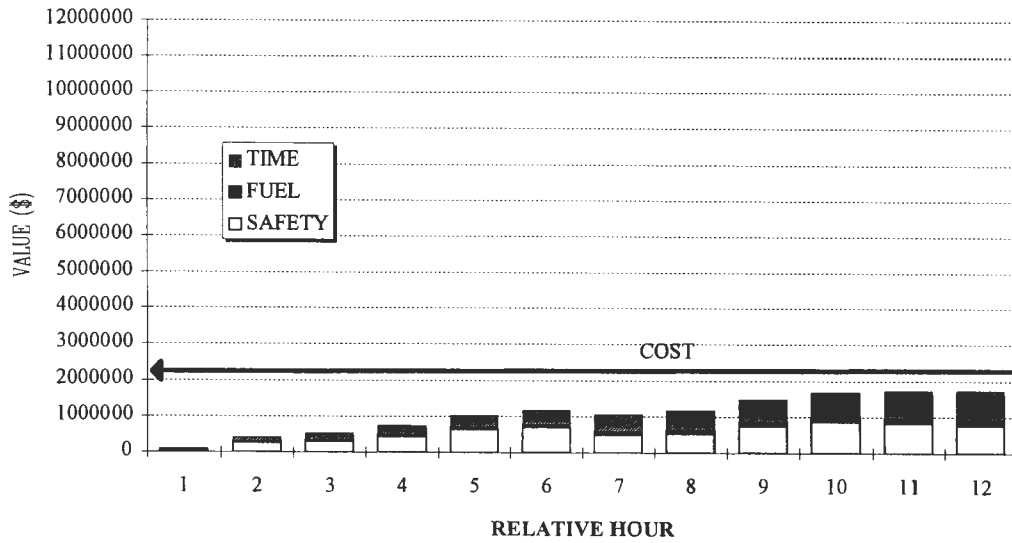
FIGURE 3   Cumulative summary of direct benefits, two-lane highways.

$30/lane-km/event for two-lane highways and $21 for freeways. This cost estimate is conservative because it excludes major storms. (As noted earlier, major storms were not analyzed in this study because of multiple applications.

The total cost of all winter maintenance regular events (3,045 subevents) was approximately $2,106,000 for two-lane highways and $158,000 for freeways. A full discussion of the calculations is presented elsewhere (15).

Winter Maintenance Benefits

The individual components of direct benefits of winter maintenance in the after period are shown as savings in travel time (marked "time"), savings in gasoline consumption (marked "fuel"), and savings in accident reduction (marked "safety") for the cumulative hours after zero

hour in Figures 3 and 4 for two-lane highways and freeways, respectively. If accidents increased in the after period, the increased cost is shown as a negative saving.

The results of the cumulative benefits by hour after zero hour (top of the bar graph for each hour) along with the costs (a solid bold line) for all regular events are shown in Figures 3 and 4 for two-lane highways and freeways, respectively.

The total benefits for all regular events was approximately $1,740,000 on two-lane highways and $424,000 on freeways.

For two-lane highways, the regular winter maintenance events did not recover costs at any time during the first 12 hr analyzed. The benefit-cost ratio for these events was approximately 0.6 for the first 6 hr after zero hour and 0.8 for 12 hr after.
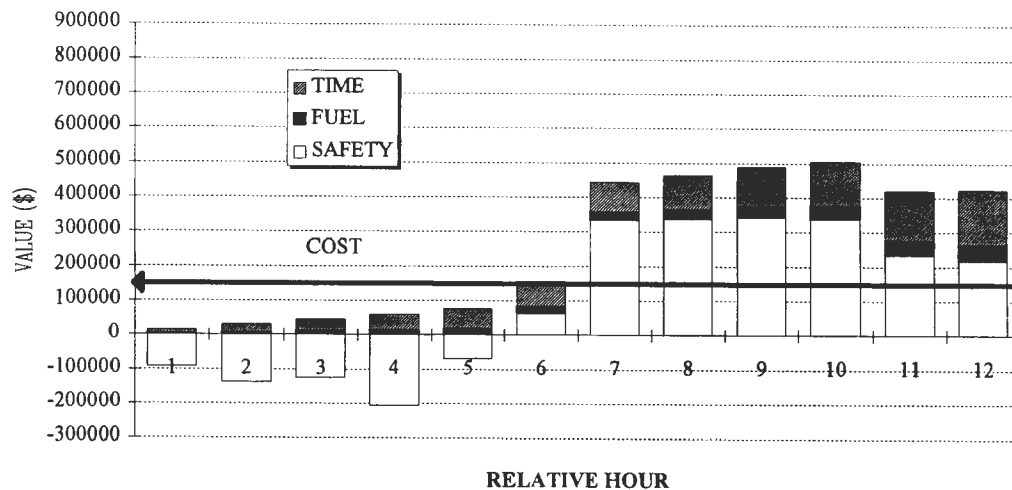
FIGURE 4   Cumulative summary of direct benefits, freeways.

For freeways, the regular winter maintenance events recovered costs after 6 hr. The benefit-cost ratio was 1.0 after the first 6 hr after zero hour and 2.7 after 12 hr. A plot of these cumulative benefit-cost ratios is shown in Figure 5 for both two-lane highways and freeways.

COMPARISON OF STUDY DATA

A final goal of this study was to compare the results of winter maintenance using salt-abrasive mixtures (data labeled "Salt II," and conducted from 1992 to 1994) with a study conducted by Marquette University (1,8,10) of agencies that used salt only (data labeled "Salt I", conducted from 1990 to 1991). Appropriate adjustments to both benefit and cost calculations were made to allow economic comparisons.

Maintenance Policies

In the earlier study of agencies that used salt only, all (Illinois, New York, and Wisconsin) had a bare pavement policy. New York was included in both studies but with different maintenance districts and maintenance policies. In the later study on salt-abrasive mixtures, some highway classifications (freeways) had bare pavement as a goal, but on two-lane highways some states had a lower level of service (one bare wheel path, for example).

Size of Database

Information about test sections is presented in the following table.

Database	Salt Only	Salt-Abrasives
Kilometers of Test Section	912	881.6
Travel, MKT 24 hr range		
Two-lane (millions)	3.36–4.64 m	0.8–1.76 m
Freeway (millions)	1.28–2.08 m	1.44–2.72 m
Winter Maintenance		
Events	226	781
Subevents	4,600+	3,045
Accidents		
Two-lane, 12 hr before	184	22
Freeways, 12 hr before	13	21

Accident Rate Reduction Before and After

A comparison of cumulative percentage accident reductions is shown for two-lane highways and freeways (Figures 6 and 7). For freeways in Figure 7, the reduction is negative because accidents increased in 3 of the first 4 hr.

Benefit-Cost Ratios and Recovery of Cost Periods

Cumulative benefit-cost ratios are shown for both studies, without the detail of breakdown in benefit component, for two-lane highways in Figure 8 and for freeways in Figure 9. Winter maintenance cost lines are indicated for each study separately.

When salt only was used on two-lane highways, the operation paid for itself in 25 min after zero hour. The
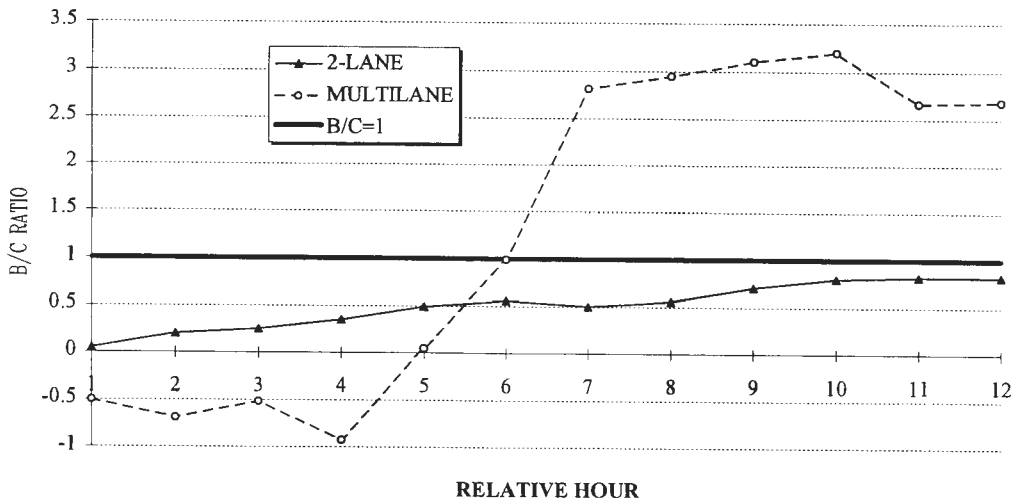
FIGURE 5   Cumulative benefit-cost (B/C) ratios for both highway groups.
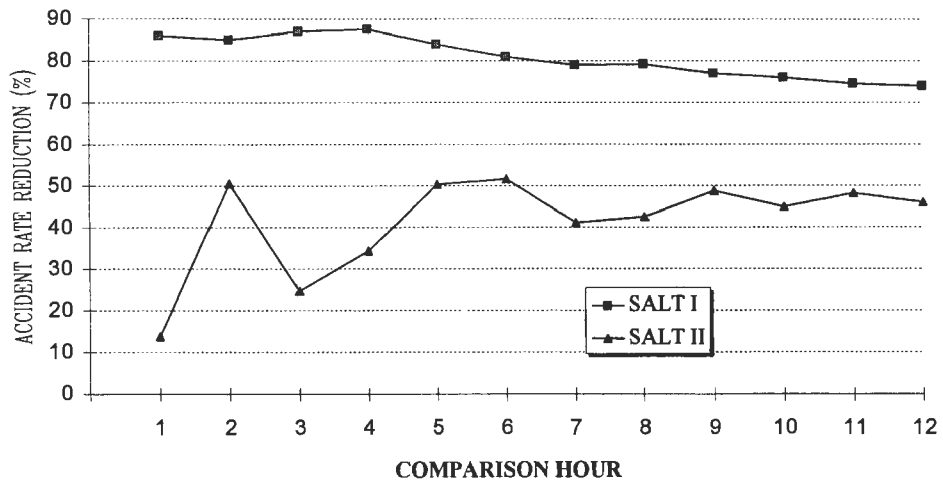
FIGURE 6   Comparison of accident rate reduction, two-lane highways.
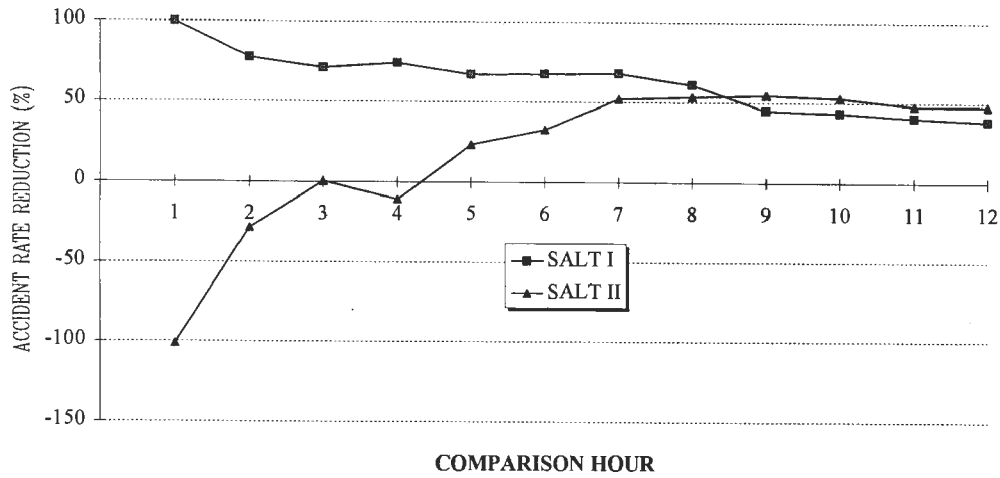
FIGURE 7   Comparison of accident rate reduction, multilane highways.
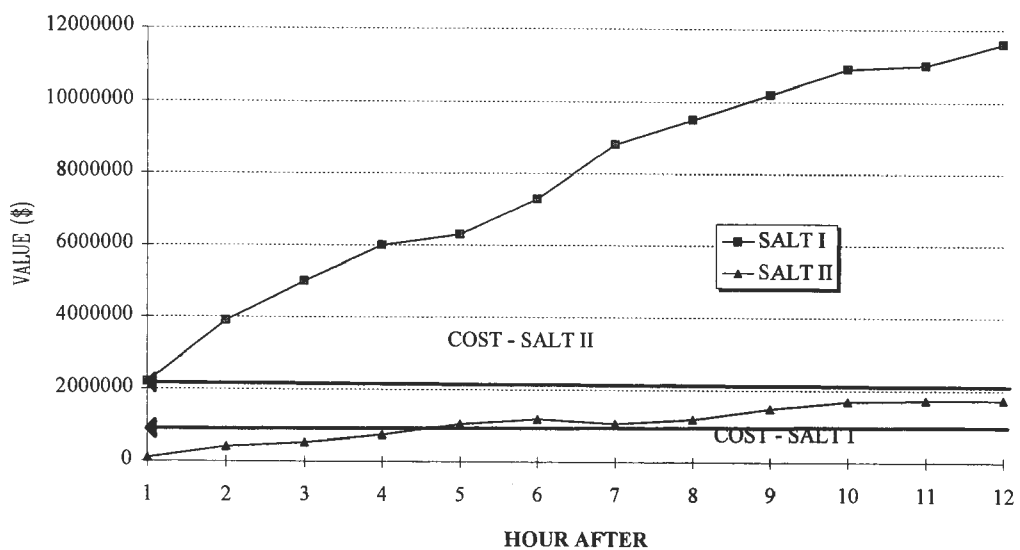
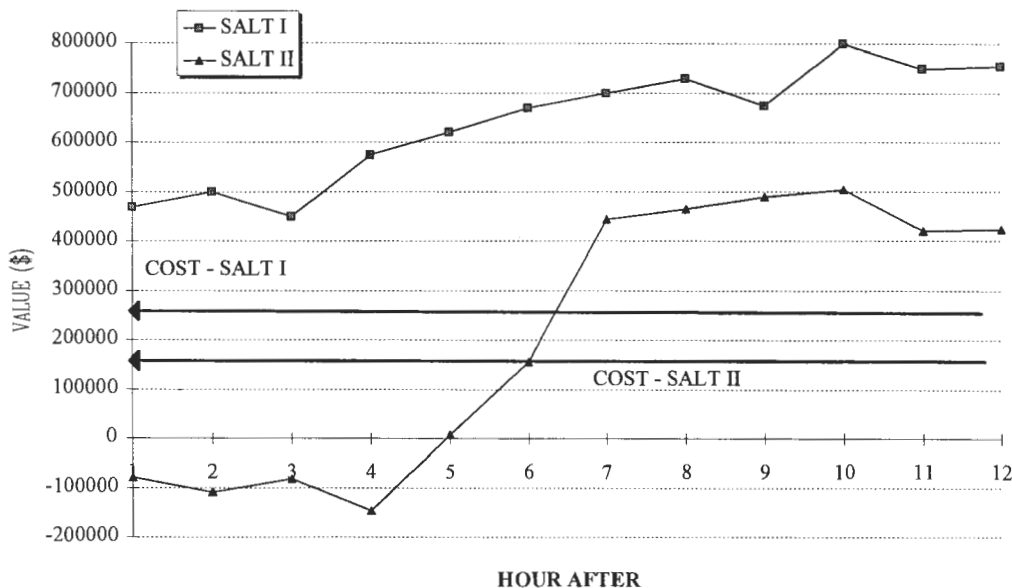FIGURE 8   Comparison of cumulative benefits, two-lane highways.

FIGURE 9 Comparison of cumulative benefits, multilane highways.

cumulative benefit-cost ratio for 12 hr after was approximately 12:1. When salt-abrasive mixtures were used, the operation did not pay for itself in 12 hr, with a benefit-cost ratio of less than 1.0.

When salt only was used on freeways, the operation paid for itself in the first 35 min after zero hour. The benefit-cost ratio for 12 hr after was approximately 3:1. When abrasive salt mixtures were used, the operation paid for itself after the first 6 hr. The benefit-cost ratio for 12 hr after was approximately 2.4:1. Note that it was negative for the first 5 hr because of the higher accident rates.

ANALYSIS OF COMPARISONS BETWEEN TWO STUDIES

Study Databases

Although every effort was made to obtain comparable lengths of highway test sections with similar volume characteristics by using AADT, it is obvious that volume data used to select highway test sections did not result in the same winter traffic volumes on highways. This resulted in lower MKT and hence lower number of accidents.

In addition, there was a difference (and change) in accident reporting limits between the states used in the two studies. In the salt-only study, Illinois, Wisconsin, and New York had minimum reporting limits of $250, $500, and $600, respectively. In the salt-abrasive study, Iowa and Minnesota had $500 limits, New York had a $1,000 limit, and Pennsylvania used the injury or tow-away criteria for reporting. To assess the effects of this change, a brief study was made of all reported accidents in New York for 1990 (lower limits) and 1992 (higher limits). In

1992, the first year of increase, there were approximately 63,000 fewer reported property damage accidents, a 40 percent reduction.

Differences in Variables Between Studies

Differences in any other variables that could exist in accident studies were also reviewed. It is believed that because of the large number of events, the other variables of weather, time of day, driver differences, and vehicle differences were likely to exist equally during both studies, so that any conclusions drawn need not be tempered by those differences.

Accident Rates

Differences in accident rates can be only partly hypothesized on two-lane highways by the lower traffic volumes and lower frequency of accidents. The accident database was not sufficient to draw accident conclusions for two-lane highways.

The database for freeways was comparable and conclusions about differences can be made. There was a substantial difference in accident reduction on freeways, even with changes in reporting limits (more accidents under the higher reporting limits).

The low frequency of accidents on two-lane highways resulted in either no significance for the first 4 hr or lower degrees of confidence (95 percent instead of 99 percent) in later hours.

The comparable number of accidents on freeways resulted in substantial significance in the salt-only study for

the first 8 hr after zero hour and significance in the last 6 hr for the salt-abrasive study. In effect, it took much longer for the rate reduction on freeways to occur in the salt-abrasive study. This was because of the accident rate increase the first 4 hr after zero hour.

Benefit-Cost Ratios

Because accidents are a major portion of the benefit-cost ratio, the ratio was much less for two-lane highways in the salt-abrasive study than in the salt-only study. On freeways, the ratio was comparable after 12 hr but after 6 hr there was a much greater ratio (2.5 : 1 versus 1.0 : 1) on the salt-only study than on the salt-abrasive study.

Conclusions

Conclusions reached from data gathered in this study (salt-abrasives) and compared to conclusions from an earlier study (salt only) are as follows (the salt-only study is called the first study and the salt-abrasives the second study).

1. The methodology used in each study was comparable. The number of events was larger in the second study. MKT was less in the second study for two-lane highways and comparable for freeways.
2. Accident rate reductions on two-lane highways were less with salt-abrasives than with salt only (Figure 6). Accident rate reductions on freeways were substantially different for the two studies. Accident rates dropped dramatically after achievement of bare pavement with salt only but more slowly with salt-abrasives (Figure 7).
3. Accident rate reductions in the second study were not as significant as those in the first study for two-lane highways. For freeways, rate reductions in both studies were significant. Significance alone, however, does not explain the difference in behavior of the accident rates between the studies. Figures 7 and 8 graphically portray the differences. Clearly, salt-only provided an improved road surface more quickly and controlled accidents sooner than did salt-abrasive mixtures.
4. Benefit-cost ratios in the first study were 12 : 1 for two-lane highways with the operation paying for itself the first 25 min after zero hour. In the second study, the benefit-cost ratio was 0.8 : 1, and the operation never paid for itself during the 12 hr of analysis after zero hour (Figures 3, 5, and 8). The use of abrasives and salt-abrasive mixtures was cost ineffective.
5. The benefit-cost ratio in the first study was 3 : 1 for freeways over the 12 hr of analysis, and the operation paid for itself the first 35 min after zero hour. For the second study, the ratio was 2.8 : 1 after 12 hr, but it took 6 hr after zero hour for the operation to pay for itself (Figures 4, 5, and 9). It took 6 hr for salt-abrasive mixtures to pay for the operation compared to 35 min for salt-only treatments.
6. The study goal of determining the relative effectiveness by percent of salt in the salt-abrasive mixture was not achieved. Because of insufficient events in the lowest salt percentage and insufficient accident data, the results are inconclusive. A much larger database would be needed for that type of determination.

References

1. Kuemmel, D., and R. Hanbali. Accident Analysis of Ice Control Operations. Presented at 3rd International Symposium on Snow and Ice Control, Minneapolis, Minn., Sept. 1992.
2. Special Report 235: Highway Deicing: Comparing Salt and Calcium Magnesium Acetate. TRB, National Research Council, Washington, D.C., 1991.
3. Guidelines to Reduce Air Pollution from Street Sanding. Regional Air Quality Council, Denver, Colo., Nov. 1991.
4. Snow and Ice Control—Instructional Memorandum. Iowa Department of Transportation, Highway Division, Office of Maintenance, Ames, Feb. 1992.
5. Ice and Snow Removal Manual. Minnesota Department of Transportation, St. Paul, June 1986.
6. Highway Maintenance Guidelines—Snow and Ice Control. New York Department of Transportation, Albany, Dec. 1993.
7. Maintenance Manual, Snow and Ice Control. Pennsylvania Department of Transportation, Harrisburg, April 1985.
8. Hanbali, R. M. Influence of Winter Road Maintenance on Traffic Accident Rates. Ph.D. dissertation, Department of Civil and Environmental Engineering, Marquette University, Milwaukee, Wis., 1992.
9. Hanbali, R., and D. Kuemmel. Traffic Volume Reductions Due to Winter Storm Conditions. In Transportation Research Record 1387, TRB, National Research Council, Washington, D.C., 1993, pp. 159–164.
10. Hanbali, R. M. Economic Impact of Winter Road Maintenance on Road Users. In Transportation Research Record

1442, TRB, National Research Council, Washington, D.C., 1994, pp. 151–161.

11. Claffey, P. Passenger Car Fuel Consumption as Affected by Ice and Snow. In *Highway Research Record 383*, HRB, National Research Council, Washington, D.C., 1972, pp. 32–37.

12. American Association of State Highway Officials. *A User Benefit Analysis of Highway and Transit Improvements.* National Cooperative Research Program Project 2–12 and 2–12/1, American Association of State Highway and Transportation Officials, Washington, D.C., 1977.

13. Welch, R. *Passenger Car Fuel Consumption as Affected by Ice and Snow.* National Pooled Fund Study. Report FHWA RD-77-20, Federal Highway Administration, U.S. Department of Transportation, 1976.

14. National Safety Council. *Accident Facts—1993.* Chicago, Ill., 1995.

15. Urban Institute. *The Costs of Highway Crashes.* Report FHWA-RD-91-055, Federal Highway Administration, U.S. Department of Transportation, 1991.

16. Bari, Q. *Accident Analysis of Abrasives and Abrasive/Salt Mixtures Used as a General Procedure for Snow and Ice Control.* Ph.D. dissertation. Department of Civil and Environmental Engineering, Marquette University, Milwaukee, Wis. (in process).

17. Kuemmel, D., and Q. Bari. *Accident Benefit Cost Comparison of Salt Only vs. Salt/Abrasive Mixtures Used in Winter Maintenance in the USA.* Final Report, Salt Institute, Alexandria, Va., June 1996.

18. Hanke, H., and C. Levin. *Influence of Winter Road Maintenance on Traffic Safety and Transport Efficiency* (in German). Darmstadt Technical University, Germany, 1988. English summary published in *Curtailing Usage of Deicing Agents in Winter Maintenance*, Organization for Economic Cooperation and Development, Paris, France, 1989.

19. Weed, R. Revised Decision Criteria for Before-and-After Analyses. In *Transportation Research Record 1068*, TRB, National Research Council, Washington, D.C., 1984, pp. 8–17.

Socioeconomic Calculations for Winter Tires

Gudrun Öberg, *Swedish National Road and Transport Research Institute*

The socioeconomic consequences that may be expected from a ban on studded tires and the effects of a requirement on winter tires in certain periods during the winter or during slippery conditions were calculated and are presented. The requirement for winter tires (mud and snow tires) means that summer tires are not allowed, but both studded and unstudded winter tires may be used. The calculations were made for the winters of 1993–1994 and 1999–2000. The conditions for winter 1993–1994, a fairly normal winter, form the basis for the calculations. The conditions for 1999–2000 are the same except for the assumptions that all studded tires will have been replaced by tires with lightweight studs and that wear-resistant pavements will be more common. All other factors for 1999–2000, such as winter maintenance, are the same as for 1993–1994. A large part of the project was to calculate the changes in vehicle mileage with different tires in various winter road conditions.

The socioeconomic calculations include the following effects: (*a*) the traffic safety effects of ice and snow conditions and pavement wear; (*b*) road wear on pavement and road markings and subsequent sign cleaning; (*c*) car costs, including costs for tires and rims, changes in fuel consumption, and car-washing changes caused by the use of studs; and (*d*) environmental effects, which include only use of stronger agents for car washing when studs are used (other environmental costs are not included).

Sweden has 8.7 million inhabitants, 5.3 million of whom have driving licenses; there are 3.9 million vehicles (*1*). The total road length is about 415 000 km. Almost 100 000 km are state-administered roads and 38 000 km are municipal roads. The vehicle mileage is almost 70 billion vehicle-km (*2*). More than 80,000 accidents are reported by police annually. In 1993, 632 persons were killed in traffic accidents (*3*). The traffic safety level in Sweden is high as demonstrated by the following statistics:

- Persons killed per 100,000 inhabitants, 7.2;
- Persons killed per 10,000 vehicles, 1.6; and
- Persons killed per 100 million vehicle-kilometers, 0.9.

In socioeconomic calculations the accident costs are calculated according to the formula.

$$OLKOST = (a \times EO + b \times LS + c \times SS + d \times D)/ANTOL \quad (1)$$

where

EO = property damage
LS = slightly injured person
SS = seriously injured person
D = a fatality
$ANTOL$ = number of police reported accidents.
a = kronar (SKr) 100,000 ($15,150)
b = SKr 230,000 ($34,850)
c = SKr 5,400,000 ($820,000)
d = SKr 12,100,000 ($1,830,000)

U.S. dollar conversions are at August 1, 1996, rates. The costs, including human value, are according to the 1992 price level of a police-reported accident. The av-

152

erage accident cost for the whole year is for rural areas SEK 1,300,000 and in urban areas SEK 520,000. The costs include an estimate of the accidents that are not reported to the police. In winter the average accident cost is somewhat lower.

WINTER TIRE PROJECT

During winter 1993–1994, the Swedish National Road Administration received considerable criticism for its winter maintenance, in particular for the high consumption of road salt. This led to discussions on changing the rules for winter maintenance, allowing a little ice and snow on salted roads and performing maintenance on more roads without salt. In addition, changes intended to influence vehicle equipment and driver behavior were to be studied.

The purpose of the investigation described here was to calculate the socioeconomic consequences that may be expected from a requirement on winter tires in various circumstances. The study started with a calculation of the socioeconomic consequences that may be expected from a ban of studded tires (4). That calculation was made to compare with earlier calculations (5,6). In this paper that result is transformed into the effect of the use of winter tires (with or without studs) in the winter compared with the effect if all cars used summer tires. The calculations were made for winter 1993–1994 and for winter 1999–2000. The conditions in winter 1993–1994, a fairly normal winter, form the basis for the calculations. During that winter it is estimated that 17 percent of the vehicles with studded tires had lightweight studs. The conditions in 1999–2000 are the same, except it is assumed that studded tires will have been replaced by tires with lightweight studs and that wear-resistant pavements will have become more common. All other factors, such as winter maintenance, are the same as for 1993–1994.

Several effects were studied, as follows.

- Accidents (direct, because of slippery pavement; indirect, because of pavement wear);
- Road wear (pavement and road markings, dirty signs);
- Car costs (tires and rims, fuel consumption, washing); and
- Environment (car washing).

EFFECT OF WINTER TIRES VERSUS SUMMER TIRES

The proportion of cars and the proportion of vehicle mileage (in ice and snow) using different tires are shown below:

	Cars (Percentage) %	Vehicle Mileage on Ice/Snow (Percentage)
Studded tires	64	76
Studless winter tires	13	15
Summer tires	23	9

When studded tires are used, the effects on road safety are a 40 percent decrease in accidents in icy or snowy road conditions on rural roads and a 35 percent decrease in accidents in built-up areas compared with use of summer tires. The corresponding figures for other winter tires are 25 percent and 20 percent. Each type includes both good and bad tires in use at the beginning of 1990 (7,8).

The number of car accidents in icy or snowy conditions during winter 1993–1994 was 16,271. The following may be calculated:

Number of car accidents in icy or snowy conditions if all cars have summer tires   23,848

Number of car accidents in icy or snowy conditions if studded tires are banned   19,538

The results obtained on the use of winter tires indicate an accident decrease of just more than 7,500 accidents per winter. There are also indirect accident effects caused by the use of studded tires, such as higher wet friction on pavements, because studs create a coarse surface texture and produce wheeltracks and dirt spray (9,10). The sum of these indirect effects is decrease of 600 to 700 accidents because of the use of winter tires. The number of fatalities in road accidents has decreased somewhat, by about 40, the seriously injured by around 350, and the slightly injured by about 1,500. The values are uncertain.

For measurement of road wear from traffic with studded tires, the SPS index normally is used. SPS is the Swedish abbreviation for specific wear and indicates the number of tonnes of abraded asphalt per kilometer of road and million vehicles with studded tires, or the number of grams of abraded asphalt per kilometer of road and vehicle with studded tires. The average SPS index has been calculated after measurements on roads with various annual average daily traffic values. With steel studs, the SPS index varied between 22 and 35 g/km for the various classes of traffic, with an average of 26 g/km. The SPS index for lightweight studs is half this figure (11).

During winter 1993–1994, it is estimated that 17 percent of the vehicles with studded tires had lightweight studs. This gives a weighted SPS index of 24 g/km, which implies total wear of 300 000 tonnes, valued at approximately SEK 150 million. To compensate for winters with more troublesome wear levels, the cost of wear can be

said to be in the range of SEK 150 million to 200 million. Costs of wear on road markings and the washing of dirt spray from road signs is estimated to cost SEK 35 million to 70 million a year.

In 1999–2000, when all studded tires will have light-weight studs and wear-resistant pavements are more common, the average SPS index is calculated to be 11 g/km, giving total road wear of about 130 000 tonnes, worth SEK 65 million to 90 million at today's prices. Costs of wear on road markings and the washing of dirt spray from road signs is put at SEK 20 million to 35 million a year.

Compared with use of summer tires the whole year, the costs of motorists' using winter tires have increased. The motorist pays for winter tires and extra rims and the cost of wheel changing. The annual cost will be about SEK 330 million.

Petrol consumption is calculated to increase by SEK 90 million because of an assumed difference of 2 percent between summer tires and winter tires. It is also assumed that no difference exists between studded and studless winter tires.

The use of studded tires means that vehicles must be cleaned more often because road wear will increase. In this study, two calculations are made. The first is that studs necessitate two to four extra washes during a winter, and the second is that all 13 washes during the winter take somewhat longer and that half an extra wash is required. The first alternative gives a somewhat larger dispersion in costs and this alternative is therefore the one used. It entails a cost to car owners of SEK 300 million to 700 million, which could be avoided. Because of road wear in 1999–2000, the cost will be only SEK 130 million to 300 million.

Vehicle washing requires stronger agents than would be necessary if tire studs were not used. Emissions of petroleum-based solvents attributable to use of studded tires would then amount to 1500 to 3000 tonnes for 1993–1994. On the basis of the Swedish National Road Administration's environmental valuation, this would lead to an environmental cost of SEK 25 million to 50 million a year. In 1999–2000, the environmental cost of vehicle washing necessitated by the use of studded tires will have fallen to SEK 10 million to 20 million.

The effect of winter tires on accidents is considerable, and the benefit of the decrease in accidents due to the use of such tires is not offset by other cost increases. The effect on the environment, however, is difficult to measure and evaluate, and therefore only vehicle washes are included in Table 1. With the results for the other effects, this means that the total environmental effect may become fairly large before equilibrium is reached. In or near 2000, the difference between the advantages and disadvantages of winter tire use will be even greater. The lightweight stud will then be the only type of stud available, leading to lower car and wear costs and thereby a

TABLE 1   Cost Changes, Winter Tires (Studded or Unstudded) Versus Summer Tires (in SKr Million/Year)

	Decrease	Increase	
		1993/1994	1999/2000
Accidents			
– direct	2,750–3,370		
– indirect	240–290		
Road wear			
– pavement		150–200	65–90
– road markings signs		35–70	20–35
Car costs			
– tires/rims		330	330
– fuel consumption		90	90
– washing		300–700	130–300
Environment			
– car washing		25–50	10–20
– the rest		?	?
TOTAL	2,990–3,660	930–1,440 +?	645–865 +?

reduction in environmental effects, at the same time as the effect of studded tires on road safety is maintained.

REQUIREMENT FOR WINTER TIRES IN SLIPPERY CONDITIONS

In the case of a requirement for winter tires in slippery conditions, it is possible that all vehicle mileage with summer tires on ice and snow will be eliminated; vehicle mileage with summer tires in icy or snowy conditions will be replaced by travel in bare road conditions; and motorists will change to winter tires.

In the calculations (12), the requirement for use of winter tires is compared with the use in the winters of 1993–1994 and 1999–2000 (Table 2). Most often, minimum and maximum alternatives for a redistribution of the vehicle mileage are calculated. It is then possible to interpolate between these alternatives. The distribution of vehicle mileage among different tires controls the change in benefit-cost implied by the various alternatives, on the basis of conditions in winter 1993–1994. The distribution used here is that of the 23 percent of drivers that now use only summer tires in the winter, 15 percent will use stud-

TABLE 2 Projected Changes Under Requirement
for Winter Tires on Slippery Surfaces Compared with
Tire Use in Winter 1993–1994

	Decrease	Increase	
		1993/1994	1999/2000
Accidents			
– direct	385–485		
– indirect	75–95		
Road wear			
– pavement		25–35	10–15
– road markings/signs		10	5
Car costs			
– tires/rims		200	200
– fuel consumption		30	30
– washing		50–120	20–50
Environment			
– car washing		5–10	0–5
– the rest		?	?
TOTAL	460–580	320–405 +?	265–305 +?

ded tires, 5 percent will use winter tires, and 3 percent will not drive when the roads are slippery.

The road safety benefit of this requirement is greater than the known negative effects of the requirement. When slipperiness is unexpected it is possible that some vehicle mileage with summer tires will take place, which will decrease the highest traffic safety value in Table 2. The number of car accidents reported by the police will decrease by 1,100 to 1,400, the number of persons killed in traffic by 6 to 7, the number seriously injured by 50 to 60, and the number slightly injured by 200 to 250. The values are uncertain.

Conclusions

The requirement for winter tires in slippery conditions will, compared with the use of summer tires, cause a decrease in accident costs by SEK 3,450 million to 4,240 million a year. The increase in costs for roads, cars, and the environment (considering only car washing) will be SEK 1,250 million to 1,845 million in 1993–1994 and SEK 910 million to 1,170 million in 1999–2000.

The decrease in police-reported accidents will be about 9,200 to 9,600 per winter. This is a winter reduction of more than 20 percent.

As a result of this project, the government suggested that winter tires be required during slippery conditions. The suggestion has been referred to authorities for consideration, and a decision will follow.

Acknowledgment

References

1. Statistical Yearbook of Sweden 1994. Statistiska centralbyrån. In English.
2. Thulin, H., and G. Nilsson. *Vägtrafik, exponering, skaderisker och skadekonsekvenser för olika färdsätt och åldersgrupper (Road traffic, exposure, injury risks and injury consequences for different travel modes and age groups)* (English summary). Rapport 390. Statens Väg- och transportforskningsinstitut, 1994.
3. *Nationellt trafiksäkerhetsprogram, 1995–2000 (National Traffic Safety Program, 1995–2000)* (in Swedish). Vägverket, Rikspolisstyrelsen och Svenska Kommunförbundet.
4. Carlsson, A., P. Centrell, and G. Öberg. Studded tyres. Socio-economic calculations (in English). Statens Väg- och Transportforskningsinstitut. Meddelande 756A.
5. Carlsson, A., O. Nordström, and H. Perby. Effekter av dubbdäck. Konsekvenser av ändrade bestämmelser (The effects of studded tyres. Consequences of amended regulations) (English summary). Statens Väg- och Trafikinstitut. Meddelande 674.
6. Piggdekk og vintervedlikeholdsstrategi. (Studded tyres and winter maintenance in the Nordic Countries) (English summary). Nordisk Vegteknisk Forbund, Rapport nr 6, 1992.
7. Öberg, G., O. Junghard, and M. Wiklund. En studie av metoder för att beräkna samband mellan dubbdäcksanvändning och trafiksäkerhet (A study of methods of calculating the connection between the use of studded tyres and road safety) (English summary). Statens Väg- och Trafikinstitut. Meddelande 722.
8. Nordström, O., and E. Samuelsson. *Vinterdäcks väggrepp på is (Road grip of winter tyres)* (English summary). Rapport 354. Statens Väg- och Trafikinstitut.
9. Kallberg, V.-P. *Uuden, vähan tietä kuluttavan nesta tyypin vaikututs liikenteen käyttö—kustannuksiin (The effects of a new stud type on the running costs of road traffic)* (in Finnish). Meddelande 914. Statens Tekniska Forskningscentral, Väg- och trafiklab., 1988.
10. Hemdorff, S., et al. *Trafiksäkerhet och vägytans egenskaper (TOVE). Slutrapport (Traffic safety and the properties of road surfaces. Final report)* (English summary). Statens Tekniska Forskningscentral. Meddelande 1075, 1989.
11. Gustafson, K. *Prov med lättare däckdubb i VTIs provvägsmaskin (Test with lightweight studs in the VTI's pavement testing machine)* (English summary). Rapport 377. Statens Väg- och Trafikinstitut.
12. Carlsson, A., and G. Öberg. *Winter tyres. Effects of proposed rules* (in English). Statens Väg- och Transportforskningsinstitut. Meddelande 757A.

Field Test Results of Intelligent Delineator System

Intelligent Transport System Technology Research and Development for Winter Traffic

Yasuhiko Kajiya, Yoshifumi Fukuzawa, and Keishi Ishimoto,
   Hokkaido Development Bureau, Civil Engineering Research Institute, Japan
Hajime Ishimaru, *Meisei Electric Company*

The intelligent delineator system is a light-emitting delineator incorporating a pole-type visibility meter and a car halt surveillance radar. When visibility is reduced it emits light to warn drivers, and it detects stopped cars to warn followers. The development of this system was begun in 1993. Initially a pole-type visibility meter was developed for this system, and its performance was examined in field tests in winter 1993–1994. The light-emitting delineator with this pole-type visibility meter was installed at a median strip on a national highway near Sapporo, Japan, in winter 1994–1995 for the on-site test. It was found that the pole-type visibility meter has sufficient accuracy and stability in operation. A car halt surveillance radar, which uses milliwave technology to detect stopped cars in blowing snow conditions, also was developed. Its performance was examined in field tests and on the same highway in winter 1995–1996. The car halt surveillance radar and the total system have shown enough possibility for further practical development. The Hokkaido Development Bureau is now developing a special research plan focusing on intelligent transport system (ITS) technology research and development for winter traffic, called the ITS/Win Research Program. The development and the field test results of the intelligent delineator system are reported, and research-and-development challenges for the ITS technology for winter traffic in Hokkaido are addressed.

Reduced visibility caused by blowing snow on highways has been a key issue for winter traffic safety in Hokkaido, Japan. In recent years, high-grade trunk roads have expanded in Hokkaido and many multi-vehicle winter collisions have occurred. Following drivers must know immediately when a car is stopped because of an accident or difficulty in driving under reduced visibility conditions. Lack of warning may be a cause of multiple-vehicle collisions. In fact, on March 17, 1992, the largest accident in Japan occurred under reduced visibility conditions in snow on the expressway near Sapporo. It involved 186 vehicles.

Development of the intelligent delineator system was begun in 1993 (*1*). The system is a light-emitting delineator incorporating a pole-type visibility meter and a car halt surveillance radar (CHSR) using milliwave technology. When visibility is reduced because of blowing snow or other causes, the system emits light to warn drivers, and it detects halted vehicles and warns the followers. Figure 1 (*1*) shows the composition of the intelligent delineator system. Figure 2 (*1*) shows the concept of the intelligent delineator system installed on a median strip. The CHSR detecting an accident in reduced visibility conditions is shown.

POLE-TYPE VISIBILITY METER

The pole-type visibility meter was specially developed for the intelligent delineator system. Because it is used in combination with a light-emitting delineator, the measuring part is in the shape of a vertical pole with a diameter as small as possible. Figure 3 shows the block diagram of the pole-type visibility meter. It emits near-infrared rays. The measuring area is formed by crossing light-receiving
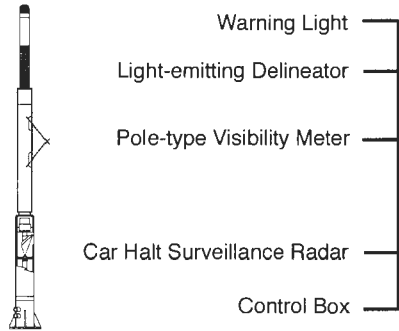
FIGURE 1 Composition of intelligent delineator system.

FIGURE 3 Pole-type visibility meter.

beams only in a sampling zone. The projected rays are scattered to the front or diagonally to the front by particles of snow flying into this zone, and the intensity of scattered rays is measured by the detector. The received signals are then processed by an amplifier, a signal discriminator, and an output discriminator, and reduced visibility signals are generated. In signal processing, background light is removed by high-speed modulation, and a feedback function to automatically stabilize light sources is performed. Output signals are obtained based on the visibility categories of "Good," "Caution," and "Danger" with a timer (1 to 999 sec).

Figure 4 (1) shows the calibration curve of this device and visibility during the daytime. From the field observations in winter for 3 years and comparative experiments in a smoke test room, the practicality of this new pole-type visibility meter has been proved.

CHSR

The CHSR is a milliwave (59.5 GHz, 70 mW) FM-CW radar. It measures the direction and distance of the target object by using rotating horizontal pencil beams ap-

FIGURE 2 Concept of intelligent delineator system.

proximately 80 cm above the ground. It judges the existence of halted vehicles by referring to the calibration data collected when there were no halted vehicles. Whereas the maximum detection distance of the system used in the test in the winter of 1994–1995 was 60 m, it was extended to 110 m in the winter of 1995–1996. This was achieved by improvement of software to limit the measurement area on the road.

Figure 5 shows the block diagram of the CHSR. An offset parabolic antenna rotates once every 2 to 3 sec in a cylindrical frame. This causes the transmission of sharp waves of beams sweeping continuously and horizontally at about 80 cm above the road surface. Because reflected waves are received every 4° between the angles of 0° and 90°, a total of 23 steps of signal can be obtained. Analog-to-digital conversion and fast Fourier transformation (FFT) processing of these signals yield a total of 128 power spectra. By representing the frequency on the abscissa axis and the intensity of signal on the ordinate axis of a bar graph, spectral arrays are obtained.

Figure 6(a) shows the monitor screen at the evaluation of the CHSR. The upper part shows the received waves (beat signals) and the lower part is the spectrum diagram after FFT processing. On the monitor screen in Figure 6(b), the horizontal axis represents the distance and the vertical axis represents the angle. The angle was measured every 4° starting from 0°, and the height of the wave represents the level of received waves. As the measurement area was limited on the road by 23 sweeping beams, the signals are hyperbolically interrupted.

Field Tests of CHSR in Winter 1994–1995

A test to detect halted cars on a winter road was conducted in February 1995. The test was conducted in light snowfall and in heavy snowfall artificially made by using a rotary snowplow. Snow was blown to a height of about 20 m and a stable snowstorm and reduced visibility conditions throughout the test site were created.
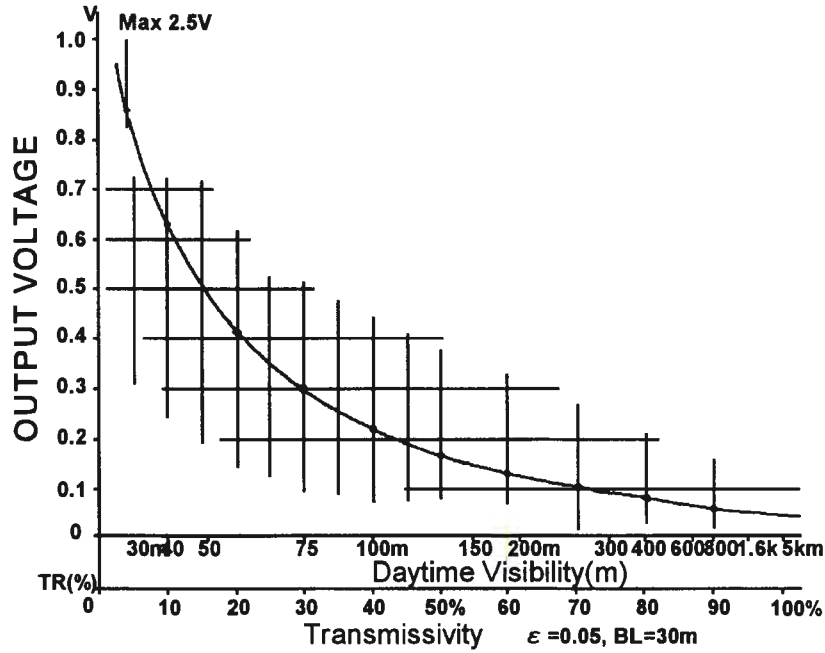
FIGURE 4   Visibility conversion curve.

Figure 7 shows the field test of the CHSR in the winter of 1994–1995. The detection results were satisfactory. A small vehicle about 40 m away could be detected without fail even when the visibility was as low as 10 m. The presence or absence of snowstorm conditions makes almost no difference in the figure. Moreover, a warning signal to indicate the existence of a halted car was sent out even when the car was buried under snow.

Field Tests of CHSR in Winter 1995–1996

On the basis of improvements to the system that were produced experimentally in the winter of 1994–1995, fields tests were conducted in the winter of 1995–1996 to detect vehicles in reduced visibility conditions caused by snowstorms. The maximum detection distance was confirmed and the response time was verified. The tests

(a)

(b)

FIGURE 6   Monitor screen at evaluation of car halt surveillance radar.

FIGURE 5   Car halt surveillance radar.
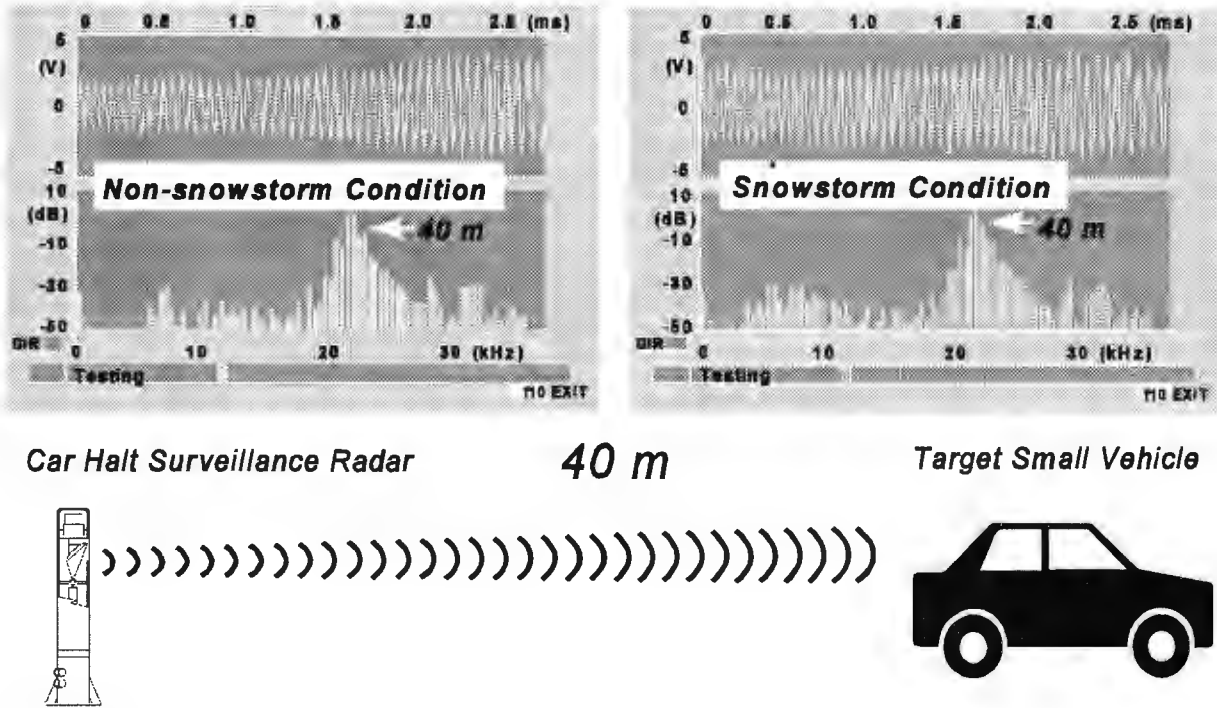
FIGURE 7   Field test of car halt surveillance radar in winter 1994–1995.

were conducted twice at the Ishikari Blowing Snow Test Field, on January 18 and March 22, 1996, and once on the Ebetsu section of National Route 12 on February 22.

Tests were conducted using four types of vehicles—a mini, a subcompact, a recreational vehicle, and a bus—to simulate actual driving conditions. Figure 8 shows the CHSR and a test condition in which the CHSR was placed at the 0-m point on a 10-m-wide, 120-m-long test road to detect cars every 20 m (Figure 9).

Tests on January 18, 1996

On January 18, 1996, a northwesterly wind was blowing at speeds of 5 to 8 m/sec, the temperature was –11°C, and visibility was 20 to 100 m. Four types of vehicles

FIGURE 8   Car halt surveillance radar and field test in winter 1995–1996.

were stopped at intervals of 20 m, and the confirmation of detection and measurement of response time were done at the same time. The measurement was conducted at each interval for each car type. Although all the cars were detected, the response time was 15 to 30 sec and stable results could not be obtained. The area-setting and automatic measurement programs used in the test were still under development.

Tests on March 22, 1996

On March 22, 1996, a northwesterly wind was blowing at speeds of 5 to 6 m/sec, the temperature was –2°C, visibility was 100 to 200 m, and there was snowfall. The test was conducted for four types of vehicles on the same road setting as for the previous test, and the improved area-setting and automatic measurement programs were used. Vehicles up to 110 m away could be detected without fail. The response time, which was thought to be a problem on January 18, was 6 sec at all points (at this stage, the rotation speed was 2 sec per rotation and detection was made for three rotations) and stable detection was confirmed. To verify the detection, the measured data were recorded on the hard disk of a personal computer and lighting of the red lamp was checked visually. The test results are shown in Table 1. Although the milliwave has been proved to be an all-weather sensor that is not affected by snow, fog, or other weather conditions, the detection of all types of vehicles in the

FIGURE 9   Field test layout of car halt surveillance radar in winter 1995–1996.

heavy snowstorm with visibility of 100 m was considered significant.

Field Test of CHSR on National Highway Route 12

The CHSR was installed at the side of National Highway Route 12 (Ebetsu Section). It has been working automatically without an operator since January 1996. Its performance has been checked by manual test (Figure 10) and by using images from an ITV camera installed near the system. ITV camera images showed that the CHSR could detect snowplows and other halted vehicles.

ITS/Win RESEARCH PROGRAM

The development of technologies for the intelligent transport system (ITS) has been under way nationwide in Japan. Through advancement of information communication technologies and the development of vehicle and highway intelligence technologies, the system will allow the unified functioning of people, vehicles, and highways. It will also lead to the improvement of traffic safety and efficiency, amelioration of the environment, a more enjoyable driving experience, and the founding of new industries. The Hokkaido Development Bureau (HDB) has established the Committee of Intelligent

Transport Systems within the bureau to consider the application of ITS technology. The committee is developing the ITS/Win Research Program, which focuses on ITS technology research and development for winter traffic. It includes 17 research projects, such as the development of the intelligent delineator system, the intelligent ITV camera, and a highway information system using Internet technologies (i.e., Intranet technology).

The program is categorized by three concepts: (a) directly avoiding danger by introducing intelligent ancillary road facilities (the Intelligent Winter Highway System); (b) indirectly reducing accidents via advanced highway information systems, thereby decreasing anticipated dangers (the Winter Highway Information System for Traffic Safety and Efficiency of the 21st Century); and (c) building a comprehensive highway disaster prevention information system. The goals of the ITS/Win Research Program are to (a) formulate solutions to traffic problems specific to Hokkaido winters; (b) increase efficiency of snow removal and road surface maintenance and management during winters; (c) create sophisticated response systems for disasters such as large-scale earthquakes; (d) resolve the year-round traffic safety problem in Hokkaido; and (e) provide improved road service specially tailored for Hokkaido.

The intelligent ITV camera has been developed to detect unexpected phenomena through image processing and to transmit messages widely and efficiently on the computer network in conjunction with the e-mail and

TABLE 1   Detection Results for Different Types of Vehicles

Car Type	Direction	20 m	40 m	60 m	80 m	100 m	110 m	120 m
Mini	Rear	D[a]	D	D	D	D	D	ND[c]
Sub-compact	Rear	D	D	D	D	D	D	ND
Recreational Vehicle	Rear	D	D	D	D	D	D	UD[b]
Bus	Rear	D	D	D	D	D	D	UD

[a]D: Detection   [b]UD: Unstable Detection   [c]ND: No Detection

FIGURE 10   Field test of car halt surveillance radar on National Highway Route 12.

World Wide Web server systems. Digitized image information will be transmitted in various forms and will change the ITV camera from a simple monitoring tool to a part of a monitoring network with an operator. HDB has long been aware of the potential for using Internet technologies in highway information systems. The Internet's multimedia, on-demand, and interactive functions could be useful to the system. In fact, a system that provides real-time images of mountain passes where there are severe weather conditions during the winter is being built on the Internet. The Civil Engineering Research Institute of HDB opened an Internet homepage called Northern Roads (http://www2.ceri.go.jp/eng/index.htm), which introduced research and development activities including the ITS/Win Research Program in Hokkaido. HDB, in conjunction with the World Road Association's World Interchange Network program, is hoping to exchange information about the ITS/Win Research Program with all snowy, cold countries and regions that have similar problems with winter traffic safety and efficiency.

CONCLUSIONS

The intelligent delineator system is a light-emitting delineator incorporating a pole-type visibility meter and a CHSR. When visibility is reduced, the system emits light to warn drivers, and it detects halted vehicles and warns the followers. Evaluation tests were conducted on the pole-type visibility meter in the winter of 1993–1994 and on the CHSR by using milliwave technology in the winter of 1994–1995 and 1995–1996. It was confirmed that the pole-type visibility meter had sufficient accuracy and stability in operation. As for the CHSR, in the test of the winter of 1994–1995, a subcompact car could be detected from about 40 m away without fail in about 10-m visibility conditions, which were created artificially by a rotary snowplow. In the 1995–1996 winter, three tests were conducted from January to March; a mini, a sub compact, a recreational vehicle, and a bus all could be detected from 110 m away without fail in 100- to 200-m visibility conditions caused by natural blowing snow. The authors are convinced that the system is feasible for further development toward future field use. The milliwave is not affected by snowfall and it is strongly expected to be basic ITS technology indispensable for a winter driving support system.

Winter driving conditions are severe because of slippery road surfaces and reduced visibility conditions caused by snow. However, these conditions may be alleviated by ITS, which has the potential to significantly increase safety by supporting winter driving. The ITS/Win Research Program, which HDB is currently developing, is expected to make a large contribution to the improvement of winter traffic safety.

REFERENCE

1. Kajiya, Y., Y. Fukuzawa, and K. Ishimoto. Development of Intelligent Delineator System. *Proc., 2nd World Congress on Intelligent Transport Systems*, Yokohama, Japan, October 1995, Vol. III, pp. 1193–1198.

Author Addresses

Lars Bäckman, Swedish National Road and Transport Research Institute, S-581 95 Linköping, Sweden.

Quazi Bari, Southern New Hampshire Planning Commission, 438 Dubuque Street, Manchester, New Hampshire 03102.

Robert R. Blackburn, Blackburn and Associates, 17029 East Aloe Drive, Fountain Hills, Arizona 85268.

Jörgen Bogren, Department of Physical Geography, Göteborgs University, S-413 81 Göteborg, Sweden.

Brian H. Chollar, Federal Highway Administration, U.S. Department of Transportation, Turner Fairbank Research Center, HNR-30, 6300 Georgetown Pike, McLean, Virginia 22101.

Edward J. Fleege, Transportation District One, Minnesota Department of Transportation, 1123 Mesaba Avenue, Duluth, Minnesota 55811-2798.

Lennart Folkeson, Swedish National Road and Transport Research Institute, S-581 95 Linköping, Sweden.

Kazunori Fujisawa, Public Works Research Institute, Ministry of Construction, Tsukuba City, Ibaraki Pref., 305, Japan.

Takashi Fujiwara, Civil Engineering Department, Hokkaido University, Kita 13, Nishi 8, Kitaku, Sapporo, 060, Japan.

Yoshifumi Fukuzawa, Hokkaido Development Bureau, Civil Engineering Research Institute, 1-3 Hiragishi, Toyohira-ku, Sapporo, 062, Japan.

Kent Gustafson, Swedish National Road and Transport Institute, S-581 95 Linköping, Sweden.

Torbjörn Gustavsson, Department of Physical Geography, Göteborgs University, S-413 81 Göteborg, Sweden.

Toru Hagiwara, Civil Engineering Department, Hokkaido University, Kita 13, Nishi 8, Kitaku, Sapporo, 060, Japan.

Anita Ihs, Swedish National Road and Transport Institute, S-581 95 Linköping, Sweden.

Hajime Ishimaru, Meisei Electric Company, Moriya Factory, 249-1 Moriyakou, Moriya-cho, Ibaragi-ken, 302-01, Japan.

Keishi Ishimoto, Hokkaido Development Bureau, Civil Engineering Research Institute, 1-3 Hiragishi, Toyohira-ku, Sapporo, 062, Japan.

Zuwei Jin, Department of Chemical Engineering, The Ohio State University, 140 West 19th Avenue, Columbus, Ohio 43210.

Yasuhiko Kajiya, Hokkaido Development Bureau, Civil Engineering Research Institute, 1-3 Hiragishi, Toyohira-ku, Sapporo, 062, Japan.

Stephen A. Ketcham, Cold Regions Research and Engineering Laboratory, U.S. Army Corps of Engineers, 72 Lyme Road, Hanover, New Hampshire 03755.

Robert F. Kubichek, Department of Electrical Engineering, University of Wyoming, P. O. Box 3295, Laramie, Wyoming 82071-3295.

David A. Kuemmel, Center for Highway and Traffic Engineering, Marquette University, P. O. Box 1881, Milwaukee, Wisconsin 53201-1881.

P. J. Lister, Vaisala TMI, Vaisala House, Bristol Road, Birmingham B5 7SW, United Kingdom.

Masaru Matsuzawa, Hokkaido Development Bureau, Civil Engineering Research Institute, 1-3 Hiragishi, Toyohira-ku, Sapporo, 062, Japan.

L. David Minsk, 24 Rayton Road, Hanover, New Hampshire 03755.

Kazuyuki Morohashi, Foundation System Research and Development Institute of Japan, Tomihisacho 16-5, Shinjuku-ku, Tokyo 162, Japan.

Takashi Nakatsuji, Civil Engineering Department, Hokkaido University, Kita 13, Nishi 8, Kitaku, Sapporo, 060, Japan.

Maarten Noort, Meteo Consult, P. O. Box 617, 6700 AP Wageningen, The Netherlands.

Gudrun Öberg, Swedish National Road and Transport Research Institute, S-581 95 Linköping, Sweden.

Yuki Onodera, Civil Engineering Department, Hokkaido University, Kita 13, Nishi 8, Kitaku, Sapporo, 060, Japan.

Hidetsugu Onuma, Hokkaido Development Bureau, Civil Engineering Research Institute, 1-3 Hiragishi, Toyohira-ku, Sapporo, 062, Japan.

Yrjö Pilli-Sihvola, Finnish National Road Administration, Kauppamiehenkatu 4, FIN-45100 Kouvola, Finland.

Zoltán Radó, Norsemeter, Norway.

Jianmin Shao, Vaisala TMI, Vaisala House, Bristol Road, Birmingham B5 7SW, United Kingdom.

Akihiro Shimojo, Hokkaido Development Bureau, Civil Engineering Research Institute, 1-3 Hiragishi, Toyohira-ku, Sapporo, 062, Japan.

Hideki Takagi, Hokkaido Development Bureau, Civil Engineering Research Institute, 1-3 Hiragishi, Toyohira-ku, Sapporo, 062, Japan.

Masao Takeuchi, Japan Weather Association, Hokkaido Head Office, N-4, W-23, Chuo-ku, Sapporo, 064, Japan.

Baskin I. Tapkan, Department of Electrical Engineering, University of Wyoming, P. O. Box 3295, Laramie, Wyoming 82071-3295.

Teruyoshi Umemura, Department of Mechanical Engineering, Nagaoka University of Technology, Kamitomiokamachi 1603-1, Nagaoka, Niigata 940-21, Japan.

J. C. Wambold, CDRM, Inc., 1911 East College Avenue, P. O. Box 1277, State College, Pennsylvania 16804.

Shang-Tian Yang, Department of Chemical Engineering, The Ohio State University, 140 West 19th Avenue, Columbus, Ohio 43210.

Suzanne Yoakum-Stover, Department of Physics and Astronomy, University of Wyoming, P. O. Box 3295, Laramie, Wyoming 82071-3295.

TRANSPORTATION RESEARCH BOARD
National Research Council
2101 Constitution Avenue, N.W.
Washington, D.C. 20418

ADDRESS CORRECTION REQUESTED

NATIONAL ACADEMY PRESS
ISBN 0-309-06216-0